0008-7114

Caryologia

International Journal of Cytology, Cytosystematics and Cytogenetics

2022
Vol. 75 - n. 4

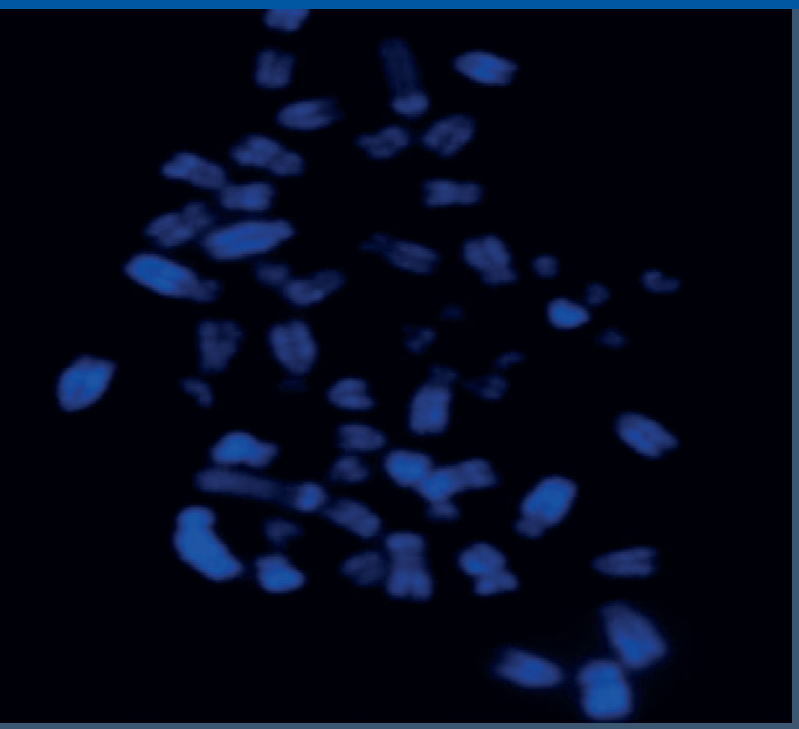

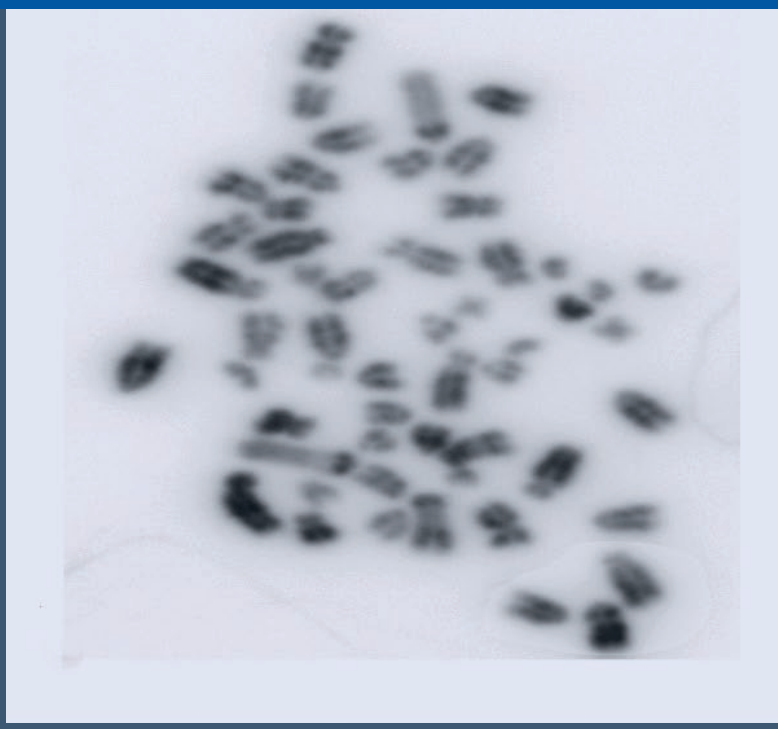

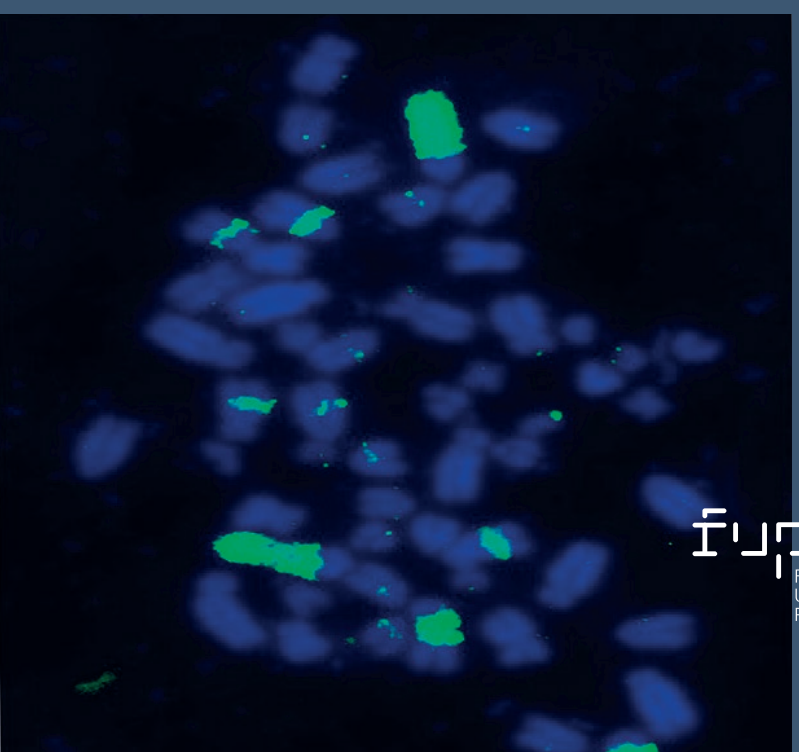

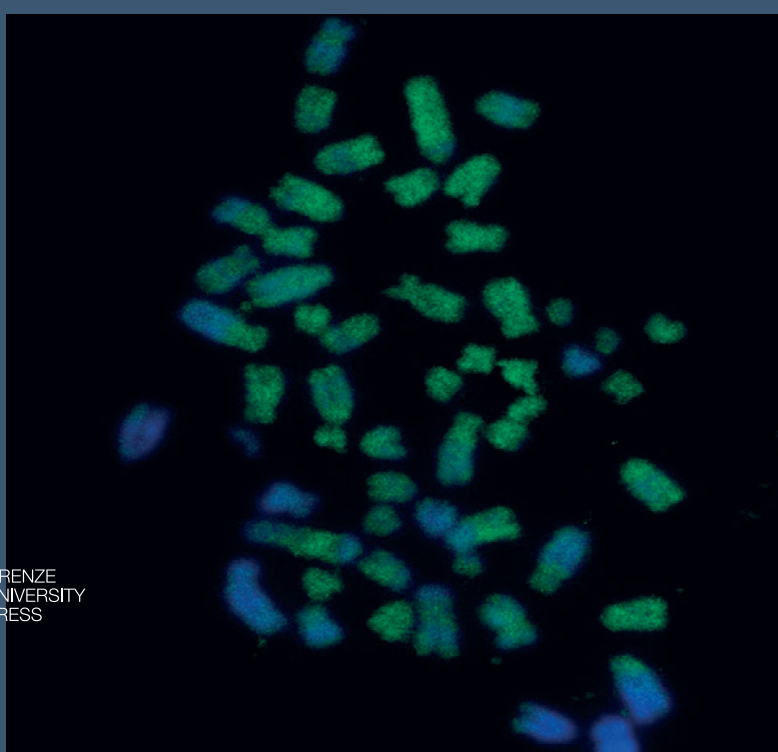

FIRENZE
UNIVERSITY
PRESS

Caryologia. International Journal of Cytology, Cytosystematics and Cytogenetics
Caryologia is devoted to the publication of original papers, and occasionally of reviews, about plant, animal and human karyological, cytological, cytogenetic, embryological and ultrastructural studies. Articles about the structure, the organization and the biological events relating to DNA and chromatin organization in eukaryotic cells are considered. *Caryologia* has a strong tradition in plant and animal cytosystematics and in cytotoxicology. Bioinformatics articles may be considered, but only if they have an emphasis on the relationship between the nucleus and cytoplasm and/or the structural organization of the eukaryotic cell.

Cover: figure from the article inside by Simona Ceraulo, Francesca Dumas. "Mapping CAP-A satellite DNAs by FISH in *Sapajus cay paraguay* and *S. macrocephalus* (Platyrrhini, Primates)".

Caryologia

International Journal of Cytology, Cytosystematics and Cytogenetics

Volume 75, Issue 4 - 2022

Firenze University Press

***Caryologia*. International Journal of Cytology, Cytosystematics and Cytogenetics**
Published by
Firenze University Press – University of Florence, Italy
Via Cittadella, 7 - 50144 Florence - Italy
http://www.fupress.com/caryologia

Caryologia
International Journal of Cytology, Cytosystematics and Cytogenetics

Firenze University Press
www.fupress.com/caryologia

OPEN ACCESS

Citation: Laleh Malekmohammadi, Masoud Sheidai, Farrokh Ghahremaninejad, Afshin Danehkar, Fahimeh Koohdar (2022). *Avicennia* genus molecular phylogeny and barcoding: A multiple approach. *Caryologia* 75(4): 3-13. doi: 10.36253/caryologia-1592

Received: March 02, 2022

Accepted: October 20, 2022

Published: April 28, 2023

Data Availability Statement: All relevant data are within the paper and its Supporting Information files.

Competing Interests: The Author(s) declare(s) no conflict of interest.

Avicennia genus molecular phylogeny and barcoding: A multiple approach

Laleh Malekmohammadi[1], Masoud Sheidai[1,*], Farrokh Ghahremaninejad[2], Afshin Danehkar[3], Fahimeh Koohdar[1]

[1] *Department of Plant Sciences and Biotechnology, Faculty of Life Sciences and Biotechnology, Shahid Beheshti University, Tehran, Iran*
[2] *Department of Plant Sciences, Faculty of Biological Sciences, Kharazmi University, Tehran, Iran*
[3] *Department of Environmental Sciences, Faculty of Natural Resources, University of Tehran, Karaj, Iran*
*Corresponding author. E-mail: msheidai@sbu.ac.ir

Abstract. The genus *Avicennia* contains of 8 species which show a great extent of morphological and genetic variability, which make taxonomy of the genus difficult. Molecular barcoding along with advancement in computational approaches may be proper methods to investigate and assess the efficiency of different molecular genetic regions in *Avicennia* species delineation and also produce data on species evolution and divergence. The aims of present study were to utilize multiple genetic data for the species delineation and study the phylogeny of the genus. Moreover, we developed a hypothesis on biogeography of these species with respect to barcode divergence. The results showed that both Internal transcribed spacer (ITS) and trnHG–psbA intergenic spacer (trnHG-psbA) sequences may be used in *Avicennia* species delineation. Barcode gap analysis and nucleotide difference of the studied taxa showed significant Fst for pairwise species comparison and the role of nucleotide changes in *Avicennia* speciation.

Keywords: *Avicennia*, Barcode-gap analysis, Genetic differentiation, Nucleotide difference speciation.

INTRODUCTION

DNA barcoding is applied to plant and animal species with the aim to improve organismal identification and taxonomic clarification. The main principles of DNA barcoding are standardization, minimalism, and scalability, which means selection one or a few standard loci that can be sequenced routinely and reliably in very large and diverse sample sets, and obtaining a reliable and conveniently comparable data to differentiate the species in question from one another (Hollingsworth et al. 2011).

Controversy exits on the use and choosing the plant molecular barcode markers. Different researches resulted in general agreement that several different marker combinations produce equivalent performance, and that none of the proposed barcodes is perfect in every respect (Seberg and Petersen

2009). Utilizing a multiple approach for a better species differentiation has been suggested by several authors (see for example, Fazekas et al. 2008).

In most of the studies, researchers use of a common, easily amplified and aligned region such as *rbcL*, *trn L-F* spacer regions, *mat K*, *trnHG-psbA*, *nrITS1*, *nrITS2* or the full *ITS1-5.8S-ITS2* (*nrITS*), as suggested by the CBOL Plant Working Group and BOLD (Cbol 2009; Ratnasingham and Hebert 2007).

The genus *Avicennia* is composed of eight species of mangrove trees which grow in intertidal zones in tropical and temperate regions of the world. These plant species are economically important as they are extensively used as medicinal plants. In fact, different parts of these plants have ethno medicinal applications for treatment of various diseases such as cancer, diabetes, malaria, rheumatism, asthma, small pox and ulcer (Hrudayanath et al. 2016). These species show variation and are taxonomically complex due to vast geographical distribution and introgressive hybridization (Mori et al. 2015). Therefore, the aims of present study are: 1- Assessment of different molecular markers in *Avicennia* species delineation through barcode analysis, 2- Species relationships based on molecular markers, and 3- Biogeographical distribution of these species with regard to DNA sequence divergence.

Table 1. Voucher information and GenBank accession numbers of taxa sampled for the genus *Avicennia* based on trnL-F data.

Sp	Accession number
Avicennia officinalis	KT074999.1
Avicennia officinalis	MH215695.1
Avicennia officinalis	MH215694.1
Avicennia officinalis	MH215693.1
Avicennia officinalis	MH215692.1
Avicennia officinalis	MH215691.1
Avicennia officinalis	MH215690.1
Avicennia officinalis	MH215689.1
Avicennia alba	MH215683.1
Avicennia alba	MH215682.1
Avicennia alba	MH215681.1
Avicennia alba	MH215680.1
Avicennia alba	MH215679.1
Avicennia marina	KT074998.1
Avicennia marina	MH215688.1
Avicennia marina	MH215687.1
Avicennia marina	MH215686.1
Avicennia marina	MH215685.1
Avicennia marina	MH215684.1
Avicennia marina	KM888791.1
Avicennia marina	JQ728990.1

MATERIALS AND METHODS

In this study, we used published data on *trn L-F*, *trnHG-psbA* and *ITS* sequences for a number of *Avicennia* species which are reported from different parts of the world in NCBI site (Table 1, 2 and 3).

Data analyses

DNA sequences obtained were initially aligned by MUSCLE program and cured accordingly. The total length, polymorphic sites, average of p distance, Genetic diversity within the studied species, the Fst values for the sequences and Maximum Liklihod phylogenetic tree based on these sequences as well as Tajimas'D test was performed as implemented in MEGA ver. 7 (Kumar et al. 2016). Mantel test performed with 1000 permutations, for showing significant association between nucleotide difference of the studied species and population to the geographical longitude and altitude. The range of Bayesian probability value obtained for species with Mr. Bayes analysis (Ronquist et al. 2012). Barcoding analysis and windows sliding of nucleotides were performed by BarcodingR, and spider package, while Skyline plot and mismatch distribution of nucleotides were determined by ape, and pegas package in R. Monophyletic phylogenetic tree and its statistical test of Rosenberg (2007), as implemented in R package. We used RASP (Reconstruction of ancestral states in phylogeny) program ver. 4.2 in the RASP-Bayesian analyzed phylogenetic tree.

RESULTS

Species delimitation and barcode gap analysis

We used published data on *trn L-F*, *trnHG-psbA* and *ITS* sequences for a number of *Avicennia* species which are reported from different parts of the world (Table 1). In the first step, we evaluated the efficiency of these molecular markers in species delineation, and finally, we extracted different evolutionary information from the one with the highest degree of efficiency.

Details of the studied sequences with regard to *Avicennia* species differentiation and species phylogeny are presented below. Available data on *trn L-F* sequence is very limited and is available for only 21 samples of *Avicennia officinalis*, *A. marina*, and *A. alba*. These sequences had a total length 296 bp, with only 14 polymorphic sites, and average p distacne = 0.006. The ML phyloge-

Table2 . Voucher information and GenBank accession numbers of taxa sampled for the genus *Avicennia* based on trnHG-psbA data.

Sp	Accession number
Avicennia officinalis	KT161361.1
Avicennia officinalis	MN117565.1
Avicennia officinalis	MN117564.1
Avicennia officinalis	MN117563.1
Avicennia officinalis	MN117562.1
Avicennia officinalis	MN117561.1
Avicennia officinalis	MN117560.1
Avicennia officinalis	MN117559.1
Avicennia alba	MN117553.1
Avicennia alba	MN117552.1
Avicennia alba	MN117551.1
Avicennia alba	MN117550.1
Avicennia alba	MN117549.1
Avicennia alba	JX448690.1
Avicennia marina	KT161360.1
Avicennia marina	MN117558.1
Avicennia marina	MN117557.1
Avicennia marina	MN117556.1
Avicennia marina	MN117555.1
Avicennia marina	MN117554.1
Avicennia marina	JX448688.1
Avicennia germinans	KC420634.1
Avicennia germinans	KJ426610.1
Avicennia germinans	HG963703.1
Avicennia bicolor	KC420633.1
Avicennia rumphiana	JX448689.1

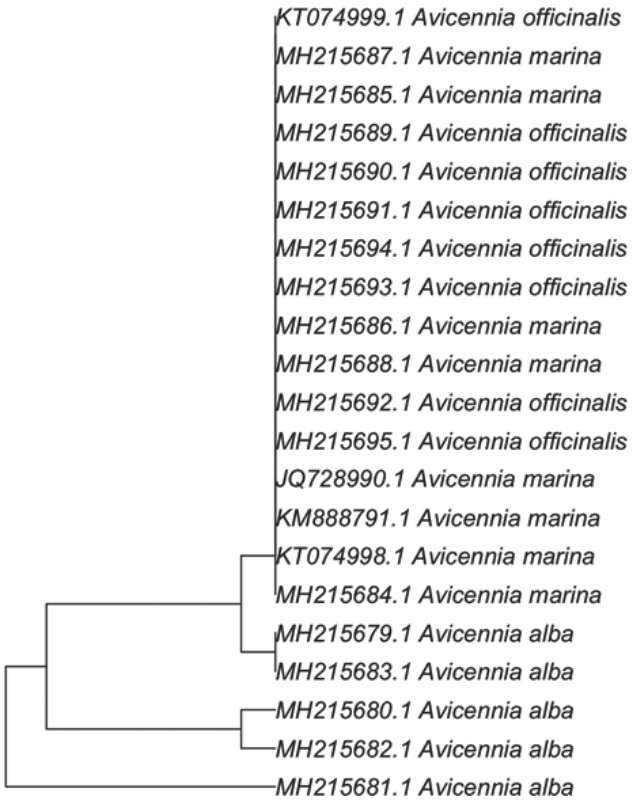

Figure 1. ML Phylogenetic tree of *Avicennia* species based on ITS sequences.

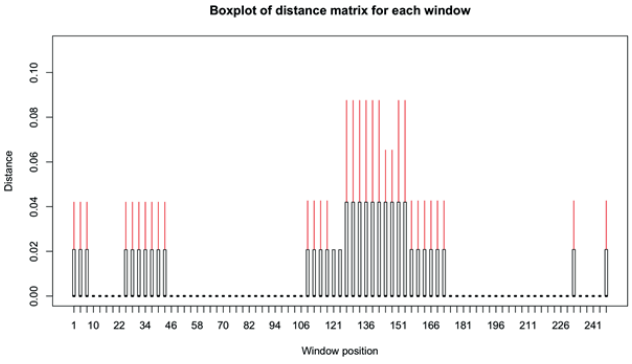

Figure 2. Mini-barcode sliding windows of *trnL-F* sequence in *Avicennia* species, showing genetic distance of *Avicennia alba* with the other studied taxa.

netic tree based on these sequences (Fig. 1), revealed that only the samples of *A. alba* can be differentiated from the other two species.

Analyses performed by Bayesian method of species barcoding as implemented in Barcoding package in R program indicated that only 25% of the studied samples have success in species identification, and the others may not be differentiated. In this analysis also the higher degree of Bayesian probability was obtained for *A. alba* (0.50-0.97). The probability value obtained for the other species was about 0.06 only. Sliding Windows of the mini-barcodes within *trn L-F* barcode sequence 9 (Fig. 2), also showed genetic distance in mini-barcodes between *A. alba* and the other species studied.

TrnHG-psbA sequence efficiency in species delineation and barcoding

TrnHG- psbA sequence data is available for 26 sample in *Avicennia* species (Table 2) namely, *A. officinalis*, *A. marina*, *A. bicolor*, *A. germinans*, *A. alba*, and *A. rumphiana*. These samples have also been reported from different parts of the world.

Preliminary analysis of *trnHG- psbA* sequences indicated that the total length of the studied sequences is 167 bp, with 52 polymorphic sites, and average p distance = 0.09.

Table 3. Voucher information and GenBank accession numbers of taxa sampled for the genus *Avicennia* based on ITS data.

Sp	Accession number
Avicennia alba	EF540977.1
Avicennia alba	AF365980.1
Avicennia alba	MH243937.1
Avicennia alba	MH243936.1
Avicennia alba	MH243935.1
Avicennia alba	MH243934.1
Avicennia alba	MG880036.1
Avicennia alba	MG880035.1
Avicennia alba	MG880034.1
Avicennia alba	MG880033.1
Avicennia alba	MG880032.1
Avicennia alba	MG880031.1
Avicennia alba	MG880030.1
Avicennia alba	MG880029.1
Avicennia alba	MG880028.1
Avicennia alba	EU528876.1
Avicennia alba	KX641594.1
Avicennia alba	KJ784551.1
Avicennia alba	KF848261.1
Avicennia bicolor	EF540988.1
Avicennia bicolor	EF540988.1
Avicennia bicolor	EF540987.1
Avicennia bicolor	EU352151.1
Avicennia bicolor	EU352150.1
Avicennia bicolor	EU352149.1
Avicennia bicolor	AF365977.1
Avicennia bicolor	EU528877.1
Avicennia germinans	EF540990.1
Avicennia germinans	EF540985.1
Avicennia germinans	EF540984.1
Avicennia germinans	EF540983.1
Avicennia germinans	EF540982.1
Avicennia germinans	EF540981.1
Avicennia germinans	EF540980.1
Avicennia germinans	EU352146.1
Avicennia germinans	EU352147.1
Avicennia germinans	KX641596.1
Avicennia germinans	MG880047.1
Avicennia germinans	MG880046.1
Avicennia germinans	MG880045.1
Avicennia germinans	MG880041.1
Avicennia germinans	MG880040.1
Avicennia germinans	MG880039.1
Avicennia germinans	MG880038.1
Avicennia germinans	MG880037.1
Avicennia germinans	DQ469846.1
Avicennia germinans	DQ469845.1
Avicennia germinans	DQ469860.1
Avicennia germinans	DQ469859.1
Avicennia germinans	DQ469858.1
Avicennia germinans	DQ469857.1
Avicennia germinans	DQ469856.1
Avicennia germinans	DQ469855.1
Avicennia germinans	DQ469854.1
Avicennia germinans	DQ469853.1
Avicennia germinans	DQ469852.1
Avicennia integra	KX641598.1
Avicennia officinalis	MH243949.1
Avicennia officinalis	MH243948.1
Avicennia officinalis	MH243947.1
Avicennia officinalis	MH243946.1
Avicennia officinalis	MH243945.1
Avicennia officinalis	MH243944.1
Avicennia officinalis	MH243943.1
Avicennia officinalis	MG880054.1
Avicennia officinalis	MG880053.1
Avicennia officinalis	MG880052.1
Avicennia officinalis	MG880051.1
Avicennia officinalis	MG880050.1
Avicennia officinalis	KX641597.1
Avicennia officinalis	KJ784553.1
Avicennia officinalis	KF848263.1
Avicennia rumphiana	KX641595.1
Avicennia schaueriana	EF540986.1
Avicennia schaueriana	DQ469862.1
Avicennia schaueriana	AB861412.1
Avicennia schaueriana	AB861385.1
Avicennia schaueriana	AB861382.1
Avicennia schaueriana	AB861365.1
Avicennia schaueriana	AB861357.1
Avicennia schaueriana	AB861354.1
Avicennia schaueriana	AB861345.1
Avicennia schaueriana	AB861327.1
Avicennia schaueriana	AB861326.1
Avicennia schaueriana	AB861325.1
Avicennia schaueriana	AB861307.1
Avicennia schaueriana	AB861306.1
Avicennia schaueriana	AB861305.1
Avicennia schaueriana	AB861287.1
Avicennia schaueriana	AB861286.1
Avicennia schaueriana	AB861285.1
Avicennia schaueriana	AB861284.1
Avicennia schaueriana	AB861280.1
Avicennia schaueriana	AB861270.1
Avicennia schaueriana	AB861266.1
Avicennia schaueriana	AB861265.1
Avicennia schaueriana	AB861263.1
Avicennia schaueriana	AB861257.1
Avicennia schaueriana	AB861251.1
Avicennia schaueriana	AB861246.1

Sp	Accession number
Avicennia schaueriana	AB861245.1
Avicennia schaueriana	AB861244.1
Avicennia schaueriana	AB861240.1
Avicennia schaueriana	AB861231.1
Avicennia schaueriana	AB861226.1
Avicennia schaueriana	AB861225.1
Avicennia schaueriana	AB861224.1
Avicennia schaueriana	AB861222.1
Avicennia schaueriana	AB861220.1
Avicennia marina	MF063712.1
Avicennia marina	MF063711.1
Avicennia marina	MF063710.1
Avicennia marina	MF063709.1
Avicennia marina	MF063708.1
Avicennia marina	EF540978.1
Avicennia marina	AF477771.1
Avicennia marina	AF477770.1
Avicennia marina	MN883387.1
Avicennia marina	MN883386.1
Avicennia marina	MN883385.1
Avicennia marina	MN883384.1
Avicennia marina	MH243942.1
Avicennia marina	MH243941.1
Avicennia marina	MH243940.1
Avicennia marina	MH243939.1
Avicennia marina	MH243938.1
Avicennia marina	MG880049.1
Avicennia marina	MG880048.1
Avicennia marina	MK027295.1
Avicennia marina	EU528879.1
Avicennia marina	KM652500.1
Avicennia marina	KF848262.1
Avicennia marina	DQ469861.1
Avicennia marina subsp. *marina*	KX641593.1
Avicennia marina subsp. *eucalyptifolia*	KX641592.
Avicennia marina subsp. *australasica*	KX641591.
Avicennia marina subsp. *australasica*	AF365978.1

Bayesian method analysis of barcoding for *trnHG-psbA* sequences, reveals that about 53% of the samples are identified with success. Bayesian probability value obtained for *A. officinalis* samples, ranged from 0.24 to 0.96. The same value for *A. germinans*, ranged from 0.5-0.95, for *A. marina* and *A. alba* the value ranged from was 0.2 to 0.96.

Monophyletic phylogenetic tree and its statistical test of Rosenberg (2007), as implemented in R package is presented in Fig. 3. The red circles on the nodes of this phylogenetic tree indicates that monophyly has passed the significant test at p = 0.05. Therefore, we observe the

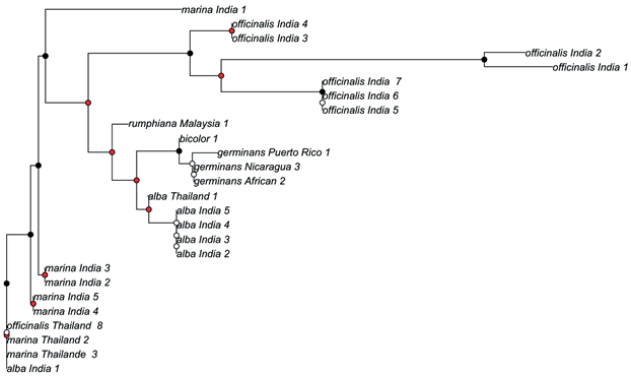

Figure 3. Monophyly analysis of *Avicennia* species based on *trn-HG-psbA* sequences. [a]The red circles on the nodes indicate that the clade is significant at p = 0.05.

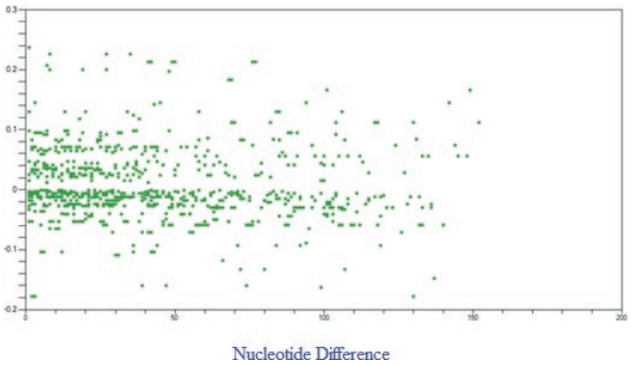

Figure 4. *trnHG-psbA* nucleotide difference among *Avicennia* species.

presence of significant monophyletic groups for some of the sample in *A. officinalis*, *A. alba*, *A. germinans*, and *A. marina*. We have also some cases of admixture between the studied species which makes that clade non-monophyletic.

TrnHG- psbA nucleotide difference in the studied *Avicennia* species is presented in Fig. 4. This plot shows a great difference of the *trnHG- psbA* nucleotides, which is a significant difference according to chi-square and Snn test of Hudson (Hudson, 2000).

The Fst values for *trnHG- psbA* sequences in the studied species ranged from 0.40-0.65. Inter-specific genetic differentiation estimates obtained for the *trnHG- psbA* nucleotide produced chi-square = 63.321, with P-value = 0.0012. Similarly, Hudson Snn after 1000 permutations produced Snn = 0.86, P<0.01. These values indicate significant difference among the studied samples.

Pair-wise mismatch plot of these sequences (Fig. 5), revealed that, almost all the studied species-pairs differ significantly in their *trnHG- psbA* nucleotides.

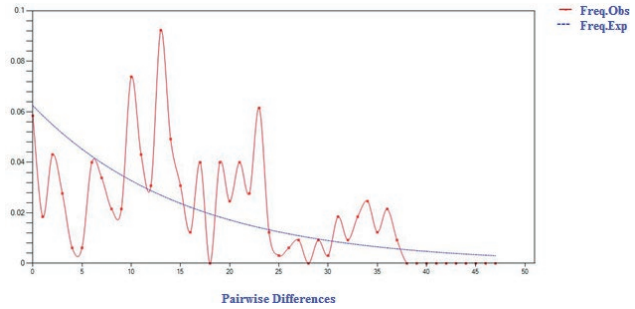

Figure 5. Pair-wise mismatch plot of *trnHG-psbA* sequences in *Avicennia* species.

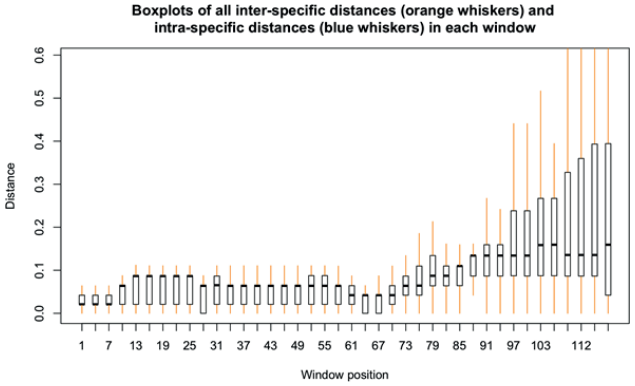

Figure 6. Window sliding of *trnHG-psbA* sequences in *Avicennia* species, showing that these species differ in mini-barcodes.

Mini-barcode analysis by windows sliding (Fig. 6), also showed that *trnHG- psbA* sequences contain mini-barcodes which differs among *Avicennia* species. Therefore, *trnHG- psbA* sequences could be utilized for *Avicennia*. species delineation.

Mini-barcode analysis by windows sliding (Fig. 7), also showed that *trnHG- psbA* sequences contain mini-barcodes which differs among *Avicennia* species. Therefore, *trnHG- psbA* sequences could be utilized for *Avicennia* species delineation.

ITS sequences species delineation and barcoding

ITS sequences (Table3) obtained had total length 494 bp, with polymorphic sites = 88, and average p dist = 0.038. Bayesian method analysis revealed that about 42% of the samples are identified correctly. Bayesian probability value obtained for *Avicennia alba* ranged from 0.12 to 0.99, for *A. bicolor* ranged from 0.20 to 0.99, and for *A. germinans*, ranged from 0.16 to 1.00. Almost the same ranges were obtained for other species. ML phylogenetic tree of 135 species samples (Fig. 8), pro-

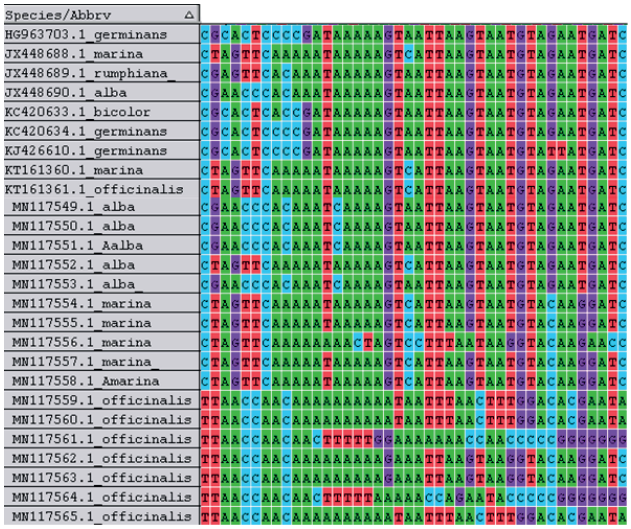

Figure 7. *TrnHG-psbA* sequences in *Avicennia* species, showing mini-barcodes which differentiate the studied taxa.

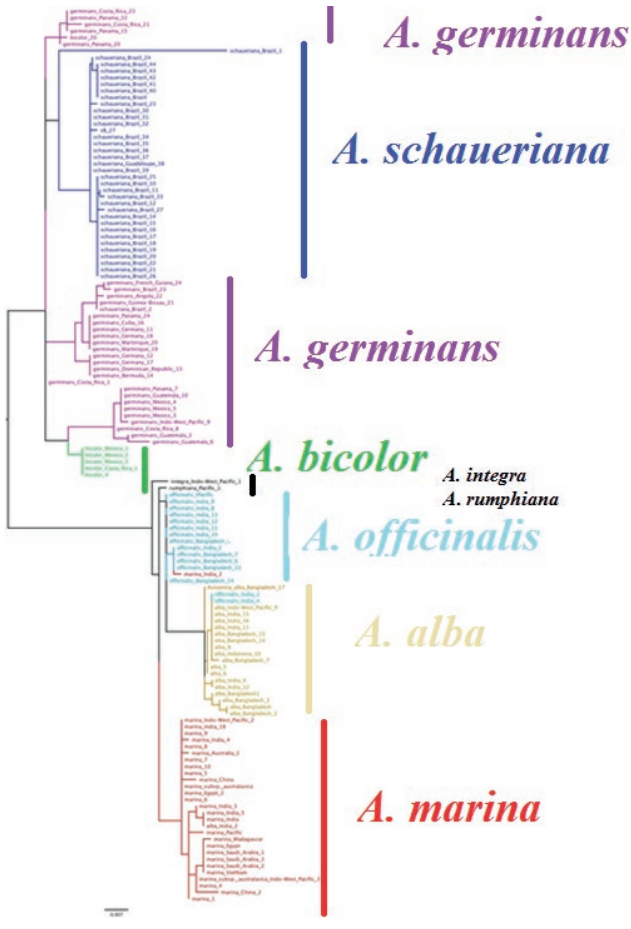

Figure 8. ML Phylogenetic tree of *Avicennia* species based on ITS sequences.

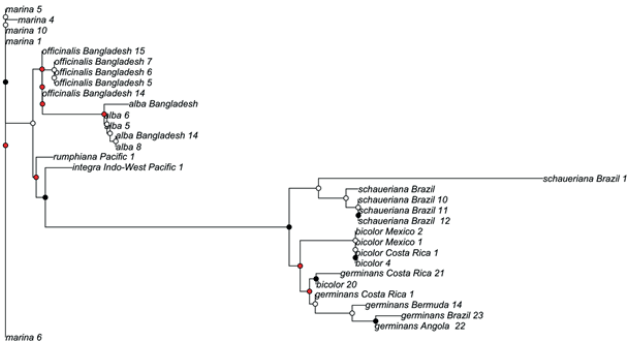

Figure 9. Monophyly test of the studied *Avicennia* species based on ITS sequences. [a]The red circles on the. nodes indicate a significant monophyletic clade.

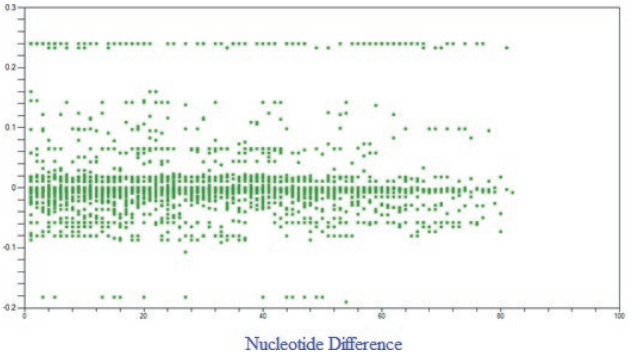

Figure 10. The nucleotide difference in ITS sequences among *Avicennia* species.

duced almost distinct separate clades for the studied species, but some degree of admixtures was observed too. For the test of monophyly, we kept randomly some of the replicates of each species. The result of monophyly and its statistical test of Rosenberg is presented in Fig. 9. The red circles on some of the tree nodes indicates the monophyletic clade which is significant at p = 0.05.

We also obtained monophyletic clades for some of the sample in *A. officinalis*, *A. alba*, *A. germinans*, *A. bicolor* and *A. marina*. We have also some cases of admixture between the studied species which makes some of the clade non-monophyletic.

The nucleotide difference in ITS sequences of the studied *Avicennia* species is presented in Fig. 10. The plot shows a great difference, which is a significant difference according to chi-square and Snn test of Hudson.

The Fst values for ITS sequences ranged from 0.43-0.99. The inter-specific genetic differentiation estimates obtained for the ITS nucleotide produced chi-square = 90.26, with P-value = 0.001. Similarly, Hudson Snn after 1000 permutations produced Snn = 0.82, P<0.001. These

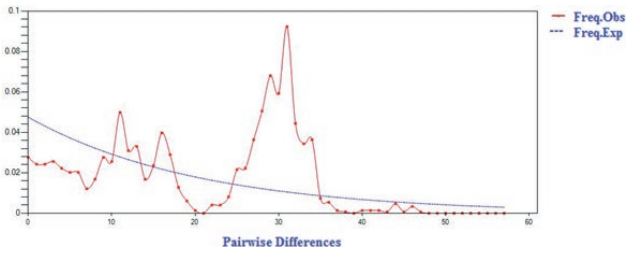

Figure 11. Mismatch plot of ITS sequences in *Avicennia* species.

1	alba_Bangladesh	C	T	T	G	C	C	C	C	G	C	G	G	T	T	A	G
2	alba_India	C	T	T	G	C	C	C	C	G	C	G	G	T	T	A	G
3	alba_India_1	C	T	T	G	C	C	C	C	G	C	G	G	T	T	A	G
4	alba_Indonesia	C	T	T	G	C	C	C	C	G	C	G	G	T	T	A	G
5	alba_Indo-West_Pacific	C	T	T	G	C	C	C	C	G	C	G	G	T	T	A	G
6	bicolor	T	G	C	T	T	A	T	T	C	A	A	A	C	C	C	A
7	bicolor_Costa_Rica	T	G	C	T	T	A	T	T	C	A	A	A	C	C	C	A
8	bicolor_Mexico	T	G	C	T	T	A	T	T	C	A	A	A	C	C	C	A
9	bicolor_Mexico_1	T	G	C	T	T	A	T	T	C	A	A	A	C	C	C	A

Figure 12. ITS Barcode sequences differentiating *Avicennia alba* and *A. bicolor*.

values indicate significant difference among the studied samples. Mismatch plot of ITS sequences (Fig. 11), revealed that, almost all the studied species-pairs differ significantly in their *trnHG- psbA* nucleotides. Moreover, Tajimas'D obtained was 0.32, which indicates the presence of a positive selection on ITS sequences and therefore ITS changes may be in some way related to speciation events in the genus *Avicennia*.

Windows sliding of ITS sequences also revealed the occurrence of mini-barcodes in these sequences which also differed greatly among the studied species. For example, barcode sequences in some of the species are provided in Figs 12 and 13.

Genetic diversity within the studied species ranged from 0.03 in *A. alba* to 0.12 in *A. germinans*, while inter-specific genetic distance, 0.04 between *A. alba* and *A. officinalis*, and 0.08 between *A. marina* and *A. integra*, to 0.43, between *A. germinans* and *A. alba*.

DNA barcoding gap analysis of ITS sequences is presented in Fig. 14. Both intra- and inter-specific sequence gaps, supports the use of ITS sequences for delineation of *Avicennia* species.

Mantel test performed with 1000 permutations, showed no significant association between nucleotide difference of the studied species and population to the geographical longitude and altitude (Correlation r = 0.044, p = 0.1456).

Details of *Avicennia* species diversification based on ITS sequences and in relation with geographical distri-

1	alba_Bangladesh	C	T	G	C	C	C	C	G	C	C	C	G	G	T	T	A	G
2	alba_India_2	C	T	G	C	C	C	C	G	C	C	C	G	G	T	T	A	G
3	alba_India_4	C	T	G	C	C	C	C	G	C	C	C	G	G	T	T	A	G
4	alba_Indonesia_10	C	T	G	C	C	C	C	G	C	C	C	G	G	T	T	A	G
5	alba_Indo-West_Pacific_9	C	T	G	C	C	C	C	G	C	C	C	G	G	T	T	A	G
6	germinans_Angola__22	T	C	T	T	A	T	T	C	T	T	A	A	A	C	C	C	A
7	germinans_Bermuda_14	T	C	T	T	A	T	T	C	T	T	A	A	A	C	C	C	A
8	germinans_Brazil_23	T	C	T	T	A	T	T	C	T	T	A	A	A	C	C	C	A
9	germinans_Costa_Rica_1	T	C	T	T	A	T	T	C	T	T	A	A	A	C	C	C	A
10	germinans_Costa_Rica_8	T	C	T	T	A	T	T	C	T	T	A	A	A	C	C	C	A
11	germinans_Cuba_16	T	C	T	T	A	T	T	C	T	T	A	A	A	C	C	C	A
12	germinans_Dominican_Republic_13	T	C	T	T	A	T	T	C	T	T	A	A	A	C	C	C	A
13	germinans_French_Guiana_24	T	C	T	T	A	T	T	C	T	T	A	A	A	C	C	C	A
14	germinans_Germany_11	T	C	T	T	A	T	T	C	T	T	A	A	A	C	C	C	A
15	germinans_Germany_12	T	C	T	T	A	T	T	C	T	T	A	A	A	C	C	C	A
16	germinans_Guatemala_10	T	C	T	T	A	T	T	C	T	T	A	A	A	C	C	C	A
17	germinans_Guatemala_6	T	C	T	T	A	T	T	C	T	T	A	A	A	C	C	C	A
18	germinans_Guinea-Bissau_21	T	C	T	T	A	T	T	C	T	T	A	A	A	C	C	C	A
19	germinans_Indo-West_Pacific_9	T	C	T	T	A	T	T	C	T	T	A	A	A	C	C	C	A
20	germinans_Mexico_3	T	C	T	T	A	T	T	C	T	T	A	A	A	C	C	C	A
21	germinans_Mexico_4	T	C	T	T	A	T	T	C	T	T	A	A	A	C	C	C	A
22	germinans_Panama_15	T	C	T	T	A	T	T	C	T	T	A	A	A	C	C	C	A
23	germinans_Panama_7	T	C	T	T	A	T	T	C	T	T	A	A	A	C	C	C	A

Figure 13. Barcode ITS sequences differentiating *Avicennia alba* and *A. germinans*.

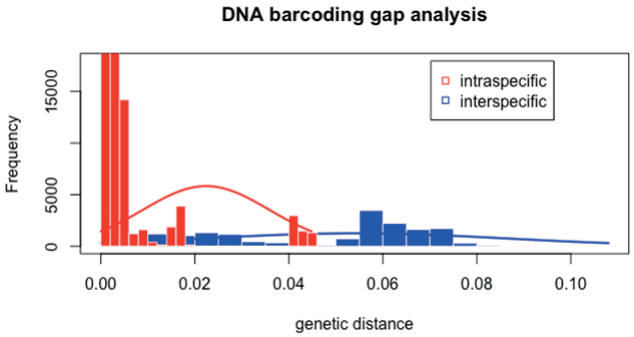

Figure 14. Barcode gap analysis of ITS sequences revealing both intra- as well as inter-specific sequence difference in *Avicennia* species studied.

bution of these species is presented in the RASP-Bayesian analyzed phylogenetic tree (Fig. 15).

Two main clades are present in this phylogenetic tree. The species of *A. alba*, *A. officinalis*, *A. marina*, *A. rumphiana*, and *A. integra*, comprised the first major clade, while, *A. schueriana*, *A. germinnas*, and *A. bicolor* formed the second major clade.

Looking at details of each major clade points out some interesting results. For example, most of *A. marina* samples were grouped together due to sequence similarity. Though Mantel test revealed no association between nucleotide difference and geographical longitude and latitude of the studied taxa, some interesting relationships between *A. marina* geographical populations can be seen

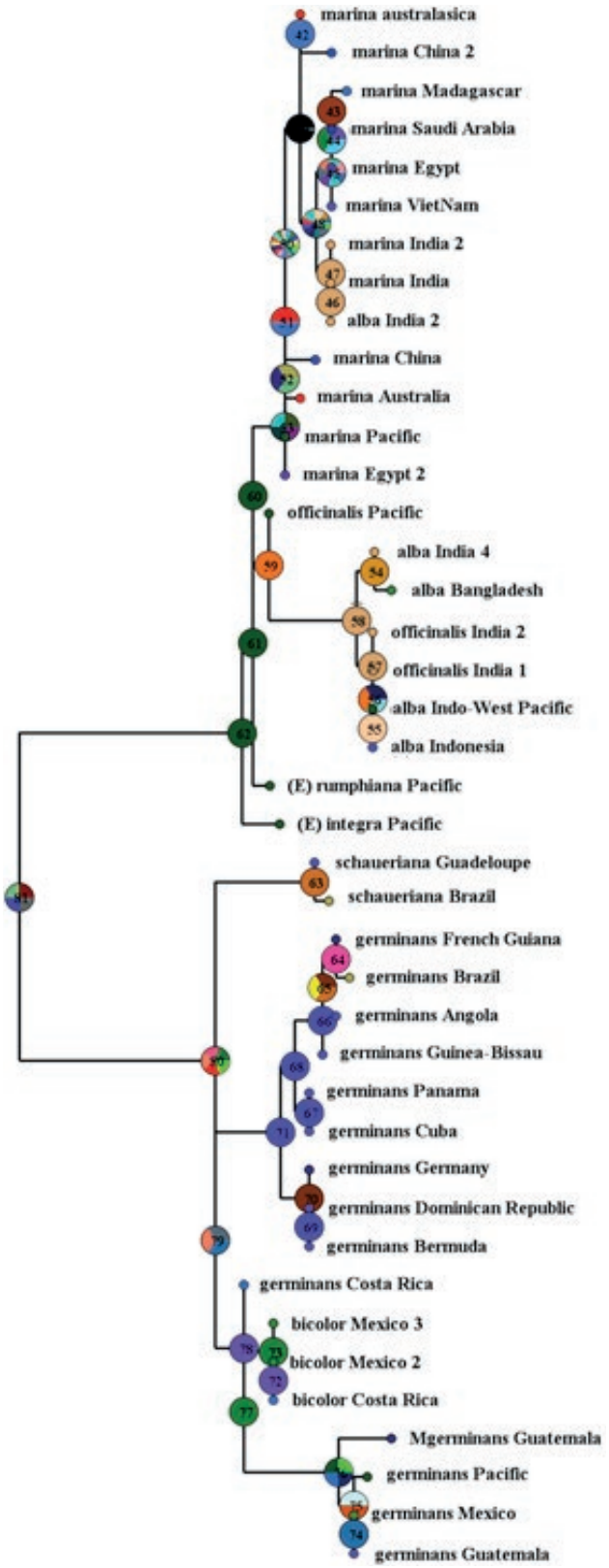

Figure 15. RASP Bayesian tree of ITS data, placing the species studied in two major clades.

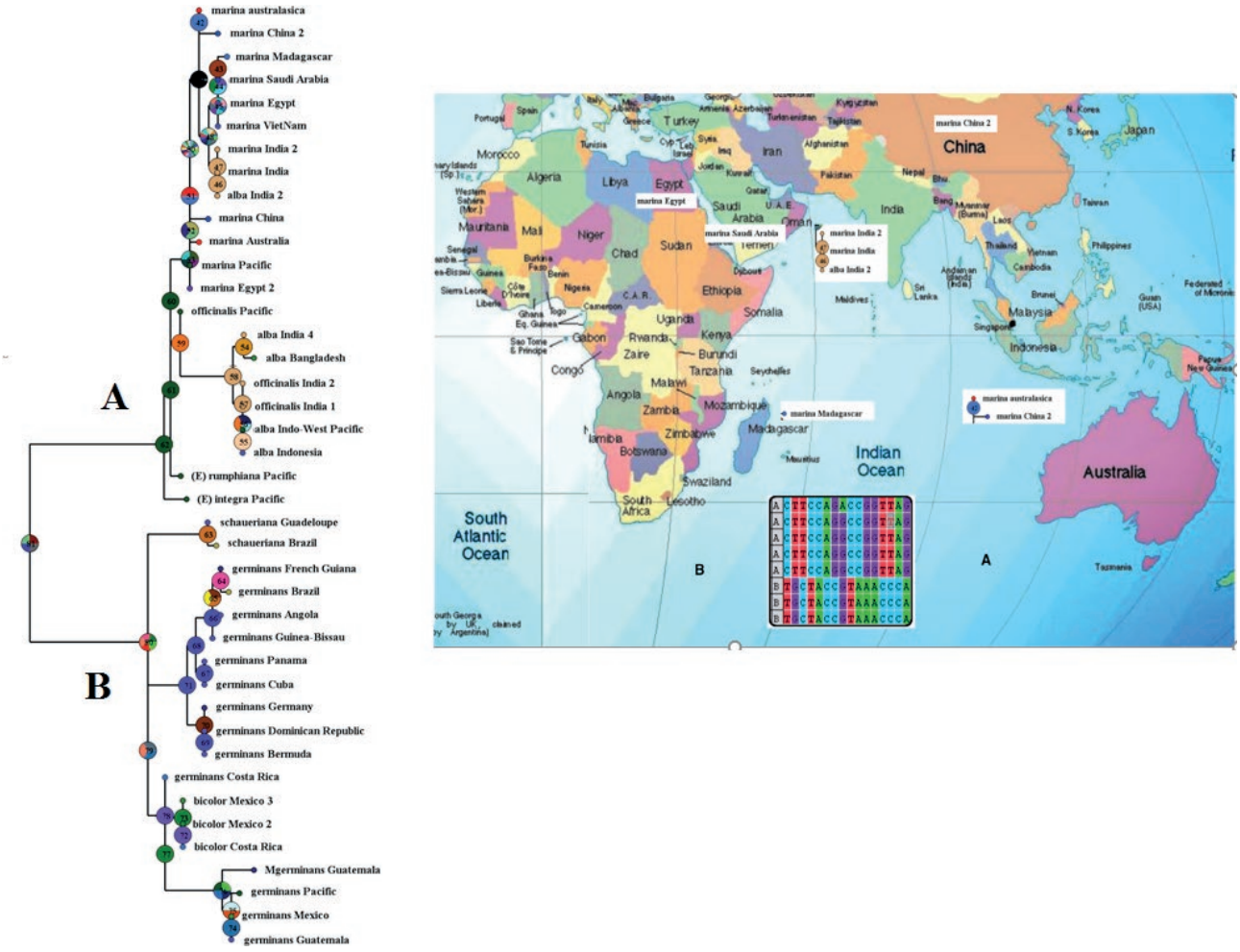

Figure 16. Biogeographical distribution of *Avicennia* marina populations based on ITS sequences.

when we plot these studied specimens on the world map. For example, *A. marina* specimens studied from Saudi-Arabia and Egypt show sequence affinity and are placed close to each other in the phylogenetic tree. Moreover, the specimens studied from Madagascar, is placed close to the above said specimens. Madagascar is some-what close to and connected by Indian ocean to Saudi-Arabia and Egypt.

Similarly, *Avicennia marina* samples from China and Australia, also show sequence similarity and form a separate sub-clade from the other specimens studied. The studied specimens from India stand in a separate sub-clade, far from the sub-clade of China-Australia.

If we consider all the samples studied, biogeographical distribution reveals that the species of *A. marina*, *A. alba*, and *A. officinalis* are mostly found in Asia and Australia region (Denoted A. in Fig. 16), while *A. terminals*, *A. bicolor*, and *A. schauriena*, are distributed in South America (Denoted B in Fig. 16). This may indicate speciation events in *Avicennia* in two different regions of the world. We have also provided barcodes for geographical regions A and B, which shows nucleotide changes possibly associated / or the outcome of speciation in these two areas (Fig 16).

DISCUSSION

The present study showed that based on ITS sequence analysis, *A. alba* and *A. officinalis* show close affinity and comprise sister-clades. *A. marina* joins these two with some distance.

A. germinans samples form three separate clades, which indicates a potential presence of infra-specific taxon rank within this species. This is in accordance with earlier consideration which propose three different vari-

eties for this species, which were later on were merged into a single species with no variety.

A. bicolor showed close relationship to one of the clades of *A. germinans*. Sample of *A. schaueriana* comprise a single distinct clade based on ITS data.

However, the species relationships were partly distorted by trnHG- psbA sequence data. The three species of *A. officinalis*, *A. marina*, and *A. alba*, were placed inter-mixed to some degree. Close affinity bet ween *A. germinans* and *A. bicolor* are similar to ITS results. The close affinity between *A. officinalis*, *A. marina*, was also indicated by Li et al. (2016). These authors showed closer relationship between *A. rumphiana* and *A. alba,* which in agreement with our trnHG- psbA tree, and to some extent also with ITS-baes phylogenetic tree.

According to Li et al. (2016), even though the first fossil record of *Avicennia* in the IWP region dates back to the late Eocene of southwest Australia, *Avicennia* speciation was active during the Miocene. Similarly, they suggest that distribution of ancestral *Avicennia* was likely to have been similar to its present location, extending from Japan to Borneo and from the Marshall Islands to the Red Sea. Therefore, the materials studied in this project, may have migrated from Japan, china or India, through red sea and reached to the countries like Iran, Egypt, and Sauidi-Arabia. In these migration path, *Avicennia* speciation may have resulted in formation of *A. marina*, *A. officinalis* and *A. alba*, as well as *A. integra*, and *A. rumpiana*.

If we consider our ITS-based phylogenetic tree, we observe the species of the region B, viz. *A. bicolor*, *A. germinans*, *A. schaueriana*. are related through *A. rumpiana* and *A. integra*, to the species of region A. Therefore, we may suggest a preliminary hypothesis that through migration of either or both of *A. rumpiana* and *A. integra*, new speciation events resulted in the formation of other species found in South America countries. We believe that more works are required to second this raw and immature hypothesis.

Mangroves in general, have a broad distributional patterns, ability in long-distance dispersal and can adapt to rigorous environmental constraints associated with regular seawater inundation. However, the present day distributions of individual taxa show several instances of finite dispersal limitations, especially across open water. These dis-continuities, in the absence of current dispersal barriers, may be explained by persistent past barriers (Duke et al. 2002).

In present study we report genetic diversity both with the studied *Avicennia* species and between these taxa. A high levels of genetic diversity were also reported among the central populations of many mangrove species including *Avicennia* in the Indo-West Pacific (IWP) (Mantiquilla et al. 2021). Mori et al. (2015), suggest that *A. bicolor, A. germinans* and *A. schaueriana* are three evolutionary lineages that present historical and ongoing hybridization. They also consider gene flow between *A. germinans,* and *A. schaueriana* by propagules rather than pollen in *A. schaueriana*.

We also reported distinct inter-specific genetic distance and significant Fst value among different species both within those species distributed in the A geographical region (Australia, India, China), and those distributed in the B region (South America in general). In a similar investigation performed presence of a strong genetic structuring resulting in divergence among mangrove populations of Indian Ocean and South China Sea, as well as between South China Sea and Southwestern Pacific was reported (Mantiquilla et al. 2021).

CONCLUSION

With regard to *Avicennia* species taxonomy and the presence of high level of genetic diversity within these species, we provided distinct molecular barcodes for species delineation. We suggest it is suitable to utilize a combination of ITS nuclear sequences along with *trnHG- psbA* spacer region of chloroplast genome for taxonomic purpose.

LIST OF ABBREVIATIONS

ITS: Internal transcribed spacer
ML: Maximum Liklihod
RASP: Reconstruction of ancestral states in phylogeny
MEGA: Molecular Evolutionary Genetics Analysis

ACKNOWLEDGEMENTS

We thank the Iran National Science Foundation (INSF), for partial financial supportof this project (No.4002299).

AUTHOR CONTRIBUTION STATEMENT

Masood Sheidai: conceptualization of the project and corresponding author, Farrokh Ghahremaninejad: conceptualization of the project and data collection, Afshin Danehkar: conceptualization of the project and plant collection, Fahimeh Koohdar: conceptualization of the project and lab work, Laleh malekmohammadi: data collection and lab work and data analysis.

REFERENCES

CBOL Plant Working Group (2009) A DNA barcode for land plants. Proc Natl Acad Sci 106, 12794±12797

Fazekas AJ, Burgess KS, Kesanakurti PR, Graham SW, Newmaster SG, Husband BC, Percy DM, Hajibabaei M, BarrettScH (2008) Multiple multilocus DNA barcodes from the plastid genome discriminate plant species equally well. PLoS ONE 3: e2802.

Hollingsworth PM, Graham SW, Little DP (2011) Choosing and Using a Plant DNA Barcode. PLoS ONE 6(5): e19254

Hudson RR (2000) A new statistic for detecting genetic differentiation. Genetics 155: 2011-2014

Hrudayanath T, Dibyajyoti S, Swagat KD (2016) The genus *Avicennia*, a pioneer group of dominant mangrove plant species with potential medicinal values. Front Life Sci 9: 267-291.

Mantiquilla JA, Shiao MSh, Shih HCh, Chen WH, Chiang YCh (2021) A review on the genetic structure of ecologically and economically important mangrove species in the Indo-West Pacific. Ecol Genet Genom 18: 100078.

Kumar S, Stecher G, Tamura K (2016) MEGA7: Molecular Evolutionary Genetics Analysis Version 70 for Bigger Datasets. Mol Biol Evol 33(7):1870-1874.

Li X Duke, NC Yang, Y Huang L, Zhu Y, Zhang Z, Zhou R, Zhong C, Huang NY, Shi S (2016) Re-Evaluation of Phylogenetic Relationships among Species of the Mangrove Genus *Avicennia* from Indo-West Pacific Based on Multilocus Analyses. PLoS ONE 11(10): e0164453

Mori GM, Zucchi MI, Sampaio I Souza, AP (2015) Species distribution and introgressive hybridization of two *Avicennia* species from the Western Hemisphere unveiled by phylogeographic patterns. BMC Evol Biol 15: 61

Duke NC, Lo EYY, Sun M (2002) Global distribution and genetic discontinuities of mangroves – emerging patterns in the evolution of *Rhizophora.* Trees 16: 65–79

Ratnasingham S, Hebert PD BOLD (2007) The Barcode of Life Data System. Mol Ecol Notes 7: 355±364 https://doiorg/101111/j1471-8286200701678x PMID: 18784790

Ronquist F, Teslenko M, Mark PVD, Ayres DL, Darling A, Höhna S, Larget B, Liu L, Suchard MA, Huelsenbeck, JP (2012) MrBayes 32: Efficient Bayesian Phylogenetic Inference and Model Choice Across a Large Model Space Syst Biol61(3): 539–542.

Rosenberg N A (2007) Statistical tests for taxonomic distinctiveness from observations of monophyly. Evolution 61 (2): 317-323

Seberg O, Petersen G (2009) How many loci does it take to DNA barcode acrocus?. PLoS ONE 4: e4598

Caryologia
International Journal of Cytology, Cytosystematics and Cytogenetics

Firenze University Press
www.fupress.com/caryologia

OPEN ACCESS

Citation: Basoz Sadiq Muhealdin, Sahar Hussein Hamarashid, Fairuz Ibrahim Ali, Nakhshin Omer Abdulla, Syamand Ahmad Qadir (2022). Studying some morphological responses of stevia (*Stevia rebaudiana* Bertoni) to some elicitors under water deficiency. *Caryologia* 75(4): 15-24. doi: 10.36253/caryologia-1922

Received: November 08, 2022

Accepted: December 14, 2022

Published: April 28, 2023

Data Availability Statement: All relevant data are within the paper and its Supporting Information files.

Competing Interests: The Author(s) declare(s) no conflict of interest.

Studying some morphological responses of stevia (*Stevia rebaudiana* Bertoni) to some elicitors under water deficiency

Basoz Sadiq Muhealdin[1], Sahar Hussein Hamarashid[1,*], Fairuz Ibrahim Ali[1], Nakhshin Omer Abdulla[1], Syamand Ahmad Qadir[2]

[1] *Agricultural Project Management Department, Technical College of Applied Science Halabja, Sulaimani Polytechnic University, Iraq*
[2] *Medical laboratory techniques department/Halabja Technical Institute, Research center/ Sulaimani Polytechnic University, Sulaymaniyah, Iraq*
*Corresponding author. E-mail: sahar.rashid@spu.edu.iq

Abstract. This research evaluated the effect of foliar spraying of different elicitors on modulating the effect of water stress on the stevia. The experimental design was the split-plot based on a randomized complete block design with three repetitions. Experimental treatments included different irrigation regimes (90% FC, 65% FC, and 40% FC) and foliar application of different elicitors (control, chitosan, salicylic acid, and melatonin). In this study, the content of chlorophyll A and b was reduced by intensifying the water deficit stress. Also, the highest content of the two pigments was allocated to the treatment of melatonin application. In the present study, melatonin foliar application under 90% FC irrigation conditions had the highest plant height, leaf area index, biomass, and carotenoid content, Moreover, the highest content of proline, phenol, DPPH, rebaudioside A, and steviosid was assigned to melatonin foliar application treatment under 40% FC irrigation conditions. Results revealed, although water stress reduced plant height, leaf area index, and plant biomass, the application of melatonin and salicylic acid under different irrigation conditions moderated the effect of water stress on these traits. Application of melatonin and salicylic acid under water deficit stress conditions also increased the content of proline, phenol, DPPH, rebaudioside, and steviosid.

Keywords: Drought stress, Enzyme activities, Foliar spraying, Pigment.

INTRODUCTION

About 230-220 species have been recorded for stevia, one of the most economically important species is S. rebaudian (Al Hassan *et al* 2017). The distinguishing feature of *S. rebaudiana (stevia*) from other species is the relatively high production of non-toxic and non-nutritive diterpenoid anticorn glycosides in the leaves of this species, the sweetness of which is 300 times of sucrose (Aghighi Shaverdi *et al.,* 2018). Consumers' desire for a natural zero-calorie sweetener has made the cultivation, production, and extraction of glycosides in this plant attractive (Aghighi Shaverdi *et al.,* 2018). Among the glycosides in

stevia leaves and tissues, the most abundant glycosides are rebaudioside A (Reb-A) and steviosid (Arnon 1949)

Drought is known as one of the most destructive stresses that affect the growth, development, and reproduction of plants (Bi et al 2021). A typical effect of water deficit is to cause oxidative damage through the widespread accumulation of reactive oxygen species (ROS) (Duan *et al*., 2022). ROS overproduction leads to lipid peroxidation, enzyme inactivation, impaired protein structure / function, and nucleic acid damage (Duncan 1955). Plants, in turn, use enzymatic and non-enzymatic antioxidant systems to prevent the accumulation of ROS (Duncan 1955). Some stimulants of biological origin or eustress or with appropriate dosage and length, not only activate chemical defense in plants, but also increase plant productivity (Elizabeth Abreu and Munné-Bosch 2008). One of the purposes of plant physiologists is to identify and introduce substances that improve the resistance of plants to biotic and abiotic stresses. Salicylic acid is one of these substances. Salicylic acid treatment with appropriate dose has increased resistance to environmental stresses in different species. Regulation of tougher pressure and activation of the antioxidant system are the mechanisms of salicylic acid in improving water shortage stress resistance (Eraslan *et al*., 2007). Another substance that plays a role in modulating environmental stresses is chitosan. It is a natural polymer derived from chitin, which is used as a biological elicitor in agriculture (EFSA 2010).

Chitosan treatment enhances photosynthesis and stomatal closure by ABA synthesis (Guo et al., 2022; 2021). This substance increases antioxidant enzymes through the H_2O_2 and NO signaling pathways and induces the produces sugars, amino acids, organic acids, and other metabolites needed to signal stress, osmotic balance, and energy metabolism under unfavorable environmental conditions (Gao et al., 2016).

Another compound that increases plant resistance to biological and non-biological stresses is melatonin (N-acetyl-5-methoxytryptamine) (Janda et al., 1999; Meng et al., 2014; Ma et al., 2018; Porra et al., 1989; Peng et al., 2021; Su et al., 2019; Sun et al., 2021). A wide range of physiological reactions has been attributed to melatonin, which can moderate the adverse effects of environmental stresses such as drought and salinity on plants. Melatonin has an antioxidant activity and can detoxify ROS in cells (Karimi et al., 2015). Melatonin can increase photosynthetic capacity by increasing the absorption of water and nutrients and increasing the expression of genes associated with mitogen-activated protein kinases (LI et al., 2021). It has been reported that the use of melatonin under drought stress conditions prevents the accumulation of abscisic acid in the cell and has a synergistic effect with cytokinin (Lehmann et al., 2010; Liang et al., 2019; Mahajanab et al., 2021). Therefore, in the present study, we investigate the role of chitosan, salicylic acid, and melatonin on the physiological and biochemical responses of stevia under water deficit stress conditions.

MATERIALS AND METHODS

This experiment was carried out in the two cropping years of 2019 and 2020 as a split-plot based on a randomized complete block design with three replications in a research farm in the city of Sulaymaniyah located in the north of Iraq. The experimental area was located at 45°11' N; 45°58' E longitude and altitude, respectively, 690 m above sea level. The average annual rainfall in the experimental area was about 250 mm and the average maximum and minimum temperatures were 22 and 9 degrees, respectively. The soil properties of the test site are listed in Table 1.

Experimental treatments included different irrigation regimes (90% FC, 65% FC, and 40% FC) and foliar application of different elicitor (control, chitosan (2 gL^{-1}), salicylic acid (100 mg L^{-1}), and melatonin (100 µM), which were assigned to main and sub-plots, respectively.

Table 1. Soil physical and chemical properties of the experimental site.

Physical Properties	Value	Unit	Chemical properties	Value	Unit
sand	133.6	g kg^{-1}	Organic mater	20	g Kg^{-1}
silt	244.3	g kg^{-1}	pH	7.57	
clay	622.1	g kg^{-1}	ECe	1.4	dS m^{-1}
soil texture	Clay		Total nitrogen	20	mg Kg^{-1}
Bulk density	1200	Kg m^{-3}	Phosphors (soluble)	19	mg Kg^{-1}
Field capacity (33 k Pa)	320	g kg^{-1}	Potassium (soluble)	13.7	Meq Kg^{-1}
Wilting point (1500 k Pa)	188	g kg^{-1}	Calcium (soluble)	7.5	Meq Kg^{-1}

The seedlings obtained by tissue culture were initially cultivated in peat moss medium to select the well-established plantlets. After three weeks, the uniform seedlings were trans-planted into soil in May each year.

In this experiment, the dimensions of each plot were considered 2×2.5 m. Each plot also included four rows of crops. In this study, the distance between the rows was 50 and the distance between the plants was 30 cm.

The first two weeks the soil moisture was maintained within the range of field capacity and, then, the irrigation treatments were applied as 90, 65, and 40% of field capacity (FC). The soil moisture content was measured using the gravimetric method. Irrigations for each plat were conducted to replenish 100% of soil field capacity.

Chitosan, salicylic acid, and melatonin were sprayed three times after 30, 40, and 50 days from transplanting in both years.

Harvesting was done 62 days after transplanting the seedlings to the field. In the first stage, the leaves and stems were separated and then weighed.

Evaluating morphological characteristics

At the time of harvest, the plants in each plot were carefully removed from the soil and the roots of each sample were washed to remove soil residues. Stem length, leaf area index, and biological yield of each sample were measured.

Leaf area index was calculated according to Formula (1), in which LA leaf area and LG land area were occupied LAI = LA/LG photosynthetic pigments
80% of acetone extract with adsorption readings at 663, 646, and 440 nm was used to measure the concentration of photosynthetic pigments according to Arnon's (18) method. In addition to quantify the measurements, Porra et al. (19) method was used
Chlorophyll a = 12.25×A663–2.55×A646
Chlorophyll b = 20.31×A646–4.91×A663
Carotenoids = 4.69×A440–0.267× (A663×A646)
Pigment content was expressed as mg/gDW.

Proline content

To determined the proline content. 50 mg of leaf dry matter was homogenized in 5 ml of ethanol: Water mixture (60:40) and the homogenized solution was incubated for 24 h at +4 °C. After centrifugation at 10,000 rpm, the supernatant was collected. In the next step, 100 mL of ninhydrin acid 1% was mixed with 500 µL of supernatant of the extracted solution. The samples (reaction mixture) were placed in a water bath at 95 °C for 20 min and, then, cooled to the room temperature. After cooling, the reaction absorbance was measured at 520 nm and using proline as standard, the proline content of the samples was measured. The proline content of the samples was expressed based on mg proline / g fresh weight Zheng et al. (2018).

Secondary metabolite analysis

To extract phenol, plant samples were dried and, then, macerated in 80% methanol ((HPLC grade). In the next step, the samples were incubated for 24 h at 4 °C.

The incubated samples were centrifuged at 2000 rpm for 15 min and the supernatants of the extracts were collected for further analysis. Finally, Wolf et al.'s (20) method was used to analyze the phenol content. In this method, folin-ciocalteu reagent and gallic acid were used as the standard. The total antioxidant capacity was determined by the DPPH (2,2-diphenyl-1-picrylhydrazyl) assay according to Karimi et al. (21).

Analysis of steviol glycosides

To estimate the glycoside content of the leaves, at the time of harvest, the leaves in each plot were randomly selected and dried at 40 °C in an air oven. Then, 100 g of the powdered leaf sample was placed in a 25 ml flask containing 10 ml of methanol and filtered for 24 hours. The reduced pressure filter was vacuum dried and, then, defatted with n-hexane. Afterwards, the moving phase was used to solve the samples (HPLC grade-acetonitrile: water in the ratio 1:1). Filters with pores of 0.22 µm were used to re-filter the samples. Filtered samples were used to determine the content of stevoside, Reb-A by liquid chromatography-mass spectrometry (LCMS-Shimadzu, 2020 system) (22). Standard curves with the samples were used to quantify glycoside content; these curves are used for standard stevoside and Reb-A samples (22).

Statistical analysis

Analysis of variance was performed using SAS software, also the comparison of the mean of treatments with the Duncan (1955) method was performed at a level of 5% probability.

RESULTS

Results showed the effect of irrigation regimes on all the traits was significant at the level of 1% probability.

A significant difference was detected among the different treatments in terms of the effect on plant height, leaf area index, biological yield, proline, chlorophyll a, chlorophyll b, phenol, rebaudioside A, and steviosid at the probability level of 1% and in terms of carotenoid content at the level of 5% probability. There was a significant interaction effect of irrigation and allicator treatments on plant height, biological yield, proline, phenol content, DPPH, rebaudioside A, and steviosid at 1% probability and on leaf area index and carotenoid content at 5% probability level was observed (Table 2).

Plant Height

In this study, the highest plant height with the average of 37.17 cm was allocated to normal irrigation conditions (90% FC) and the foliar application of salicylic acid. With the intensification of water stress, the plant height significantly decreased; but, in treatment of the 65% FC, application of salicylic acid could significantly increase plant height compared to the control treatment. There was no significant difference between the control treatment and other treatments using growth stimulants (Table 4). The results also showed that under irrigation conditions of the 40% FC, there was no considerable difference among the control treatment and the application of elicitors. Results revealed, the lowest plant height was allocated to irrigation treatment of the 40% FC in all the four growth elicitor treatments (Table 4).

Leaf Area Index

The results of mean comparisons showed that melatonin application under normal irrigation conditions (90% FC) had the highest leaf area index, while the control and chitosan treatment in the treatment of 40% FC showed the lowest amount. In this study, although in the irrigation treatment of 65% FC, there was no considerable difference between the control treatment and the other elicitor treatments, in the irrigation treatment of 40% FC, the use of salicylic acid increased the leaf area index significantly compared with the control and other treatments (Table 4).

Biological Yield

Among the interactions of irrigation and plant growth stimulant treatments, the use of melatonin in 90% FC treatment with the average of 49.34 g/plant showed the maximum biological yield. The lowest biological yield with the average of 12.14 and 10.97 g/plant was allocated to the control treatment and application of chitosan under irrigation conditions of 40% FC. Results showed that although biological yield decreased with exacerbation of water deficit, the melatonin spraying was able to improve this trait in the treatment of the 65% FC by 45.61% compared with the control treatment, In addition there was no remarkable difference among control treatment and elicitors application treatments in the irrigation treatment of the 40% FC (Table 4).

Table 2. Combine analysis of variance of irrigation and spraying elicitors on studied traits in stevia (*Stevia rebaudiana Bertoni*).

SOV	Df	Mean square										
		Plant Height	LAI	Biomass	Proline	Chlorophyll a	Chlorophyll b	Carotenoid	Phenol	DPPH	Rebaudioside A	Steviosid
Year (Y)	1	39.01^{ns}	1.25^{ns}	0.60^{ns}	0.0004^{ns}	0.0004^{ns}	0.008ns	0.00021^{ns}	0.027^{ns}	0.056^{ns}	0.50^{ns}	2.72^{ns}
Year (Replication)	4	13.08	0.85	0.21	0.0005	0.0002	0.004	0.0006	0.018	0.021	0.64	1.24
Irrigation levels (I)	2	1606.57**	305.92**	4182.82**	0.0029**	0.0057**	28.32**	0.0031**	0.065**	42.81**	27.73**	98.38**
Y× I	2	7.76^{ns}	17.36^{ns}	10.06^{ns}	0.0001^{ns}	0.0004^{ns}	0.0024ns	0.00007^{ns}	0.017^{ns}	0.18^{ns}	5.50^{ns}	4.05^{ns}
Error 1	8	13.56	5.88	60.04	0.0006	0.0007	4.33	0.000012	0.011	3.71	5.91	11.73
Elicitors (E)	3	37.29**	31.62**	289.38**	0.0075**	0.0147**	29.94**	0.0013*	0.040**	1.95^{ns}	13.47**	216.91**
Y×E	3	19.94^{ns}	0.45^{ns}	0.06^{ns}	0.0074^{ns}	0.0004^{ns}	0.052^{ns}	0.000025^{ns}	0.012^{ns}	0.092^{ns}	0.47^{ns}	7.16^{ns}
I × E	6	41.33**	8.88*	189.68**	0.0011**	0.0005^{ns}	5.54^{ns}	0.00040*	0.332**	3.98**	8.39**	46.95*
Y×E×I	6	10.36^{ns}	1.54^{ns}	11.16^{ns}	0.0004^{ns}	0.0004^{ns}	0.0011^{ns}	0.000032^{ns}	0.031**	0.05^{ns}	0.46^{ns}	6.27^{ns}
E2	36	11.12	3.41	48.21	0.0003	0.0006	2.12	0.00013	0.011	1.05	0.98	14.34
CV%	-	12.56	14.20	24.78	15.16	19.01	16.96	20.57	10.52	9.67	13.51	15.55

ns, *, and ** were significant at levels 1 and 5% respectively.

Table 3. Mean comparison of main effects of irrigation and spraying elicitors treatments of on studied traits in Stevia (*Stevia rebaudiana Bertoni*).

Irrigation	Plant Height (cm)	LAI	Biomass (g plant-1)	Proline (Mg gFW-1)	Chlorophyll a (Mg gFW-1)	Chlorophyll b (Mg gFW-1)	Carotenoid (Mg gFW-1)	phenol mgGAE gDW-1	DPPH (%)	Rebaudioside A (%)	Steviosid (%)
90% FC	34.50a	16.71a	41.13a	0.108b	0.149a	0.096a	0.069a	0.961b	9.36c	6.48b	22.34b
65% FC	26.99b	12.75b	28.19b	0.120a	0.133b	0.086b	0.052b	1.026a	10.45b	7.03b	24.36ab
40% FC	18.16c	9.58c	14.73c	0.130a	0.118c	0.074c	0.047b	1.067a	12.00a	8.55a	26.39a
Elicitors											
Control	24.41b	11.49c	23.08b	0.148a	0.094c	0.068c	0.046c	0.822d	10.49a	6.63b	21.63b
Chitosan	27.42a	12.64bc	27.56ab	0.119b	0.141b	0.087b	0.056b	1.174a	10.52a	6.43b	21.09b
Salicylic acid	26.99ab	14.68a	28.57ab	0.108bc	0.136b	0.089ab	0.055b	0.993c	10.31a	8.11a	27.33a
Melatonin	27.38ab	13.23ab	32.85a	0.102c	0.163a	0.098a	0.067a	1.087b	11.07a	8.24a	27.39a

Data in columns followed by different letters are significantly different ($p \leq 0.01$) by Duncan's multiple range test.

Table 4. Mean comparison of irrigation and spraying elicitors interaction treatments of on studied traits in Stevia (*Stevia rebaudiana Bertoni*).

Irrigation	Elicitors	Plant Height (cm)	LAI	Biomass (g plant-1)	Proline (Mg gFW-1)	Carotenoid (Mg gFW-1)	Chlorophyll a (Mg gFW-1)	Chlorophyll b (Mg gFW-1)	Phenol mgGAE gDW-1	DPPH (%)	Rebaudioside A (%)	Steviosid (%)
90% FC	Control	30.35bcd	14.73bcd	32.88bcd	0.0937d	0.062bc	0.109a	0.081a	1.1197bc	8.11f	5.887ghi	18.76f
	Chitosan	33.95abc	15.94abc	38.84abc	0.0957cd	0.058b-e	0.147a	0.091a	1.1017bc	9.29ef	6.65f-h	20.81ef
	Salicylic acid	37.17a	17.65ab	43.45ab	0.1207bcd	0.07b	0.164a	0.102a	0.6317d	10.03de	5.302i	26.65bc
	Melatonin	36.53ab	18.51a	49.34a	0.123bcd	0.087a	0.176a	0.068a	0.674d	9.94de	8.088cd	23.15c-f
65% FC	Control	23.08ef	11.36def	20.61def	0.1033cd	0.047de	0.086a	0.111a	0.6747d	11.12bcd	6.328f-i	22.49c-f
	Chitosan	26.57de	13.69cd	28.26cde	0.1237bcd	0.056cde	0.149a	0.082a	1.1567ab	10.37de	5.649h-i	20.40ef
	Salicylic acid	30.02cd	14.03bcd	26.82cde	0.1063cd	0.045e	0.134a	0.089a	1.1683ab	9.92de	8.883bc	29.10b
	Melatonin	28.89cde	11.9def	37.07abc	0.1498ab	0.059bcd	0.164a	0.105a	1.108bc	10.4de	7.277def	25.43bcd
40% FC	Control	19.8f	8.39f	12.14f	0.1113cd	0.031f	0.088a	0.055a	1.0033c	12.24ab	7.7de	23.66cde
	Chitosan	18.9f	8.3f	10.97f	0.1057cd	0.055cde	0.126a	0.094a	1.2647a	11.91abc	7.018d-g	22.06def
	Salicylic acid	17.22f	12.36cde	20.05def	0.1313bc	0.048cde	0.11a	0.07a	1.18ab	10.98cd	10.15a	26.25bcd
	Melatonin	16.71f	9.28ef	15.75ef	0.1733a	0.055cde	0.148a	0.079a	1.151ab	12.88a	9.362ab	33.60a

Data in columns followed by different letters are significantly different ($p \leq 0.01$) by Duncan's multiple range test.

Proline

The results revealed that the leaf proline content increased with exacerbation of drought, so that the irrigation conditions of the 40% FC with spraying of melatonin with the average of 0.173 (Mg/gFW) had the maximum proline content. Results demonstrated that spraying of melatonin in both 65% FC and 40% FC conditions was able to improve the proline content compared with the control by 41.62 and 55.85%, respectively. The lowest proline content was assigned to 90% FC treatment with all four eliminator treatments (Table 4).

Photosynthetic Pigments

The results showed that irrigation conditions of 40% FC and 65% FC reduced the chlorophyll content by 10.85 and 20.91 percent, respectively, compared to 90% FC irrigation conditions (Table 3).

In the present study, the use of melatonin with the average of 0.163 (Mg/gFW) had the highest leaf chlorophyll a content and increased the amount of this trait compared to the use of chitosan, salicylic acid, and control by 15.60, 15.60, and 72.30 percent, respectively. In this study, the control treatment with the average of 0.094 (Mg/gFW) had the lowest chlorophyll a content (Table 3).

Chlorophyll b content decreased due to water shortage so that the supply of the 90% FC and 40% FC had the maximum and minimum chlorophyll b contents, respectively (Table 3).

Results revealed that melatonin application had the highest chlorophyll b content. The difference between melatonin and salicylic acid was not significant. The lowest chlorophyll content was recorded for control treatment of foliar application (Table 3).

In our experiment spraying of melatonin in irrigation treatments of 90% FC improved carotenoid content compared with the control treatment by 40.32 percent and had the maximum carotenoid content (Table 4). In our study, although in irrigation treatment of 60% FC, there was no notable difference among the control treatment and elicitors, in the irrigation treatment of 40% FC, foliar spraying of chitosan, salicylic acid, and melatonin increased the carotenoid content by 77.41, 54.88, and 77.10 percent compared to the control.

Phenol content

Based on the results, with the intensification of water deficit stress, the phenol content was increased, so that the foliar spraying of chitosan and salicylic acid in irrigation treatment of 60% FC and the use of chitosan, salicylic acid, and melatonin in irrigation treatment of 40% FC had the highest phenol content and enhanced the amount of this trait remarkable compared with the control. The lowest phenol content was allocated to irrigation treatment of 90% FC and the foliar spraying of salicylic acid and melatonin (Table 4).

DPPH

In our study water stress rose the amount of DPPH, so that the treatment of melatonin, chitosan, and control under irrigation treatment of 40% FC had the highest amount of DPPH activity. The minimum DPPH content was recorded in the control treatment under 90% FC irrigation conditions (Table 4). In our experiment, water shortage and foliar application of elicitors had a synergistic effect on DPPH activity.

Rebaudioside A

Results revealed that water deficit stress and foliar spraying of salicylic acid and melatonin had a synergistic effect on rebaudioside A content. Irrigation treatment with 40% FC with foliar spraying of salicylic acid and melatonin had the highest amount of glycoside rebaudioside A. It should be noted that the application of these two treatments in the irrigation regime of 65% FC significantly increased the amount of rebaudioside A in comparison to the control and foliar spraying chitosan treatments (Table 4). The lowest amount of rebaudioside A was recorded under normal irrigation (90% FC) and salicylic acid application.

Steviosid

In our study irrigation regime of 40% FC along with melatonin foliar spraying had the highest steviosid glycoside content, Furthermore foliar spraying of salicylic acid under 90% FC irrigation conditions, foliar spraying of salicylic acid and melatonin under 65% FC irrigation conditions, and application of melatonin under 40% FC irrigation conditions could significantly improved steviosid glycoside content compared with control and other treatments (Table 4).

DISCUSSION

Our research findings showed water deficit diminished plant height, but spraying of salicylic acid, especially in irrigation treatment of the 65% FC, was able to moderate the negative effect of water deficit on plant height. Under drought stress, cell elongation and cell differentiation are reduced due to decreased total water potential inside the plant (Xu et al., 2021). It seems that the application of salicylic acid can mitigate the adverse effect of drought stress on plant growth by preventing a reduction in cell divisions and cell size (Yan et al., 2018). In the study by Karimi et al. (Tardieu et al., 2000) on stevia, drought stress decreased plant height, while the use of external SVglys could not affect this trait.

In this study, foliar application of melatonin under normal irrigation conditions produced the maximum leaf area index. leaf area index decreased with the intensification of water shortage. Results revealed the use of salicylic acid in the irrigation treatment of 40% FC, increased the leaf area index significantly compared to the control and other treatments. Probability salicylic acid can improve nutrient uptake, especially under stress, which in turn can increase growth (25). It seems that salicylic acid can increase photosynthesis and, thus, increase growth by increasing the amount of chlorophyll in the leaves that are at the beginning of the aging process (26). Karimi et al. (21) showed that drought stress decreased leaf growth in stevia, but the external application of SVglys reduced the leaf losses.

In our research, the use of melatonin under normal irrigation had the highest biological yield, This trait was reduced by reducing the available water of the plant. The results also revealed that foliar application of melatonin under water shortage conditions increased biological yield compared to the non-foliar spraying treatment. Increased biological yield in the present study can be due to the positive effect of foliar application on leaf area index and photosynthetic pigments under different irrigation, leaf area development and photosynthetic pigments increased the rate of photosynthesis and accelerate plant vegetative growth. One of the adverse effects of drought stress is accelerating the production of reactive oxygen species (ROS) (Ucar et al., 2016), which leads to cell damage, reduced growth and biomass production, and ultimately cell death.

The result showed that under irrigation conditions of the 40% FC with the use of melatonin had the highest proline content. Results also revealed that the use of melatonin in both 65% FC and 40% FC conditions was able to raise the proline content compared to the control treatment. Proline acts as an osmolytic / sprotactant factor under water deficit stress (Zheng et al., 2018). The results of our study showed a significant increase in proline content under water deficit stress treatments. It has been reported that the use of melatonin under water deficit conditions induces drought resistance in plants by increasing proline biosynthesis (Zhang et al., 2015). Consistent with the results of the present study, Liang et al. (Zhao et al., 2017) in *Actinidia cinnis*, Campos et al. (2019) in *Brassica napus*, and Li et al. (2019) in *Cophea Arabica* have found that melatonin application significantly increases leaf proline content in these plants. In the study by Ghanbari et al., the use of chitosan and salicylic acid in milk thistle (*silybum marianum* L.) remarkably raised the proline content under drought stress.

Water deficit causes the ROS accumulation, resulting in the degradation of the molecular structure of chlorophyll, and finally declining plant photosynthesis. Under moisture shortage conditions, a decrease in Chl content was considered a typical sign of oxidative stress. The decrease in Chl content under drought stress is mainly due to degradation of Chl as the result of ROS activity (Zhang, et al ,2022). Reduction of chlorophyll content due to water deficiency, in chickpea, maize , and basil , has been documented in previous investigations. In the present study, the use of melatonin had the highest leaf chlorophyll a and b content. Similar to other photosynthetic pigments, water deficit decreases carotenoid content, but the use of all three elicitors increased carotenoid compared with non-foliar spraying treatment (control) under irrigation treatment of 40% FC. Under water deficit conditions stress, the use of elicitors can prevent the degradation of pigments molecules. Decreased pigments molecule degradation after melatonin treatment may be due to decreased down-regulation of genes of chlorophyll-degrading enzymes such as Chlase, PPH, and Chl-PRX.

The results showed that induction of water deficit stress and foliar application of elicitors increased leaf phenol content so that the use of chitosan and salicylic acid under irrigation treatment of 60% FC and the use of chitosan, salicylic acid, and melatonin in irrigation treatment of 40% FC showed the highest amount of phenol content. As mentioned, drought stress increases the accumulation of ROS in cells that can damage cellular structures. The use of elicitors can increase the activity of antioxidant enzymes to strengthen the plant's defense system and prevent accumulation of ROS in cells. Increased phenol content in response to melatonin treatment under drought stress had been reported in the study by Sharma et al. (2017) on Grafted (*Carya cathayensis*). In the study by Karimi et al. (2017), the highest values of antioxidant capacity in stevia were allocated to water deficit conditions and plants treated with SVglys, while the lowest values were reported under normal irrigation conditions and no use of SVglys. Application of salicylic acid by regulating the activity of antioxidant enzymes can improve plant tolerance to adverse conditions (Li, *et al*, 2021; Sun, *et al.* 2021; Xu, *et al*, 2021; Zhang, *et al.* 2022).

The results showed the spraying of melatonin and chitosan under irrigation treatment of 40% FC showed the maximum amount of DPPH activity. Consistent with our results, the use of melatonin had a protective role against water shortage in corn and oats . In the study by Ahmed et al. (42), water deficit increased rebaudioside A and stevioside content in steva. compatible solutes such as soluble sugars under melatonin treatment increase, These substances are responsible for maintaining the turgor and osmotic pressure of plant cells under water deficit conditions. In the study by Jalal et al. (2018), salicylic acid treatment increased sugar content on plant in both drought stress and control treatments. Salicylic acid increases plant resistance to drought stress by stimulating sugar production in the cell. Karimi et al. (2019) showed that drought stress increased rebaudioside A content in stevia (Bi, *et al.,* 2021; Duan, *et al.,* 2022; Guo, *et al*, 2021; Guo, *et al,* 2022).

The results showed that application of salicylic acid under 90% and 65% FC irrigation conditions and application of melatonin under 40% FC irrigation had a positive effect on increasing steviosid glycoside content,

therefore, the content of this substance increased in all irrigation conditions in response to different elicitors. In a study on milk thistle (*silybum marianum* L.), the highest soluble sugars was reported in the application of chitosan and salicylic acid under water stress conditions. The positive effect of melatonin on increasing the amount of soluble sugars has also been reported in the studies by Liang et al. (2011), Campos et al. (2012), and Li et al. (2018).

CONCLUSION

To summarize, the findings of this research revealed that water deficit stress markedly decreased plant growth and increased the proline, phenol, DPPH, rebaudioside, and steviosid contents. However, exogenous application of salicylic acid and melatonin enhanced tolerance of the *stevia* to water deficit stress by increasing the growth, anti-oxidative enzyme activities, chlorophyll (Chlo) content, and synthesis of rebaudioside and steviosid. Therefore, salicylic acid and melatonin mitigated the adverse effect of drought stress in stevia and their spraying on the leaves was beneficial for plant recovery and growth under water deficit stress.

REFERENCES

Aghighi Shaverdi M, Omidi H, Tabatabaei S. 2018 Morpho-physiological response of stevia (*stevia rebaudiana* bertoni) to salinity under hydroponic culture condition (a case study in Iran). Appl Ecol Environ Res. 16(1): 17-28. DOI:10.15666/aeer/…

Al Hassan M, Chaura J, Donat-Torres M P, Boscaiu M, Vicente O. 2017. Antioxidant responses under salinity and drought in three closely related wild monocots with different ecological optima. AoB Plants. 9(2): plx009. https://doi.org/10.1093/aobpla/plx009

Arnon DI. 1949. Copper enzymes in isolated chloroplasts. Polyphenoloxidase in Beta vulgaris. Plant Physiol . 24: 1–15.

Bi, D., C. Dan, M. Khayatnezhad, Z. Sayyah Hashjin, Z. Y. Ma 2021. Molecular Identification And Genetic Diversity In Hypericum L.: A High Value Medicinal Plant Using Rapd Markers Markers. Genetika *53*(1): 393-405.

Chen, Weimiao; Khayatnezhad, Majid; Sarhadi, Nima 2021. Protok gena i struktura populacije kod allochrusa (Caryophylloideae, Caryophyllaceae) pomocu molekularnih markera. Genetika 53(2): 799-812.

Duan, F., Fei Song, Sainan Chen, Majid Khayatnezhad, Noradin Ghadimi, 2022. Model parameters identification of the PEMFCs using an improved design of Crow Search Algorithm. International Journal of Hydrogen Energy, *47*(79): 33839-33849.

Duncan, D. B.1955. Multiple range and multiple 'F' tests. Biometrics., 11(1): 1-42. https://doi.org/10.2307/300147

Elizabeth Abreu M, Munné-Bosch S. 2008. Salicylic acid may be involved in the regulation of droughtinduced leaf senescence in perennials: A case study in field-grown Salvia officinalis L. plants. Environ Exp Bot, 64:105–112. https://doi.org/10.1016/j.envexpbot.2007.12.016

Eraslan F, Inal A, Gunes A, Alpaslan M. Impact of exogenous salicylic acid on growth, antioxidant activity and physiology of carrot plants subjected to combined salinity and boron toxicity. Scientia Horticulturae, 2007; 113: 120–128.

EFSA (European Food Safety Authority). , 2010. Panel on food additives and nutrient sources (ans): scientific opinion on safety of steviol glycosides for the proposed uses as a food additive. EFSA J. 8 (4): 1537

Guo, H., Wei Gu, Majid Khayatnezhad, Noradin Ghadimi, (2022): Parameter extraction of the SOFC mathematical model based on fractional order version of dragonfly algorithm. International Journal of Hydrogen Energy, **47**(57):24059-24068.

Guo, L.N., She, C., Kong, D.B., Yan, S.L., Xu, Y.P., Khayatnezhad, M. and Gholinia, F. 2021. Prediction of the effects of climate change on hydroelectric generation, electricity demand, and emissions of greenhouse gases under climatic scenarios and optimized ANN model. Energy Reports **7:** 5431-5445.

GaoW, Zhang Y, Feng Z, Bai Q, He J, Wang Y. 2016. Effects of melatonin on antioxidant capacity in naked oat seedlings under drought stress. Molecules, 23:1580. DOI: 10.3390/molecules23071580

Janda T, Szalai G, Tari I, Paldi E. 1999. Hydroponic treatment with salicylic acid decreases the effect of chilling injury in maize (*Zea mays* L.) plants. Planta. 208:175-180.

Jia, Y., M. Khayatnezhad, s. mehri (2020). Population differentiation and gene flow in Rrodium cicutarium: A potential medicinal plant. Genetika 52(3): 1127-1144.

Karimi M, Ahmadi A, Hashemi J, Abbasi A, Tavarini S, Pompeiano A, Guglielminetti L, Angelini L G. 2015. The positive role of steviol glycosides in stevia (*Stevia rebaudiana* Bertoni) under drought stress condition. Plant Biosystems. 150 (6): 1323-1331 . doi.org/10.1080/11263504.2015.1056857.

LI, ANG; MU, Xinyuan; Zhao, Xia; Xu, Jiamin; Khayat-

nezhad, Majid; Lalehzari, Reza; (2021):Developing the non-dimensional framework for water distribution formulation to evaluate sprinkler irrigation; Irrigation and Drainage, **70:** 659-667

Lehmann S, Funck D, Szabados L, Rentsch D. 2010. Proline metabolism and transport in plant development. J Amino Acids. 39(4): 949-962. DOI: 10.1007/s00726-010-0525-3

Liang D, Ni Z, Xia H, Xie Y, Lv X, Wang J, Lin L, Deng Q, Luo X. 2019. Exogenous melatonin promotes biomass accumulation and photosynthesis of kiwifruit seedlings under drought stress. Sci. Hortic. 246: 34–43. doi.org/10.1016/j.scienta.2018.10.058

Liu, S., Wang, Y., Song, Y., Khayatnezhad, M., & Minaeifar, A. A. 2021. Genetic variations and interspecific relationships in Salvia (Lamiaceae) using SCoT molecular markers. Caryologia, 74(3), 77-89.

Mahajanab M, Kumar B, Probir Kumar T. . 2021. Moisture stress and nitrogen availability modulate the secondary metabolite profiles, enzymatic activity, and physiological and agronomic traits of Stevia rebaudiana. Plant Physiol Biochem 162: 56-68. doi.org/10.1016/j.plaphy.2021.02.018

Meng JF, Xu TF, Wang Z Z, Fang Y L, Xi ZM, Zhang ZW. 2014. The ameliorative efects of exogenous melatonin on grape cuttings under water-deficient stress: Antioxidant metabolites, leaf anatomy, and chloroplast morphology. J. Pineal Res. 57: 200–212. DOI: 10.1111/jpi.12159

Ma, S., M. Khayatnezhad, A. A. Minaeifar. 2021. Genetic diversity and relationships among Hypericum L. species by ISSR Markers: A high value medicinal plant from Northern of Iran. Caryologia, 74(1): 97-107.

Mehri, H. Shirafkanajirlou, I. Kolbadi 2020. Genetic diversity, population structure and chromosome numbers in medicinal plant species *Stellaria media* L. VILL.. *Caryologia* 73(1): 57-65. doi: 10.13128/caryologia-680

Ma X, Zhang J, Burgess P, Rossi S, Huang B. 2018. Interactive efects of melatonin and cytokinin on alleviating drought-induced leaf senescence in creeping bentgrass (*Agrostis stolonifera*). Environ. Exp. Bot. 145: 1–11.

Porra RJ, Thompson WA, Kriedemann PE. 1989. Determination of accurate extinction coefficients and simultaneous equations for assaying chlorophylls a and b extracted with four different solvents: verification of the concentration of chlorophyll standards by atomic absorption spectrometry. Biochim Biophys Acta. 975: 384–394. doi.org/10.1016/S0005-2728(89)80347-0

Peng, X., Khayatnezhad, M. and Ghezeljehmeidan, L. 2021: Rapd profiling in detecting genetic variation in stellaria l. (caryophyllaceae). Genetika-Belgrade *53:* 349-362.

Shi, B., Khayatnezhad, M., Shakoor, A. 2021. The interacting effects of genetic variation in Geranium subg. Geranium (Geraniaceae) using scot molecular markers. Caryologia, 74(3), 141-150.

Su X, Fan X, Shao R. Guo J. Wang Y, Yang J, Yang Q, Guo L. 2019. Physiological and iTRAQ-based proteomic analyses reveal that melatonin alleviates oxidative damage in maize leaves exposed to drought stress. Plant Physiol Biochem. 142:263–274. DOI: 10.1016/j.plaphy.2019.07.012

Sun, Q., Deli Lin, Majid K., Mohammad T., 2021. Investigation of phosphoric acid fuel cell, linear Fresnel solar reflector and Organic Rankine Cycle polygeneration energy system in different climatic conditions. Process Safety and Environmental Protection, **147**:993-1008.

Xu, Y.-P., Ping Ouyang, Si-Ming Xing, Lu-Yu Qi, Majid khayatnezhad, Hasan Jafari,2021. Optimal structure design of a PV/FC HRES using amended Water Strider Algorithm. Energy Reports, **7:** 2057-2067.

Tardieu F, Reymond M, Hamard P, Granier C, Muller B. 2000. Spatial distributions of expansion rate, cell division rate and cell size in maize leaves: a synthesis of the effects of soil water status, evaporative demand and temperature. J. Exp. Bot. 51: 1505–1514.

Wang, J., Ye, Q., Zhang, T., Shi, X., Khayatnezhad, M., Shakoor, A. 2021. Palynological analysis of genus Geranium (Geraniaceae) and its systematic implications using scanning electron microscopy. Caryologia, 74(3), 31-43.

Yan Y, Pan C, Du Y, Li D, Liu W. 2018. Exogenous salicylic acid regulates reactive oxygen species metabolism and ascorbate–glutathione cycle in *Nitraria tangutorum* Bobr. under salinity stress. Physiol Mol Biol Plants. 24(4):577–589. DOI: 10.1007/s12298-018-0540-5

Ucar E, Ozyigit Y, Turgut K. 2016.The Effects of Light and Temperature on Germination of Stevia (*Stevia rebaudiana* BERT.) Seeds. Türkiye tarım araşt. Derg. 3(1): 37-40. DOI:10.19159/tutad.76528.

Zheng J, Ma X, Zhang X, Hu Q, Qian R. 2018. Salicylic acid promotes plant growth and salt-related gene expression in *Dianthus superbus* L. (*Caryophyllaceae*) grown under different salt stress conditions. Physiol Mol Biol Plants. 24(2):231–238. doi: 10.1007/s12298-017-0496-x

Zhang M, Jin ZQ, Zhao J, Zhang G, Wu F. 2015. Physiological and biochemical responses to drought stress in cultivated and Tibetan wild barley. Plant Growth Regul. 75(2): 567-574.

Zhao P, Lu GH, Yang YH. 2017. Salicylic acid signaling and its role in responses to stresses in plants. In: Pandey G (ed) Mechanism of plant hormone signaling under stress, 1st edn, vol 11.

Zhang, J., M. Khayatnezhad, and N. Ghadimi, 2022. Optimal model evaluation of the proton-exchange membrane fuel cells based on deep learning and modified African Vulture Optimization Algorithm. Energy Sources, Part A: Recovery, Utilization, and Environmental Effects, *44*(1):287-305.

Caryologia
International Journal of Cytology, Cytosystematics and Cytogenetics

Firenze University Press
www.fupress.com/caryologia

OPEN ACCESS

Citation: Wendy Ozols-Narbona, José Imery-Buiza (2022). Morphological and cytogenetic characterization in experimental hybrid *Aloe jucunda* Reyn. x Aloe vera (L.) Burm. f. (Asphodelaceae). *Caryologia* 75(4): 25-35. doi: 10.36253/caryologia-1886

Received: November 05, 2022

Accepted: December 28, 2022

Published: April 28, 2023

Data Availability Statement: All relevant data are within the paper and its Supporting Information files.

Competing Interests: The Author(s) declare(s) no conflict of interest.

Morphological and cytogenetic characterization in experimental hybrid *Aloe jucunda* Reyn. x *Aloe vera* (L.) Burm. f. (Asphodelaceae)

Wendy Ozols-Narbona*, José Imery-Buiza

Departamento de Biología, Universidad de Oriente, Cumaná, 6101, Venezuela
*Correspondign author. E-mail: wozolsnarbona@gmail.com

Abstract. *Aloe* L. includes plants of economic interest worldwide for their medicinal properties and ornamental character. In this study, morphological and cytogenetic traits were evaluated in a hybrid obtained using *Aloe jucunda* Reyn. as pollen donor and *A. vera* (L.) Burm. f. as female parent, to characterize it, determine its ornamental and agronomic potentialities and aspects related to its reproduction. Conventional protocols for morphometric studies and cytogenetic analysis described for succulent plants were applied. Progeny showed intermediate expressiveness in most of the characteristics, except in the colour of the leaves and flowers (hybrid = *A. jucunda*), as well as for the length of teeth, number, and area of leaf spots and angle between continuous leaves, where it surpassed the expression of both parents, giving it a high ornamental value. The length, width, and thickness of the leaves improved with respect to the paternal genome, so its potential for the exploitation of the gel and latex of its leaves cannot be ruled out. Root tip cells showed a karyotype 2n = 2x = 14 = 8L + 6S = 1L(smsat) + 1L(sm) + 3L(st) + 3L(smsat) + 1S(m) + 5S(sm). Microsporogenesis showed chromosomal abnormalities in 47.4% of the meiocytes, the most frequent being micronuclei in prophase-I, sticky chromosomes in metaphase-I, one or two dicentric bridges accompanied or not by acentric fragments in anaphase-I, -II, and telophase-I, - II, as well as one or two additional microspores. These abnormalities reduce the fertility of their pollen grains and limit their sexual reproduction, providing a better explanation for their sterility.

Keywords: *Aloe*, hybrid, morphological attributes, karyotype, microsporogenesis.

INTRODUCTION

Manual hybridization in plants has aroused interest in the genetic improvement of plants that represent crops of economic interest worldwide (Marasek-Ciolakowska et al. 2018). Among these plants are those included within the genus *Aloe* L., which comprises about 519 species with variable vegetative characteristics depending on their geographical location, temperature, fertility conditions, and availability of water in the soil (Smith and Van-Wyk 2008; MBG 2022). These species are xerophytic and monocotyledonous plants that are characterized by being perennial herbs, shrubs or small trees

with thick roots and rosette-shaped leaves (Carter 1994) with succulent tissues of economic importance for their ornamental attributes and therapeutic uses (Rowley 1997, Imery 2011).

Aloe vera (L.) Burm. f. (=*A. barbadensis* Mill.) is native to the Arabian Peninsula and now cultivated in several warm climatic zones of world including Asia, America, and Europe (Grace et al. 2015, Giannakoudakis et al. 2018). The *A. vera* industry has expanded throughout the world and the mucilaginous gel from the parenchymatous cells in the inner leaf pulp is used in many products, including fresh gel, juice, and multiple formulations for health, medicinal, and cosmetic purposes (Saleem et al. 2022). Its leaf extracts are rich in nutrients and contain over 200 active compounds including simple/complex polysaccharides, amino acids, proteins, enzymes, terpenoids, flavonoids, saponins, minerals, vitamins, phenols, and other metabolites, allowing a broad spectrum of medicinal applications (Saniasiaya et al. 2017). Other industrial perspectives also include the use of *A. vera* derivatives as corrosion inhibitors (Singh et al. 2016), obtaining biodiesel (Silva et al. 2015), growth enhancer (El Sherif 2017), germination accelerator and root development stimulant (Tucuch-Haas et al. 2022), post-harvest coating treatments (Farina at al. 2020), improvement of the swelling capacity of commercial acrylic hydrogels (Guancha-Chalapud et al. 2022), nanobiotechnologies (Arshad et al. 2022, Song et al. 2022), decreased methane release in dairy cows (Singh et al. 2021), bioremediation (Giannakoudakis et al. 2018), among others. The global *A. vera* extracts market value is projected to increase from USD 2,454.5 Million in 2022 to USD 5,153.71 Million by 2032, showing opulent growth of 7.7% (FMI 2022).

On the other hand, *Aloe jucunda* Reyn. evolved separately further south, in the Somali desert, and it is considered an exclusively ornamental plant due to its small size, adaptability, and beauty of its bright green variegated leaves and pink pendant flowers (Reynolds 1950). *A. vera* and *A. jucunda* only coexist in botanical gardens, nurseries, or research laboratories, both species present reproductive barriers such as protandry and self-incompatibility, which is why these plants propagate asexually (Imery and Cequea 2008). However, in reciprocal crosses trials, Imery (2011) obtained viable progeny, using *A. jucunda* as the donor species for the pollen grains and *A. vera* as the female parent. The need to obtain information as a contribution to scientific knowledge about a completely unpublished genotype not yet described, led to the realization of this work, which aimed to evaluate morphological and cytogenetic traits that would allow characterizing this experimental hybrid.

MATERIALS AND METHODS

Vegetal material

A. jucunda and *A. vera* adult plants (over eight years old) growing in the germplasm bank of succulent species of the Biology Department from Universidad de Oriente, located at 10°26'32'' N and 64°09'14'' W, in an area of very dry tropical forest in Cumaná city (Venezuela) were used. Specimens of *A. jucunda* (P2) were originally acquired in local nurseries and those of *A. vera* (P1) came from Península de Araya naturalized population, located at 10°34'15'' N and 64°12'08'' W (Albornoz and Imery 2003). Both species were identified considering the morphotaxonomic descriptions of Jacobsen (1955), Carter (1994) and Van-Wyk and Smith (1996). Five specimens of each of the evaluated genotypes were deposited in the IRBR Herbarium. Other fresh specimens are preserved in the already identified germplasm bank.

Morphological evaluation

Following of the morphometric traits were determined in the progeny and their parents (Figure 1): number, length, width, thickness, and volume (VH=π*LH*AH*EH/12) of the leaves (Hernández-Cruz et al. 2002), number and length of leaf teeth, number and area of leaf spots, leaf insertion angle, angle between continuous leaves, number of suckers, and flower colour, according to Imery and Cequea (2012). Ten adult plants of each genotype (*A. jucunda*, *A. vera*, and experimental progeny) were characterized.

Quantitative variables were analysed using ANOVA and LSD tests at $p \leq 0.05$ (Sokal and Rohlf 1979).

Cytogenetic evaluation

Mitotic chromosomes were studied from temporal slide prepared with meristems of root tips collected at 7:30-8:00 a.m., pre-treated with colchicine (0.05% m/v) for 2 h, fixed in Carnoy II solution (5:3:1 ethanol: glacial acetic acid: chloroform) for 30 min, hydrated in distilled water for 10 min, hydrolysed with HCl (1N) for 10 min and 24ºC, rehydrated in distilled water for 10 min, coloured with orcein (2% m/v) lactopropionic (45% v/v) for 4 min and gently squashed (Fukui and Nakayama 1996). Chromosomes according to their size (Stebbins 1971), length of the short arm (Brandham 1971) and centromere position (Levan et al. 1964) were classified. Microsporogenesis was evaluated in flower buds between 3.7-4.3 mm in length, fixed in Carnoy II and

Figure 1. Vegetative traits of the hybrid and its parents. (a) *Aloe jucunda*, (b) hybrid, (c) *A. vera*, (d) cross section in leaves of *A. jucunda* (upper), hybrid (middle), and *A. vera* (lower), (e) leaf lengths in the three genotypes, (f) contrasting details in the colour of the leaves, spots, and foliar teeth of the three genotypes evaluated, g) differences in the number of leaf spots between the adaxial face and the abaxial face in the leaves of the experimental hybrid, vegetative (h) and floral (i) details of the experimental hybrid. Scale bars = 2 cm.

staining the content of an anther with lactopropionic orcein (Alcorcés et al. 2012). At least five flower buds in meiosis for each genotype were analysed. All slides were systematically evaluated using a Nikon LABPHOT-2 microscope.

Photomicrographs at 400 and 1000 X with a Sony 7.2 digital camera were captured and the images on a computer using the PhotoImpact and SigmaScan Pro 5 programs were examined. Karyological data (chromosomal length, relative length, and long/short arm index) for ANOVA between genotypes and "t-student" tests between homologous chromosomes were used.

Viability of pollen grains

Fertility of the experimental hybrids was estimated by means of the *in vitro* germination of the pollen grains and pollen tube growth according to Sunderland and Roberts (1977) in culture medium with nutrient agar (6 $g.l^{-1}$) and sucrose (0.125 $mol.l^{-1}$), previously standardized for this genotype. Culture medium was autoclaved at 15 PSI for 15 min and five drops were added to ten slides. It was allowed to gel (10 min, 25ºC) and then the pollen grains of flowers kept in a humid chamber were dispersed until anthesis. Observation was carried out in a Nikon optical microscope, model LABPHOT-2 at 100X, after 60 min in the 10 slides of the microcultures established and covered by a Petri dish to avoid desiccation. For a better contrast, two drops of Astra Blue were added to each slide to colour the pollen tubes (Danti et al. 2011). A viable pollen grain was expected when the length of the pollen tube was greater than or equal to the length of its polar axis (Kalinganire et al. 2000). The percentage of *in vitro* germination of pollen grains was estimated using the relationship between the number of germinated pollen grains and the total number of pollen grains contained in each microscopic field.

RESULTS AND DISCUSSION

Genotypes evaluated (P1: *A. vera*, P2: *A. jucunda*, and H: hybrid) were significantly different ($p \leq 0.05$) in all the morphological variables studied. In most of the characteristics, the progeny was expressed in an intermediate way between its parents, except in the colour of the leaves, flowers and the presence of spots, which were inherited from the paternal genome of *A. jucunda*, as well as for the length of the teeth, angle between continuous leaves, number of spots on the adaxial side and number and area of leaf spots on both the adaxial and abaxial sides, in which the hybrid exceeded the expression of both parents (Table 1). The bright green colour and variegated character of its leaves thanks to the presence of spots because of the contribution of the paternal genome of *A. jucunda*, give this hybrid a high ornamen-

Table 1. Morphological attributes evaluated in adult plants of the progeny and their parents *Aloe jucunda* and *A. vera*, under nursery conditions in Cumaná (Venezuela).

Attribute/Genotype	A. vera (P1)	A. jucunda (P2)	Hybrid (H)	P1/P2	H/P1	H/P2
Leaf colour	Grey-green	Pine-green	Pine-green	-	-	-
Number of leaves	24.90 ± 2.85^{a}	18.90 ± 3.38^{c}	23.40 ± 2.22^{b}	1.32	0.94	1.24
Leaf length (cm)	57.41 ± 5.24^{a}	7.19 ± 0.28^{c}	28.28 ± 3.27^{b}	7.98	0.49	3.93
Leaf width (mm)	74.79 ± 5.31^{a}	15.74 ± 1.40^{c}	35.61 ± 4.64^{b}	4.75	0.48	2.26
Leaf thickness (mm)	21.74 ± 2.34^{a}	9.42 ± 0.83^{c}	17.82 ± 1.63^{b}	2.31	0.82	1.89
Leaf volume (cm^3)	244.39 ± 41.21^{a}	2.81 ± 0.45^{c}	47.47 ± 11.48^{b}	86.97	0.19	16.89
Leaf insertion angle (°)	31.71 ± 2.93^{c}	79.06 ± 7.30^{a}	38.44 ± 5.78^{b}	0.40	1.21	0.49
Angle between leaves (°)	80.90 ± 2.99^{c}	105.37 ± 19.15^{b}	124.72 ± 14.64^{a}	0.77	1.54	1.18
Number of leave teeth	35.08 ± 1.05^{a}	20.30 ± 1.37^{c}	23.43 ± 1.84^{b}	1.73	0.66	1.15
Teeth length (mm)	2.75 ± 0.22^{b}	1.38 ± 0.20^{c}	3.61 ± 0.47^{a}	1.99	1.31	2.62
Number of spots (adaxial)	0.00 ± 0.00^{c}	51.13 ± 6.06^{b}	59.27 ± 19.69^{a}	0.00	∞	1.16
Number of spots (abaxial)	0.00 ± 0.00^{c}	225.37 ± 15.65^{a}	194.37 ± 28.43^{b}	0.00	∞	0.86
Adaxial spot area (mm^2)	0.00 ± 0.00^{c}	1.82 ± 0.48^{b}	16.35 ± 6.35^{a}	0.00	∞	8.98
Abaxial spot area (mm^2)	0.00 ± 0.00^{c}	0.93 ± 0.27^{b}	15.56 ± 7.59^{a}	0.00	∞	16.73
Number of basal suckers	6.80 ± 2.04^{a}	4.10 ± 0.99^{c}	5.10 ± 3.03^{b}	0.75	0.63	1.24
Flower colour	Yellow	Orange-pink	Orange-pink	-	-	-

Values indicate mean ± standard deviation with n = 10 plants. Numbers followed by same letter are not significantly different (LSD $p \leq 0.05$) between genotypes.

tal value. Traits such as the length, width, thickness, and volume of the leaves were significantly improved in the progeny because of the contribution of the maternal genome (*A. vera*). In these cases, the magnitude of the improvements was between 1.24 to 16.89 times higher than the expression of the parent *A. jucunda* (smaller parent), so its possible agronomic potential for exploitation is not ruled out both of gel and latex of its leaves (Figure 1).

Another attribute of interest is the increase in the dimensions of the foliar teeth, which gives this new genotype an advantage as a defence mechanism against some predators. Watson et al. (2003) comment that the overexpression of some characteristic in hybrid descendants could be attributed to the accumulation of numerous loci in heterozygosis, propitiated by the interaction of two different genomes, in this case, that intervene in the organogenesis of the spines or biomass leaf to the edges. On the other hand, the prolific vegetative propagation guarantees the hybrid to perpetuate itself over time, compensating for its sterility, since it has not formed fruits and seeds through sexual reproduction, which, according to Imery and Cequea (2008), could be attributed to self-incompatibility mechanisms inherited from the maternal genome of *A. vera*.

Morphometric characterization of the progeny reveals a considerable ornamental value in this new genotype and the possibility of incorporating it as a model for studying the inheritance of traits of ornamental value and/or agronomic importance or for future crosses in the search for new genotypes, and complementary research.

Root tip meristematic cells presented bimodal karyotypes and chromosomal classifications (Levan et al. 1964) described by the formulas $2n = 2x = 14 = 8L + 6S = 2L(smsat) + 4L(st) + 2L(stsat) + 2S(m) + 4S(sm)$ in *A. vera* with eight large chromosomes (L) measuring 13.4-15.5 µm and six small chromosomes (S) measuring 5.1-5.9 µm; $2n = 2x = 14 = 8L + 6S = 2L(sm) + 2L(st) + 4L(stsat) + 5S(sm) + 1S(m)$ in *A. jucunda* with eight L chromosomes (14.7-16.9 µm) and six S chromosomes (5.5-6.3 µm); and $2n = 2x = 14 = 8L + 6S = 1L(smsat) + 1L(sm) + 3L(st) + 3L(stsat) + 1S(m) + 5S(sm)$ in the hybrid with eight L chromosomes (13.8-15.8 µm) and six S chromosomes (5.2-6.2 µm) (Figure 2).

Heteromorphisms between the homologues of chromosome pairs L2 and S1 were determined in the hybrids named VJ6 and VJ10, respectively (Figure 2c,d). As the genotypes evaluated did not show significant differences in the length of each of their chromosomes, the possibility that heteromorphisms between homologues of the progeny are caused by chromosomal mutations such as deletions is ruled out. In this regard, Brandham (1976) evaluated the karyotypes of 1543 diploid plants of the *Aloe*, *Gasteria*, and *Haworthia* genera without finding evidence of deletion. However, in polyploid species of the genus *Aloe* he found a frequency of 5.8%, indicating that structural mutations of this type have a lethal effect in diploid species. That is why heteromorphisms between homologous chromosomes are mainly attributed to the fact that their chromosomal complement comes from two different genomes.

Chromosomal abnormalities were found in 47.4% of the meiocytes evaluated. The most frequent meiotic aberrations were formation of micronuclei in prophase-I, sticky chromosomes, and acentric fragments in metaphase-I and -II, dicentric bridges accompanied or not with acentric or linked fragments in anaphase-I and -II, occasionally persistent in prophase-II, asynchrony between telophase-I and prophase-II, bridges, fragments, and micronuclei in telophase-I and -II, one or two additional microspores of variable size at the end of microsporogenesis (Figure 4). Although 31.6% of the pollen grains evaluated in the present investigation germinated under *in vitro* conditions (Figure 5), the absence of fruits and seeds in this new genotype forces this plant to depend exclusively on vegetative propagation for its multiplication.

Reproductive barriers such as gametophytic and sporophytic self-incompatibility have been described for most species of the *Aloe* genus (Newton 2004), including *A. vera* (Imery and Cequea 2008) and *A. jucunda* (Riley and Majumdar 1979), limiting then its self-fertilization with those pollen grains not affected by microsporogenic irregularities. This leads to the deduction that the impossibility of sexual reproduction of the experimental hybrids is also related to incompatibility genes inherited from both parents.

Swamy and Krishnamurthy (1980) and Imery (2011), argue that many plant species are forced to propagate asexually due to the existence of chromosomal alterations (deletions, inversions, and translocations), transmitted from their parents, either because they were present in their genomes or because they originated during the formation of their sex cells.

Additional bridges, fragments, micronuclei, and microspores are frequent in *Aloe* species with heterozygous paracentric inversions (Riley and Majumdar 1979, Ahirwar and Verma 2013). The pairing between the inverted chromosome and its pachytene homologue must involve the formation of a loop where crossovers occur between homologous chromatids that generate fine chromatin threads linked to two centromeres and totally unlinked fragments of these, causing the loss of

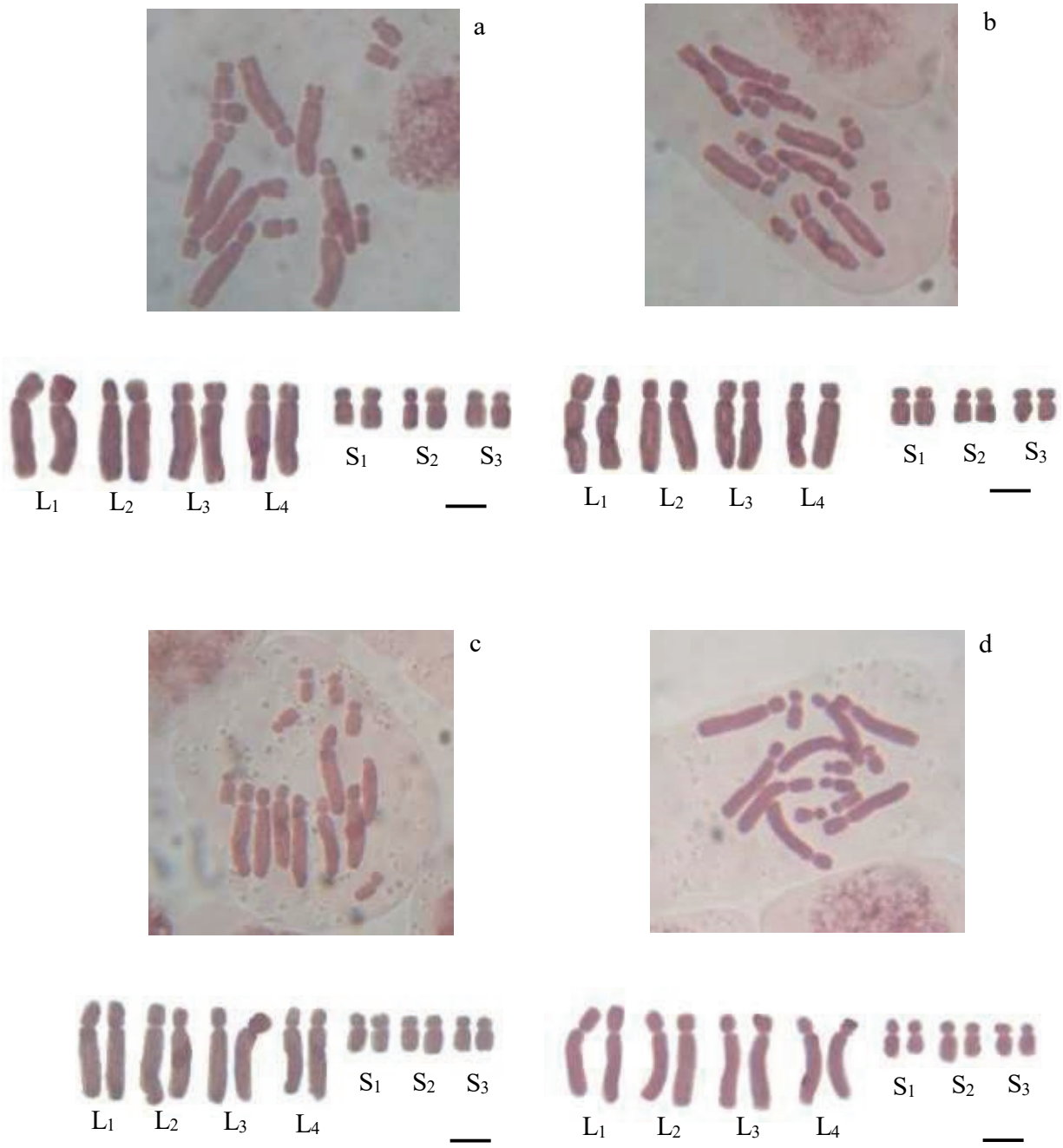

Figure 2. Mitotic chromosomes in root tip cells and bimodal karyograms (2*n*=2x=14=8L+6S) of a) *Aloe jucunda*, b) *A. vera*, c, d) experimental hybrids with greater heteromorphisms between homologous chromosomes. Typing of large (L) and small (S) chromosomes according to Brandham (1971). Scale bars = 5 µm.

genes that reduce the fertility of gametes. Chromosomal fragments present individually or linked to dicentric bridges during anaphase-I or telophase-I generally form additional micronuclei that increase the number of microspores at the end of meiosis and cause gene deficiencies (Ahirwar and Verma 2013). These aberrations may be present in clones that were formed by vegetative propagation from carrier individuals (populations of *A. vera* from Eastern Venezuela) and may have been inherited by the progeny or may be generated during the formation of sexual cells (Cequea et al. 2003, Imery 2011).

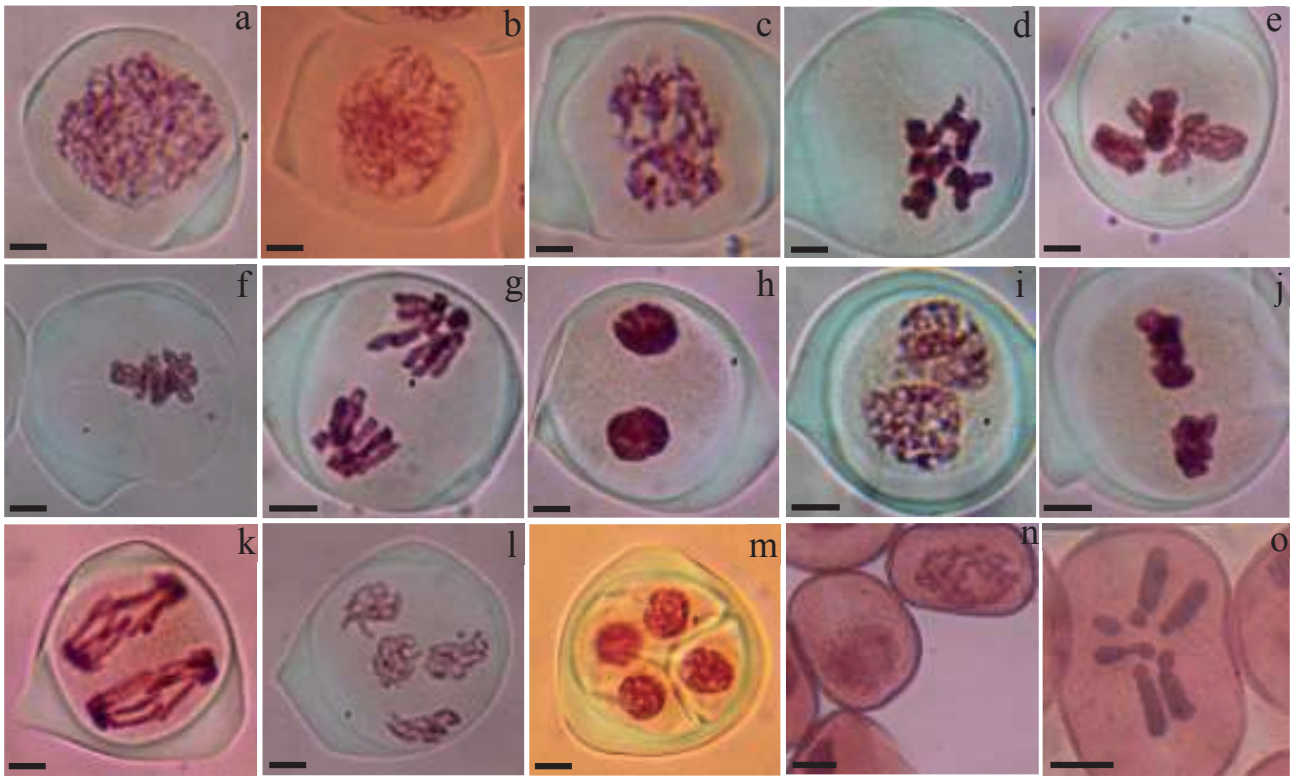

Figure 3. Microsporogenesis and microspore mitosis of the experimental hybrid *Aloe jucunda* x *A. vera*. a) Prophase-I (Leptotene), b) Prophase-I (zygotene), c) Prophase-I (pachytene), d) Prophase-I (diplotene), e) Prophase-I (diakinesis), f) Metaphase-I , g) anaphase-I, h) telophase-I, i) prophase-II, j) metaphase-II, k) anaphase-II, l) telophase- II, m) tetrad, n) microspores initiating first mitosis, o) microspore in metaphase showing haploid chromosomes (n=x=7=4L+3S). Scale bars = 10 µm.

On the other hand, Baptista et al. (2000) mention that the high frequency of sticky chromosomes or agglutination could be due to a genetic-environmental interaction associated with high temperatures, causing chromatin instability mainly in metaphase-I. Sapre (1975) suggests that the participation of neocentric activity in early displacement of smaller chromosomes is the main cause of dicentric bridges between large homologues; however, Imery and Cequea (2002) attributes this to early dissolution of the synaptonemal complex between small homologous chromosomes.

Other causes that have been mentioned to explain the presence of failures during meiosis are environmental conditions. Palmer et al. (2000), obtained discrepancies in the percentage of abnormalities between *Glycine max* plants that grew in different environmental conditions. These authors argue that the plants analysed grew in two contrasting environments and that the high temperatures increased the frequency of meiotic aberrations. A cytogenetic study in *Abies sibirica* (gymnosperm) conducted by Bazhina et al. (2008) revealed the same trend, noting that temperature fluctuations in the different months of the year affected the frequency of abnormalities. In this case, the plants evaluated during the dry season of summer registered a greater number of anomalies with respect to those analysed in the cool season of spring. Imery (2011) points out the possibility that the environmental conditions associated with high temperatures, solar radiation, and low humidity could promote the increase in the concentration of some substances typical of the plant (anthrones, anthraquinones) that alter the normal division of pollen mother cells in *A. vera*. It is possible, then, that the high environmental sensitivity and the existence of structural mutations already reported in *A. vera* were inherited to their sexual descendants *A. jucunda* x *A. vera* explain the origin of the abnormalities observed in this investigation.

Failures in the union of the kinetochores to the meiotic spindle could explain the presence of lagging or asynaptic chromosomes in metaphase and anaphase-I and -II, causing an independent behaviour of the rest of the chromosomes that make up the nucleus (Ishii and Akiyoshi 2022), and the depolymerization of spindle at different times in each cell nucleus could be the reason

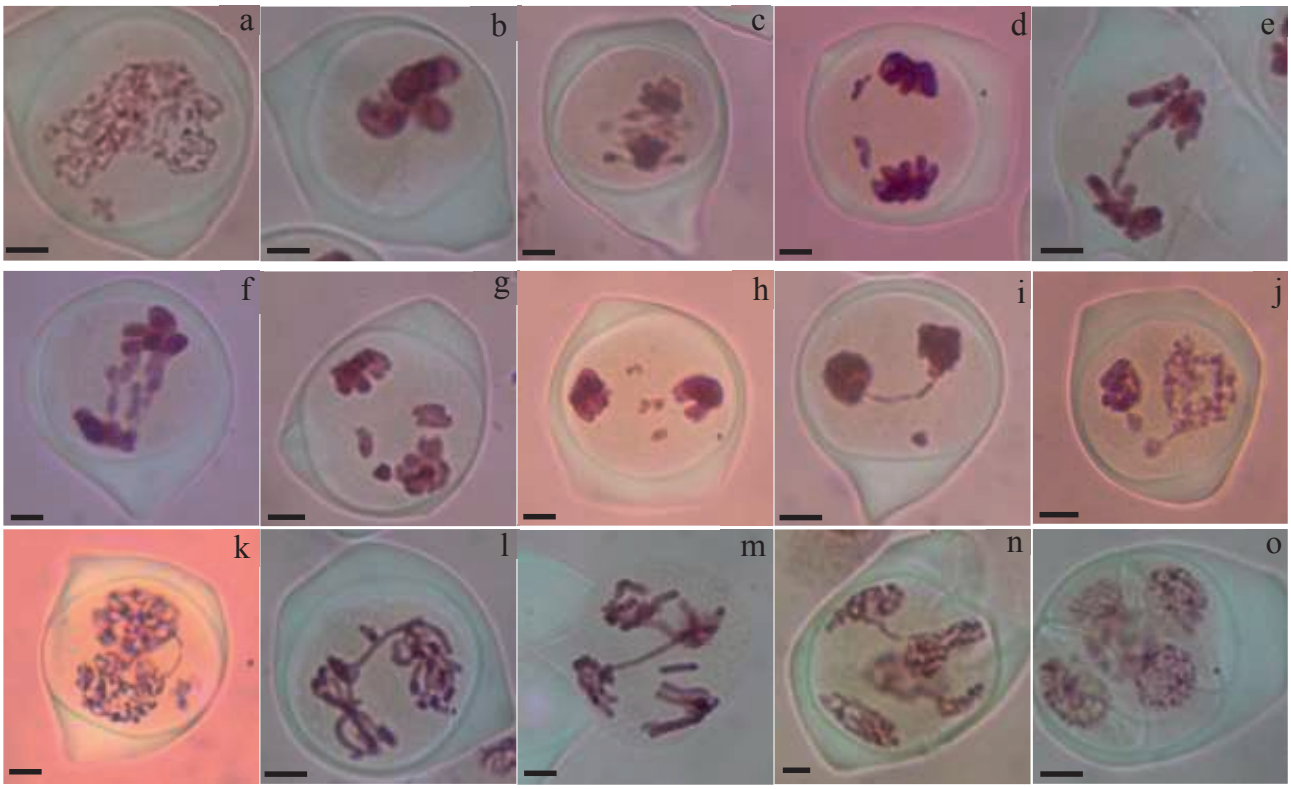

Figure 4. Most frequent meiotic abnormalities in the hybrid *Aloe vera* x *A. jucunda*. (a) Micronucleus in prophase-I; (b-c) sticky chromosomes and early displacement of small chromosomes in metaphase-I; (d-h) acentric fragments in anaphase-I and telophase-I; (e-f) one and two dicentric bridges in anaphase-I; (g) lagging chromosomes in anaphase-I; (i-k-n) bridge and fragment in telophase-I, -II and prophase-II; (j) phase asynchrony between telophase-I and prophase-II; (l) bridging and metaphase-II fragment; (m) bridge and fragment in anaphase-II and (o) additional microspore at the end of microsporogenesis. Scale bars = 10 µm.

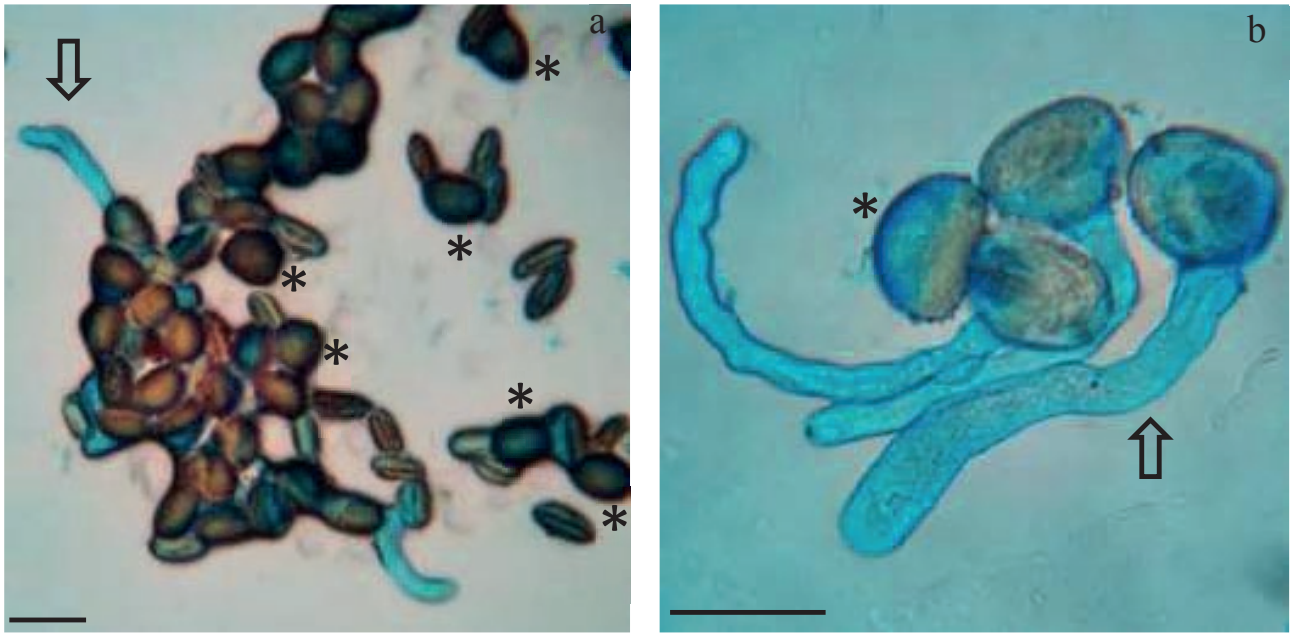

Figure 5. Pollen grains of the experimental hybrid *Aloe jucunda* x *A. vera*. Viability test of pollen cultured in vitro with agar-sucrose medium. Arrows point to pollen tubes of germinated pollen grains considered viable, while the (*) indicate non-germinated or non-viable pollen grains. Scale bars = 50 µm.

for the phase asynchrony between telophase-I/prophase-II and anaphase-I/telophase-II (Alcorcés et al. 2007).

CONCLUSIONS

Experimental hybrids of *Aloe vera* x *A. jucunda* showed superiority of vegetative traits such as the length of the foliar teeth, angle between continuous leaves, number and area of the spots compared to their parents, conferring them a high ornamental value. Traits such as the length, width, thickness, and volume of the leaves improved considerably with respect to the paternal genome, so its possible agronomic potential for the exploitation of the gel and latex of its leaves cannot be ruled out. Root tip cells presented the expected bimodal karyotype and number of chromosomes for the species of this genus. The meiotic abnormalities present in the progeny decrease the fertility of the pollen grains and show the reasons for their limited sexual reproduction, providing a better explanation for the absence of fruits and seeds in all their flowering periods.

ACKNOWLEDGEMENTS

The authors are highly thankful to the Consejo de Investigación de la Universidad de Oriente for the partial financing of this work through project CI-5-010101-1223/05.

REFERENCES

Ahiwar R, Verma R. 2013. Spontaneous Inversion Heterozygotes in *Aloe barbadensis*
Mill. Cytologia. 78:51-54. DOI: 10.1508/cytologia.78.51.

Albornoz A, Imery J. 2003. Evaluación citogenética de ocho poblaciones de *Aloe vera* L. de la península de Araya-Venezuela. Ciencia (LUZ). 11:5-13.

Alcorcés N, Lárez A, Mayz F. 2007. Additions to the cytogenetic knowledge of *Tithonia diversifolia* (Hemsl.) A. Gray (Asteraceae). Acta Bot Venez. 30:267-275. <https://www.jstor.org/stable/41740838>

Arshad H, Saleem M, Pasha U, Sadaf S. 2022. Synthesis of *Aloe vera*-conjugated silver nanoparticles for use against multidrug-resistant microorganisms. EJBT. 55:55-64. DOI: 10.1016/j.ejbt.2021.11.003.

Baptista F, Pagliarini M, Almeida J. 2000. Multiple anaphase bridges on meiosis in Brazilian oats (*Avena sativa* L.). Nucleus. 43:58-63.

Bazhina E, Kvitko O, Muratova E. 2008. Meiosis at microsporogenesis in Siberian fir (*Abies sibirica* Ledeb.) in natural populations and in an arboretum. Eurasian J For Res. 11:41-49. <https://hdl.handle.net/2115/33064>

Brandham P. 1971. The chromosome of the Liliaceae. III. Polyploidy and karyotype variation in the Aloineae. Kew Bull. 25:381-399. DOI: 10.2307/4103181.

Brandham P. 1976. The frequency of spontaneous structural change. In: Jones K, Brandham P, editors. Current Chromosome research. Elsevier North Holland Biomedical Press, Amsterdam, p. 77–87. <https://scholar.google.com/scholar_lookup?title=The%20frequency%20of%20spo ntaneous%20structural%20change&pages=77- 87&publication_year=1976&author=Brandham%2CP.E.>

Carter S. 1994. Flora of tropical east Africa. Aloaceae. Royal Botanic Gardens, Kew. <https://scholar.google.com/scholar_lookup?&title=Flora%20of%20Tropical%20E ast%20Africa%3A%20Aloaceae&publication_year=1994&author=Carter%2CS>

Cequea H, Díaz D, Imery J, Nirchio M. 2003. Cytogenetics study of paracentric inversions in *Tridax procumbens* (Compositae). Cytologia. 68:329-333. DOI: 10.1508/cytologia.68.329.

Danti R, Della G, Calamassi R, Mori B, Mariotti M. 2011. Insights into a hydration regulating system in *Cuppresus* pollen grains. Ann Bot. 108:299-306. DOI: 10.1093/aob/mcr144.

El Sherif F. 2017. *Aloe vera* leaf extract as a potential growth enhancer for *Populus* trees grown under *in vitro* conditions. Am J Plant Biol. 2:101-105. DOI: 10.11648/j.ajpb.20170203.13.

Farina V, Passafiume R, Tinebra I, Palazzolo E, Sortino G. 2020. Use of *Aloe vera* gel- based edible coating with natural anti-browning and anti-oxidant additives to improve post-harvest quality of fresh-cut ´Fiji´ apple. Agronomy. 10:515. DOI: 10.3390/agronomy10040515.

Future Market Insights (FMI). 2022. *Aloe vera* extracts market. <https://www.futuremarketinsights.com/reports/aloe-vera-extracts-market>

Fukui K, Nakayama S. 1996. Plant chromosomes: laboratory methods. CRC Press, Boca Ratón. <https://scholar.google.es/scholar?q=%22Plant+chromosomes:+laboratory+methods%22&hl=es&as_sdt=0&as_vis=1&oi=scholart>

Giannakoudakis D, Hosseini-Bandegharaei A, Tsafrakidou P, Triantafyllidis K, Kornaros M, Anastopoulos I. 2018. *Aloe vera* waste biomass-based adsorbents for the removal of aquatic pollutants: A review. J Environ Manage. 227: 354-364. DOI: 10.1016/j.jenvman.2018.08.064.

Grace O, Buerki S, Symonds M, Bisque F, Van-Wyk A, Smith G, Klopper R, Bjora C, Neale S, Demissew S, Simmonds M, Ronsted N. 2015. Evolutionary history and leaf succulence as explanations for medicinal use in aloes and the global popularity of *Aloe vera*. BMC Evol Biol. 15:29. DOI: 10.1186/s12862-015-0291-7.

Guancha-Chalapud M, Serna-Cock L, Tirado D. 2022. *Aloe vera* rind valorization to improve the swelling capacity of commercial acrylic hydrogels. Fibers. 10:73. DOI: 10.3390/fib10090073.

Hernández-Cruz L, Rodríguez-García R, Jasso D, Angulo-Sánchez J. 2002. *Aloe vera* response to plastic mulch and nitrogen. In: Janick J, Whipkey A, editors. Trends in new crops and new uses. ASHS Press, Alexandria, p. 570-574.

Imery J, Cequea H. 2002. Anormalidades cromosómicas en la microsporogénesis de *Aloe vera* (L.) Burm. f. (Aloaceae). Acta Bot Venez. 25:143-152. <https://www.jstor.org/stable/41740752>

Imery J, Cequea H. 2008. Autoincompatibilidad y protandría en poblaciones naturalizadas de *Aloe vera* de la península de Araya, Venezuela. Polibotanica. 09:113-125. <https://www.scielo.org.mx/scielo.php?pid=S1405-27682008000200005&script=sci_arttext>

Imery J, Cequea H. 2012. Estudio morfológico y citogenético del híbrido experimental *Aloe vera* (L.) Burm. f. x *A. jacksonii* Reyn. Rev. Cient. UDO Agric. 12:267-274. < https://www.bioline.org.br/abstract?id=cg12034>

Imery J. 2011. *Aloe vera*. In: Singh R, editor. Genetic Resources, Chromosome Engineering and Crop Improvement. Medicinal Plant, Vol. 6. CRC Press, Boca Ratón, p. 849-886.

Ishii M, Akiyoshi B. 2022. Plasticity in centromere organization and kinetochore composition: Lessons from diversity. Curr Opin Cell Biol. 74:47-54. DOI: 10.1016/j.ced.2021.12.007.

Jacobsen H. 1955. Succulent plants. Description, cultivation, and uses of succulent plants, other than cacti (authorized translation by Higgins V.). Ernest Benn Limited. London.

Kalinganire A, Harwood C, Slee M, Simona A. 2000. Floral structure, stigma receptivity and pollen viability in relation to protandry and self-incompatibility in silky oak (*Grevillea robusta* A. Cunn.). Ann Bot 86:133-148. DOI: 10.1006/anbo.2000.1170.

Levan A, Fredga K, Sandberg A. 1964. Nomenclature for centromeric position on chromosomes. Hereditas. 52:201-220. DOI: 10.1111/j.1601-5223.1964.tb01953.x.

Marasek-Ciolakowska A, Nishikawa T, Shea D, Okazaki K. 2018. Breeding of lilies and tulips: interspecific hybridization and genetic background. Breed Sci. 68:35-52. DOI: 10.1270/jsbbs.17097.

Missouri Botanical Garden (MBG). 2022. <http://tropicos.org>

Newton L. 2004. Aloes in habitat. In: Reynolds T, editor. Aloes. The Genus *Aloe*. CRC Press, Boca Ratón, p. 3-14.

Palmer R, Sun H, Zhao L. 2000. Genetics and cytology of chromosome inversions in Soybean Germplasm. Crop Sci. 40:683-687. DOI: 10.2135/cropsci2000.403683x.

Reynolds G. 1950. The aloes of South Africa. Aloes of South Africa books Fundation, Johannesburg.

Riley H, Majumdar D. 1979. The Aloineae; a biosystematic survey. University Press, Kentucky.

Rowley G. 1997. A history of succulent plant. Strawberry Press. California.

Saleem A, Naureen I, Naeem M, Murad H, Maqsood S, Tasleem G. 2022. *Aloe vera* gel effect on skin and pharmacological properties. Sch Int J Anat Physiol. 5:1-8. DOI: 10.36348/sijap.2022.v05i01.001.

Saniasiaya J, Salim R, Mohamad I, Harun A. 2017. Antifungal effect of Malaysian *Aloe vera* leaf extract on selected fungal species of pathogenic otomycosis species in *in vitro* culture medium. OMJ. 32:41-46. DOI: 10.5001/omj.2017.08.

Sapre A. 1975. Meiosis and pollen mitosis in *Aloe barbadensis* Mill. (*A. perfoliata* var. *vera* L., *A. vera* Auth. Non Mill.). Cytologia. 40:525-533. DOI: 10.1508/cytologia.40.525.

Silva M, Machado A, Da Rocha B, Castro A, De Castro T, Santana L, Murras R, Carvalho B. 2015. Technical aspects of the production process of *Aloe vera* gel biodiesel: pre- treatment and transesterification. SHEWC. 15:25-28. DOI: 10.14684/SHEWC.15.2015.25-28.

Singh A, Mohapatra S, Pani B. 2016. Corrosion inhibition effect of *Aloe vera* gel: Gravimetric and electrochemical study. JIEC. 33:288-297. DOI: 10.1016/j.jiec.2015.10.014.

Singh P, Hundal JS, Patra AK, Wadhwa M, Sharma A. 2021. Sustainable utilization of *Aloe vera* waste in the diet of lactating cows for improvement of milk production performance and reduction of carbon footprint. J Cleaner Prod. 288:125118. DOI: 10.1016/j.jclepro.2020.125118.

Smith G, Van-Wyk B. 2008. Aloes in Southern Africa. New Holland Pub. Cape Town.

Sokal R, Rohlf R. 1979. Biometría, principios y métodos estadísticos en la investigación biológica. Blume. Madrid.

Song Y, Yang F, Ma M, Kang Y, Hui A, Quan Z, Wang A. 2022. Green synthesized Se– ZnO/attapulgite nano-

composites using *Aloe vera* leaf extract: Characterization, antibacterial and antioxidant activities. LWT. 165:113762. DOI: 10.1016/j.lwt.2022.113762.

Stebbins G. 1971. Chromosomal evolution in higher plants. Edward Arnold Pub. London. Sunderland N, Roberts M. 1977. New approaches to pollen culture. Nature. 270:236-238. DOI: 10.1038/270236a0.

Swamy B, Krishnamurthy K. 1980. From flower to fruit, Embryology of flowering plants. Tata McGraw-Hill Pub. Company. New Delhi.

Tucuch-Haas C, Cen-Caamal J, Kancab-Uc, Tucuch-Haas J. 2022. Uso de gel de *Aloe vera* en la producción de plántulas de *Capsicum chinense*. Biotecnia. 24:116-121. DOI: 10.18633/biotecnia.v24i1.1542.

Van-Wyk B, Smith G. 1996. Guide to the Aloes of South Africa. 5th Ed. Briza Publications, Pretoria.

Watson D, Gilman M, Witkowski J, Zoller M. 2003. DNA ricombinante. Zanichelli editore S.p.A., Bologna.

Caryologia
International Journal of Cytology, Cytosystematics and Cytogenetics

Firenze University Press
www.fupress.com/caryologia

OPEN ACCESS

Citation: Seyedeh Mahsa Hosseini, Sepideh Kalatejari, Mohsen Kafi, Babak Motesharezadeh (2022). Assessment of the absorption ability of nitrate and lead by japanese raisin under salt stress conditions. *Caryologia* 75(4): 37-48. doi: 10.36253/caryologia-1827

Received: April 18, 2022

Accepted: December 04, 2022

Published: April 28, 2023

Data Availability Statement: All relevant data are within the paper and its Supporting Information files.
The data that support the findings of this study are openly available in [repository name e.g "Zenodo"] at http://doi.org/[10.5281/zenodo.6344758].

Competing Interests: The Author(s) declare(s) no conflict of interest.

Assessment of the absorption ability of nitrate and lead by japanese raisin under salt stress conditions

Seyedeh Mahsa Hosseini[1], Sepideh Kalatejari[1], Mohsen Kafi[2,*], Babak Motesharezadeh[3]

[1] *Department of Horticultural Science and Agronomy, Science and Research Branch, Islamic Azad University, Tehran, Iran*
[2] *Department of Horticultural Science, University College of Agriculture & Natural Resource, University of Tehran, Karaj, Iran*
[3] *Department of Soil Science, Faculty of Agricultural Engineering & Technology, University College of Agriculture & Natural Resources, University of Tehran, Karaj, Iran*
Corresponding author. E-mail: mkafi@ut.ac.ir

Abstract. Heavy metals pollution is an important challenge that was cussed by human activity, this stress decreases under salinity. The aim of this study was to investigate the ability of Japanese raisin in the absorption of nitrate (0, 30, and 60 mgL^{-1}) and lead (0, 300, and 600 mgL^{-1}) under salinity stress (0 as control and 3 and 6 dSm^{-1}). Results showed that the studied plant continued to uptake nitrate and potassium under stress conditions of Pb and salinity. Although Na and Cl uptake were observed as a defense mechanism in the plant, the K/Na ratio, and K content increased from 1 to 6 and from 1.8 to 5%, respectively. Also, the most appropriate physiological responses were observed at treatments under contamination level of 300 mg Pb and salinity level of 3 dSm^{-1}, so that the synthesis of malondialdehyde (MDA) and enzymatic activity increased at these levels of HMs and salinity. Based on the results, the studied species were able to uptake moderate concentrations of Pb (34.1-71mg kg^{-1}) under experimental conditions. Hence, its potential for the clean-up of some contaminants in the environment can be considered by researchers for further research.

Novelty statement. This study investigated the cleaning up of some heavy metals and nitrate from the environment and plants' physiological responses under stressful conditions. The plant species (Japanese raisin) characteristics and the results have enough novelty and will be published for the first time. Most hardwood trees such as walnut, oak, beech, poplar, etc. have a slow growth rate. But Japanese raisin tree a new and unknown plant in Iran has very important features. This tree is one of the few trees that in addition to having hardwood, has a very high growth rate. Which can be useful in creating artificial forests, Landscapes, as well as in industrial applications, buildings, and furniture industries. So far, no special research has been done on the phytoremediation characteristics of this plant and the selection of this plant in the present study and the study of the ability of this plant to absorb nitrate and lead under salinity stress is a completely new and innovative topic.

Keywords: Antioxidant enzymes, Heavy metal, Phytoremediation, Proline, Malondialdehyde, Salinity.

1. INTRODUCTION

Metal pollution is harmful for human health and the environment. Human activities have been considered an important factor in the contamination of the soil with heavy metals (HMs) (Akinci and Guven 2018; Motesharezadeh et al, 2016). The presence of HMs reduces soil fertility, crop yield, and soil microbial activity (Pinto et al, 2004; Sumiahadi and Acar, 2018). Lead (Pb), a HM pollutant in industrial ecosystems, is important in plant life because of its easily absorption by the plant roots, which is induced by its high accumulation in the surface area of the soil (Mosaferi et al, 2008; Wang et al, 2019). In addition to natural processes, Pb is also produced through the artificial sources (exhaust fumes from automobiles, factories, battery tanks, and pesticides). After Pb is absorbed by roots, it causes changes in metabolic activities of plants, disrupting their growth and development (Sharma and Dubey, 2005; Oguntade et al, 2018). Presence of Pb, leads to a disruption of membrane carriers' activity of the root cells, depleting nutrients such as magnesium, calcium, and iron. As a result of an experiment, deficiency symptoms of these nutrients were reported in Pb-treated plants (Sharma and Dubey, 2005). Moreover, the overuse of nitrate fertilizers in agriculture fields leads to nitrate pollution of ground and surface waters (Castro-Rodríguez et al, 2016).

Climate change and water deficit is the important challenge in agriculture activities all over the world and soil salinity is the one of most important problem that cause by these challenges (Isayenkov and Maathuis, 2019). There are many studies have reported that salinity stress induced by NaCl restricts agriculture and crop yield (Isayenkov and Maathuis, 2019). Plant resistance to salinity depends on some mechanisms such as antioxidants activity, ion homeostasis, biosynthesis of osmolytes, and gene expression. Phytoremediation is a useful technic based on the living plant's ability to absorb ionic compound by their roots or leaves and clean up soil, air and water contamination (Berti and Cunningham, 2000). There are many reports on phytoremediation, such as phytoremediation of high levels of nitrate with poplar trees (Castro-Rodriguez et al, 2016), zinc (Zn) and Pb nitrates with sunflowers (Adesodun et al, 2010), nitrate with *Salvinia molesta* (Ng and Chan, 2017) and Zn, Cd, and Pb with *Typha angustifolia* and *Eichhornia crassipes* (Sricoth et al, 2018). Generally, stresses such as salinity and heavy metals in which salinity increases the uptake of heavy metals, occur simultaneously in the environment. The results of a study indicated that the presence of Cd along with NaCl in the root environment of four barley cultivars significantly reduced soil Cd concentration and increased its uptake by plants (Huang et al, 2007). Similarly, Abbasi et al. (2013) investigated the effect of irrigation water salinity on the rate of heavy metals uptake in *Potamogeton berchtoldi* and reported that the concentration of heavy metals (Pb and Cd) in plant increased with the increasing salinity up to 4 and 6 dSm^{-1}, respectively. In general, based on the results of the numerous studies, it can be concluded that under conditions of HMs (such as Pb and Cd) and salinity stresses, the plant's nutritional needs for nutrients such as N, P and K will increase (Khoshgoftarmanesh, 2010; Yan et al, 2020). In fact, the recommendation for more application of these nutrients under stress conditions, is a strategic management to prevent reducing plant dry matter. It should be mentioned that nitrate, in principle, increases the resistance to salinity, which has been similarly reported in several studies (Bai et al, 2021).

However, there are limited reports on the phytoremediation ability of Japanese raisin or its ability to grow in the contaminated soils. Based on this background, this study was aimed to assess the potential use of Japanese raisin for the phytoremediation of a nitrate/Pb polluted soil under conditions of salt stress.

2. MATERIAL AND METHODS

2.1. Plant material and growth condition

One-year old seedlings of Japanese raisin (*Hovenia dulcis* L.) were prepared from Hirkania greenhouse (Nowshahr, Mazandaran, Iran). Seedlings were grown in plastic bags (25×30 cm), and fertilized with NPK fertilizer and a Hoagland based solution during the test period (Motesharezadeh et al, 2016), also the average temperature and the humidity were 25 °C and 70%, respectively (Ramesh et al, 2006). The seedlings were kept for five months and then harvested. Due to the stress induced by moving seedlings from a distant place in the north of the country, it was necessary to apply some treatments to plants reinforcement (Table S[1]1). Therefore, to improve the seedlings growth and before the application of experimental treatments, complete fertilizer and Hoagland nutrient solution were used and also leaching was considered.

[1] Supplementary data.

2.2. Experimental design

To execute the experiment, a neutral culture media (a combination of 70% non-enriched cocopeat and 30% perlite) was used. In order to investigate the capability of Japanese raisin for the phytoremediation of a NO_3^- / Pb polluted soil under conditions of NaCl stress, a factorial greenhouse trial was arranged in a completely randomized design with four replications. The treatments consisted of (1) NaCl salinity as the primary factor at three levels of 0 (control), 3, and 6 dSm^{-1}, according to previous reports (Salimi et al, 2012); (2) Nitrate derived from potassium nitrate, as the secondary factor, was applied at three levels (0, 30, and 60 mgL^{-1}) (Gheshlaghi et al, 2015); and (3) Pb form the source of lead nitrate (0, 300, and 600 mgL^{-1}) (Shabani et al, 2015) as the third factor. To have only the effect of nitrate, equivalent of potassium added in the treatments (from the source of potassium nitrate), potassium sulfate was added to other pots. In order to avoid the negative effect of possible stress on plant, potassium nitrate was applied during the holding period every two weeks via irrigation water.

2.3. Biochemical measurements

2.3.a Lead content measurement

Dry ashing method was used to analyze plant samples and measure Pb (Wallis, 1996). During the method, to measure metals, plants organic matter is destroyed with controlled heat. Based on the method, one gram of dried and powdered sample of the plant was poured into a crucible and placed in an electric oven at 550 degrees for 4 hours. After leaving the crucibles out of the furnace and reaching ambient temperature, samples were transferred to small beakers using 10 ml of 2 M hydrochloric acid. Then, the beakers were placed on an electric stove until the first white vapors appeared. Next, after reaching the ambient temperature, the contents of beakers were filtered through a filter paper inside a 100 ml volumetric flask and made up to volume with distilled water. Finally, Pb concentrations were reported in samples extract by use of ICP-OES (Inductively Coupled Plasma Atomic Spectroscopy). Pb uptake was measured and reported by multiplying its concentration by the plant dry matter (Sharma et al, 2012).

2.3.b Total Nitrogen and Nitrate content measurement

Total concentration of nitrogen (N) in plant samples was measured by Kjeldahl method (Horneck and Miller,1998). In this method ground plant material were digested to H_2SO_4 at high temperatures by the help of metal catalyst. Total nitrogen of plant was changed to ammonium (NH_4^+), which is then by titration the concentration of N was quantified. To measure the nitrate of the plant samples, ion-selective electrode method was used (Miller, 1988).

2.3.c Potassium/sodium ratio and chlore content measurements

Sodium and potassium concentrations were determined based on the method of wet digestion with hydrochloric acid using flame photometer ELEA (Ryan et al, 2002).

In order to measure the chlore (Cl) content in the plant material (Liu, 1998), after extraction, the Cl in the filtrate was analyzed using the colorimetric method on the TRAACS 800TM Auto-Analyzer. In this method, the sample is mixed with the color reagent and dialyzed into the color reagent again. The procedure is based on the release of thiocyanate ions from mercuric thiocyanate by Cl ions in the sample. The liberated thiocyanate reacts with ferric iron to form a red color complex of ferric thiocyanate. The color of the resulting solution is stable and directly proportional to the original Cl concentration. The color complex is measured at 480 nm using a 10-mm flow cell. Nitrite (NO_2), sulfide, cyanide, thiocyanate, bromide, and iodine ions cause interferences when present in sufficient amounts.

2.4. Antioxidant enzymes activity measurement

In order to evaluate the effect of salinity, nitrate and lead contamination stresses on plant physiological responses, the changes in enzymatic activity were measured. Among plant enzymes, catalase (CAT) and superoxide dismutase (SOD) are considered as sensitive enzymes indicating plant resistance mechanisms under stress conditions (Khadem Moghadam et al, 2016). Hence, these two enzymes were selected for this goal of the present study. Total protein content was determined following the method described by Bradford (1976). Protein content was determined using spectrophotometry at a wavelength of 595 nm. Also, the modified method of Chance and Maehly (1955) was used to measure the activity of peroxidase (POD) enzyme. The activity of superoxide dismutase, the basis of which is its ability to inhibit the photochemical reduction of nitro blue tetrazolium (NBT), was determined according to the method described by Dhindsa et al. (1981).

2.5. Soluble carbohydrate content measurement

The method of Irigoyen et al. (1992), was used to measure soluble carbohydrates. For this purpose, leave sample were ground in liquid nitrogen, 100 mg of them were blended with 5 mL of 70 % ethanol (wv^{-1}) for 5 min, then centrifuged at 3500 rpm for 10 min at 4 °C. After that 200 mL of the supernatant were added to 1 mL of an anthrone solution, then the absorbance was read by UV/vis spectrophotometer at 625 nm.

2.6. Malondialdehyde level assessment

Malondialdehyde (MDA) concentration was measured by thiobarbituric acid method by spectrophotometry. Its concentration was calculated using the extinction coefficient MDA-TBA for the complex (Dandekar et al., 2002).

2.7. Proline content measurement

To measure proline level, the procedure of Bate et al. (1973) were used. First, 10 ml of acid sulfuric were added to 100 mg of fresh leaf, they were then passed through filter paper. After 2ml ninhydrin and 2ml acid acetic glacial were added to 2 ml of extract and kept in benmary counter for 1 h, then toluene was added to them. After 2 h the supernatant was extracted. The absorbance at 520 nm was recorded.

2.8. Lipid peroxidization measurement

To quantify the amount of this enzyme, the modified Chance and Maehly (1955) method was used. In this method, 1 ml of potassium phosphate buffer (pH = 6.7) was poured into the cuvette and 17.6 µl of hydrogen peroxide and 17.6 µl of leaf extract were added to it. The resulting solution was immediately read in a spectrophotometer at a wavelength of 240 nm for 2 minutes at intervals of 15 seconds to calculate the activity of this enzyme according to the amount of light absorption.

2.9. Statical analysis

The present study was executed based on a factorial trial arranged in a completely randomized design (CRD) with four replications. Data were analyzed using SAS 9.2 and MSTATC software. Differences between treatments were determined following Duncan's Multiple Range Test (DMRT), ($P \leq 0.05$). figures were drawn using Excel 2010 software.

3. RESULTS

3.1. Biochemical content measurements

3.1.a. Plants lead level

According to the variance analysis results, the interactions of salinity, NO_3^-, and Pb significantly affected Pb concentration (Table S2). Based on the means comparison results, salinity at levels of 3 and 6 dSm^{-1} reduced Pb content by 13% and 36%, respectively; nitrate at levels of 30 and 60 mgL^{-1} decreased Pb content by 11% and 12%, respectively; and Pb at levels of 300 and 600 mgL^{-1} increased Pb content by 45% and 53%, respectively. Also, the highest Pb content (69 mg kg^{-1}) belonged to the treatments of S1N0Pb2 and S0N0Pb2, and the lowest one was observed at treatments with no added Pb (Fig. 1).

To better understand the ability of the studied plant how cope with stress and phytoremediation, the uptake rate was calculated for different treatments (Fig. 2). Results showed that in high salt concentration the high uptake of lead was observed in high nitrate concentration. Accordingly, Pb uptake and accumulation can be considered as a reliable indicator for phytoremediation under salinity stress conditions.

3.1.b. Plants total nitrogen and nitrate level

Regarding nitrogen content, it is understandable that there was a significant ($P \leq 0.01$) interaction between salinity, NO_3^-, and Pb. Additionally, NO_3^- significantly affected shoot nitrogen content ($P \leq 0.01$) (Table S2). The application of 30 and 60 mgL^{-1} NO_3^- increased N content by 10% and 18%, respectively. The highest N content (7.3%) was

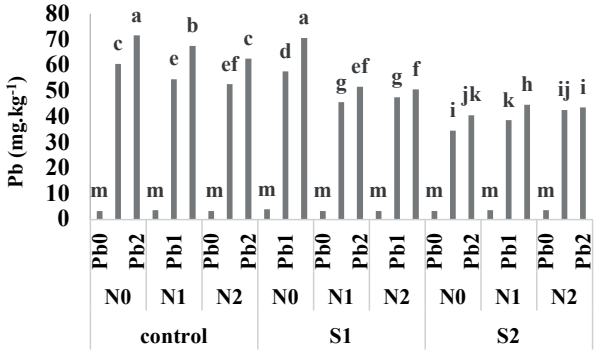

Figure 1. Lead (Pb) content in Japanese raisin in response to salinity (S0: Control, S1: 3 and S2: 6 dSm^{-1}), nitrate (N0: 0, N1: 30 and N2: 60 mgL^{-1}), and Pb (Pb0: 0, Pb1: 300 and Pb2: 600 mgL^{-1}). Values in each group followed by the same letter are not significantly different according to DMRT at $P \leq 0.05$

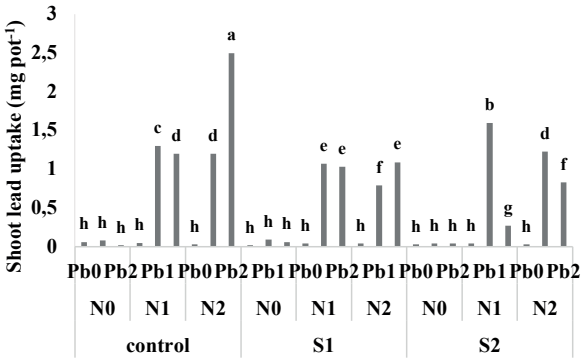

Figure 2. Shoot lead (Pb) uptake in Japanese raisin in response to salinity (S0: Control, S1: 3 and S2: 6 dSm^{-1}), nitrate (N0: 0, N1: 30 and N2: 60 mgL^{-1}), and Pb (Pb0: 0, Pb1: 300 and Pb2: 600 mgL^{-1}). Values in each group followed by the same letter are not significantly different according to DMRT at P≤0.05

observed in S0N2Pb0 and S2N1Pb2 treatments, while the lowest N content (3.3%) was recorded for S1N0Pb2.

Based on the results, the interaction of salinity, NO_3^-, and Pb, significantly affected shoot NO_3^- content (Table S2). NO_3^- content reduced by 11% and 21% with the application of 3 and 6 dSm^{-1} salinity. However, application of 30 and 60 mgL^{-1} of NO_3^- increased NO_3^- content by 24% and 36%, respectively. The interaction between all three treatments showed that the highest NO_3^- content (0.61%) was recorded for the treatment of S0N1Pb0, while the lowest NO_3^- content (0.05%) was observed at the treatment of S2N0Pb2.

3.3.c Plants sodium, potassium and chlore level

In accordance with the obtained results, the interactions of salinity, NO_3^-, and Pb significantly (P≤0.01) affected shoot potassium content (Table S2). The lowest values of shoot K concentration were observed at salinity treatments of 3 and 6 dSm^{-1}, which were reported to be 1.85% and 1.95%, respectively; while NO_3^- application at levels of 30 and 60 mgL^{-1} increased K by 4% and 22%, respectively. The interaction between the treatments indicated that the highest shoot K concentration (5.05%) belonged to the treatment of S0N2Pb0, that was almost 3 times more than the lowest one at treatment of S1N1Pb0, S1N0Pb0 and S2N0Pb2 (1.85%).

As results showed, the interactions of salinity, NO_3^-, and Pb significantly (P≤0.01) affected shoot Na concentration (Table S2). Considering to the data, it can be found that shoot Na concentration increased up to the 39% by salinity application of 3 or 6 dSm^{-1}, while NO_3^- application at levels of 30 and 60 mgL^{-1} decreased shoot Na content by 26% and 25%, respectively. Based on the interactions of studied factors, the highest shoot Na concentration)2.77% (belonged to the treatments of S2N0Pb0, S2N1Pb0 that was fivefold of the S2N2Pb2 treatment as the lowest one.

Considering to the K/Na ratio shown in Table 2, it can be found that the accumulation of K effectively controlled salinity stress. The highest ratio was recorded in the SIN0Pb1treatment that was six times more than S2N0Pb2 treatment as lowest one.

According to variance analysis results it is clear that the interactive effects of salinity, NO_3^-, and Pb, significantly affected Cl concentration (Table S2). Also, the results of means comparison ~~of~~ indicated that salinity at levels of 3 and 6 dSm^{-1} increased Cl content by 17% and 30%, respectively; Nitrate at levels of 30 and 60 mgL^{-1} increased Cl content by 9% and 2%, respectively; and Pb at levels of 300 and 600 mgL^{-1} increased Cl content by 4.9% and 6.8%, respectively. The highest (4.7%) and the lowest (1.4%) values of Cl content were recorded for the treatments of S2N1Pb2 and S0N0Pb0, respectively. High Cl concentration was observed in the treatments with high salinity and nitrate concentration.

3.2. Antioxidant enzymes activity

Results showed salinity significantly affected the activities of antioxidant enzymes (Table S3), so that the levels of 3 and 6 dSm^{-1} increased the activity of POD by 11% and 6%, respectively, while they reduced the activities of SOD by 2 and 15% and CAT by 17 and 63% (Table 1), respectively. Additionally, $NO3^-$ at levels of 30 and 60 mgL^{-1} significantly decreased the activities of POD by 12% and 20%, SOD by 9% and 24%, and CAT by 20% and 15% (Table 1), respectively. Furthermore, Pb at levels of 300 and 600 mgL^{-1} significantly increased the activities of POD by 12% and 11% and CAT by 27% and 34%, respectively, while they reduced the activity of SOD by 39% and 50%, respectively (Table 1). Considering to the results, it can be found that the highest enzymatic activity of SOD, POD and CAT, which are the best indicators of assessing stress conditions, were observed at treatments of 3 dSm^{-1} salinity + 30 mgL^{-1} nitrate (without Pb), 3 dSm^{-1} salinity + 600 mgL^{-1} Pb (without nitrate) and 600 mgL^{-1} Pb + 30 mgL^{-1} nitrate application (without salinity), respectively. (Table 1). In other words, with increasing the studied stresses levels including Pb contamination up to 600 mg, salinity up to 6 dSm^{-1} and nitrate up to 60 mgL^{-1}, the enzymatic activity reduced indicating the reduction of plant defense mechanisms under severe stress conditions.

Generally, the relationships between biochemical traits and nutrients status can provide a clear under-

Table 1. Activities of antioxidant enzyme in response to treatments.

Salinity (dSm^{-1})	Nitrate (mgL^{-1})	Pb (mgL^{-1})	POD	SOD	CAT
Control	0	0	0.52^{d*}	161.9^{c}	5^{kl}
		300	0.29^{lmn}	82.15^{ijk}	56.37^{cd}
		600	0.36^{hij}	87.87^{ij}	21.83^{gh}
	30	0	0.19^{p}	68.63^{lmn}	3.01^{l}
		300	0.35^{h-k}	93.02^{i}	54.08^{cd}
		600	0.38^{ghi}	128.4^{ef}	86.26^{a}
	60	0	0.45^{ef}	120.7^{fg}	30.8^{f}
		300	0.56^{cd}	140.1^{d}	58.77^{c}
		600	0.58^{c}	117.5^{g}	67.41^{b}
3	0	0	0.34^{ijk}	67.05^{mn}	72.25^{b}
		300	0.34^{ijk}	132.9^{de}	50.19^{d}
		600	0.8^{a}	175.5^{b}	55.34^{cd}
	30	0	0.54^{cd}	188.5^{a}	43.41^{e}
		300	0.69^{b}	154.3^{c}	11.05^{jk}
		600	0.31^{klm}	59.99^{no}	9.76^{jkl}
	60	0	0.23^{op}	52.44^{o}	53^{cd}
		300	0.27^{mno}	74.59^{klm}	10.55^{jkl}
		600	0.33^{jkl}	86.29^{ij}	14.98^{hij}
6	0	0	0.48^{e}	115.2^{gh}	3.52^{jl}
		300	0.57^{c}	132.3^{de}	25.93^{fg}
		600	0.36^{hij}	105.6^{h}	27.79^{fg}
	30	0	0.42^{fg}	106.3^{h}	14.84^{hij}
		300	0.36^{hij}	79.4^{jkl}	12.66^{ij}
		600	0.38^{ghi}	89.69^{ij}	20.79^{gh}
	60	0	0.23^{op}	49.88^{o}	8^{jkl}
		300	0.39^{gh}	114.4^{gh}	18.7^{hi}
		600	0.26^{no}	58.77^{no}	10.07^{jkl}

* Means within a column followed by the same letters are not significantly different at $P \leq 0.05$ according to Duncan's multiple range test.

standing of positive and negative correlations among whole studied parameters. For this purpose, the correlation between traits were calculated. The results showed the high positive correlation between proline and MDA by R^2=0.879, N and K by R^2= 0.718, soluble carbohydrate and MDA by R^2= 0.612 and lipid peroxidase and MDA by R^2= 0.574 (Table 2).

3.3. Soluble carbohydrates content

To evaluate the biochemical and physiological responses of plant against studied stresses, soluble carbohydrates were measured. Based on the results, the most values of soluble carbohydrates were reported at treatments of S1N0Pb2 and S0N0Pb2, indicating that HMs stress had more effect on this trait in comparison with salinity. The highest content of soluble carbohydrate was recorded in S0N0Pb2 that was 3 time more than S2N2Pb2 as lowest treatment.

3.4. Malondialdehyde level of plants

Also, there was a significant difference in proline concentration among different studied treatments compared to control. Malondialdehyde was measured as an important indicator of plant response to abiotic stresses. Results showed, the most values of this parameter were observed at moderate levels of Pb application (without salinity) and also the synthesis of this biochemical product significantly reduced by the expansion of HMs, salinity and nitrate stress. Lowest value of MDA was recorded in S2N2Pb2 treatment that show this parameter were deceased in high salt, nitrate and lead concentration.

3.5. Proline level of plants

The most values of proline were observed at moderate levels of Pb application (without salinity) and also the synthesis of this biochemical product significantly reduced by the expansion of HMs, salinity and nitrate stress. The highest value of proline was recorded in the S0N0 treatment that was twofold higher than S2N2 treatment as last one.

3.6. Lipid peroxidation

The increasing trend was observed for lipid peroxidation and the most values of this parameter belonged to the treatments with low levels of stress (without salinity and without nitrate). Highest content was observed in the S0N0 treatment, while the treatment with high level of nitrogen and lead ranked last treatment.

4. DISCUSSION

4.1. Biochemical traits affected by different level of nitrate and lead under salinity stress

4.1.a lead uptake and concentration were affected under different nitrate level

Based on the results, Pb pollution caused more salinity (Na) uptake. In other words, salinity can increase HMs stress, which means the intensification of the stress induced by salinity and also has been

Table 2. Pearson correlation coefficients between characteristics.

	N	NO3	K	Na	K/Na	Cl	Pb Con.	Pb Uptake	Sol. Carb	Proline	MDA	Lipid	POX	SOD	CAT
N	1														
$NO3^-$	0.495**	1													
K	0.768**	0.575**	1												
Na	-0.093ns	0.071ns	0.049ns	1											
K/Na	0.468**	0.359**	0.520**	-0.721**	1										
Cl	0.497**	0.409**	0.412**	0.104ns	0.249*	1									
Pb Con.	0.340**	0.158ns	0.344**	-0.331**	0.259*	0.145ns	1								
Pb Uptake	-0.209ns	-0.217ns	-0.198ns	-0.174ns	0.086ns	0.060ns	-0.149ns	1							
Sol. Carb	-0.084ns	0.083ns	-0.065ns	0.215ns	-0.140ns	0.022ns	-0.484**	0.008ns	1						
Proline	-0.006ns	0.179ns	0.189ns	0.366**	-0.180ns	-0.094ns	-0.249*	-0.222*	0.504**	1					
MDA	-0.126ns	0.064ns	-0.054ns	0.009ns	0.016ns	-0.136ns	-0.418**	0.042ns	0.818**	0.612**	1				
Lipid	0.056ns	0.215ns	0.195ns	0.302ns	-0.067ns	-0.071ns	-0.234*	-0.288**	0.475**	0.879**	0.574**	1			
POX	-0.221*	-0.146ns	-0.032ns	0.259*	-0.293**	0.131ns	-0.205ns	0.165ns	0.256*	0.106ns	0.122ns	0.004ns	1		
SOD	-0.113ns	-0.140ns	-0.085ns	0.037ns	0.067ns	-0.285**	0.218ns	0.073ns	0.328**	0.158ns	0.363**	0.206ns	0.386**	1	
CAT	-0.213ns	-0.270*	-0.099ns	-0.299**	0.163ns	-0.240*	-0.050ns	-0.219*	0.202ns	0.302**	0.373**	0.276*	-0.081ns	0.222*	1

** represent significant difference at $P \leq 0.01$, * represent significant difference at $P \leq 0.05$, n.s represent no significant difference

considered by many researchers. Generally, when the stress inhibits plant growth and reduces transpiration, the increase in contaminant uptake will be stopped or reduced. Accordingly, in the present experiment, the salinity stress without HMs contamination, led to reduce contaminant (Pb) uptake. The critical level of Pb contamination in soil, considered by researchers, is 50 mg kg^{-1} soil (Prasad, 2004). Also, the normal range of Pb in plant tissues is between 0.2 to 20 mg kg^{-1}, but its critical and contamination levels in plant is more than 20 mg kg^{-1}, reducing the yield and plants dry matter (Alloway, 1990). Accordingly, high concentrations (34.6-71.6 mg kg^{-1}) of Pb accumulated in treatments of Pb contamination indicating the ability of the studied species for HMs phytoremediation. In fact, the studied plant has an appropriate potential for phytoremediation under conditions of simultaneous stresses.

4.1.b N and Nitrate level improved the plant resistance under salinity stress

The percentage of N and NO_3 and the accumulation of K, Na and Cl represent the intensity of plant response to the studied stresses (HMs and salinity). Results indicated that salinity or Na content reduced by supplying nitrate. It should be mentioned that nitrate increases plants resistance to salinity, which also has been reported in numerous researches (Kafkafi et al, 1992). Some researchers believe that reduction of nitrate concentration is because of the negative interaction between Cl and nitrate and antagonistic effect of Cl on nitrate uptake. While, others attribute it to the plant's response under saline conditions reducing water uptake (Lauter and Munns, 1986). The results of a study showed that phytoremediation of HVs (Co, Cu, Cr, Ni, and Pb) pollution by aquatic hyacinth was only effective at high concentrations of nitrate and by decreasing nitrate concentration the phytoremediation efficiency decreased (Tangahu et al, 2011; Bai et al, 2021). Loska and Wiechula (2003) reported that the presence of any type of contaminants in water and soil resources led to pollutants accumulation in plant organs, changing enzymatic activities. Similarly, the results of the present study are consistent with those of recent studies (Dayani et al, 2009; Husejnovic et al, 2018).

4.1.c High potassium to sodium ratio improve phytoextraction in contract to Chlore

Khoshgoftar et al. (2004) reported that HMs uptake from the soil solution increased with the increase of NaCl level, while no such effect was observed for $NaNO_3$. It is assumed that chloride ion positively affected HMs (Pb and Cd) solubility in soil and their uptake by plants. Generally, chloride ion increases the dynamics and adsorption capacity of the metals. Having high salinity tolerance, is another important strategy of plants for resistance against salinity. For example, grasses and Atriplex/Salicornia are capable to grow at the salinity levels up to 1.2-1.7 dSm^{-1} and 21-28 dSm^{-1}, respectively.

Regarding to the results of the present study, it seems that the Japanese raisin (*Hovenia dulcis*) can be considered as a relatively tolerant species at moderate salinity levels due to its appropriate responses to salinity levels of 3 and 6 dSm^{-1}, the accumulation of K and Na and also the high ratio of K/Na in different stress treatments. In addition to salinity stress, Pb contamination also has a specified critical level based on soil and plant studies. Potassium accumulation is probably a defense mechanism and increasing the ratio of K/Na is a strategic way for resistance to salinity stress (Kibria and Hoque, 2015). Generally, these results indicated the intensity of the effect of stress treatments (HMs and salinity) on the one hand and the plant resistance responses to Pb and salinity. Also, Kibria and Hoque (2015) conducted a field experiment to investigate the effect of the mitigation of soil salinity on rice by application of K and Zn fertilizers. The results demonstrated that K^+/Na^+ ratio in the grains significantly affected by the application of K. Therefore, it may be induced by the fact that the application of higher doses of K and Zn fertilizers could alleviate the adverse effects of salinity in rice via increasing nutrient uptake and maintaining a higher K^+/Na^+ ratio. Boudaghi Malidareh et al. (2014) reported a significant relationship between the amount of K fertilizer and HMs pollution (cadmium concentration) in the soil. Furthermore, the results of a study demonstrated that soil salinity can be improved by the application of nitrogen and potassium fertilizers (Shanker, 2005). Azari et al. (2005) investigated the role of potassium on nitrate and Cd contamination in potato and onion. They found that the concentrations of nitrate and cadmium in potato and onion tubers significantly decreased following the application of potassium and zinc fertilizers, and the highest nitrate and Cd contamination was recorded for the treatment with the unbalanced fertilizer use. Under salinity stress, the concentrations of potassium and phosphorus in the stem significantly decreased, while the concentration of sodium in the leaves increased. The similar results were also reported by Khalilpoor and Jafarinia (2017) and Yousefinia and Ghasemiyan (2016).

4.2. Antioxidant enzymes activity was affected by different levels of HM and salt stress

It seems that the increase in enzymatic activity is one of the main strategies tolerating HMs contamination and salinity stresses (Malar et al, 2016). Accordingly, the changes in activity of SOD enzyme are considered as the appropriate indicators of stress management. The results of the present study showed that the increased SOD activity under stress conditions was due to the plant's survival on the one hand and contaminants purification on the other hand. However, the simultaneous increase in the stresses of HMs contamination, salinity and nitrate, up to the maximum levels, reduced the activity of all three studied enzymes. Malar et al. (2016) reported that plants use different mechanisms to cope with HMs toxicity. Alizadeh (2012) reported that the contamination lead and cadmium disrupted the growth of two poplar species and plant biomass significantly reduced at high levels of pollutants. Furthermore, the reduced vegetative growth caused by HMs stress in plants may be because of the suppressed activities of catalase and superoxide dismutase (Schutzendubel and Polle, 2002). Jabeen and Ahmad (2012) reported that salinity increased the activity of peroxidase but decreased that of catalase. Similar results were also reported on canola (Abili and Zare, 2014) and maize (AbdElgawad et al, 2016). Michalak (2006) has found that antioxidant enzymes can scavenge reactive oxygen species (ROS) when the plant grows under HMs stress. Also, Verma and Dubey (2003) observed that Pb toxicity changed the activity of antioxidant enzymes in rice plants. Barandeh and Kavousi (2017) reported that the activities of antioxidant enzymes, including superoxide dismutase, catalase, and ascorbate peroxidase significantly increased in lentil seedlings with the increasing in Cd concentration. Similarly, Hendry et al. (1992) illustrated that HMs are also a reason for oxidative stress via the production of free radicals of reactive oxygen which can react with lipids and finally lead to the lipid peroxidation, membrane damage, and enzymatic inactivation (Dixi et al, 2001). Similar results were reported by Verma and Dubey (2003) and AbdElqawad et al. (2016). Generally, it has been reported that stress increases the activities of antioxidant enzymes (Meloni et al, 2003) but at an intolerable intensity obviously reduces their activities (Amiriyan Mojarad et al, 2018). The results of the present study in agreement with previous reports showed the increment of SOD, POD and CAT by increasing the HM and salt stresses level.

4.3. Soluble carbohydrate was affected by different levels of HM and salt stress

Soluble carbohydrate content was affected by different nitrate level and stress condition. The results of current study showed the decreasing trend by increasing salt and lead level. Weisany et al. (2014) reported that at all three growth stages (pre-flowering, post-flowering, and seed filling), salinity stress decreased shoot fresh and dry weights, plant yield, root and leaf also soluble carbohydrate content of these tissue in soybean, but the

application of zinc fertilizer alleviated these negative effects. Decreased biomass production induced by HMs stress may be because of a disturbance in uptake and transmission of nutrients and water into the aerial parts of plants (Sudova and Vosatka, 2007).

4.4. Malondialdehyde synthesis were changed under HM and salt stress

The synthesis of biochemical compounds such as malondialdehyde has been considered as another important mechanism to withstand stress conditions. The stress-adapted plants seem to be more capable to synthesis these metabolites. There are numerous studies confirming the increased synthesis of malondialdehyde and some plant biochemical/enzymatic compounds as a response to stress conditions (Juknys et al, 2012; Aljahali and Alhassan, 2020). Based on the results of the present study, there was a significant and negative correlation between shoot Pb concentration with MDA synthesis and also between the activity of POX with the K/Na ratio. The similar results have been reported by Aljahali and Alhassan (2020).

4.5. Proline level affected under stress condition

Proline is a non-enzymatic antioxidant known as bio-marker that showed plants response to the stress (Petrovic et al, 2020). In the water caltrop plant, they suggested proline accumulation as a good biomarker of HMs stress (Petrovic et al, 2020; Bi, *et al.,* 2021; Duan, *et al.,* 2022; Guo, *et al*, 2021; Guo, *et al,* 2022). The results of proline accumulation, showed the decreasing trend by increasing the nitrate concentration under high level of lead. These results indicated the positive effect of nitrate to deceasing the side effect of HMs and salt stress as mentioned before. Similarly, Bai et al, (2021) suggested that phytoremediation of HVs pollution by sweet sorghum was only effective at high concentrations of nitrate and by decreasing nitrate concentration the phytoremediation efficiency decreased.

4.6. Lipid peroxidation were affected under stress condition

Heavy metals pollution, causes changes in some plant processes such as lipid peroxidation (Ashraf et al, 2017). The results of this study showed the high lipid peroxidation under control treatment. Similar results were reported on rice, that by increasing lead level the lipid peroxidation was decreased (Ashraf et al, 2017; Li, *et al*, 2021; Sun, *et al.* 2021; Xu, *et al*, 2021; Zhang, *et al.* 2022).

5. CONCLUSIONS

Based on the obtained results of the present study, it can be concluded that with the increasing in salinity stress from 0 to 3 dSm^{-1}, the content of N (from 5.69% to 5.26%), K (from 4% to 3.21%) and nitrate (from 0.36 to 0.28 mg kg^{-1}) significantly reduced. Also, results showed that with the increasing in salinity stress (from 3 to 6 dSm^{-1}) and nitrate level (from 30 to 60 mgL^{-1}) in the soil, plant Pb concentration significantly decreased. Additionally, under conditions of Pb stress, the uptake of nutrients (especially macronutrients) significantly improved with the increasing in the nitrate level from 30 to 60 mgL^{-1}. It appears that stress conditions increased plant's nitrate requirement, which could be considered as a strategy for the improvement of plant tolerance under HMs stress. On the other hand, the increase in K ranged from 1.8 to 5% and also K/Na ratio ranged from 1 to 6 can be considered as a resistance mechanism of plants under salinity stress. In addition, the synthesis of MDA and other biochemical compounds in Japanese raisin, grown under Pb contamination stress, has been reported for the first-time providing ideas for future studies. It should be mentioned that the studied species absorbed the moderate concentrations of Pb (34.1-71 $mgkg^{-1}$) indicating its potential for HMs phytoremediation. Generally, based on the results of the present study described before, Japanese raisin can be considered as a relatively susceptible to salt stress.

REFERENCES

Abbasi SM, Chorom N, Zamir E. 2013. The effect of salinity and heavy metals (Cd and Pb) on phytoremediation of Potamogeton berchtoldi. 2nd National conference on sustainable agriculture and health environment. 12 September. Hamedan, Iran.

AbdElgawa H, Zinta G, Hegab MM, Pandey R, Asard H, Abuelsoud W. 2016. High salinity induces different oxidative stress and antioxidant responses in maize seedlings organs. Journal of Frontiers in Plant Science. **7**: 276. https:/ DOI:org/10.3389/fpls.2016.00276.

Abili J, Zare S. 2014. Evaluation of antioxidant enzymes activity in canola under salt stress. Journal of Advances in Agriculture. **2**(2), 88-92.

Adesodun JK, Atayese MO, Agbaje TA, Osadiaye BA, Mafe OF, Soretire AA. 2010. Phytoremediation potentials of sunflowers (*Tithonia diversifolia* and *Helianthus annuus*) for metals in soils contaminated with zinc and lead nitrates. Journal of Water, Air, and Soil Pollution. **207**(1-4),195-201.

Bi, D., C. Dan, M. Khayatnezhad, Z. Sayyah Hashjin, Z. Y. Ma 2021. Molecular Identification And Genetic Diversity In Hypericum L.: A High Value Medicinal Plant Using Rapd Markers Markers. Genetika **53**(1): 393-405.

Duan, F., Fei Song, Sainan Chen, Majid Khayatnezhad, Noradin Ghadimi, 2022. Model parameters identification of the PEMFCs using an improved design of Crow Search Algorithm. International Journal of Hydrogen Energy, 47(79): 33839-33849

Gholamin, R. & Khayatnezhad, M. 2020a. Assessment of the Correlation between Chlorophyll Content and Drought Resistance in Corn Cultivars (Zea Mays). Helix, 10, 93-97.

Gholamin, R. & Khayatnezhad, M. 2020b. The effect of dry season stretch on Chlorophyll Content and RWC of Wheat Genotypes (Triticum Durum L.). Bioscience Biotechnology Research Communications, 13, 1833-1829.

Gholamin, R. & Khayatnezhad, M. 2020c. Study of Bread Wheat Genotype Physiological and Biochemical Responses to Drought Stress. Helix, 10, 87-92.

Gholamin, R. & Khayatnezhad, M. 2020d. The Study of Path Analysis for Durum Wheat (Triticum durum Desf.) Yield Components. Bioscience Biotechnology Research Communications, 13, 2139-2144.

Gholamin, R. & Khayatnezhad, M. 2021. Impacts of PEG-6000-induced Drought Stress on Chlorophyll Content, Relative Water Content (RWC), and RNA Content of Peanut (Arachis hypogaea L.) Roots and Leaves. Bioscience Research, 18, 393-402.

Gheshlaghi Z, Khorasani R, Haghnia Gh, Kafi M. 2015. Effect of nitrate and harvest time on yield and concentration of iron, zinc and copper in lettuce. Journal of Crop Production and Processing. Isfahan University of Technology. 5 (16), 315-330. https://DOI: 10.18869/acadpub.jcpp.5.16.315. (Abstract in English with full paper in Persian).

Guo, H., Wei Gu, Majid Khayatnezhad, Noradin Ghadimi, 2022. Parameter extraction of the SOFC mathematical model based on fractional order version of dragonfly algorithm. International Journal of Hydrogen Energy, **47**(57):24059-24068.

Guo, L.N., She, C., Kong, D.B., Yan, S.L., Xu, Y.P., Khayatnezhad, M. and Gholinia, F. 2021. Prediction of the effects of climate change on hydroelectric generation, electricity demand, and emissions of greenhouse gases under climatic scenarios and optimized ANN model. Energy Reports **7:** 5431-5445.

Husejnovic MS, Bergant M, Jankovic S, Zizek S, Smajlovic A, Softic A, Antonijevic OB. 2018. Assessment of Pb, Cd and Hg soil contamination and its potential to cause cytotoxic and genotoxic effects in human cell lines (CaCo-2 and HaCaT). Environmental geochemistry and health. pp.1-16. https://DOI: 10.1007/s10653-018-0071-6. PMID: 29362944.

Huang, D., Wang, J. & Khayatnezhad, M. 2021. Estimation of Actual Evapotranspiration Using Soil Moisture Balance and Remote Sensing. Iranian Journal of Science and Technology, Transactions of Civil Engineering, 1-8.

Isayenkov SV, Maathuis FJM. 2019. Plant salinity stress: Many unanswered questions remain. Front Plant Sci. 15;10:80. https://DOI: 10.3389/fpls.2019.00080. PMID: 30828339; PMCID: PMC6384275.

Jia, Y., Khayatnezhad, M. & Mehri, S. 2020. Population differentiation and gene flow in Rrodium cicutarium: A potential medicinal plant. Genetika, 52, 1127-1144.

Juknys R, Kacienė G, Racaite M, Vencloviene J. 2012. The impacts of heavy metals on oxidative stress and growth of spring barley. Central European Journal of Biology. 7(2), 299-306, https://DOI: 10.2478/s11535-012-0012-9.

Kafkafi U, Siddiqi MY, Ritchie RJ, Glass ADM, Ruth TJ. 1992. Reduction of nitrate ($^{13}NO_3$) in flux and nitrogen (^{13}N) translocation by tomato and melon varieties after short exposure to calcium and potassium chloride salts. Journal of Plant Nutrition. 15: 959–975.

Karasakal, A., Khayatnezhad, M. & Gholamin, R. 2020a. The Durum Wheat Gene Sequence Response Assessment of Triticum durum for Dehydration Situations Utilizing Different Indicators of Water Deficiency. Bioscience Biotechnology Research Communications, 13, 2050-2057.

Khadem Moghadam N, Motesharezadeh B, Maali Amiri R. 2016. Changes in antioxidative systems and membrane stability index of canola in response to saline soil and fertilizer treatment application.Global NEST. 18(3): 508-515.

Khalilpoor M, Jafarinia A. 2017. Investigation the effects of salinity and nitric oxide on the changes of chlorophyll a fluorescence in Oat (*Avena sativa* L.) plant probed by JIP-Test. Iranian Journal of Plant Biology. 31, 87-98.

Khoshgoftar AH, Shariatmadari H, Karimian N, Kalbasi M, Van Der Zee S, Parker DR. 2004. Salinity and Zinc Application Effects on Phytoavailability of Cadmium and Zinc. Soil Science Society of America Journal. 68 (6). https://DOI: org/10.2136/sssaj2004.1885.

Khoshgoftarmanesh AH. 2010. Advanced concepts in plant nutrition. 383 pp. Publication No. 74. Isfahan University of Technology Press.

Kibria MG, Hoque MA. 2015. Alleviation of soil salinity in rice by potassium and zinc fertilization Inter-

national Journal of Experimental Agriculture. 5(3), 15-21.

Li, Ang; Mu, Xinyuan; Zhao, Xia; Xu, Jiamin; Khayatnezhad, Majid; Lalehzari, Reza; Developing the non-dimensional framework for water distribution formulation to evaluate sprinkler irrigation; Irrigation and Drainage, **70:** 659-667

Malar A, Wang P, Ali A, Awasthi MK, Lahori AH, Wang Q. 2016. Challenges and opportunities in the phytoremediation of HMs contaminated soils.a review. Journal of Ecotoxicology and environmental safety. 126, 111-121.

Miller RO. 1988. Extractable nitrate in plant tissue: Ion-Selective Electrode Method. In: Y.P. Kalra (Editor). Handbook of reference methods for plant analysis. CRC Press, Taylor and Francis Group, 6000 Broken Sound Parkway NW, Suite 300. Boca Raton FL 33487-2742.

Malidareh HB, Mahvi A, Yunesian M, Alimohammadi M. 2014. Effect of Fertilizer Application on Paddy Soil HMs Concentration and Groundwater in North of Iran. Middle East Journal of Scientific Research. 20(12):1721-1727. https://DOI:10.5829/idosi.mejsr.2014.20.12.13633.

Castro-Rodríguez V, García-Gutiérrez A, Canales J, Cañas RA, Kirby EG, Avila Canovas CFM. 2016. Poplar trees for phytoremediation of high levels of nitrate and applications in bioenergy. Plant biotechnology journal. 14(1), 299-312.

Ng YS, Chan DJC. 2017. Wastewater phytoremediation by *Salvinia molesta*. Journal of Water Process Engineering. 15, 107-115.

Oguntade OA, Odusanya O, Olagunju SO, Olagbenro TS, Adewusi KM, Adegoke AT. 2018. Assessment of composted kitchen waste and poultry manure amendments on growth, yield and heavy metal uptake by Jute mallow Corchorus olitorius Linn. International Journal of Recycling of Organic Waste in Agriculture. https://DOI.10.1007/s40093-018-0232-8

Petrovic D, Krivokapic S. 2020. The Effect of Cu, Zn, Cd, and Pb Accumulation on Biochemical Parameters (Proline, Chlorophyll) in the Water Caltrop (Trapa natans L.), Lake Skadar, Montenegro. Plants, 9, 1287. https://DOI.org/10.3390/plants9101287

Pinto AP, Mota AM, Varennes AD, Pinto FC. 2004. Influence of organic matter on the uptake of cadmium, zinc, copper and iron by sorghum plants. Journal of Science of Total Environment. 326, 239-247.

Peng, X., Khayatnezhad, M. and Ghezeljehmeidan, L. 2021. Rapd profiling in detecting genetic variation in stellaria l. (caryophyllaceae). Genetika-Belgrade **53**: 349-362.

Prasad MNV. 2004. Heavy metal stress in plants, From Biomolecules to Ecosystems. Second Ed. Norosa Publishing House. USA.

Ramesh K, Singh V, Megeji NW. 2006. Cultivation of Stevia [*Stevia rebaudiana* (Bert.) Bertoni]. A Comprehensive Review. Advances in Agronomy 89,137-177.

Ryan J, Estefan G, Rashid A. 2002. Soil and plant analysis laboratory manual. International Center for Agricultural Research in the Dry Areas.

Salimi M, Amin M, Ebrahimi A, Ghazifard A, Najafi P, Amini H. 2012. Influence of electrical conductivity on the phytoremediation of contaminated soils to Cd^{2+} and Zn^{2+}. International Journal of Health Engineering. Vol: 1. 11-19.

Schutzendubel A, Polle A. 2002. Antioxidants and reactive oxygen species in plants. Journal of Experimental Botany. 53(372), 1351–1365.

Shabani E, Sajjadinia A, Tabatabaee S. 2015. Investigating the amount of lead tolerance in petroleum using ecophysiological properties. Journal of Science and technology of greenhouse planting. 6(23), 89-94 (In Persian with abstract in English)

Shanker AK, Cervantes C, Loza-Tavera H, Avudainayagam S. 2005. Chromium toxicity in plants, Environment International. 31 (2005), pp. 739-753

Sharma NK, Jeet Singh R, Kumar K. 2012. Dry matter accumulation and nutrient uptake by wheat (*Triticum aestivum* L.) under poplar (*Populus deltoides*) based agroforestry system. International Scholarly Research Network. https://Doi.org/10.5402/2012/359673

Sricoth T, Meeinkuirt W, Pichtel J, Taeprayoon P, Saengwilai P. 2018. Synergistic phytoremediation of wastewater by two aquatic plants (*Typha angustifolia* and *Eichhornia crassipes*) and potential as biomass fuel. Journal of Environmental Science and Pollution Research. 25(6), 5344-5358.

Sudova R, Vosatka M. 2007. Differences in the effects of three arbuscular mycorrhizal fungal strains on P and Pb accumulation by maize plants. Plant Soil. 296, 77-83.

Sumiahadi A, Acar R. 2018. A review of phytoremediation technology: heavy metals uptake by plants, IOP Conference Series: Earth and Environmental Science, Volume 142. https://Doi:10.1088/1755-1315/142/1/012023

Sun, Q., Deli Lin, Majid K., Mohammad T., 2021. Investigation of phosphoric acid fuel cell, linear Fresnel solar reflector and Organic Rankine Cycle polygeneration energy system in different climatic conditions. Process Safety and Environmental Protection, 147:993-1008.

Xu, Y.-P., Ping Ouyang, Si-Ming Xing, Lu-Yu Qi, Majid khayatnezhad, Hasan Jafari, 2021. Optimal struc-

ture design of a PV/FC HRES using amended Water Strider Algorithm. Energy Reports, **7:** 2057-2067.

Yan A, Wang Y, Tan SN, Mohd Yusof ML, Ghosh S, Chen Z. 2020. Phytoremediation: A Promising Approach for Revegetation of Heavy Metal-Polluted Land. Front. Plant Sci, 30. https://DOI.org/10.3389/fpls.2020.00359.

Zare S, Pakniyat H. 2012. Changes in activities of antioxidant enzymes in oilseed rape in response to salinity stress. International Journal of Agriculture and Crop Sciences. Vol, **4** (7), 398-403.

Zhang, J., M. Khayatnezhad, and N. Ghadimi, 2022. Optimal model evaluation of the proton-exchange membrane fuel cells based on deep learning and modified African Vulture Optimization Algorithm. Energy Sources, Part A: Recovery, Utilization, and Environmental Effects, **44**(1):287-305.

Caryologia
International Journal of Cytology, Cytosystematics and Cytogenetics

Firenze University Press
www.fupress.com/caryologia

OPEN ACCESS

Citation: Ekram Abdelhaliem, Hanan M.Abdalla, Ahmed A. Bolbol, Rania S. Shehata (2022). Assessment of protein and DNA polymorphisms in corn (*Zea mays*) under the effect of non-ionizing electromagnetic radiation. *Caryologia* 75(4): 49-66. doi: 10.36253/caryologia-1716

Received: June 27, 2022

Accepted: November 23, 2022

Published: April 28, 2023

Data Availability Statement: All relevant data are within the paper and its Supporting Information files.

Competing Interests: The Author(s) declare(s) no conflict of interest.

Assessment of protein and DNA polymorphisms in corn (*Zea mays*) under the effect of non-ionizing electromagnetic radiation

Ekram M. Abdelhaliem[1],*, Hanan M.Abdalla[1], Ahmed A. Bolbol[1], Rania S. Shehata[1,2]

[1] *Department of Botany and Microbiology, Faculty of Science, Zagazig University, 44519, Egypt*
[2] *Biology Department, Faculty of Science, Jazan University, 45142, Saudi Arabia*
*Corresponding author. E-mail: ekram.esa@gmail.com

Abstract. Many reports highlight biological responses of crop plants after non-ionizing electromagnetic radiation (EMR) exposure based on the phenotypic and physiological levels. So, this study aimed to estimate genetic alterations in proteins, isozymes, and DNA banding patterns as well as the extent of nuclear DNA damage of economic corn (*Zea mays*) under the stress of EMR using accurate and reliable bio-assays like sodium dodecyl sulfate-polyacrylamide gel electrophoresis (SDS-PAGE), isozymes (Leucine- aminopeptidase, Esterases, Peroxidase, and Catalases), random amplified polymorphic DNA- polymerase chain reaction (RAPD-PCR), and Comet Assay, respectively. SDS-PAGE analysis showed distinct polymorphisms (96.66%) between EMR exposed and non-exposed corn seedlings depending on the number and type of bands, their intensities as well as molecular weight which ranged from (60.27 to 192.35 kDa), gain, and loss of bands. The four isozymes generated varies isozymatic polymorphisms based on relative front, zymogram number, and optical intensities. RAPD analysis generated 85 amplified DNA products with high polymorphism values ranged from 90.91 to 100% based on primers, band type, DNA sizes which ranged from 153 to 1008-bp, lose, gain, and intensity of DNA bands. Comet Assay scored highest extent of loosed DNA from nuclei (DNA damage) reached the value of (tailed ratio 20%) at EMR exposed corn nuclei for 5 days compared to non-exposed nuclei which reached the value of (tailed ratio 3%). This study concluded that each EMR exposure time had unique interaction with proteins, isozymes, and DNA of corn cells exhibiting wide range of genotoxic stress and subsequently, adversely effect on growth and yield of this sensitive crop plants.

Keywords: Electromagnetic radiation, *Zea mays*, SDS-PAGE, isozymes, RAPD-PCR, single cell gel electrophoresis.

INTRODUCTION

Nowadays, non-ionizing electromagnetic radiation (EMR) arise from both natural and wide human made sources such as variety of electronic devices (Rio & Rio, 2013) can influence the growth, yield, and quality of

plants based on flux of EMR and exposure time (Nyakane et al., 2019). Important components of cells are proteins that classified into varies classes according to their functions. The stress proteins generated from abiotic stressor like EMR consider a new class from these proteins with functions related to protection of cell (Iderawumi and Friday 2020). When EMR interact with the DNA can stimulate the synthesis of this stress protein, causing DNA strand breaks which increase by increasing of EMR energy (Blank & Goodman, 2012,

Shabrangi et al., 2011). Field parameters and characteristics (frequency, intensity, and wave-shape), cell type, and exposure duration all influence EMR genetic effects. The gene expression changes (for example, genes implicated in cell cycle arrest, apoptosis and stress responses, and heat-shock proteins) are consistent with the results that EMR causes genetic damage (Lai, H 2021).

The study of Ruiz-Gómez and Martínez-Morillo (2009) reported that a major concern of the genotoxic effects of non-ionizing electromagnetic field (EMF) is overproduction of ROS in cells and inducing oxidative stress on protein and DNA because of EMF exposure can induce DNA strand breaks and acts as a co-inductor of DNA damages rather than as a genotoxic agent. The genetic mechanisms by which EMR interact with protein and DNA are radical pair recombination led to increasing the concentration, activity, and lifetime of reactive oxygen species (ROS), which might cause changes in cell cycle, genetic mutation, damage to DNA which can lead to changes in cellular functions and cell death, modification of protein expression and oxidation of proteins, inhibition of enzymes (Kıvrak *et al*., 2017).

Higher plant species differ in their sensitivity and response to environmental stresses because they have a variety of stress perception, signaling, and response skills (Ahanger *et al*., 2017). Corn (*Zea mays*) is one of the world's major cereals and food crops for humans, it belonging to family *Gramineae* and genus *Zea*. Several physical abiotic stresses affect the total production of maize due to damage in its DNA, like EMF (Yan, *et al.,* 2011). It provides a promising genetic bio-monitors model to detect genotoxicity of environmental stress and DNA lesions induced by abiotic stress (Grant & Owens, 2006; Erturk, *et al*., 2014).

Many studies focused on the effect of EMF on plant growth and its development (Ortiz, *et al*., 2015) but rarely concerned with their effects on banding patterns and genetic polymorphisms of proteins, isozymes and DNA. This attracted the attention of this study to explore the interaction of low frequency EMFs (60 Hz^{+}) with proteins (enzymatic and non- enzymatic) using SDS-PAGE and isozymatic technique, respectively and DNA using RAPD- PCR and Single cell gel electrophoresis bioassays.

Identification of the biochemical and molecular mechanisms for plant tolerance like maize to environmental stress is important. Detection of proteins and isozymes alterations at the gene product level is carried out by biochemical markers which measuring allele frequencies for specific genes (Hailu&, Alatawi 2014). Meanwhile, molecular markers monitored differences (polymorphisms) within nucleotide sequences to indicate alterations at the DNA level, such as nucleotide changes: deletion, duplication, inversion, and/or insertion (Qi *et al*., 2014).

SDS-PAGE (Sodium dodecyl sulphate polyacrylamide gel electrophoresis) is a biochemical bioassay that is used to detect genetic differences in polypeptide banding patterns and to profile proteins induced by abiotic stress due to changes in the DNA coding sequences and active structural genes leading to modifications of structure protein, protein interaction, and stressed oxidative proteins (Karaca, 2013). On the other hand, isozyme analysis is a sophisticated biochemical approach that has a wide range of applications in detecting genetic alterations in plant cells (Hailu et al., 2014). Isozymes are enzymatic proteins, arise from multiple gene loci coding for distinct structural polypeptide chains, and their electric charge depends on the amino acids they contain (Hailu et al., 2014). They have different molecular forms showing the same substrate specificity due to changes in the nucleotide sequence of the DNA that codes for the protein, they differ in size, molecular weight, electrophoretic mobility, electric charge, and amino acid content (Karaca, 2013). Native polyacrylamide gel electrophoresis (Native PAGE) is used to differentiate protein variants in isozyme analysis, and an enzyme-specific staining combination, which contains a substrate, co-factor, and oxidized salt, is used to visualize them. (Karaca, 2013).

Recently mutations induced by genotoxic stress, damage and fragmentation of DNA can be estimated using molecular cytogenetic techniques such as RAPD-PCR and the single cell gel electrophoresis (Comet assay) which can determine the direct genotoxic effect of exogenous factors on plant genotypes at the nuclear DNA level (Cenkci *et al*., 2009; Santos, Pourrut, Ferreira de Oliveira, 2015). RAPD (random amplified polymorphic DNA) is a PCR-based technology that uses short randomized nucleotide sequence primers to amplify random DNA segments of genomic DNA without the need for prior genomic DNA knowledge. It can be used to detect genotoxicity, nucleotide sequence polymorphism, and alteration in RAPD profiles induced by environmental genotoxic stresses which lead to changes in the structure

of DNA in living organisms, such as point mutations, tiny insertions and deletions of DNA, and rearrangement of nucleotide sequences, all of which cause DNA damage and lesions (Atienzar & Jha, 2006).

Comet assay, also known as single cell gel electrophoresis, is one of the most modern procedures for analyzing DNA damages brought to agricultural sciences and genetic toxicology in recent years, reflected as single and double-strand breaks, oxidative-induced base damage and DNA-DNA/DNA protein cross linking induced by oxidative and genotoxic environmental factors (Nandhakumar *et al*., 2011). Comet-like shape of nuclei (with a head, the nuclear region and a tail which contains DNA fragments) is formed after electrophoresis and staining with a fluorescent dye and observed by a fluorescence microscopy (Dikilitas *et al*., 2009).

The aim of this study is to investigate biochemical and molecular mechanisms of non- ionizing electromagnetic radiation (EMR) on proteins and DNA of corn (*Zea mays*) based on SDS-PAGE, isozymatic analyses, RAPD-PCR, and comet assay to estimate genetic polymorphism in economic corn crop under the stress of EMR as well as understand how this plant was adapted.

MATERIAL AND METHODS

Plant material

The bio-monitor plant material in this investigation was maize grains (hybrid-323) supplied from the (Agronomy Research Department, Field Crops Institute, Agriculture Research Center, Giza, Egypt). Grains were checked for viability and homogeneity size before being divided into two groups: non-exposed and exposed to electromagnetic radiation (EMR). 30 grains of each group were sterilized and germinated in earthenware pot 60 cm in diameter containing soil obtained from the agriculture field until reached seedlings after thirty-days-old.

EMR Exposure facility

Electromagnetic radiations (EMR) are created when electric current flows: the greater the current, the stronger the magnetic intensity. So, (EMR) have magnetic and electrical properties that surround plant samples within that field. EMR generator system was designed a locally and presented at Biophysics Department, Faculty of science, Zagazig University, Egypt. This system consists of two coils, each formed by 1,000 turns of 1 mm copper wire, with a mean diameter of 260 mm and 25 cm length. EMR were generated by a handmade cylindrical shaped coil that was connected to a 220V AC power supply (ED-345BM, China), to generate electrical current of 60 Hz. EMR intensities were measured through use of magnetic flux meter type 4048 with probe T- 4048, 001, manufactured by USA. To keep the temperature from rising, a standard fan was used. The temperature was measured with a thermometer to be 22+1°C. Thus, a vertical sinusoidal magnetic field of 10 mT was generated in the central zone of the coils system when a 60 Hz sinusoidal electric current passed through the coils.

Corn seedlings were put in a vessel (a glass jar with diameter of 7 cm and height of 12 cm) by placing a glass jar daily in the center zone of the coils system, and then subjected to strengths of EMR (10 mT) for four different durations of exposure 1, 3, and 5 days, termed as (Ex-1, Ex-3, and Ex-5 days) while EMR non-exposed seedlings termed as (Ex-0). Leaves of ten corn seedlings were collected from EMR exposed, and non-exposed, and thoroughly cleaned with distilled water, for removal of any debris and then completely dried in air conditions and then subjected to biochemical and molecular cytogenetic analyses.

Biochemical and molecular cytogenetic bioassays

Dried leaves of EMR exposed, and non-exposed Corn seedlings were defatted and processed into leaf powder according to the methods outlined by Hojilla-Evangelista & Evangelista, (2006) and used for SDS-PAGE, isozymatic, RAPD-PCR, single cell gel electrophoresis analyses.

Biochemical bioassays

Protein extraction and SDS-PAGE analysis

Protein extraction from leaves was carried out as stated in the work of Abdelhaliem and Al-Huqail (2016) with some modifications. 0.2 g of powdered and defatted leaves was added to extraction buffer (0.5 M Tris-HCl, pH 6.8, 2.5% SDS, 5% urea, and 5% 2-merkaptoethanol) in an Eppendorf tube and mixed thoroughly by overtaxing. Extraction buffer was boiled for 5 min before centrifugation at 10,000 *g* for 5 min at 4°C and the supernatant was used. To visualize the mobility of protein on the gel, bromophenol blue was added to the supernatant as a tracking dye. SDS-PAGE was used to examine proteins using 10% SDS-polyacrylamide gels, as described by Laemmli (1970). The protein bands were observed after electrophoresis using Coomassie brilliant blue G-250 staining. Marker proteins (Fermentas) were

used as references.The molecular weights (kDa) of the polypeptide bands formed in the electropherogram were compared to the standard Pharmacia protein marker. To capture the image and determine band

intensities, gels were digitally photographed and analyzed using the Gel Doc Viller Lourmat system.

Data analysis of polypeptide banding patterns

The Bio-Rad video densitometer, Model Gel Doc 2000, was used to determine the number, concentration, and band density of polypeptide bands on each gel lane. Electropherograms of each germplasm of EMR exposed and non-exposed corn plants were evaluated for the presence (1) or absence (0) of protein bands to assess variance in the protein banding pattern. Protein polymorphisms were evaluated based on previous polypeptide banding pattern differences.

Isozymes extraction and Isozymatic analysis

Identification of isozymatic variations induced in EMR exposed, and non-exposed corn seedlings were performed using the sodium dodecyl sulphate-native polyacrylamide gel electrophoresis (PAGE) according to the methods of Majumder, Hassan , Rahim, Kabir (2012). Four isozymes, Leucine-aminopeptidase (LAP. E.C. 3.4.1 1. I), Esterases (EST, E.C. 3.1.1.1), Peroxidase, (PRX E.C. 1.11.1.7), Catalases (CAT, 1.11. 1.6), were used in this study. Isozymes of each sample was extracted according to method of Majumder et al. (2012) that described briefly in the study of Abdelhaliem & Al-Huqail, (2014).

The staining of gel of LAP and CAT isozymes was performed according to protocol of Pasteur, Pasteur, Bouhomme, Catalan, Davidian (1988) while EST and PRX isozymes followed the protocol of Tiwari & Bakshi (2015) for. The Vilber Lourmat gel documentation system was used to photograph the gels. The most common allele at each locus for each isozyme was assigned as relative front mobility (R_f) value. The value R_f was calculated in equation (1).

R_f = Distance of zymograms migrated / Distance of marker dye migrated (Eq. 1)

PAGE and data analyses

Zymograms of each enzyme were observed and studied against an intense fluorescent light. After the staining of LAP, EST, PEX, and CAT isozymes, the isozymatic data were collected and immediately only consistent and clear zymograms were scored. The isozymatic banding patterns were compared among of EMR non-exposed, and exposed corn seedlings based on their relative front (R_f) values on gel electrophoresis, zymogram number, their intensities, and the percentages of polymorphic, unique and non-unique loci. Different isozymatic patterns were scored as discrete variables, the presence "1" or absence "0" of zymogram. Alterations of isozymatic patterns and zymograms at each locus were calculated using the POPGENE 32 version 1.31 software based on the computer program (Labate, 2000).

Molecular cytogenetic bioassays

Genomic DNA isolation and RAPD-PCR analysis

RAPD analysis was performed to analyze the genotoxic effects of EMR exposed, and non- exposed corn DNA. Genomic DNA of powdered and defatted leaves were isolated following a modified Hexadecyl trimethyl ammonium bromide (CTAB) buffer protocol Kit & Chandran (2010) as described briefly in the study of Abdelhaliem & Al-Huqail, (2013). The absorbance of diluted DNA solution at 260 nm and 280 nm was used to measure the purity and concentration of DNA. The DNA quality was evaluated using ethidium bromide-stained agarose gel electrophoresis.

DNA amplification process by PCR

Reactions of DNA amplification by PCR, analysis of amplification products by agarose gel electrophoresis were conducted following the protocol of Williams Williams, Kubelik, Livak, Rafalski, Tingey (1990) with some modifications. The mixture of PCR amplification reaction as described briefly in the study of Abdelhaliem, & Al-Huqail (2016) was consisted of 2.5 µL 10X buffer with 15 mM $MgCl_2$ (Fermentas, Vinius, Lithuania), with 0.25 mM each of dATP, dCTP, dGTP and dTTP (Sigma, St. Louis, MO, USA), 0.5 U Taq DNA polymerase (Sigma), 0.3 mM primer and 50 ng template DNA. The PCR was performed in a Palm thermal Cycler apparatus (Corbett Research) was programmed using the following method: initial denaturation of 4 min at 95°C followed by 45 cycles of 1 min at 95°C, 1 min at 38°C, and 2 min at 72°C with final extension at 72°C for 10 min and a hold temperature of 4°C. Only five primers (P-02, 06, 08, 10, and 14) effectively generated reproducible amplified products after a total of 20 random DNA oligonucleotide primers

(10 mer) were employed in the PCR (University of British Columbia, Canada). Amplification DNA products were analyzed by electrophoresed on 1.5% agarose gel (Sigma) in TAE buffer (0.04 M Tris-acetate, 1 mM EDTA, pH 8). The run lasted one hour at a constant voltage of 100 volts. For 15 minutes, gels were stained with 0.2 mg/mL ethidium bromide. A UV light transilluminator was used to examine the PCR products. To determine band sizes, a 100-bp DNA ladder (Gibco-BRL, Grand Island, NY, USA) was put into the first lane of each gel. A gel documentation system was used to photograph the gels under UV light (Bio-Rad, Hercules, CA, USA).

Analyses of DNA banding patterns

Visualization of amplified DNA products on agarose gel electrophoresis was carried out using Photo Print (Vilber Lourmat, France) imaging system. Banding patterns generated by RAPD were analyzed using one-dimensional software (Advanced American Biotechnology and Imaging, Fullerton CA 92831, USA) while DNA polymorphisms in RAPD profiles included disappearance of a band and appearance of a new band with respect to the non-exposed profile, were calculated using several amplified DNA parameters such as losses of normal bands, appearance of new bands, the number of polymorphic (unique and non-unique DNA bands), and monomorphic DNA bands, and the molecular sizes of DNA bands as well as intensity of bands for each EMR exposed sample compared to non-exposed one. Amplified DNA products were scored based on the presence (1) or absence (0) of DNA bands for each primer and DNA band intensity estimated by using image analysis software. Polymorphic DNA bands (unique and non-unique) and monomorphic bands were also scored.

Estimation of genetic Polymorphisms

Polymorphism (*P*, in %) of protein or isozyme or DNA were estimated according to Gjorgieva *et al.*, (2013) based on the lost bands (non-unique) and the appearance of a new band (unique bands) as well as the monomorphic bands (bands with the same loci at all samples) as in equation (2).

$$\text{Polymorphism } \% = [a+b/c] \times 100 \quad \text{(Eq. 2)}$$

Where *a* is the number Polymorphic bands (a is new bands unique, *b* is the number of lost non- unique bands and *c* is the total number of scored bands (Polymorphic and monomorphic bands).

Isolation of nuclei and Comet Assay (Single cell gel electrophoresis) technique

Isolation of nuclei and slide preparation

The nuclei of EMR exposed, and non-exposed corn leaves were isolated following the protocol of Juchimiuk *et al.*, (2006). Five hundred mg of leaves were rinsed in distilled water twice, dried with a paper towel and then placed in a glass petri dishes containing 200 µL of cold Tris-HCl buffer, pH 7.5 (on ice). Under yellow light, leaves were carefully sliced into a "fringe" with a new razor blade to release nuclei into the buffer. This approach of nuclei isolation found to be the most effective in obtaining low DNA lesions in non-exposed samples. Each slide was covered with a mixture of 55 l nuclear suspension and 55 l LMP agarose (1% generated with phosphate-buffered saline) and cover slipped at 40°C after being coated with 11% NMP agarose and dried. After putting the slide on ice for at least 5 min., the coverslip was removed. The coverslip was then replaced after 110 l of LMP agarose (0.5%) was poured on the slide. The coverslip was removed after 5 minutes on ice.

Single cell gel electrophoresis technique

Comet assay slides were prepared as described by Juchimiuk et al. (2006). The corn nuclei slides were horizontally put in a gel electrophoresis tank with freshly prepared cold electrophoresis buffer (300 mM NaOH, 1 mM EDTA, pH > 13) and incubated for 15 min. At 4°C, electrophoresis was carried out at 16 V, 300 mA for 30 min. The gel was then neutralized by washing three times in 400 mM Tris-HCl, pH 7.5, and then stained for five minutes with ethidium bromide (20 g/mL). The gels were immediately dipped in ice-cold distilled water after staining and examined.

Comet imaging and software analysis

The level of DNA damage in 50 randomly chosen nuclei was examined in each slide using a computerized image analysis system or a fluorescence microscope with an excitation filter of 546 nm and a barrier filter of 590 nm (Komet Version 3.1. Kinetic Imaging, Liverpool, UK). Tail DNA (TD percent, relative proportion of DNA in the comet tail) and tail moment (TM, integrated value of density multiplied by DNA migration distance from nuclei) were used as DNA damage parameters to quantify nuclear DNA damages (Juchimiuk et al., 2006). The

percentage of nuclei having tails was also estimated, as well as relative tail length.

RESULTS

Biochemical genetic bioassays

SDS-PAGE bioassay

The electrophoretic profiling of polypeptide banding patterns based on molecular weight (kDa), band number, band intensity, fractionation of bands, appearance of new bands and the loss of some bands as parameters of polypeptide banding showed variations between EMR exposed and non-exposed corn seedlings by SDS-PAGE analysis (Table 1 and Figure 1). There were 39 polypeptide bands with molecular weights ranging from 60.27 to 192.35 kDa, 29 of which were polymorphic with a value of 74.36%, according to the data obtained, (24 unique bands with a value of 61.54%, plus 5 non-unique bands with value of 12.82%) in addition to one monomorphic band value of 2.56%.SDS-PAGE analysis indicated distinctive polymorphism value of 96.66% based previous banding variations. When comparing EMR exposure samples to non-exposed samples, there were noticeable differences in the number of polypeptide bands and molecular weight. The highest number of polypeptides bands was 12, with a value 30.77% scored at corn seedlings exposed to EMF for 5 days while the lowest number was 8, with a value 20.51% for non-exposed samples (control).

Unique polypeptide bands obtained from SDS-PAGE were varied in molecular weight (kDa), and in number and intensity of bands among EMR exposed and non-exposed samples (Table 1). As a result, unique bands can be employed as a tool for the appearance new characteristic polypeptide bands that are specific for each EMR exposure time. The highest number of unique polypeptides bands was 9, with a value of 37.50% for samples exposed to EMR for 5 days while the lowest number (4 unique bands), and with a value of 16.67 scored at samples exposed to EMR for one a day (Table 1).

Isozymatic bioassay

LAP, EST, PRX, and CAT isozymes used in this study revealed clear isozymatic polymorphisms among EMR exposed and non-exposed Zea mays reached the values of 91.66 % for LAP and EST, 88.89% for CAT, and 80.00% for PEX based on zymograms number, loci, R*f* values, and optical densities generated by each isozyme, separately (Tables 2, 3, 4 and 5; Figures 2 and 3 A and B).

A total of 72 different electrophoretic zymograms produced by the four isozymes showed varied relative front (R*f*) values, varying from 0.01 to 1.20 and varied values of optical densities (OD). Of these zymograms, 38 with a value of 52.77% were polymorphic (27 unique zymograms with a value of 37.5% plus 11 non- unique zymograms with a value of 15.28%). The higher number of zymograms was (19) generated by EST and PRX while LAP and CAT isozymes generated 17 zymograms. The four enzymes scored maximum number of zymograms (21) at corn seedling exposed to EMF for 5 days compared with 13 zymograms scored for non-exposed samples.

On the other hand, LAP , EST, PRX, and CAT isozymes generated unique zymograms varied in R*f* values and optical densities. The highest number of unique zymograms produced by four isozymes was 9; with a value of 33.33% recorded for samples exposed to EMR for 1 and 5 days, in comparison to 5 unique zymograms; with a value of 18.51 % for non-exposed samples (Tables 2, 3, 4 and 5).

Molecular cytogenetic bioassays

RAPD-PCR bioassay

Profiles and banding patterns of amplified DNA bands generated by RAPD exhibited clear variations among corn seedlings exposed to EMR compared to non-exposed one (Table 6 and Figure 4). Only five of the 20 random decamer primers examined revealed distinct alterations in the amplified DNA banding patterns and provided specific and reliable results and consistent bands. 85 DNA bands were produced by RAPD analysis, the sizes of these bands ranged from 153 and 1008 bp in length. The RAPD analysis, on the other hand, identified three types of amplified DNA bands (polymorphic, monomorphic, and polymorphic), which differed quantitatively and qualitatively in band number, size (bp), and intensity on an agarose gel (Table 6). There were, 59 bands were polymorphic (unique and non-unique bands) with a value of 69.41% (36 unique bands with a value of 42.35% and 23 non-unique bands with a value of 27.06%) and 5 monomorphic bands with a value of 5.88%. An average of 17 bands per primer was scored. Furthermore, Table 6 shows the total polymorphisms produced by the five primers, which reached a value of 97.01%. The primers differed with respect to the value of polymorphisms detected. The highest level of polymorphism (100%) was revealed by primers (P-14) because of it do not detect any monomorphic bands, followed by primers (P-02 and P-10) which recorded polymorphism value of 90.91%, P-06 recorded polymorphism value of (88.89%)

Table 1. Sodium dodecyl sulfate-polyacrylamide gel electrophoresis (SDS-PAGE) analysis of proteins of EMF exposed and non-exposed *Zea mays* seedlings for days of exposure times (Ex-0, Ex-1, Ex-3,and Ex-5) using the documentation system Gel Doc Bio Rad system 2000. Lanes 1–4 represented the days of exposure times (Ex-0, Ex-1, Ex-3,and Ex-5), respectively.

Lanes Rows	Molecular weight (kDa)	Polypeptide bands in each lane								
		Lane1		Lane 2		Lane 3		Lane 4		Band types
		kDa	%	kDa	%	kDa	%	kDa	%	
1	192.35	0	-	0	-	1	10.90	0	-	U
2	184.13	1	2.27	0		0	-	0	-	U
3	180.15	0	-	1	5.67	0	-	0	-	U
4	158.02	0	-	0	-	0	-	1	6.67	U
5	154.61	0	-	0	-	1	5.98	0	-	U
6	148.00	0	-	1	4.08	0	-	0	-	U
7	145.31	1	10.40	0	-	0	-	0	-	U
8	138.81	0	-	0	-	1	5.31	1	1.55	Non-U
9	130.19	0	-	1	1.17	0	-	0	-	U
10	126.66	0	-	0	-	1	2.23	0	-	U
11	118.79	1	11.10	0	-	0	-	0	-	U
12	115.57	0	-	1	17.40	1	13.00	0	-	Non- U
13	112.44	0	-	0		0		1	17.60	U
14	105.45	1	10.40	1	5.51	0	-	0	-	Non-U
15	104.49	0	-	0	-	1	6.53	0	-	U
16	89.84	1	28.30	1	27.60	1	21.50	1	24.60	M
17	80.24	0	-	0	-	0	-	1	8.28	U
18	76.16	1	2.70	0	-	0	-	0	-	U
19	75.50	0	-	0	-	0	-	1	1.43	U
20	71.66	0	-	0	-	0	-	1	4.24	U
21	71.04	0	-	1	15.20	0	-	0	-	U
22	70.42	0		0		1	13.40	0	-	U
23	67.43	0	-	0	-	0	-	1	2.07	U
24	66.27	1	13.40	0		0	-	0	-	U
25	63.66	0	-	0	-	0	-	1	2.07	U
26	62.00	0	-	1	16.90	1	13.90	1	1.00	Non-U
27	62.22	0	-	0	-	0	-	1	10.30	U
28	61.45	1	21.50	0	-	0	-	0	-	U
29	60.91	0	-	1	6.46	1	7.12	0	-	Non-U
30	60.27	0	-	0	-	0	-	1	21.20	U
No. of polypeptide bands			8		9		10		12	
Total polypeptide bands						39				
% of total bands			20.51		23.07		25.64		30.77	

	Unique (U) bands		(Non-U) bands		Polymorphic bands		Monomorphic bands		Polymorphisms %
	No	%	No	%	No	%	No	%	
Frequency of polypeptide bands and Polymorphisms	24	61.54	5	12.82	29	74.36	1	2.56	96.66

	Lane1		Lane2		Lane 3		Lane 4	
	No.	kDa	No.	kDa	No.	kDa	No.	kDa
No.and MW(kDa) of unique polypeptide bands	6	184.13–145.31-76.16–66.27–61.45	4	180.1501–48.00–130.19–71.04	5	192.35–154.61 126.66–104.49–70.42	9	158.02–112.44–80.24–75.50–71.66–67.43–63.66–62.22-60.27
Total unique bands					24			
% of unique bands		25		16.67		20.83		37.50

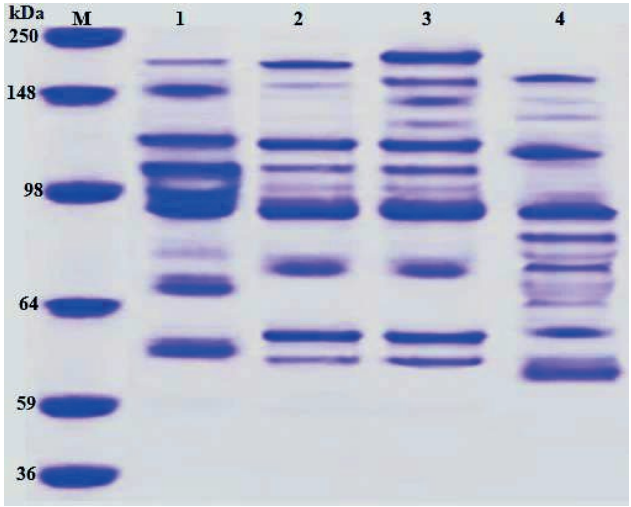

Figure 1. Polypeptide banding patterns analyzed by Sodium dodecyl sulfate-polyacrylamide gel electrophoresis (SDS-PAGE) technique of non-exposed and EMR exposed seedlings of *Zea mays* for days of exposure times (Ex-0, Ex-1, Ex-3,and Ex-5) based on relative front (R*f*) Values and optical densities (OD). Lanes 1–4 represented the days of exposure times (Ex-0, Ex-1, Ex- 3,and Ex-5), respectively.

while primer (P-08) scored the lowest level of polymorphism value of (81.83%). These genetic DNA polymorphisms based on the gain and/or loss of DNA bands in EMR exposed samples compared to the non-exposed one (control). Besides, the number of RAPD amplified DNA bands varied among EMR exposed corn seedlings compared to control and correlated positively with increasing exposure time of EMR. The highest number of amplified DNA bands was 26, with a value of 30.59%, which was produced by five primers and was detected in EMR exposed sample for 5 days exposure time compared to 21 DNA bands, with a value of 24.71% which recorded at non-exposed samples. Unique amplified DNA bands created by RAPD analysis were distinctive loci specific for one exposure time based on their number, their molecular sizes, and optical intensities. The highest number of unique DNA bands produced by five primers was 13, with a value of 36.11% recorded in EMR exposed samples for 5 days exposure time compared to 10 DNA unique bands, with a value of 27.78% which recorded at non-exposed samples, while the lowest number of unique DNA bands was six, with a value of 16.67% for EMR exposed samples for one days exposure time (Table 6).

Single Cell Gel Electrophoresis Technique bioassay

The Comet Assay or single cell gel electrophoresis assay (SCGE) is one of the very widely used assays to microscopically detect DNA damage at the level of a single cell. Cells containing damaged DNA have the appearance of a comet with a bright head and tail. The SCGE or comet test was employed in this investigation to identify nuclear DNA (nDNA) damage caused by an electromagnetic radiation stressor in corn seedlings for different exposure times (Table 7 and Figure 5). The extent of DNA migration from nuclei (tailed ratio), tail length μm, % of tailed DNA (TD percent), and tail moments(TM) were utilized to evaluate the level of DNA damage caused by the comet assay. The recent findings revealed that each EMR exposure time led to inconsistent differences in the level of DNA damage in corn nuclei. EMR exposed samples for 5 days exposure time (Ex-5) detected the highest DNA migration from corn nuclei (tailed ratio 20%) with tail length (2.88 μm), TD% (2.79%), and TM (8.04); this demonstrated that this EMR exposure time had clastogenic and genotoxic stress increased nDNA damage of corn cells in comparison to non-exposed nuclei (Ex-0) which detected the lowest DNA migration (tailed ratio 3%) with tail length (0.99 μm), TD% (1.05%), and TM (1.73).

DISCUSSION

The current study used SDS-PAGE and isozymatic, RAPD-PCR, and SCGE as accurate, reliable, to detect genetic effect of 60 Hz EMR on proteins, isozymes, and DNA, respectively. SDS PAGE and isozymatic analyses are biochemical bioassays generated genetic polymorphisms at the level of gene product such as alterations in non-enzymatic and enzymatic proteins (storage proteins and isozymes, respectively) and amino acids. SDS-PAGE analysis revealed varied polypeptide banding patterns and high level of protein polymorphisms among EMR exposed corn seedlings and non-exposed samples depend on number of bands, their molecular weights, and band intensity, the gain of new protein bands (unique bands) and the loss of normal bands (non-unique bands). The banding pattern of electrophoretic polypeptide may be due to interaction of EMR with the transcriptional events occurring during the expression of genes under EMR stressor leading to different mutations in sequencing of mRNA and changes in amino acids of proteins as end products and consequently, polypeptide banding patterns of proteins on electrophoretic gel of SDS-PAGE (Sadia *et al.*, 2009).

On the other hands, the high levels of polymorphisms based on the gain of polypeptide bands or loss of others which generated by SDS-PAGE analysis may be resulted from conformational changes in the amino acid

Table 2. Distribution of leucine-aminopeptidase (LAP) zymograms of EMF non-exposed and exposed *Zea mays* seedlings for days of exposure times (Ex-0, Ex-1, Ex-3, and Ex-5) based on relative front (R*f*) Values and optical densities (OD). Lanes 1–4 represented the days of exposure times (Ex-0, Ex-1, Ex- 3, and Ex-5), respectively.

Rows	R*f* Values	Leucine-aminopeptidase (LAP) zymograms								Zymogram types
		Lane 1		Lane 2		Lane 3		Lane 4		
		R_f	OD	R_f	OD	R_f	OD	R_f	OD	
1	0.19							√	38.4	U
2	0.25	√	34.9							U
3	0.35			√	5.15					U
4	0.40							√	10.8	U
5	0.43			√	28.3					U
6	0.46					√	32.4			U
7	0.66	√	35.1	√	33.6	√	25.9	√	31.3	M
8	0.85							√	30.4	U
9	0.88	√	29.9							U
10	0.90					√	41.7			U
11	0.95			√	38.1					U
12	1.20			√	7.23	√	4.34	√	3.05	Non-U
No. zymograms		3		5		4		5		
Total zymograms		17								
% of zymograms		17.64		29.41		23.53		29.41		

	Lane 1		Lane 2		Lane 3		Lane 4	
	No.	R*f*	No.	R*f*	No.	R*f*	No.	R*f*
No. and R*f* of unique loci	2	0.25–0.88	3	0.35–0.43–0.95	2	0.46–0.90	3	0.19–0.40–0.85
% of unique loci	20.00		30.00		20.00		30.00	

	Unique (U)		(Non-U)		Polymorphic		Monomorphic (M)		Polymorphisms
	No.	%	No.	%	No.	%	No.	%	%
Frequency of isozymetic bands and Polymorphisms	10	58.82	1	5.88	11	64.71	1	5.88	91.67

sequences of proteins, or may result from gene duplication followed by a point mutation (insertion or addition of nitrogenous base sequences) that encodes the fractionated polypeptide bands led to appearing (gain) of new bands (unique bands) or may be result from deletion of sequences or loss of genes and consequently, deficiency of amino acids between mutated sites of polypeptide chain of EMR-exposed samples led to loss of protein bands (non-unique) (Galani *et al.*, 2011). Moreover, variation in the number of polypeptide bands and band intensities observed in EMR-exposed samples in comparison to the control may be resulted from changes in nitrogenous bases of DNA, in protein sites or amino acid sequences or frameshift mutations led to changes in bands number while band intensity may be resulted from duplication of gen or point mutation which led to manufacturing of longer and shorter of polypeptide chains (Shikazono *et al.*, 2005). Additionally, EMR-exposed corn seedlings for 5 days caused alteration in profile and banding patterns of proteins as evident in increasing bands number more than non-exposed ones.

On native-PAGE, LAP, EST, PEX, and CAT isozymes employed in this work displayed numerous zymograms at various loci. These variations in electrophoretic zymogramatic patterns and isozymatic polymorphisms based on R_f values and zymograms intensi-

Table 3. Distribution of esterase (EST) zymograms of EMF non-exposed and exposed *Zea mays* seedlings for days of exposure times (Ex-0, Ex-1, Ex-3, and Ex-5) based on relative front (R*f*) Values and optical densities (OD). Lanes 1–4 represented the days of exposure times (Ex-0, Ex-1, Ex-3, and Ex-5), respectively.

Rows	R*f* Values	Esterase (EST) zymograms								Zymogram types
		Lane 1		Lane 2		Lane 3		Lane 4		
		R_f	OD	R_f	OD	R_f	OD	R_f	OD	
1	0.15			√	33.8	√	42.2			Non-U
2	0.16	√	34.3							U
3	0.29							√	57.6	U
4	0.36					√	15.6			U
5	0.38			√	10.2					U
6	0.39	√	13.5							U
7	0.57	√	25.8			√	22.9			Non-U
8	0.58			√	19.7			√	20.0	Non-U
9	0.69							√	3.62	U
10	0.78	√	26.3	√	36.3	√	19.4	√	8.54	M
11	0.97	√	1.50					√	21.40	Non-U
12	1.10			√	2.52					U
No. zymograms		5		5		4		5		
Total zymograms		19								
% of zymograms		26.31		26.31		21.05		26.31		

	Lane 1		Lane 2		Lane 3		Lane 4	
	No.	R*f*	No.	R*f*	No.	R*f*	No.	R*f*
No. and R*f* of unique loci	3	0.16–0.39–0.77	3	0.38–0.79–1.10	1	0.36	2	0.29–0.69
% of unique loci	42.86		42.86		14.29		28.57	

	Unique (U)		(Non-U)		Polymorphic		Monomorphic (M)		Polymorphisms
	No.	%	No.	%	No.	%	No.	%	%
Frequency of zymograms and Polymorphisms	7	36.84	4	21.05	11	57.90	1	5.26	91.66

ties among EMR- exposed corn seedlings for different exposure times compared to non-exposed ones. The alterations in zymogramatic patterns may be due to mutation or changes in the DNA nucleotide sequence that codes for the protein leading to the substitution of one to several amino acids or changes in amino acids compositions that result in a change in the net charge of a proteins consisted isozyme (Karaca, 2013). They might also be attributable to a gene's interaction with oxidative stress caused by EMR exposure times or to changes in enzyme conformation which altering the rate of proteins migration on PAGE and their relative front mobility as well as efficiency and stability of the isozyme (Kumar, Gupta, Misra, Modi, Pandey, 2009). On the other hand, alteration in the electrophoretic zymograms mobility may be due to changes in the sequences of encoding DNA or from the shapes and different sizes of the affected isozyme (Karaca, 2013).

Recently, RAPD-PCR and single-cell gel electrophoresis (SCGE) are molecular and cytogenetic bioassays used in this study at DNA level to detect reliable and accurate genetic polymorphisms in banding patterns and DNA damages induced by EMR-oxidative stress on nuclear DNA of corn seedlings. RAPD bioassay is used in this study to provide information about nucleotide sequence polymorphisms that might have occurred across coding and non- coding regions of the entire genome (Elsh & McClelland, 1991). The data obtained

Table 4. Distribution of peroxidase (PEX) zymograms of EMF non-exposed and exposed *Zea mays* seedlings for days of exposure times (Ex-0, Ex-1, Ex-3, and Ex-5) based on relative front (R*f*) Values and optical densities (OD). Lanes 1–4 represented the days of exposure times (Ex-0, Ex-1, Ex-3, and Ex-5), respectively.

Rows	Rf Values	Peroxidase (PER) zymograms								
		Lane 1		Lane 2		Lane 3		Lane 4		Zymogram
		R_f	OD	R_f	OD	R_f	OD	R_f	OD	types
1	0.01			√	2.5	√	1.5	√	1.0	Non-U
2	0.10	√	24.6	√	35.7	√	32.4	√	44.6	M
3	0.38	√	57.9	√	37.0	√	24.9	√	43.4	M
4	0.59					√	23.4			U
5	0.62			√	2.00					U
6	0.73	√	17.5					√	2.50	Non-U
7	0.88							√	12.00	U
8	0.89			√	27.4					U
9	0.92					√	19.2			U
10	1.20							√	2.00	U
No. zymograms		3		5		5		6		
Total zymograms		19								
% of zymograms		15.78		26.31		26.31		31.57		

	Lane 1		Lane 2		Lane 3		Lane 4	
	No.	Rf	No.	Rf	No.	Rf	No.	Rf
No. and Rf of unique loci	0	–	2	0.62–0.89	2	0.59–0.92	2	0.88–1.20
% of unique loci	0.00		33.33		33.33		33.33	

	Unique (U)		(Non-U)		Polymorphic		Monomorphic (M)		Polymorphisms
	No.	%	No.	%	No.	%	No.	%	%
Frequency of zymograms and Polymorphism	6	31.57	2	10.52	8	42.10	2	10.52	80.00

scored variations in DNA polymorphisms and banding patterns among EMR-exposed *Zea mays* compared to the non-exposed ones based on primers used, alterations in the bands number of DNA, their sizes, intensities, the gain of new amplified DNA bands (unique), and disappearance of normal bands (non-unique). Additionally, this study found that these variations was dependent on EMR exposure times.

The number of amplified DNA bands may be related to the number of nucleotides and their directions within genomic DNA sequences that are complementary to the sequence of the related primer (Abdelhaliem & Al-Huqail, 2016). DNA polymorphisms generated by RAPD analysis may be due to alterations in DNA nucleotide sequences during duplication of DNA or gene expression under the EMR stressor such as additions of the amplified DNA bands, insertions of new nitrogenous bases, and transpositions of genes within genomic DNA that led to appearance of new DNA bands (unique DNA bands) (Atienzar & Jha, 2006).or due to the deletion of existing genes present on genomic DNA or transpositions of genes from their own DNA to another DNA or due to the hybridization site of a primer in one gene that is altered at a single nucleotide in second amplified gene that can eliminate of a specific amplified nucleotide sequences from second gene amplified resulting of disappearance of amplified DNA genes (non-unique bands) (Welsh & McClelland, 1991). Therefore, the unique bands can be assumed as a characteristic bioassay specific for each corn germplasm affected by EMR.

The comet assay (single-cell gel electrophoresis) is a simple method for measuring DNA strand breaks (DNA damage) in eukaryotic nuclei. Cells containing damaged DNA have the appearance of a comet with a bright

Table 5. Distribution of catalase (CAT) zymograms of EMF non-exposed and exposed *Zea mays* seedlings for days of exposure times (Ex-0, Ex-1, Ex-3, and Ex-5) based on relative front (R*f*) Values and optical densities (OD). Lanes 1–4 represented the days of exposure times (Ex-0, Ex- 1, Ex-3, and Ex-5), respectively.

Rows	R*f* Values	Esterase (EST) zymograms								Zymogram types
		Lane 1		Lane 2		Lane 3		Lane 4		
		R_f	OD	R_f	OD	R_f	OD	R_f	OD	
1	0.02	√	2.00	√	2.34			√	1.0	Non-U
2	0.09	√	32.4	√	32.9	√	25.9	√	21.1	M
3	0.22							√	15.4	U
4	0.33			√	17.2	√	27.9			Non-U
5	0.34	√	32.9					√	21.5	Non-U
6	0.69							√	57.6	U
7	0.71	√	34.7			√	46.2			Non-U
8	0.85			√	49.9					U
9	0.94					√	3.34			U
No. zymograms		4		4		4		5		
Total zymograms		17								
% of zymograms		23.53		23.53		23.53		29.41		

	Lane 1		Lane 2		Lane 3		Lane 4	
	No.	R*f*	No.	R*f*	No.	R*f*	No.	R*f*
No. and R*f* of unique loci	0	–	1	0.85	1	0.36	2	0.29–0.69
% of unique loci	0.00		25.00		25.00		50.00	

	Unique (U)		(Non-U)		Polymorphic		Monomorphic (M)		Polymorphisms
	No.	%	No.	%	No.	%	No.	%	%
Frequency of zymograms and Polymorphism	4	23.53	4	23.53	8	47.06	1	5.88	88.89

head and tail. In contrast, undamaged DNA appears as an intact nucleus with no tail. In this study, It used to determine the degree of DNA damage induced by EMR in corn seedlings. SCGE data illustrated notable alterations in the degree of DNA damage in corn nuclei exposed to EMR for one, three-, and five-days dependent on exposing time. This may be due to interaction of EMR with the DNA can stimulate the synthesis of this stress protein, causing DNA strand breaks which increase by increasing of EMR energy (Blank & Goodman, 2012). This nuclear DNA (nDNA) damages led to increase in migration of DNA fragments (tail) from the nucleus (head). This revealed that the increased EMR-exposure of corn seedlings induced DNA lesions in their cells. The DNA lesions induced by EMR may be directly due to energy deposition in cells or indirectly due to reactive oxygen species (ROS) and oxidative DNA damage (Kıvrak et al., 2017). They showed that a major concern of the genotoxic effects of non-ionizing electromagnetic radiation (EMR) is overproduction of ROS in cells and inducing oxidative stress on protein and DNA because of EMR exposure can induce DNA strand breaks and acts as a co-inductor of DNA damages rather than as a genotoxic agent. They also interpreted the genetic mechanisms by which EMR interact with protein and DNA are radical pair recombination led to increasing the concentration, activity, and lifetime of reactive oxygen species (ROS), which might cause changes in cell cycle, genetic mutation, damage to DNA leading to changes in cellular functions and cell death, modification of protein expression and oxidation of proteins, and inhibition of enzymes.

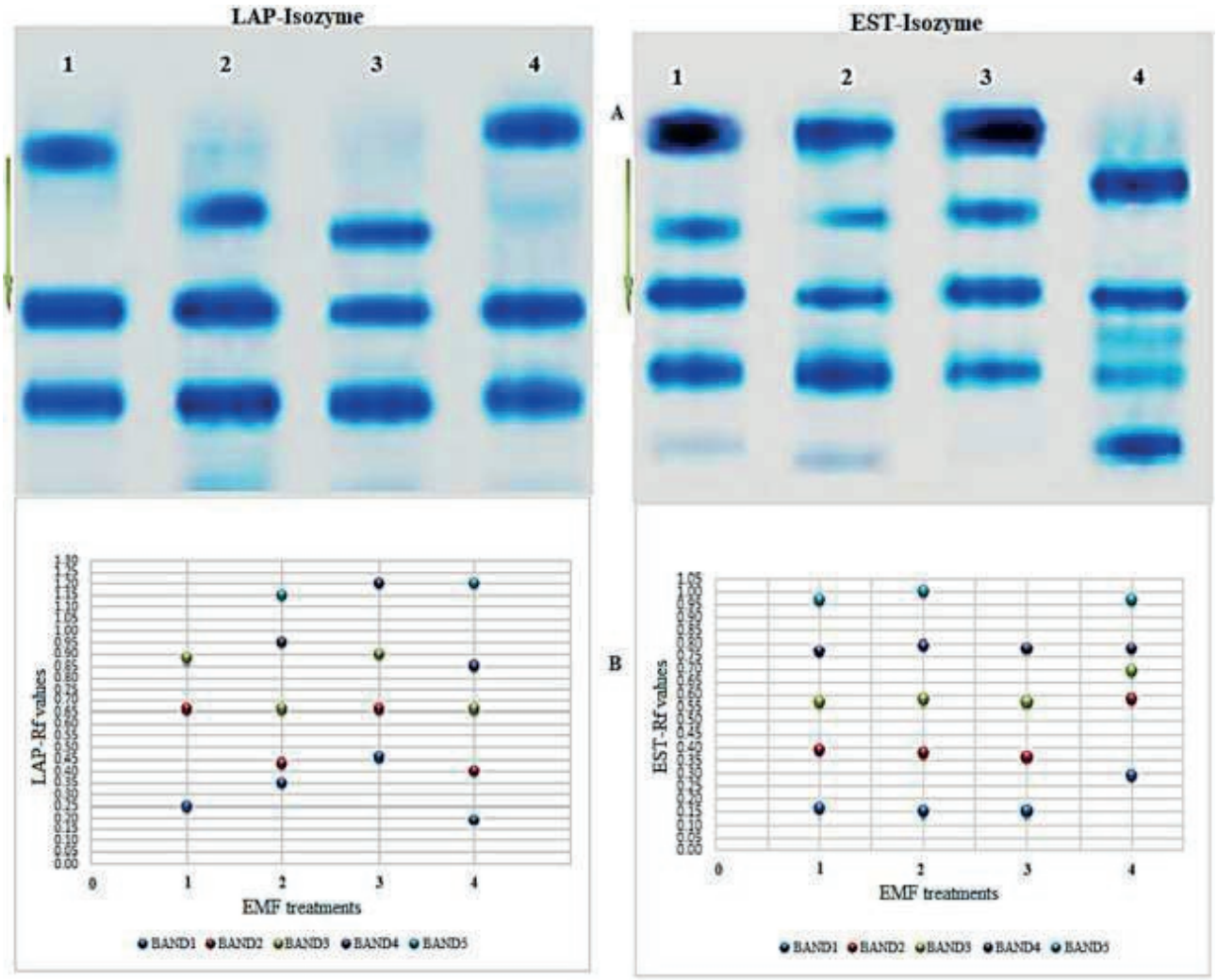

Figure 2. (A) Isozymatic patterns and (B) schematic distribution of Leucine-aminopeptidase (LAP) and Esterase (EST) zymograms (R_f values) of non-exposed and EMR exposed seedlings of *Zea mays* for days of exposure times (Ex-0, Ex-1, Ex-3, and Ex-5) based on relative front (R*f*) Values and optical densities (OD). Lanes 1–4 represented the days of exposure times (Ex-0, Ex- 1, Ex-3, and Ex-5), respectively.

CONCLUSION

The data obtained in current study observed that the longer EMR exposing time could induce notable alterations in banding patterns profile generated by SDS-PAGE, isozymatic, and RAPD bioassays in addition to distinct extent of DNA damages as estimated by comet assay. Therefore, this study concluded that each EMR exposing time had unique interaction with proteins, isozymes, and DNA in corn cells exhibiting wide range of genetic and oxidative stress on these macromolecules. Due to these distinct alteration, it might be asserted that the exposure of economic crop plants to EMR may change gene expression and subsequently, will affect their growth and grain yield. Also, it concluded that bio-assays used should be augmented for accurate and precise estimation of alterations of protein and DNA profiles after EMR exposure of crop plants and for providing excellent results and understanding how this plant was adapted.

AUTHOR CONTRIBUTION

E. M. A. and H. M.A. designed and performed the experiments. E. M. A. analyzed the data and discussed the results. E. M. A. and R. S. S. wrote the manuscript in consultation with A. A. B., and H. M.A. All of the authors read and approved the manuscript.

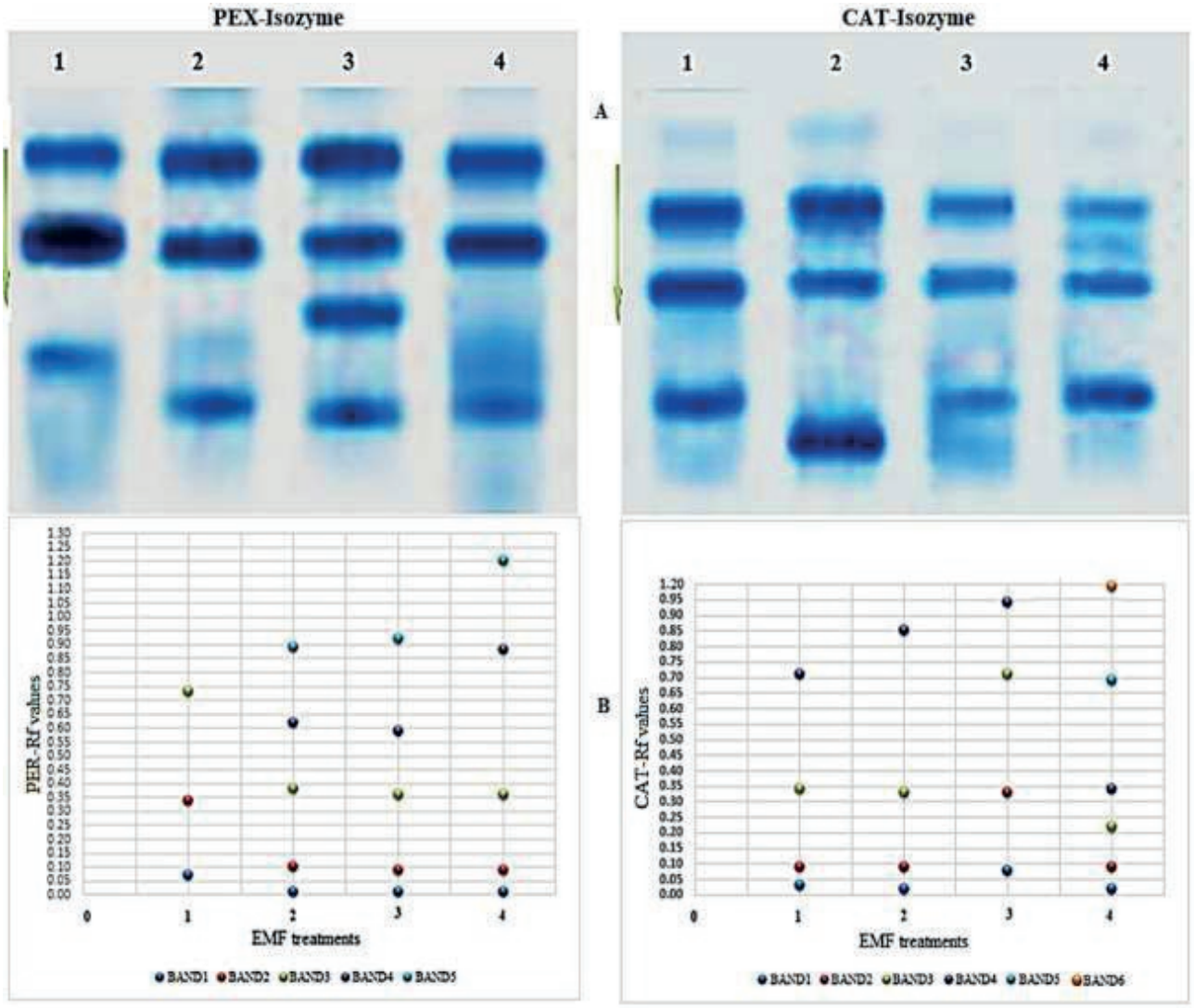

Figure 3. (A) Isozymatic patterns and (B) schematic distribution of Peroxidase (PEX) and Catalases (CAT) zymograms (R_f values) of non-exposed and EMR exposed seedlings of *Zea mays* for days of exposure times (Ex-0, Ex-1, Ex-3,and Ex-5) based on relative front (R*f*) Values and optical densities (OD). Lanes 1–4 represented the days of exposure times (Ex-0, Ex-1, Ex- 3,and Ex-5), respectively.

ACKNOWLEDGMENT

The authors would like to express their deep thanks to Professor Magda Hanafy, Biophysics Department, Science College, Zagazig University, for her effort in performing Electromagnetic radiation (EMR).

REFERENCES

Abdel Haliem E, Al-Huqail AA. 2013. Oxidative damage and mutagenic potency of fast neutron and UV-B radiation in pollen mother cells and seed yield of *Vicia faba* L. BioMed research international 2013:1:12

Abdelhaliem E, Al-Huqail AA. 2016. Detection of protein and DNA damage induced by elevated carbon dioxide and ozone in Triticum aestivum L. using biomarker and comet assay. Genetics and Molecular Research 15(2):1-19.

Ahanger MA, Akram NA, Ashraf M, Alyemeni MN, Wijaya L, Ahmad P. 2017. Plant responses to environmental stresses—from gene to biotechnology. AoB Plants 9(4): 1-17. Atienzar FA, Jha AN. 2006. The random amplified polymorphic DNA (RAPD) assay and related techniques applied to genotoxicity and carcinogenesis studies: a critical review. Mutation Research/ Reviews in Mutation Research 613(2-3):76-102.

Table 6. Amplification banding patterns and genomic template stability (GTS) of nuclear DNA analyzed by RAPD-PCR isolated from EMF non-exposed and exposed *Zea mays* seedlings for days of exposure times (Ex-0, Ex-1, Ex-3,and Ex-5) and analyzed by Bio-One D++ software (Vilber Lourmat, France). Lanes 1–4 represented the days of exposure times (Ex-0, Ex-1, Ex-3,and Ex-5), respectively.

Primer code	Primers sequences (5′→3′)	Amplicon sizes (bp)	Number of scorable bands in each lane				Types of DNA bands										Polymorphisms
							Polymorphic								Monomorphic		
							Total bands		Unique (U)		Non -U		Total				
			Lane1	Lane2	Lane3	Lane4	No	%	No	%	No	%	No	%	No	%	%
P-02	GGA CCC AAC C	1008-170	3	3	4	5	15	17.65	5	5.88	3	3.53	8	9.41	1	1.18	90.91
P-06	ACC TGA ACG G	938-709	4	3	3	5	15	17.65	4	4.71	6	7.06	10	11.76	1	1.18	88.89
P-08	GTG TGC CCC A	877-438	3	3	4	5	15	17.65	6	7.06	3	3.53	9	10.59	2	2.35	81.83
P-10	GGT CTA CAC C	774-214	5	5	3	7	20	23.53	9	10.59	5	5.88	14	16.47	1	1.18	90.91
P-14	CTT CCC CAA G	846-153	5	5	5	4	20	23.53	12	14.12	6	7.06	18	21.18	0	–	100.00
Overall total bands in each lane			21	19	19	26	85	100	36	42.35	23	27.06	59	69.41	5	5.88	92.19
Sum			85														
% of total bands in each lane			24.71	22.35	22.35	30.59											

Primer code	No. and Sizes (bp) of unique amplified DNA bands							
	Lane 1		Lane 2		Lane 3		Lane 4	
	No.	Sizes	No.	Sizes	No.	Sizes	No.	Sizes
P-02	1	985	1	979	1	1000	2	1008–450
P-06	2	688–595	0	–	0	–	2	780–640
P-08	0	–	1	706	2	650–500	3	780–520
P-10	2	600–200	2	550–418	1	366	4	690–640–493–297
P-14	5	721–652–594–528–153	2	371–153	3	797–483–406	2	846–700
Total unique bands	10		6		7		13	
Sum of unique bands	36							
% of unique bands	27.78		16.67		19.44		36.11	

Blank M, Goodman R. 2011. DNA is a fractal antenna in electromagnetic fields. International Journal of radiation biology 87(4): 409-415.

Blank M, Goodman R M. 2012. Electromagnetic fields and health: DNA-based dosimetry. Electromagnetic Biology and Medicine 31(4): 243-249.

Cenkci S, Yıldız M, Ciğerci İH, Konuk M, Bozdağ A. (2009). Toxic chemicals-induced genotoxicity detected by random amplified polymorphic DNA (RAPD) in bean (Phaseolus vulgaris L.) seedlings. Chemosphere 76 (7): 900-906.

Dikilitas M, Kocyigit A, Yigit F. (2009). A molecular-based fast method to determine the extent of DNA damages in higher plants and fungi. African Journal of Biotechnology, 8(14).

Elsh J, McClelland M. (1991). Genomic fingerprinting using arbitrarily primed PCR and a matrix of pairwise combinations of primers. Nucleic Acids Research 19:5275–5279.

Erturk FA, Agar G, Arslan E, Nardemir G, Sahin, Z. 2014. Determination of genomic instability and DNA methylation effects of Cr on maize (*Zea mays* L.) using RAPD and CRED-RA analysis. Acta Physiologiae Plantarum 36(6):1529-1537.

Galani S, Naz F, Soomro F, Jamil I, Azhar A, Ashraf A. 2011. Seed storage protein polymorphism in ten elite rice (Oryza sativa L.) genotypes of Sindh. African Journal of biotechnology 10(7): 1106-1111

Gjorgieva D, Kadifkova Panovska T, Ruskovska T, Bačeva K, Stafilov T. 2013. Influence of heavy metal stress on antioxidant status and DNA damage in Urtica dioica. BioMed Research International 2013:1-6.

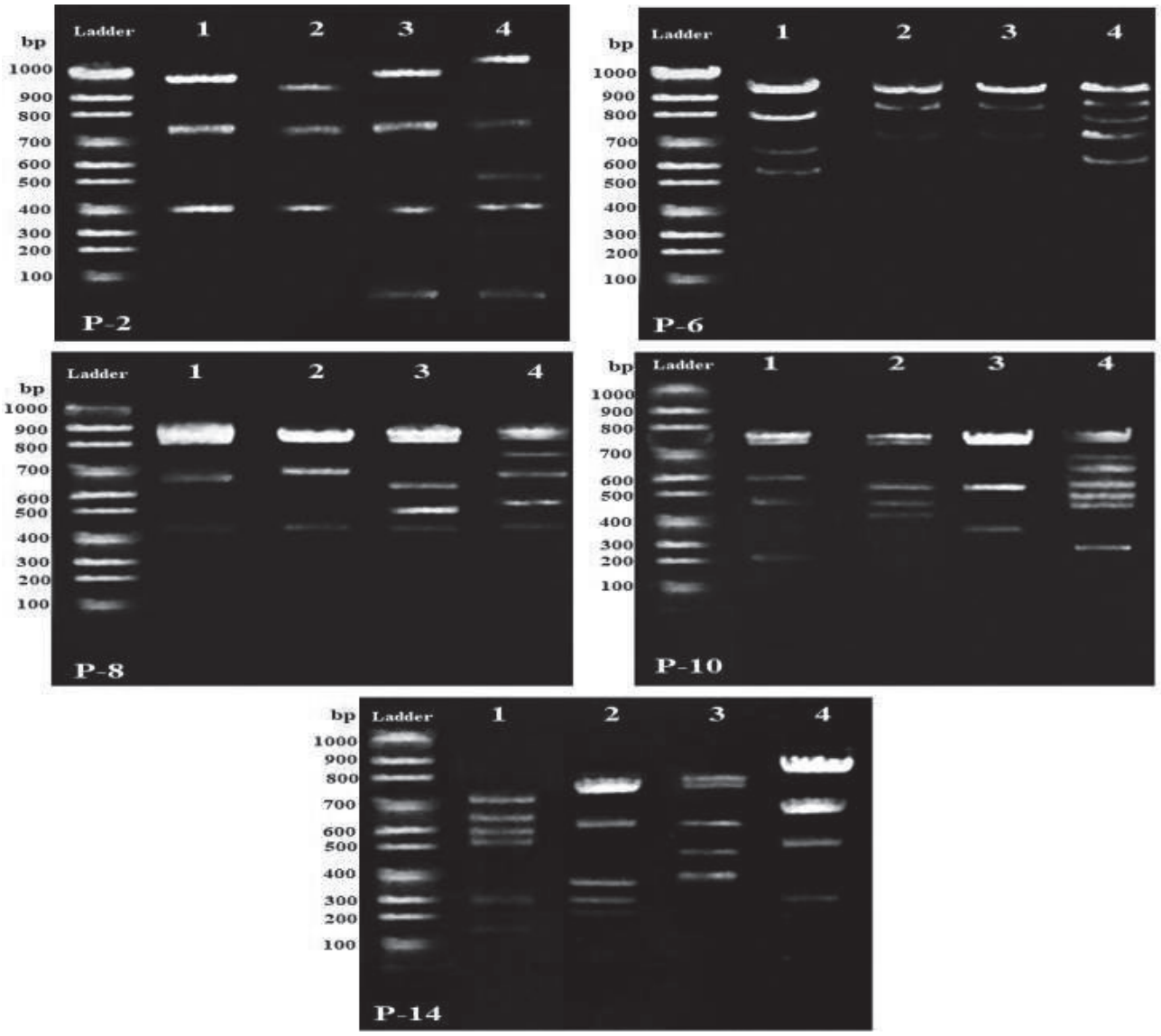

Figure 4. Amplified DNA banding patterns of genomic DNA isolated from non-exposed and EMR exposed seedlings of *Zea mays* for days of exposure times (Ex-1, Ex-3,and Ex-5) and analyzed by RAPD-PCR DNA using five random primers (P-02, 06, 08, 10, and 14). Lanes 1–4 represented the days of exposure times (Ex-0, Ex-1, Ex-3,and Ex-5), respectively.

Hailu HW, Kristiyanto DH, ALatawi ARA, Raqib SM. 2014. Isozyme electrophoresis and morphometric comparison of reed (*Imperata cylindrical*) adaptation to different altitudes. International Journal of Innovative Research in Science, Engineering and Technology 3(5):12387-12394.

Hojilla-Evangelista MP, & Evangelista RL. 2006. Effects of cooking and screw-pressing on functional properties of Cuphea PSR23 seed proteins. Journal of the American Oil Chemists' Society 83(8):713-718.

Iderawumi AM, Friday CE. 2020. Effects of magnetic field on pre-treatment of seedlings and germination. Journal of Agriculture and Research 6 (9):1-8.

Juchimiuk J, Gnys A, Maluszynska J. 2006. DNA damage induced by mutagens in plant and human cell nuclei in acellular comet assay. Folia Histochemica et Cytobiologica, 44(2):127-131.

Karaca M. 2013. Isozymes as biochemical markers in plant genetics. International Journal of Agriscience 3(11):851-861.

Kit YS, Chandran S. 2010. A simple, rapid, and efficient method of isolating DNA from Chokanan mango (*Mangifera indic*a L.). African Journal of Biotechnology 9(36): 5805- 5808.

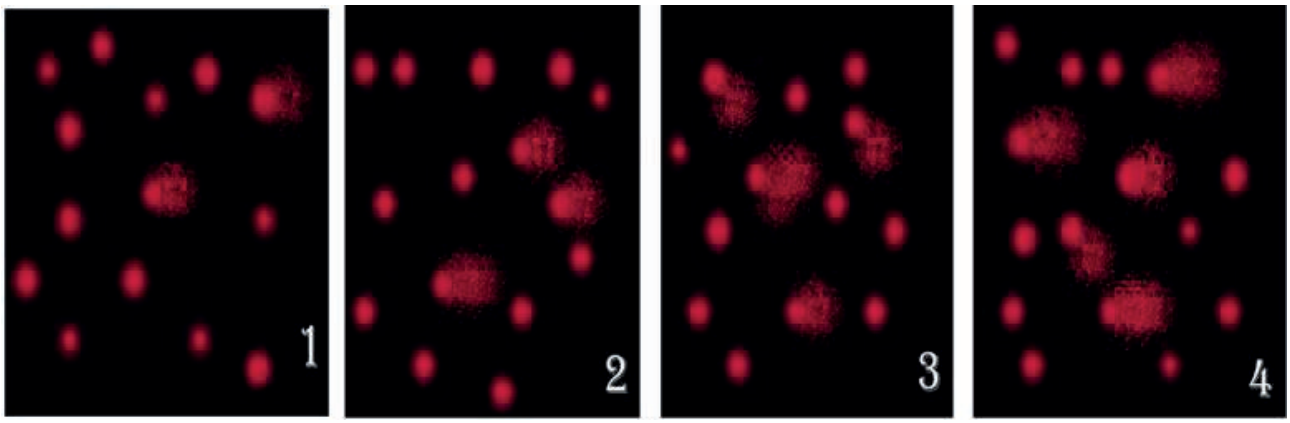

Figure 5. Comet nuclei prepared by Comet assay show the variable extent of nuclear DNA damage in the nuclei isolated from non-exposed and EMR exposed *Zea mays* for days of exposure times (Ex-1, Ex- 3,and Ex-5). Images 1–4 represented the days of exposure times (Ex-0, Ex-1, Ex-3,and Ex-5), respectively.

Table 7. Damage extent of nuclear DNA generated by Comet assays in EMF non-exposed and exposed *Zea mays* nuclei for days of exposure times (Ex-0, Ex-1, Ex-3,and Ex-5).

EME exposure time (days)	Tailed %	Un-tailed%	Tail length (μm)	Tail DNA %	Tail Moment Unit
Ex-0	3	97	0.99	1.05	1.73
Ex-1	7	93	2.05	2.19	4.49
Ex-3	12	88	2.46	2.52	6.20
Ex-5	20	80	2.88	2.79	8.04

Kıvrak EG, Yurt KK, Kaplan AA, Alkan I, Altun, G. 2017. Effects of electromagnetic fields exposure on the antioxidant defense system. Journal of microscopy and ultrastructure 5(4):167-176.

Kumar P, Gupta VK, Misra AK, Modi DR, Pandey BK. 2009. Potential of molecular markers in plant biotechnology. Plant omics 2(4): 141-162.

Labate JA. (2000). Software for population genetic analyses of molecular marker data. Crop Science 40(6): 1521-1528.

Laemmli UK. 1970. Cleavage of structural proteins during the assembly of the head of bacteriophage T4. Nature 227(5259): 680-685.

Lai, H. 2021. Genetic effects of non-ionizing electromagnetic fields. Electromagnetic Biology and Medicine 40(2): 264-273.

Nandhakumar S, Parasuraman S, Shanmugam MM, Rao KR, Chand P, Bhat BV. 2011. Evaluation of DNA damage using single-cell gel electrophoresis (Comet Assay). Journal of pharmacology & pharmacotherapeutics: 2(2): 107–111.

Nyakane NE, Markus ED, Sedibe MM. 2019. The effects of magnetic fields on plants growth: a comprehensive review. International Journal of food engineering 5(1): 79-87.

Ortiz J, Suarez D, Puentes A, Velasquez P, Santis Navarro A. 2015. Comparison of the effects in the germination and growth of corn seeds (Zea mays L.) by exposure to magnetic, electrical, and electromagnetic fields. Chemical Engineering Transactions 43: 169–174.

Pasteur N, Pasteur G, Bouhomme F, Catalan, J., Davidian, B. J. 1988 . Practical isozyme genetics. J Wiley & Sons, New York.

Qi J, Chen Y, Copenhaver GP, Ma H. 2014. Detection of genomic variations and DNA polymorphisms and impact on analysis of meiotic recombination and genetic mapping. Proceedings of the National Academy of Sciences 111(27):10007-10012.

Rio, L. C., & Rio, M. M. 2013. Effect of electro-magnetic field on the growth characteristics of okra (*Abelmoschus esculentus*), tomato (*Solanum lycopersicum*) and eggplant (*Solanum melongena*). International Journal of Scientific and Research Publications 3(10):41-45.

Ruiz-Gómez M J, Martínez-Morillo M. 2009. Electromagnetic fields and the induction of DNA strand breaks. Electromagnetic biology and medicine 28(2): 201-214.

Sadia M, Malik SA, Rabbani MA, Pearce SR. 2009. Electrophoretic characterization and the relationship between some Brassica species. Electronic Journal of Biology 5(1): 1-4.

Santos CL, Pourrut B, Ferreira de Oliveira JM. 2015. The use of comet assay in plant toxicology: recent advances. Frontiers in Genetics 6: 216.

Shabrangi A, Majd A, Sheidai M. 2011. Effects of extremely low frequency electromagnetic fields on growth, cytogenetic, protein content and antioxidant system of *Zea mays* L. African Journal of Biotechnology 10(46): 9362-9369.

Shikazono N, Suzuki C, Kitamura S, Watanabe H, Tano S, Tanaka A. 2005. Analysis of mutations induced by carbon ions in Arabidopsis thaliana. Journal of Experimental Botany 56(412): 587-596.

Tiwari C, Bakshi M. 2015. Isozymatic Characterization of Accessions of *Arundinaria falcata* (Nees). Forest Research 4(1):133-137.

Williams JG, Kubelik AR, Livak KJ, Rafalski JA, Tingey SV. 1990. DNA polymorphisms amplified by arbitrary primers are useful as genetic markers. Nucleic acids research, 18(22): 6531-6535.

Yan J, Warburton M, Crouch J. 2011. Association mapping for enhancing maize (*Zea mays* L.) genetic improvement. Crop science 51(2):433-449.

Caryologia
International Journal of Cytology, Cytosystematics and Cytogenetics

Firenze University Press
www.fupress.com/caryologia

OPEN ACCESS

Citation: Saeedeh Sadat Mirzadeh Vaghefi, Adel Jalili (2022). Chromosome counts of some species of wetland plants from Northwest Iran. *Caryologia* 75(4): 67-76. doi: 10.36253/caryologia-1674

Received: May 29, 2022

Accepted: December 06, 2022

Published: April 28, 2023

Data Availability Statement: All relevant data are within the paper and its Supporting Information files.

Competing Interests: The Author(s) declare(s) no conflict of interest.

Chromosome counts of some species of wetland plants from Northwest Iran

Saeedeh Sadat Mirzadeh Vaghefi*, Adel Jalili

Research Institute of Forests and Rangelands, Agricultural Research, Education and Extension Organization (AREEO), P. O. Box 13185-116, Tehran, Iran
*Corresponding author. E-mail: myalyssum94@gmail.com

Abstract. Wetlands scatter as microclimates in mountain areas of Iran. In this investigation, the chromosome number of species and populations from Azerbaijan provinces were studied. After seed germination and root fixation, meristem cells were stained and photographs were taken for cells in the metaphase stage by light microscope. Data were analyzed by Micromeasure and excel softwares. As many as 28 populations of 24 species were studied. The chromosome numbers of two species (viz. *Ranunculus kotschyi*) were reported for the first time. 11 populations in 9 species were reported for the first time from Iranian populations (viz. *Alisma plantago-aquatica*, *Prunella vulgaris*, *Scrophularia umbrosa*). The range of haploid chromosome numbers is between n=6 and n=21. Ideograms were depicted for each species.

Keywords: chromosome number, wetland, ideogram, Azerbaijan.

INTRODUCTION

Wetlands are considerate as microclimates in alpine areas with special species in Iran. In the steppic mountain areas of Iran are a wide range of wetland vegetation. The wetland habitats are sharply embedded within vegetation of the IranoTuranian steppes that are more characteristic of this region and are of interest both in themselves and for wider comparison with EuroSiberian wetlands (Naqinezhad, 2012).

Most of the wetlands in the northwest part of Iran develop when snowmelt and rain fill the pockmarks left on the landscape by glaciers. This kind of wetlands was categorized in Prairie potholes class (EPA 2001).

In angiosperms, the haploid chromosome number varies between $n = 2$ and $n = 132$, but the majority of them show a range between $n = 7$ and $n = 12$(Sharma, 2009). Variation or constancy in the chromosome number within taxa of different categories has been proven to be important characters for taxonomic groupings (Sharma, 2009).

We studied on chromosome number of 28 accessions of 24 species belonging to 21 genera of 12 families wetland plants of Azerbaijan Mountains of Iran. The aim of this study was to investigate on chromosome number of Wetland plants of Azerbaijan provinces.

MATERIALS AND METHODS

Plant materials

Specimens and seeds were collected from natural habitats of Azerbaijan provinces (West, East Azerbaijan and Ardebil) in 2013 and 2014. Vouchers are deposited in TARI (Table 1). The plant samples were identified by Flora of Iran (Assadi *et al*., 2018) and Flora Iranica (Rechinger, 2005).

Chromosome counts

The seeds were used for chromosome counts. Seeds were germinated at 20-25°C on moist filter paper in Petri dishes. Root tips of seeds had grown 1–1.5 cm in length were stopped from the germinating by pretreating with *alpha-bromonaphthalene* for two hours. Then fixed with acetic alcohol (1:3) for 4 h and stored in 70% alcohol at 2–4°C. Then the root tips were rinsed in water and hydrolyzed with 1 N HCl for 10–18 min at 60°C and rinsed in running water for a minimum of 3–5 min. Staining of root tips was carried out for 1–2 h and root tips were put in hematoxylin for 5–10 min to improve staining. Finally, squash preparations were made. Chromosome nomenclature follows Levan *et al*. (1964) and Stebbins (1971). The photos were taken by light microscope (BH2 Olympus × 1000).

We measured the chromosomes using MicroMeasure (version 3.3 (Reeves and Tear, 2000).

RESULTS

Our goal in this project was to create a chromosome index for the wetland plants of Azerbaijan. It is so difficult to discussion about several species from several families that collected for common goal.

Table 1. List of species examined, Family, Locality, Altitude, Voucher number, and Habitat.

Voucher no.	Alt.	Locality	Family	Species
102715	2392	East Azerbaijan, Tabriz, Arshad chamani	Alismataceae	*Alisma plantago- aquatica* L.
102769	2281	West Azerbaijan, Salmas, Jam Valley	Poaceae	*Alopecurus arundinaceus* Poir.
102752	1900	Aligo Village	Brasicaceae	*Barbarea plantaginea* DC.
8228	----	East Azerbaijan, Bostanabad	Poaceae	*Catabrosa aquatica* (L.) P.Beauv.
102750	2266	Ardebil province, Salmas, Jam Valley	Asteraceae	*Erigeron acris* L. subsp. *pycnotrichus* (Vierh.) Rech. f.
101699	2266	West Azerbaijan, Dalamper Village	Geraniaceae	*Geranium sylvaticum* L.
102751	2266	West Azerbaijan, Dalamper Village	Hypericaceae	*Hypericum perforatum* L.
102807	2266	West Azerbaijan, Dalamper Village	Asteraceae	*Inula aucheriana* DC.
102762	1688	East Azerbaijan, Hashtroud, Zalbil	Asteraceae	*Mulgedium tataricum* (L.) DC.
8239	1819	East Azerbaijan, Hashtroud, Baboneh village	Poaceae	*Phragmites australis* Trin. ex Steud.
101691	2281	West Azerbaijan, Salmas, Jam Valley	Plantaginaceae	*Plantago atrata* Hoppe.
101601	2266	West Azerbaijan, Dalamper Village	Lamiaceae	*Prunella vulgaris* L. (Dalamper)
8242	----	East Azerbaijan, Bostanabad	Lamiaceae	*Prunella vulgaris* L. (Bostanabad)
101668	2296	Ardebil, Agh Ghabali	Rannunculaceae	*Ranunculus aquatilis* var. *diffusus* With.
101670		East Azerbaijan, Varzaghan	Rannunculaceae	*Ranunculus dolusus* Fisch . & C. A. Mey.
101674	1648	Ardebil province, Ardebil to Bolaghvar	Rannunculaceae	*Ranunculus kotschyi* Boiss.
102738	1900	East Azerbaijan, Bostanabad	Scrophulariaceae	*Scrophularia umbrosa* Dumort.
102805	1688	East Azerbaijan, Hashtroud, Zalbil	Asteraceae	*Senecio pseudoorientalis* Schischk. (Hashtroud)
102761	1648	Ardebil province, Ardebil to Bolaghvar	Asteraceae	*Senecio pseudoorientalis* Schischk.)Bolaghvar)
101688	2266	West Azerbaijan, Dalamper Village	Fabaceae	*Trifolium pratense* L.
102724	2281	West Azerbaijan, Salmas, Jam Valley	Juncaginaceae	*Triglochin maritima* L. (Jam valley(
102728	1650	Ardebil province, Ardebil to Bolaghvar	Juncaginaceae	*Triglochin maritima* L. (Bolaghvar)
102753	1900	East Azerbaijan, Bostanabad	Asteraceae	*Tripleurospermum disciforme* Sch.Bip. (Bostanabad)
102784	1900	East Azerbaijan, Tabriz, Arshad chamani	Asteraceae	*Tripleurospermum disciforme* Sch.Bip. (Jam valley)
102713	2392	East Azerbaijan, Tabriz, Arshad chamani	Scrophulariaceae	*Veronica orientalis* Miller (Arshad Chamani)
102716	2281	East Azerbaijan, Bostanabad	Scrophulariaceae	*Veronica orientalis* Miller (Bostanabad)
102729	2281	East Azerbaijan, Bostanabad	Scrophulariaceae	*Veronica filiformis* Sm.
101677	1650	Ardebil province, Ardebil to Bolaghvar	Fabaceae	*Vicia variabilis* Freyn & Sint. ex Freyn

Table 2. Chromosome counts of studied species previously described in the literature.

References (viz.)	2*n*	References	N	Species
(Dobes *et al.,* 1997)(Wulff, 1939)(Love and Love., 1942)	10, 12, 14	(Kaur et al., 2011)	14	*Alisma plantago- aquatica*
(Kuzmanov, 1993)(Amosova *et al.,* 2019)(Sheidai *et al.,* 2009)	28, 42	(Koull and Gohil 1991)	14	*Alopecurus arundinaceus*
(Astanova, 1999)(Ørgaard and Linde-laursen, 2014)	16	(Aryavand, 1977) (Ghaffari, 2007)	8	*Barbarea plantaginea*
(Sawicka, 1991)(Lövkvist and Hultgård., 1999)(Sheidai *et al.,* 2009)	20			*Catabrosa aquatica.*
(Kaur *et al.,* 2011)(Bala and Gupta, 2013)(Paule *et al.*, 2017)	18			*Erigeron acris* (other subspecies)
(Petrova and Stanimirova, 2001) (Lövkvist and Hultgård 1999)(Dmitrieva, 1986)	28, 24	(Clifford Odets, 1954)	12	*Geranium sylvaticum*
(Ciccarelli *et. al.* 2001)(Lövkvist and Hultgård, 1999)(Krasnikov and Schaulo 1990)(Kalinka *et al.*, 2014((Baltisberger and Widmer, 2009((Brutovska et al., 2000)	32	(Ghaffari, 2006)	16	*Hypericum perforatum*
		(Chehregani and Hajisadeghian, 2009)	9	*Inula aucheriana*
(Probatova, 2004)	36			*Mulgedium tataricum*
(Lövkvist and Hultgård 1999)(Panahi., 1979)(Gervais *et al.*, 1993)	42,48, 72,96			*Phragmites australis*
(Petrova and Stanimirova, 2001)(Lessani and Chariat-panahi., 1979)	12, 24			*Plantago atrata*
(Lövkvist and Hultgård 1999((Krasnikov and Schaulo., 1990)	28			Prunella vulgaris
(Dahlgren and Cronberg, 1996)	32,48			*Ranunculus aquatilis* var. *diffusus*
(Baltisberger, 1991) (Agapova, 1981)(Assadi, 1989) (Ghasemi *et al.*, 2015)	28, 32			*Ranunculus dolusus*
Not reported				*Ranunculus kotschyi*
(Javurkova, 1979)(Grau, 1979)(Vitek *et al.* 1992)	26,52	(Grau, 1979)	13, 26	*Scrophularia umbrosa*
		(Ghaffari, 1999)	20	*Senecio pseudoorientalis*
(Probatova, 2000) (Krasnikov and Schaulo, 1990)(Zhang *et al.,* 1993)(Sheidai *et al.,* 1998)	14, 16			*Trifolium pratense*
(Lövkvist and Hultgård. 1999)(Krasnikov, 1991)) Rotreklova, 2004((Uchiyama, 1989)(Iwatsubo *et al.*, 1998)	48,120			*Triglochin maritima*
(Ghaffari, 1999) (Hayirlioglu-Ayaz, 2011)	18	(Ghaffari, 1999) (Razaq, et al., 1994)	9	Tripleurospermum disciforme
(Ghaffari, 1986)	32	(Ghaffari, 1987)	32	Veronica orientalis
(Pogan *et al.*, 1990)(Dzhus and Dmitrieva, 2001)(Albach *et al.*, 2009)	14	(Dobes and Vitek, 2000)	7	*Veronica filiformis*
(Hesamzadeh Hejazi and Rasuli, 2006)(Hesamzadeh Hajazi and Ziaei Nasab, 2009)	14			*Vicia variabilis*

Of 24 examined species (Table 2), 5 species have two populations (*Prunella vulgaris, Tripleurospermum disciforme*, *Pedicularis sibthorpii*, *Senecio pseudoorientalis* and *Veronica orientalis*). Another species has just one population. Asteraceae (5 species), Scrophulariaceae (3 species), Poaceae and Ranunculaceae (3 species) families have the most species respectively.

The chromosomes counts of the taxa previously reported are in Table 2. Most of them confirm our results.

Chromosome numbers of *Ranunculus kotschyi* (Fig. 2P) and *Erigeron acris* subsp. *pycnotrichus* (Fig. 1F) were reported for the first time. *Alisma plantago-aquatica* (Fig. 1A), *Prunella vulgaris* (Fig. 2M & N), *Scrophularia umbrosa* (Fig. 2Q), *Mulgedium tataricum* (Fig. 1J), *Ranunculus aquatilis* var. *diffusus* (Fig.1D), *Erigeron acris* subsp. *pycnotrichus* (Fig.1F), *Geranium sylvaticum* (Fig.1G), *Triglochin maritima* (Fig.3U&V), *Veronica filiformis* (Fig. 3Y) were reported for the first time of Iranian populations. Sporophytic count of *Barbarea plantaginea* (Fig. 1C) was reported for the first time from Iran.

The details of each taxon reported as in Table 3.

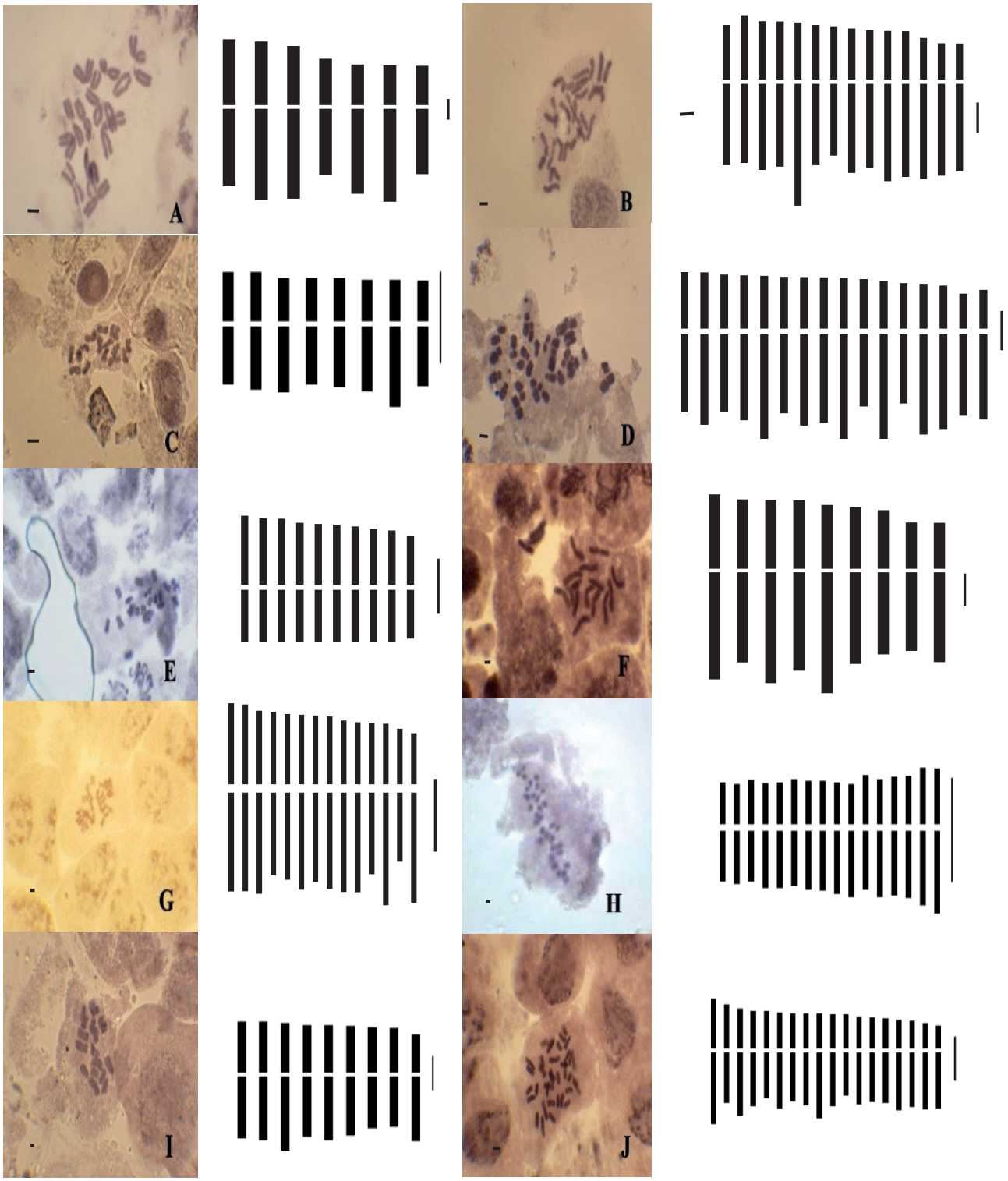

Figure 1. Somatic metaphase chromosome, Ideogram of each population is on the right side of the image: A: *Alisma plantago- aquatica* (2*n* = 14); B: *Alopecurus arundinaceus* (2*n* = 28); C: *Barbarea plantaginea* (2*n* = 16); D: *Ranunculus aquatilis* var. *diffusus* (2*n* = 32); E: *Catabrosa aquatica* (2*n* = 20); F: *Erigeron acris* subsp. *pycnotrichus* (2*n* = 18); G: *Geranium sylvaticum* (2*n* = 28); H: *Hypericum perforatum* (2*n* = 32); I: *Inula aucheriana* (2*n* = 18); J: *Mulgedium tataricum* (2*n* = 36). Scale bar: 1 μm.

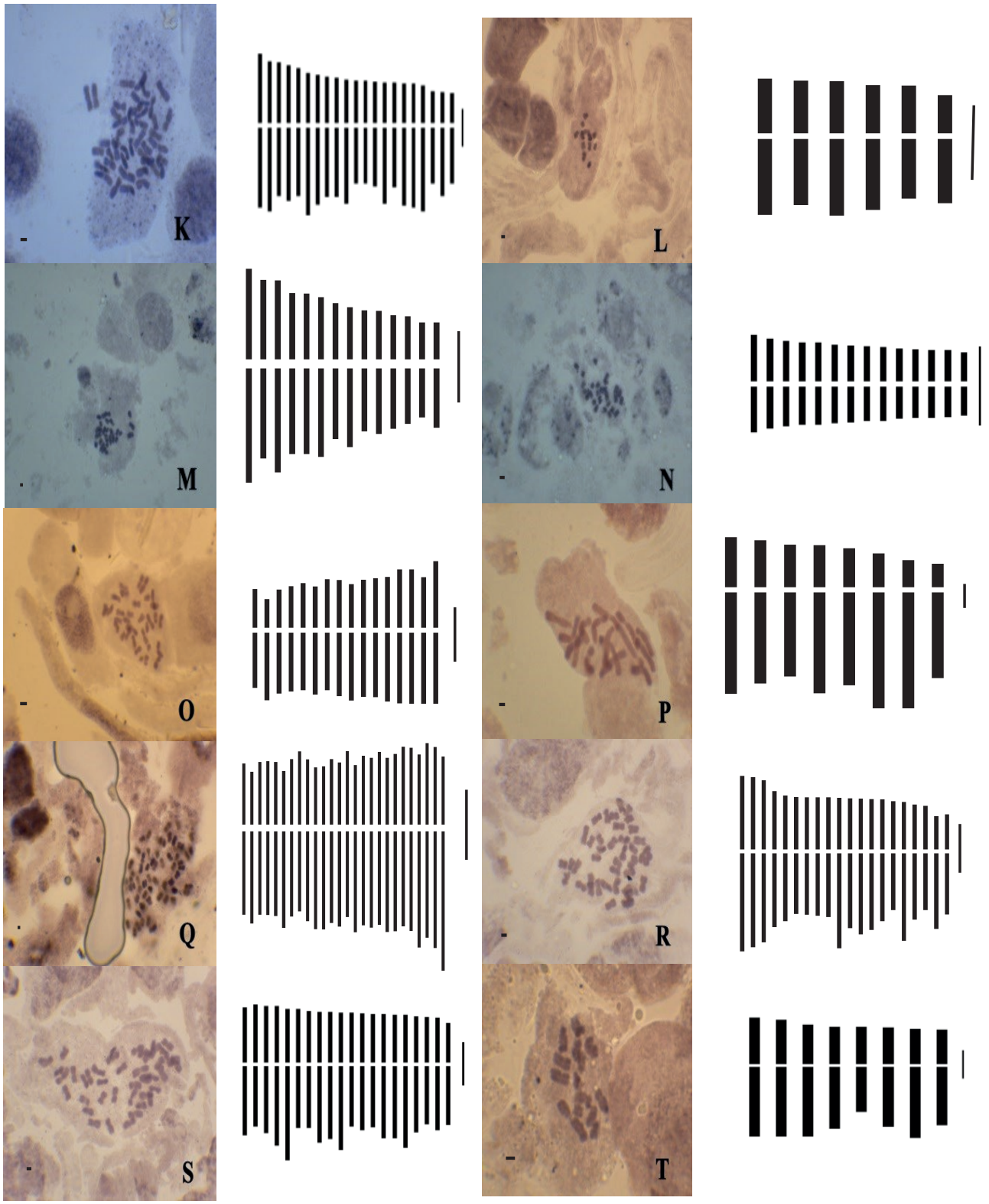

Figure 2. Somatic metaphase chromosome, Ideogram of each population is on the right side of the image: K: *Phragmites australis* (2*n* = 42); L: *Plantago atrata* (2*n* = 12); M: *Prunella vulgaris* (Dalamper) (2*n* = 28); N: *Prunella vulgaris* (Bostanabad) (2*n* = 28); O: *Ranunculus dolusus* (2*n* = 32); P: *Ranunculus kotschyi* (2*n* = 16); Q: *Scrophularia umbrosa* (2*n* = 52); R: *Senecio pseudoorientalis* (Hashtroud) (2*n* = 40); S: *Senecio pseudoorientalis*)Bolaghvar) (2*n* = 40); T: *Trifolium pratense* (2*n* = 16). Scale bar: 1 µm.

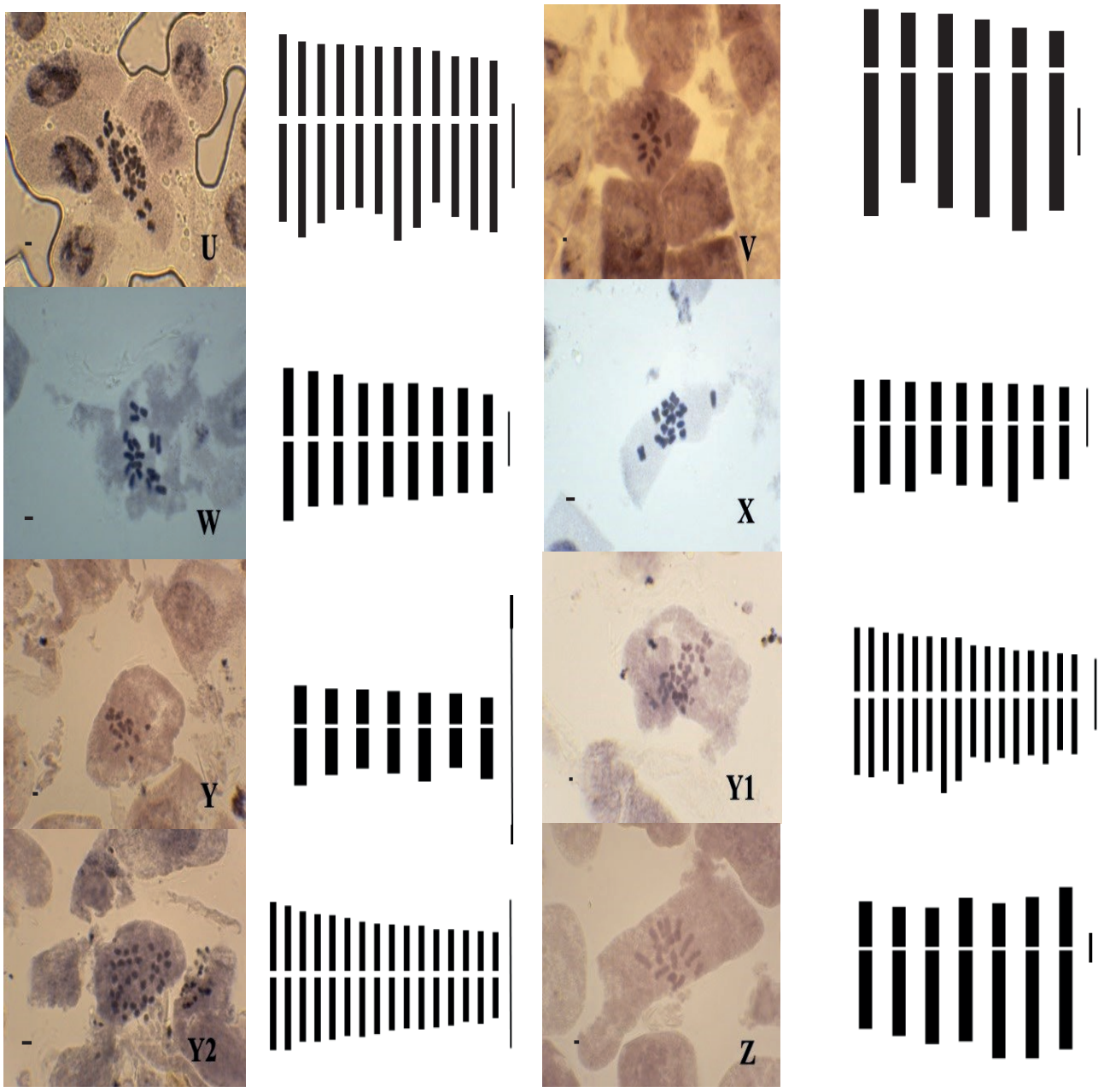

Figure 3. Somatic metaphase chromosome, Ideogram of each population is on the right side of the image: U: *Triglochin maritima* (Jam valley) (2*n* = 24); V: *Triglochin maritima* (Bolaghvar) (2*n* = 12); W: *Tripleurospermum disciforme* (Bostanabad). (2*n* = 18); X: *Tripleurospermum disciforme* (Jam valley((2*n* = 18); Y: *Veronica filiformis* (2*n* = 14); Y1: *Veronica orientalis* (Arshad Chamani) (2*n* = 32); Y2: *Veronica orientalis* (Bostanabad) (2*n* = 32); Z: *Vicia variabilis* (2*n* = 14). Scale bar: 1 µm.

Somatic metaphase and Ideograms of taxa were shown (Figs 1-3).

DISCUSSION

Only some interesting results are discussed here.

The chromosome number of the most of the species support by former studies (Table 2). The variation ranges of haploid chromosome numbers in studied species are between *n*=6 and *n*=21.

Populations in *Triglochin maritima* (Fig. 3U & V) comprise different ploidy levels (2*n* = 24, 12). Some species like *Prunella vulgaris* (Fig. 2M & N), *Veronica ori-*

Table 3. Somatic chromosome number (2n), Ploidy level, karyotype formula, ranges of chromosome length and degree of Asymmetry according to STEBBINS (1971) for the studied taxa, Figure numbers are related images in Fig 1

Figure number (Figs.1-3)	Stebbins	Chromosome range length (μm)	Karyotype formula	Ploidy level	x	2*n*	Taxa
A	B1	5.3-7.83	2sm+5m	2	7	14	*Alisma plantago- aquatica*
B	A2	4.1-5.95	8sm+6m	4	7	28	*Alopecurus arundinaceus*
C	A1	1.06-1.29	2sm+6m	2	8	16	*Barbarea plantaginea*
E	A1	2.25-3.09	10m	4	5	20	*Catabrosa aquatica*
F	A1	3.44-5.10	3sm+6m	2	9	18	*Erigeron acris* subsp. *pycnotrichus*
G	A1	1.51-2.19	2sm+12m	2	14	28	*Geranium sylvaticum*
H	A1	0.92-1.37	16m	4	8	32	*Hypericum perforatum*
I	A1	2.91-3.8	9m	*2*	9	18	*Inula aucheriana*
J	A2	2.14-3.30	5sm+13m	4	9	36	*Mulgedium tataricum*
K	A2	2.8-4.89	10sm+11m	4	An.	42	*Phragmites australis*
L	A1		6m	2	6	12	*Plantago atrata*
M	B1	0.95-2.28	14m	2	14	28	*Prunella vulgaris* (Dalamper)
N	A1	0.7-1.11	14m	2	14	28	*Prunella vulgaris (*Bostanabad)
D	A2	2.01-3.31	9sm+7m	4	8	32	*Ranunculus aquatilis* var. *diffusus*
O	A2	1.89-2.87a	4sm+12m	4	8	32	*Ranunculus dolusus*
P	A3	3.67-5.38	5sm+3st	2	8	16	*Ranunculus kotschyi*
Q	A1	1.51-3.15	4sm+22m	4	13	52	*Scrophularia umbrosa*
R	A1	2.41-4.31	4sm+16m	4	10	40	*Senecio pseudoorientalis* (Hashtroud)
S	A2	2.6-3.66	2sm+18m	4	10	40	*Senecio pseudoorientalis*)Bolaghvar)
T	A1	3.41-4.80	2sm+6m	2	8	16	*Trifolium pratense*
U	A1	1.88-2.46	3sm+9m	4	6	24	*Triglochin maritima* (Jam valley)
V	A3	4.23-5.16	3sm+3st	2	6	12	*Triglochin maritima* (Bolaghvar)
W	A1	2.14-2.7	9m	2	8	18	*Tripleurospermum disciforme* (Bostanabad).
X	B1	1.81-2.86	9m	2	9	18	*Tripleurospermum disciforme* (Jam valley(
Y1	A1	0.73-1.31	16m	4	8	32	*Veronica orientalis* (Arshad Chamani)
Y2	A1	1.38-2.19	16m	4	8	32	*Veronica orientalis* (Bostanabad)
Y	A1	0.28-0.48	1sm+6m	2	7	14	Veronica filiformis
Z	A3	1.66-2.37	3sm+4m	2	7	14	*Vicia variabilis*

An.= Aneuploidy.

entalis (Fig. 3Y1 & Y2), *Senecio pseudoorientalis* (Fig. 2R & S), *Tripleurospermum disciforme* (Fig. 3W & X) have invariant ploidy level in this study.

Alisma plantago-aquatica n = 7 (Fig. 1A), is not particularly variable; nevertheless three different chromosome numbers have been found for it viz. *n* = 5 (Wulff, 1939), 6 (Liehr, 1916; Love and Love, 1942) and 7 (Love and Love, 1942).

Combining the available chromosome studies, the *Erigeron* has relatively consistent chromosome diversification with a basic number of 9, and most species contain diploid individuals, which suggested *Erigeron* at the initial phase of polyploid diversification (Baldwin and Speese, 1955).

Phragmatis australis is represented by many polyploids, cuploids from 3x = 36 to 8x = 96 (without 5 x) and aneuploidies (2*n* = 42, 44, 46, 49, 50, 51, 52, 54). Tetraploidy and octoploidy are in majority (Gorenflot, 1979). Chromosome numbers of *Phragmatis australis* showed a high degree of aneuploidy and varied between 2*n*=42 and 2*n*=59 (Gervais *et al*., 1993). The degree of polyploidy is not in direct relation with the individual's habitus. Meiosis study shows that this complex has already passed the maturity, the diploid forms having disappeared (Gorenflot, 1979). Base on this study our case is aneuploidy.

Hypericum perforatum has the smallest chromosomes than other species of this genus. In other studies it had 2n=32 with median centromeric chromosomes as our result (Brutovska *et al*., 2000).

Most of the subgenera of *Veronic*a exhibit only one single basic number, i.e., x = 6, 7, 8, 9, 12, 17, or 20/21.

In this genus, the putative ancestral base number of 9 has been reduced several times to 8 and 7, respectively (aneuploidy/dysploidy), often associated with transition to annual life history. In contrast, no unambiguous increase of chromosome base number has been inferred (Albach *et al*., 2008). A base chromosome number reduction to x = 8 (aneuploidy), seems to have occurred in *Veronica orientalis* (tetraploid, 2*n*=4x=32*).* Previous results confirm our result (Ghaffari, 1986).

Basic chromosome number(x)

The frequency of 2x (53.57%) and 4x (46.43%) in this study are almost identical. 6x and more another nx not found. 2x and 4x are most common in flowering plants (Bala and Gupta, 2013). The present result is in agreement with the reports of earlier investigators.

Polyploidy and habit

The overall chromosome numbers during present study lie on two different levels of ploidy i.e. 2x, 4x. Among these, the diploids are the most common in terms of frequency (53.57 %), followed by tetraploids (46.43 %) (Table 3).

As reported at least 47% of species have undergone a recent polyploidy event (Wood *et al*., 2009)polyploidy has been recognized as an important phenomenon in vascular plants, and several lines of evidence indicate that most, if not all, plant species ultimately have a polyploid ancestry. However, previous estimates of the frequency of polyploid speciation suggest that the formation and establishment of neopolyploid species is rare. By combining information from the botanical community's vast cytogenetic and phylogenetic databases, we establish that 15% of angiosperm and 31% of fern speciation events are accompanied by ploidy increase. These frequency estimates are higher by a factor of four than earlier estimates and lead to a standing incidence of polyploid species within genera of 35% (n = 1,506. As Ramsey and Ramsey,(2014) indicated that; Polyploids are able to colonize larger geographic ranges and/or occur in more habitats than related diploids, similar picture occurred in our study: those species with higher ploidy level have wide spread geographical distribution than their related diploid populations or species. For example in Iran, some species such as; *Alopecurus arundinaceus, Phragmites australis, Catabrosa aquatica, Hypericum perforatum, Veronica orientalis* with higher polyploidy level showed same attitudes (Table 3) (Alinejad *et al*., 2017; Ghahremaninejad *et al*.; 2012, Khanhasani *et al*., 2021; Safikhani *et al*., 2018; Aref Tabad *et al*., 2016; Jalili *et al*., 2014)

Karyotype

Metacentric and submetacentric are commonly observed. Karyotype of ten species (35.7%) consists of chromosomes with the centromere in median regions (m). 14 species (50%) have metacentric and submetacentric chromosomes in their formula. Only 2 species have karyotypes with *submetacentric* and *subtelocentric chromosomes*. Karyotypes of most species (78.58%) were classified in the 1A and 2A Stebbins classes (Table 3).

ACKNOWLEDGMENT

This paper was supported by a research project of Research Institute of Forests and Rangelands of Iran; Project title: "Study and survey of chromosome numbers and ploidy levels in wetland plants in East Azerbaijan and Ardebil provinces".

REFERENCES

Agapova, N.D., 1981. A comparative karyological study of some *Ranunculus* species from the European part of the USSR. Bot. Zhurn. SSSR 66: 483–493.

Albach, D.C., Martínez-Ortega, M.M., Delgado, L., Weiss-Schneeweiss, H., Özgökce, F., Fischer, M.A., 2008. Chromosome numbers in Veroniceae (Plantaginaceae): Review and several new counts. Ann. Missouri Bot. Gard. 95(4): 543–566. doi:10.3417/2006094

Alinejad, K., Ramezani, E., Naqinezhad, A., Djamali, M., 2017. A preliminary floristic study of Neor high altitude wetland, Ardebil province, NW Iran. J. For. Res. Dev. 3: 221–235. doi:10.21859/ijnr-12029

Amosova, A. V., Zoshchuk, S.A., Rodionov, A. V., Ghukasyan, L., Samatadze, T.E., Punina, E.O., Loskutov, I.G., Yurkevich, O.Y., Muravenko, O. V., 2019. Molecular cytogenetics of valuable Arctic and sub-Arctic pasture grass species from the Aveneae / Poeae tribe complex (Poaceae) BMC Genetics 20(92): 1-16.

Aref Tabad, M., Jalilian, N., Maroofi, H., 2016. Study of flora, life form and chorology of plant Species in Zarivar Region of Marivan, Kurdistan. Taxon. Biosyst. 69–102.

Aryavand, A., 1977. In IOPB chromosome number reports LVIII. Taxon 26: 557–565.

Assadi, M., Massoumi, A.A., Khatamsaz, M. , Mozaffarian, V. 2018. Flora of Iran 1988-2018. Vol. 1-149, Research Institute of Forest Publication, Tehran. (In Persian)

Astanova, S.B., 1999. Chromosome numbers of some representatives of the family Brassicaceae of the flora of Tadjikistan. Citologija 41(12): 1054–1055.

Bala, S., Gupta, R.C., 2013. Male meiosis and chromosome number in Asteraceae family from district Kangra of H.P. (Western Himalayas). International Journal of Botany and Research 3: 43-58.

Baldwin, J.T., Speese, B.M., 1955. Chromosomes of Taxa of the Alismataceae in the Range of Gray's Manual. American Journal of Botany 42(4): 406-411. doi:10.2307/2438748

Baltisberger, M., 1991. IOPB chromosome data 3. Int. Organ. Pl. Biosyst.Newslett. 17: 5–7.

Baltisberger, M., Widmer, A., 2009. Chromosome numbers and karyotypes within the *Ranunculus alpestris*-group (Ranunculaceae). Org. Divers. Evol. 9: 232–243. doi:10.1016/j.ode.2009.03.003

Brutovská, R., Kušnirikova, P., Birosova, E., Cellárová, E., 2000. Karyotype Analysis of *Hypericum perforatum* L. Biol. Plant. 43(1): 133–136. doi:10.1023/A

Chehregani, A., Hajisadeghian, S., 2009. New chromosome counts in some species of Asteraceae from Iran 6–9. doi:10.1111/j.1756-1051.2009.00347.x

Ciccarelli, D., Garbari, F., Mártonfi, P., 2001. Mediterranean chromosome number reports 11 (1232). Fl. Medit. 11: 440–443.

Dahlgren, G., Cronberg, N., 1996. Species differentiation and relationships in *Ranunculus* subgenus *Batrachium* (Ranunculaceae) elucidated by isozyme electrophoresis. Symb. Bot. Upsal. 31: 91–104.

Dmitrieva, S.A., 1986. Chisla khromosom nekotorych vidov rastenij Berezinskogo Biosfernogo Zapovednika. Zapov. Beloruss. Issl. 10: 24–28.

Dobeš, CH., Hahn, B., Morawetz, W., 1997. Chromosomenzahlen zur Gefäßpflanzen-Flora Österreichs. Linzer Biol. Beiträge 29(1): 5–43.

Dobeš, CH., Vitek, E., 2000. Documented Chromosome Number Checklist of Austrian Vascular Plants. Verlag des Naturhistorischen Museums Wien, Vienna.

Dzhus, M.A., Dmitrieva, S.A., 2001. Chromosome numbers in the species of the genus *Veronica* (Scrophulariaceae) from Byelorussia. Bot. Zhurn. (Moscow & Leningrad) 86: 144–147.

EPA (Environmental Protection Agency), 2001. Types of Wetlands. United states Environmental Protection Agency.

Ghasemi, F.S., Jalili, A., Mirzadeh Vaghefi, S.S., Ashrafi, S., 2015. Chromosome numbers for *Ranunculus dolosus* and *Silene conoidea* from Iran. Iran. J. Bot. 21: 61–63.

Gervais, C., Moreno, D., Drolet, A., 1993. Chromosomiques et Reproduction 2005–2008.

Ghaffari, S.M., 1986. Chromosome number reports. XCI. Taxon 35: 407.

Ghaffari, S.M., 1987. Chromosome counts of some Angiosperms from Iran II. Iran. J. Bot. 3: 183–188.

Ghaffari, S.M., 1999. Chromosome studies in the Iranian Asteraceae II. Iran. J. Bot. 8, 91–104.

Ghaffari, S.M., 2006. New or rare chromosome counts of some angiosperm species from Iran II. Iran. J. Bot. 12: 81–86.

Ghaffari, S.M., 2007. Chromosome counts of some angiosperm species from Iran (III) Rostaniha 8: 74-83.

Ghahremaninejad, F., Naqinezhad, A., Amirgholipour Kasmani, V., 2012. Plant diversity of five important wetlands of Babol Mazandaran province, Iran. Taxon. Biosyst. J. 4: 13–24.

Gorenflot R., Sanei-Chariat Panahi, M., Liebert, J., 1979. Le complexe polypoide du *Phragmites australis* (Cav.) Trin. ex Steud. en Iran. Rev. Cytol. Biol. Veget. Bot. 2 (1): 67-81.

Grau, J., 1979. The probable allopolyploid origin of *Scrophularia auriculata* and *S. pseudoauriculata*. Webbia 34: 497–499.

Hayirlioglu-Ayaz, H.I., 2011. NIH Public Access 2010: 149–157. doi:10.1007/s00606-009-0266-5.Chromosome

Hesamzadeh Hejazi, S.M., Rasuli, M., 2006. Cytogenetic study of some species of vetch genus (*Vicia* sp.) in Ira. Iran. J. Agric. Sci. 37: 213–225.

Hesamzadeh Hejazi, S.M., Ziaei Nasab, M., 2009. Color chromosome atlas of legumes collected in natural resources gene bank od Iran.

Iwatsubo, Y., Sugimoto, M., Suyama, C., Naruhashi., N., 1998. Distribution and chromosome numbers of *Triglochin maritimum* L. s.l. (Juncaginaceae) in Chubu District, Japan. J. Phytogeogr. Taxon. 46: 195–199.

Jalili, A., Naqinezhad, A. r., Kamrani, A., 2014. Wetland Ecology (With an especial approach on wetland habitats of southern Alborz). 268 pp.

Javùrková, V., 1979. In IOPB chromosome number reports LXIV. Taxon 28: 400–401.

Kalinka, A., Mifsud, S., Popiela, A., Achrem, M., 2014. Chromosome number of *Eatine gussonei* (Sommier) Brullo (Elatinaceae) and its distribution on the Maltese islands. Acta Bot. Croat. 73(1): 267–273. doi:10.2478/botcro-2013-0022

Kaur, H., Mubarik, N., Kumari, S., Gupta, R.C., 2011. IAPT/IOPB chromosome data 11. Taxon 60(4): 1220–1223.

Khanhasani, M., Jalili, A., Khodakarami, Y., Jalilian, N., 2021. Wetland flora of Kermanshah Province, Iran. Nov. Biol. Reper. 8: 154–172. doi:10.52547/nbr.8.2.154

Koull, K., Koul, K.K., Gohil, R.N., 1991. Cytogenetic studies on some Kashmir grasses. VIII Tribe Agrostideae, Festuceae and Paniceae. Cytologia (Tokyo), 56(3): 437-452.

Krasnikov, A.A., Schaulo., D.N., 1990. Chromosome numbers in representatives of some families of vascular plants in the flora of the Novosibirsk region. II. Bot. Zhurn. (Moscow & Leningrad) 75: 118–120.

Krasnikov, A.A., 1991. Chromosome numbers in some species of vascular plants from Novosibirsk region. Bot. Zhurn. (Moscow & Leningrad) 76: 476–479.

Kuzmanov, B., 1993. Chromosome numbers of bulgarian angiosperms : An introduction to a chromosome atlas of the Bulgarian flora. Flora Mediterr. 3: 19–163.

Lessani, H., Chariat-panahi., S., 1979. In IOPB chromosome number reports LXV. Taxon 28 (4): 635–636.

Levan, A., Fredga, K., Sandberg, A.A., 1964. Nomenclature for centromeric position on chromosomes. Hereditas 52: 201–220.

Liehr, O., 1916. Ist die angenommene Verwandtschaft der Helobiae und Polycarpiae auch in ihrer Cytologie zu erkennen? Beitr. Biol. Pflanz. 13(2): 135–220.

Love, A., Love., D., 1942. Cyto-taxonomic studies on boreal plants. I. K. Kgl. Fysiogr. Sällsk. Lund Förhandl. 12(6): 1–19.

Lövkvist, B., Hultgård., U.M., 1999. Chromosome numbers in south Swedish vascular plants. Opera Bot. 137: 1–42.

Naqinezhad, A. R., 2012. Vegetation Database of Mountain Wetlands of Iran (Short Database Report). Biodivers. Ecol. 4: 306–306.

Ørgaard, M., Linde-Laursen, I.B., 2014. Cytogenetics of Danish species of *Barbarea* (Brassicaceae): chromocentres, chromosomes and rDNA sites. Hereditas, 144 (4): 159-170. doi:10.1111/j.2007.0018-0661.01987.x

Paule, J., Gregor, T., Schmidt, M., Gerstner, E.-M.,, Dersch, G., Dressler, S., Wesche, K., Zizka, G., 2017. Chromosome numbers of the flora of Germany – a new online database of georeferenced chromosome counts and flow cytometric ploidy estimates. Plant Systematics and Evolution 303(8): 1123-1129, doi:10.1007/s00606-016-1362-y.

Petrova, A., Stanimirova, P., 2001. chromosome number reports 11 (1248–1253). Fl. Medit. 11: 460–466.

Pogan, E., Jankun, A., Sawicka, Z., 1990. Further studies in chromosome numbers of Polish angiosperms, part 22. Acta Biol. Cracov., Ser. Bot. 31: 1–17.

Probatova, N.S., 2000. Chromosome numbers in some plant species from the Razdolnaya (Suifun) river basin (Primorsky Territory). Bot. Zhurn. (Moscow Leningrad) 85: 102–107.

Probatova, 2004. Chromosome numbers of some representatives of the flora of the Primorsky Territory. Bot. Zhurn. (Moscow Leningrad) 89: 1209–1217.

Ramsey, J., Ramsey, T. S., 2014. Ecological studies of polyploidy in the 100 years following its discovery. Phil. Trans. R. Soc. B: Biol. Sci. 369, 20130352. doi:10.1098/rstb.2013.0352.

Razaq, Z.A., Vahidy, A.A., Ali, S.I., 1994. Chromosome numbers in Compositae from Pakistan. Ann. Missouri Bot. Gard. 81: 800–808.

Rechinger K. H., 2005. Flora Iranica. Akademische Druck- und Verlagsanstalt, Graz.

Reeves, A., Tear, J., 2000. MicroMeasure for Windows, version 3.3. Free program distributed by the authors over the internet from.

Rotreklová, O., 2004. Chromosome numbers for some species of vascular plants from Europe. Biol. 59 (4): 425–433.

Safikhani, K., Jalili, A., Jamzad, Z., 2018. Archive of SID Wetlands Flora of Hamedan Province (Iran) Archive of SID.

Sawicka, Z., 1991. In: Further studies in chromosome numbers of Polish angiosperms, part 24. Acta Biol. Cracov., Ser. Bot. 33: 37–38.

Sharma O. P., 2009. Plant taxonomy. 2nd ed. Tata McGraw-Hill Publishing Co., New Delhi.

Sheidai, M., Hamta, A., Mofidabadi, A.J., Noori-Daloir, M. R., 1998.Keryotypic study of *Trifolium* species and cultivars in Iran. J. Sci. I.R.lran 9: 214–222.

Sheidai, M., Jafari, S., Taleban, P., Keshavarzi, M., 2009. Cytomixis and Unreduced Pollen Grain Formation in *Alopecurus* L. and *Catbrosa* Beauv. (Poaceae) 74: 31–41.

Stebbins, G.L., 1971. Chromosome evolution in higher plants. Edward Arnold, London.

Uchiyama, H., 1989. Karyomorphological studies on some taxa of the Helobiae. J. Sci. Hiroshima Univ.Ser. B, Div. 2, Bot. 22: 271–352.

Vitek, E., Kiehn, M., Pascher, K., Starlinger, F., Greimler, J., Stocker, U., Lehner, S., Beinhofer, P., Blaha, A. 1992. Beiträge zur Flora von Österreich - weitere Chromosomenzählungen. Verh. Zool.-Bot. Ges. Wien 129: 215–226.

Wood, T.E., Takebayashi, N., Barker, M.S., Mayrose, I., Greenspoon, P.B., Rieseberg, L.H., 2009. The frequency of polyploid speciation in vascular plants. Proc. Natl. Acad. Sci. U. S. A. 106: 13875–13879. doi:10.1073/pnas.0811575106

Wulff, H.D., 1939. Chromosomenstudien an der schleswig-holsteinischen Angiospermen-Flora. III. Ber. Deutsch. Bot. Ges. 57: 84–91.

Zhang, Z. p., Wu, L. h., Kang, Y. f., 1993. Analyses of karyotypes in six forage grass species of Leguminosae. Bot. Res 1:60–61.

Caryologia
International Journal of Cytology, Cytosystematics and Cytogenetics

Firenze University Press
www.fupress.com/caryologia

OPEN ACCESS

Citation: Chnar Hama Noori Meerza, Basoz Sadiq Muhealdin, Sahar Hussein Hamarashid, Syamand Ahmad Qadir,Yusef Juan (2022). Delimiting species using DNA and morphological variation in some *Alcea* (Malvaceae) species based on SRAP markers. *Caryologia* 75(4): 77-86. doi: 10.36253/caryologia-1629

Received: April 15, 2022

Accepted: December 20, 2022

Published: April 28, 2023

Data Availability Statement: All relevant data are within the paper and its Supporting Information files.

Competing Interests: The Author(s) declare(s) no conflict of interest.

Delimiting species using DNA and morphological variation in some *Alcea* (Malvaceae) species based on SRAP markers

Chnar Hama Noori Meerza[1], Basoz Sadiq Muhealdin[2], Sahar Hussein Hamarashid[2,*], Syamand Ahmad Qadir[3], Yusef Juan[4]

[1] *Food Science and Quality Control Department, Bakrajo Technical Institute, Sulaimani Polytechnic University, Sulaymaniyah, Iraq*
[2] *Agricultural Project Management Department, Technical College of Applied Science Halabja, Sulaimani Polytechnic University, Iraq*
[3] *Medical Laboratory Techniques Department, Halabja Technical Institute, Research center, Sulaimani Polytechnic University, Sulaymaniyah, Iraq*
[4] *Department of Biology, Faculty of Science, Behbahan Khatam Alanbia University of Technology, Khuzestan, Iran*
*Corresponding author. E-mail: sahar.rashid@spu.edu.iq

Abstract. Species identification is fundamentally important within the fields of biology, biogeography, ecology and conservation. The genus *Alcea* (Malvaceae) includes approximately 70 species of mainly Irano-Turanian distribution and is considered one of the most challenging genera of the Middle East, due to its uniformity and pronounced plasticity in morphological traits. In spite vast distribution of many *Alcea* species that grow in Iraq, there are not any available report on their genetic diversity, mode of divergence and patterns of dispersal. Therefore, we performed molecular (SRAP marker) and morphological studies of 80 accessions from 10 species of *Alcea* that were collected from different habitats in Iraq. The aims of present study are: 1) can SRAP markers identify *Alcea* species, 2) what is the genetic structure of these taxa in Iraq, and 3) to investigate the species inter-relationship? The present study revealed that combination of morphological and SRAP data can identify the species.

Keywords: *Alcea,* SRAP, Morphology, Species Identification.

1. INTRODUCTION

Alcea L. (Malvaceae) is considered one of the most complicated and challenging genera of the Middle Eastern flora (Iljin, 1949; Zohary, 1963b; Riedl, 1976; Townsend, 1980; Pakravan, 2001).

The Irano-Turanian floristic region (Takhtajan, 1986) stretches from central Anatolia to the highlands of central Asia and is a main center of diversity for many medium- to large-sized genera.

A well-suited system for investigating radiations in the Irano-Turanian region is the genus *Alcea*. It includes approximately 70 species, which are

mainly of Irano-Turanian distribution with extensions into the Caucasus and the eastern Mediterranean (Zohary, 1963b). Riedl (1976) has reported 39 species in Iran, but the number has been reduced to 34 due to taxonomic rearrangement among them, 15 species are endemic (Pakravan 2008b). *Alcea* species are mainly annual, biennial or perennial, mostly tall-growing hemicryptophytes. The stem is erect and rarely branched from the base or acaulescent in a few cases. The mucilage that containing the plants of the Malvaceae family are sources of carbohydrates, which are used in medicine (Azizov *et al*., 2007).

Any classifications are hampered by uniformity in many morphological and ecological traits (flower, inflorescence and fruit structure, habitat and life form) combined with a pronounced plasticity in the morphological characters considered important for species identification (indumentum, leaf shape and degree of division, calyx and epicalyx morphology, flower colour; Zohary, 1963b, c). Due to this plasticity, accurate species identification requires character state combinations of the sequence of change of leaf morphology along the main stem (hereafter leaf sequence), relative proportions of calyx and epicalyx lobes and (mature) mericarp morphology, which are rarely found together on herbarium specimens. Additionally, due to political tensions in the Middle East and the Caucasus, *Alcea* has received only limited attention in recent studies of Malvaceae (La Duke & Doebley, 1995; Alverson & al., 1998; Nyffeler & al., 2005; Tate & al., 2005; Escobar García & al., 2009). So far, only two infrageneric classification systems have been suggested. Boissier (1867) defined two sections, *Pterocarpae* Boiss. and *Apterocarpae* Boiss., distinguished by winged versus unwinged mericarps. Zohary (1963b, c) proposed nine informal groups based on overlapping character combinations (leaf shape and degree of leaf division, mericarp morphology, relative dimensions of calyx and epicalyx, indumentum).

Previous study on species delimitation and species relationship performed in this genus. Badrkhani et al (2014) sequence-related amplified polymorphism (SRAP) marker was employed to assess the genetic diversity and genetic similarity relationships among 14 species of *Alcea* collected from northwest of Iran. Two main clusters were detected using UPGMA, which did not

correspond to geographical origin of the species. Their study indicates that SRAP markers could be good candidates for assessing genetic variation in *Alcea*.

Escobar García et al. (2012) examines the phylogeny of *Alcea* using three molecular markers (nrDNA ITS and the plastid spacers *psbA-trnH* and *trnL-trnF*), their results show that while molecular data unambiguously support the circumscription of *Alcea* inferred from morphology, they prove to be of limited utility in resolving interspecific relationships, suggesting that *Alcea*s high species diversity is due to rapid and recent radiation.

Literature revealed that studies are mainly dealing with taxonomy, seed and pollen morphology, stem and leaf anatomy (Arabameri and Khodayari 2019; Escobar García et al. 2012) of *Alcea* species and also, genetic diversity of *Alcea* species have been reported in only some studies by (Badrkhani et al (2014)) but there is no attempt to study genetic diversity, ecological adaptation and intra- and inter-specific differentiation along with morphometric studies on of Iraq. Therefore, we performed morphological and molecular study of 80 collected specimens of 10 of *Alcea* species. We try to answer the following questions: 1) Is there infra and interspecific genetic diversity among studied species? 2) Is genetic distance among these species correlated with their geographical distance? 3) What is the genetic structure of populations and taxa? 4) Is there any gene exchange between *Alcea* species in Iraq?

2. MATERIALS AND METHODS

2.1. Plant materials

We performed morphological and molecular analysis of 10 *Alcea* species growing in Iraq. For morphometric studies we used 80 plant specimens (5-15 samples from each species) and for SRAP analysis, we used 80. Different references were used for the correct identification of species (Zohary, 1963b; Riedl, 1976; Townsend, 1980; Pakravan, 2001). Details of sampling sites are mentioned (Table 1).

2.2. Morphological studies

In total 36 morphological quantitative characters were studied (supplementary Table 2). Data obtained were standardized (Mean= 0, variance = 1) and used to estimate Euclidean distance for clustering and ordination analyses (Podani 2000).

2.3. Dna extraction and srapassay

Fresh leaves were used randomly from 5-11 plants in each of the studied species. These were dried by silica gel powder. CTAB activated charcoal protocol was used to extract genomic DNA. The SRAP analysis was performed as described by Li and Quiros (2001). Ten SRAP

Table 1. *Alcea* species and populations, their localities and voucher numbers.

Sp.
A. sachsachanica Iljin
A. flavovirens (Boiss. & Buhse) Iljin
A. rechingeri (Zohary) I. Riedl
A. arbelensis Boiss. & Hausskn.,
A. koelzii I. Riedl,
A. hyrcana (Grossh.) Grossh.
A. peduncularis Boiss. & Hausskn.
A. glabrata Alef.
A. tabrisiana (Boiss. & Buhse) Iljin
A. persarum Bornm.

primer combinations (PCs) were used (Table 3); these were synthesized by Bioneer (Daejeon, Korea). PCR reactions were carried in a 25µl volume containing 10 mM Tris-HCl buffer at pH 8; 50 mM KCl; 1.5 mM $MgCl_2$; 0.2 mM of each dNTP (Bioron, Germany); 0.2 µM of a single primer; 20 ng genomic DNA and 3 U of *Taq* DNA polymerase (Bioron, Germany). The amplifications' reactions were performed in Techne thermocycler (Germany) with the following program: 5 min initial denaturation step 94°C, followed by 40 cycles of 1 min at 94°C; 1 min at 52-57°C and 2 min at 72°C. The reaction was completed by final extension step of 7-10 min at 72°C. The amplification products were observed by running on 1% agarose gel, followed by the ethidium bromide staining. The fragment size was estimated by using a 100 bp molecular size ladder (Fermentas, Germany).

2.4. Data analyses

2.4.1. Morphological studies

Morphological characters were first standardized (Mean = 0, Variance = 1) and used to establish Euclidean distance among pairs of taxa (Podani 2000). For grouping of the plant specimens, The UPGMA (Unweighted paired group using average) ordination methods were used (Podani 2000). ANOVA (Analysis of variance) were performed to show morphological difference among the populations while, PCA (Principal components analysis) biplot was used to identify the most variable morphological characters among the studied populations (Podani 2000). PAST version 2.17 (Hammer et al. 2012) was used for multivariate statistical analyses of morphological data.

Table 2. Morphological characters in studied species.

No	Characters
1	Plant height (mm)
2	Length of stem leaves petiole (mm)
3	Length of stem leaves (mm)
4	Width of stem leaves (mm)
5	Length / Width of stem leaves (mm)
6	Number of segment stem leaves (mm)
7	Length of basal leaves petiole (mm)
8	Length of basal leaves (mm)
9	Width of basal leaves (mm)
10	Length / Width of basal leaves (mm)
11	Number of segment basal leaves
12	Calyx length (mm)
13	Calyx width (mm)
14	Calyx length/ width (mm)
15	Petal length (mm)
16	Petal width (mm)
17	Petal length / width (mm)
18	Fruit length (mm)
19	Mericarp length (mm)
20	Mericarp width (mm)
21	Mericarp length/width (mm)
22	Seed length (mm)
23	Seed width (mm)
24	Seed length/ width (mm)
25	Stipules length (mm)
26	Stipules width (mm)
27	Stipules length/ width (mm)
28	Bract length (mm)
29	Bract width (mm)
30	Bract length / width (mm)
31	Pedicel length (mm)
32	Peduncle length (mm)
33	Rostrum length (mm)
34	Style length (mm)
35	Stamen filament length (mm)
36	Number of flowers per inflorescence

(flower, inflorescence and fruit structure, habitat and life form) combined with a pronounced plasticity in the morphological characters considered important for species identification (indumentum, leaf shape and degree of division, calyx and epicalyx morphology, flower colour.

2.4.2. Molecular analyses

SRAP bands obtained were coded as binary characters (presence = 1, absence = 0) and used for genetic diversity analysis. Parameter like Nei's gene diversity (H), Shannon information index (I), number of effective alleles, and percentage of polymorphism were

determined (Freeland et al. 2011). Nei's genetic distance among populations was used for Neighbor Joining (NJ) clustering and Neighbor-Net networking (Freeland et al. 2011, Huson & Bryant, 2006). Mantel test checked the correlation between geographical and genetic distance of the studied populations (Podani 2000). These analyses were done by PAST ver. 2.17 (Hammer et al. 2012), DARwin ver. 5 (2012) and SplitsTree4 V4.13.1 (2013) software. AMOVA (Analysis of molecular variance) test (with 1000 permutations) as implemented in GenAlex 6.4 (Peakall and Smouse 2006), and Nei's Gst analysis as implemented in GenoDive ver.2 (2013) (Meirmans & Van Tienderen 2004) were used to show genetic difference of the populations. Moreover, populations' genetic differentiation was studied by G'ST est = standardized measure of genetic differentiation (Hedrick 2005), and D_est = Jost measure of differentiation (Jost 2008).

The genetic structure of populations was studied by Bayesian based model STRUCTURE analysis (Pritchard et al. 2000), and maximum likelihood-based method of K-Means clustering of GenoDive ver. 2. (2013). For STRUCTURE analysis, data were scored as dominant markers (Falush et al. 2007). The Evanno test was performed on STRUCTURE result to determine proper number of *K* by using delta *K* value (Evanno et al. 2005). In K-Means clustering, two summary statistics, pseudo-F, and Bayesian Information Criterion (BIC), provide the best fit for k (Meirmans 2012). Gene flow was determined by (i) Calculating Nm an estimate of gene flow from Gst by PopGene ver. 1.32 (1997) as: Nm = 0.5(1 - Gst)/Gst. This approach considers equal amount of gene flow among all populations. (ii) Population assignment test based on maximum likelihood as performed in Genodive ver. in GenoDive ver. 2. (2013). The presence of shared alleles was determined by drawing the reticulogram network based on the least square method by DARwin ver 5. (2012).

RESULTS

3.1. Species identification and inter-relationship

Morphometry

ANOVA showed significant differences (P <0.01) in quantitative morphological characters among the species studied. In order to determine the most variable characters among the taxa studied, PCA analysis has been performed. It revealed that the first three factors comprised over 76% of the total variation. In the first PCA axis with 41% of total variation, such characters as seed outline, seed length, stipules length, shape of petal, peduncle and pedicel hair, stem hair, Stipules length/ width bract and leaf hair have shown the highest correlation (>0.7). Length of bract and peduncle, length of petal, sepal hair, number of flowers per inflorescence were characters influencing PCA axis 2 and 3 respectively.

Different clustering and ordination methods produced similar results. Therefore PCA plot of morphological characters are presented here (Fig. 1). In general, plant samples of each species, were grouped together and formed separate cluster. This result show that morphological characters studied can differentiate the *Alcea* species in two different major clusters or groups. In the studied specimens we did not encounter intermediate forms. The PCA plot of morphological characters (Fig. 1) separated the species into distinct groups with no intermixing. This is in agreement with UPGMA tree.

3.2. Species identification and genetic diversity

All SRAP primer produced polymorphic bands. Genetic diversity parameters determined in the studied species (Table 3) revealed that *A. rechingeri* had the highest level of genetic polymorphism (49.13%), while the lowest level of genetic polymorphism (17.22%) occurred in *A. sachsachanica*. *A. glabrata* also had the highest values for effective number of alleles (Ne = 1.264) and Shannon information index (I =0.235).

AMOVA test showed significant genetic difference (P = 0.01) among studied species. It revealed

that 60% of total variation was among species and 40% was within species. Pair-wise FST values showed significant difference among all studied species (Table 4). Moreover, genetic differentiation of these species was demonstrated by significant Nei's GST (0.89, P = 0.01) and D_est values (0.587, P = 0.01).

NJ tree based on Nei,s genetic distance (Fig. 2), showed that *A. flavovirens*; *A. arbelensis*; *A. persarum* are separated from the other studied species and join the others with a great distance. This dendrogram showed close genetic affinity between *A. koelzii* and *A. hyrcana*. Similarly, *A. rechingeri* and *A. peduncularis* were placed close to each other, to which, *E. litvinovii* was joined with some distance. In general, this indicates that SRAP molecular markers can be used in *Alcea* species differentiation. This is in agreement with AMOVA and genetic diversity parameters presented before. The species are genetically well differentiated from each other. The Nm analysis by Popgene software also produced mean Nm= 0.78, that is considered very low value of gene flow among the studied species.

Mantel test with 5000 permutations showed a significant correlation (r = 0.24, p=0.0002) between genetic

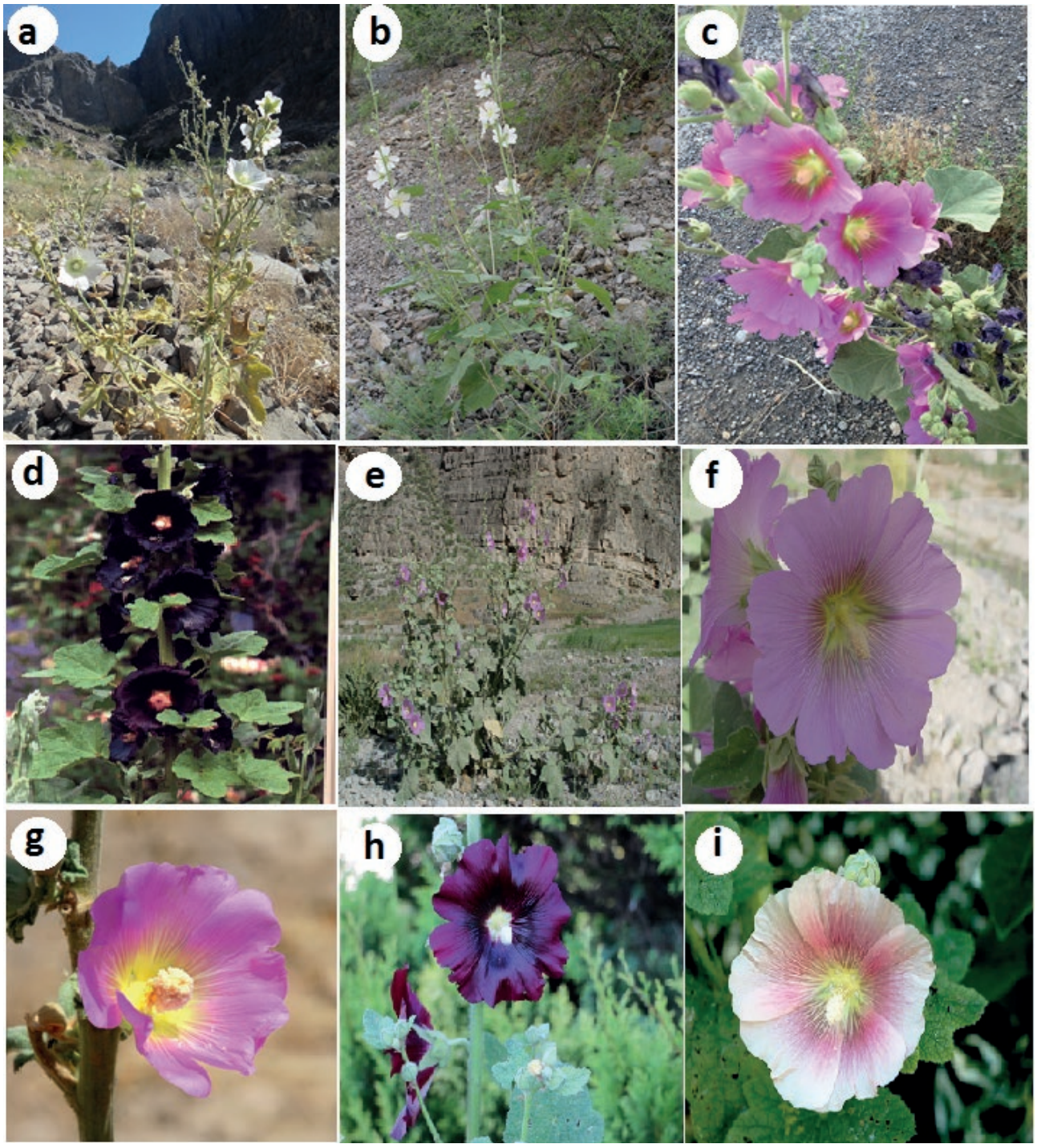

Figure 1. *Alcea* species:a, i: *A. flavovirens*; b: *A. sachsachanica*; c: *A. rechingeri*;d, h: *A. arbelensis*; e: *A. koelzii*; f, g: *A. hyrcana*

distance and geographical distance, so isolation by distance (IBD) occurred among the *Alcea* species studied.

Nei's genetic identity and the genetic distance determined among the studied species (Table is not included). The results showed that the highest degree of genetic similarity (0.83) occurred between *A. koelzii* and *A. hyrcana*. The lowest degree of genetic similarity occurred between *A. arbelensis* and *A. persarum* (0.64).

Table 3. Genetic diversity parameters in the studied *Alcea* species. (N = number of samples, Ne = number of effective alleles, I= Shannon's information index, He = gene diversity, UHe = unbiased gene diversity, P%= percentage of polymorphism, populations).

Pop	N	Na	Ne	I	He	UHe	%P
A. sachsachanica Iljin	13.000	0.178	1.017	0.016	0.002	0.019	17.22%
A. flavovirens (Boiss. & Buhse) Iljin	10.000	0.276	1.061	0.053	0.036	0.044	29.68%
A. rechingeri (Zohary) I. Riedl	17.000	0.355	1.145	0.234	0.288	0.211	49.13%
A. arbelensis Boiss. & Hausskn.,	10.000	0.301	1.009	0.211	0.154	0.177	43.23%
A. koelzii I. Riedl,	7.000	0.677	1.087	0.093	0.057	0.099	23.66%
A. hyrcana (Grossh.) Grossh.	10.000	0.699	1.156	0.143	0.094	0.205	27.96%
A. peduncularis Boiss. & Hausskn.	4.000	0.376	1.054	0.055	0.035	0.021	21.83%
A. glabrata Alef.	5.000	0.452	1.264	0.235	0.039	0.044	24.90%
A. tabrisiana (Boiss. & Buhse) Iljin	5.000	0.269	1.021	0.023	0.011	0.023	22.15%
A. persarum Bornm.	8.000	0.548	1.013	0.029	0.012	0.019	19.68%

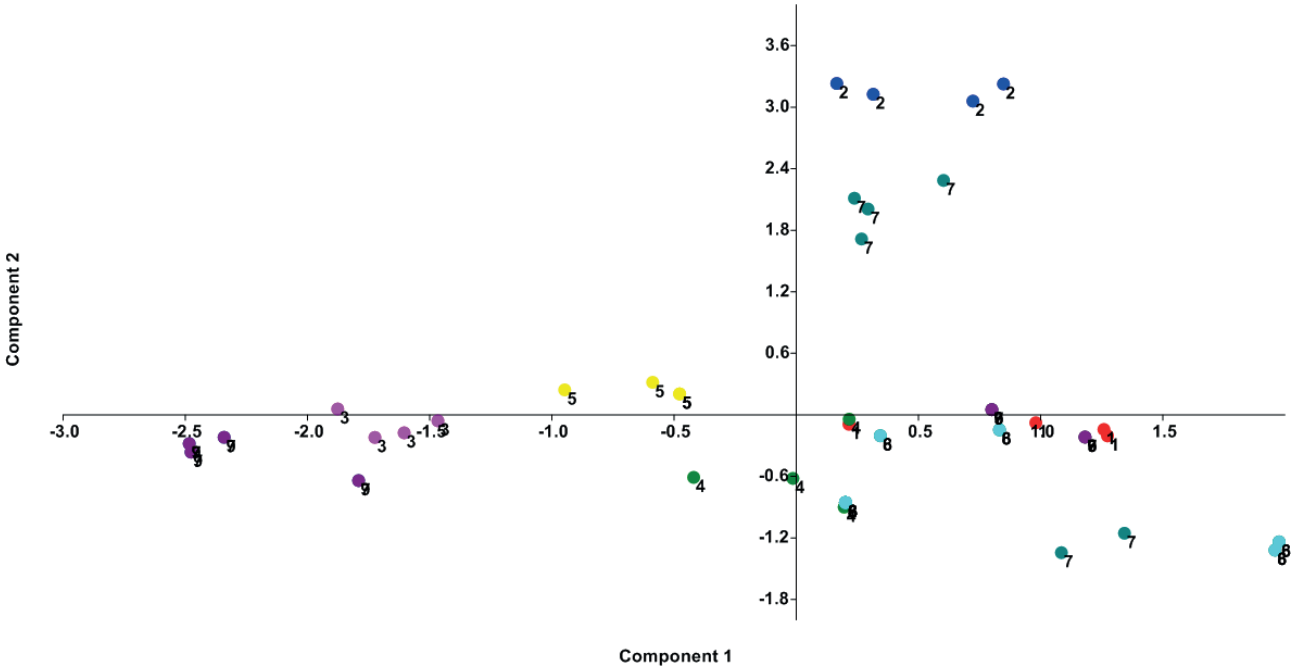

Figure 2. PCA plots of morphological characters revealing species delimitation in *Alcea* species

3.3. The species genetic structure

We performed STRUCTURE analysis followed by the Evanno test to identify the optimal number of genetic groups. We used the admixture model to illustrate interspecific gene flow or / and ancestrally shared alleles in the species studied.

STRUCTURE analysis followed by Evanno test produced ΔK =10. The STRUCTURE plot (Fig. 3) produced more detailed information about the genetic structure of the species studied as well as shared ancestral alleles and / or gene flow among *Alcea* species. This plot revealed that Genetic affinity between *A. rechingeri* and *A. arbelensis* (similarly colored), as well as *A. koelzii* and *A. hyrcana* (similarly colored) due to shared common alleles. This is in agreement with Neighbor joining dendrogram presented before. The other species are distinct in their allele composition and differed genetically from each other.

The low Nm value (0.78) indicates limited gene flow or ancestrally shared alleles between the species studied and supports genetic stratification as indicated by K-Means and STRUCTURE analyses. Population assignment test also agreed with Nm result and could not identify significant gene flow among members of

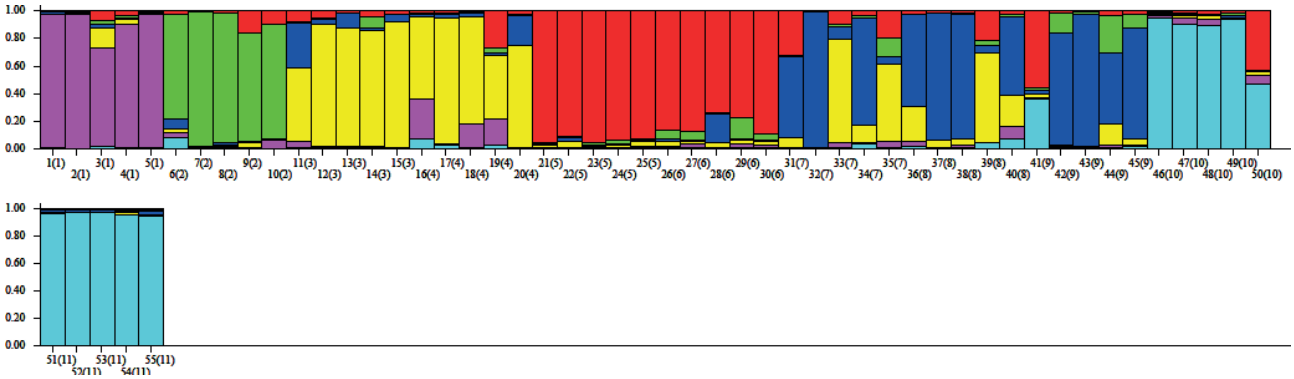

Figure 3. STRUCTURE plot of *Alcea* species based on SRAP data.

the studied species. However, reticulogram obtained based on the least square method (Figure not included), revealed some amount of shared alleles between species 2 and 1,3,5 and between 9 and 1,3-5 also between 3 and 1, 2, 9-10. As evidenced by STRUCTURE plot based on admixture model, these shared alleles comprise very limited part of the genomes in species studied and all these results are in agreement in showing high degree of genetic stratification in species studied

4. DISCUSSION

4.1. Species identification and taxonomic consideration

Species delimitation is important in different biological disciplines, like ecology, biogeography, and plant conservation (Mayr 1982). Species delimitation is done by tree-based and non-tree-based approaches (Wiens 2007). In the first method, species form distinguishing clades (phylogenetic species concept), whereas in non-tree-based method, the species are recognized on the basis of gene flow assessments (biological species concept; Pérez-Losada et al. 2005).

Wiens & Penkrot (2002), proposed to use DNA data, morphological data and character data for species delimitation while, Knowles & Carstens (2007) addressed how molecular data (i.e., gene trees from DNA sequence data) can be used in species delimitation. The latter authors used coalescent simulations to test the species limits and incorporated data from multiple loci. They showed the importance of population genetics in species delimitation. Similarly, Medrano et al. (2014), applied population genetics methods to the species delimitation problem in *Narcissus* Linnaeus (1753: 289) (Amaryllidaceae J.St.-Hil. nom. cons.) by the help of amplified fragment length polymorphism (AFLP) molecular markers.

In the present study we used morphological and molecular (SRAP) data to evaluate species relationship in *Alcea*. Morphological analyses of the studied *Alcea* species showed that they are well differentiated from each other both in quantitative measures (the ANOVA test result) and qualitative characters (The PCA plot result). In addition, PCA analysis suggests that characters like bract length, stipule length, bract shape, calyx shape, petal shape, length and width of stem-leaf, length and width of petal, peduncle and pedicel hair, mericarp hair density, mericarp surface could be used in species groups delimitation. This morphological difference was due to quantitative and qualitative characters.

4.2. Genetic structure and gene flow

This is the first study on the use of SRAP markers for genetic diversity, species delimitation and determining genetic relationships among *Alcea* species in Iraq. Alarcón, et al., (2012) showed that SRAP technique along with proper statistical tools could be successfully applied to assess the genetic diversity and phylogenetic analysis among *Alcea* species in Iraq. Our results clearly demonstrated that SRAP markers can be used in genetic diversity study as well as genetic identification of *Alcea*. Moreover, our results indicate a very high efficiency of the SRAP markers in the identification and delimitation of *Alcea* species. Similar efficiency of the SRAP markers has also been reported by other authors (Alarcón, et al., 2012; Li, *et al*, 2021; Sun, *et al.* 2021; Xu, *et al*, 2021; Zhang, *et al.* 2022).

AMOVA and STRUCTURE analysis revealed that the species of *Alcea* are genetically differentiated but have some degree of shared common alleles. Several trends in pollination mechanism can be observed in *Alcea* with gradual transition between them. Based on RAPD markers analysis, Kazemi *et al.* (2011) showed

93% polymorphism level with high variation in genetic similarity (0.31 to 0.75) within *A. rosea* populations in Iran. Öztürk *et al*. (2009) analyzed genetic profile of 18 *Alcea* species using RAPD markers and reported wide differentiation (0.13 to 0.69) among them. According to Badrkhani *et al* (2014) sequence-related amplified polymorphism (SRAP) marker was employed to assess the genetic diversity and genetic similarity relationships among14 species of *Alcea* collected from northwest of Iran. Seventeen SRAP primer combinations generated 104 fragments, of which 97 (93%) were polymorphic, with an average of 5.7 polymorphic fragments per primer. Percentage of polymorphism ranged from 50% (ME2-EM6) to a maximum of 100%, and mean polymorphism information content value obtained was 0.3. The lowest genetic similarity (0.17) was observed between *A. sophiae* and *A. flavovirens*, while the highest was found between *A. digitata* and *A. longipedicellata* (0.68). Two main clusters were detected using UPGMA, which did not correspond to geographical origin of the species. Their study indicates that SRAP markers could be good candidates for assessing genetic variation in *Alcea*. Iranian *Alcea* species have only been characterized with morphological data, so far. However, the genus has a complicated taxonomy due to small number of characters. Based on study of Pakravan (2008) on *Alcea*, only examination of the leaf sequence and configuration of the carpels would represent valuable characters. For example, *A. fl avovirens* and *A. glabrata* differ only in the size of the carpel and width of wing (Pakravan 2008). Our results grouped these two species into two different clusters.

The methods we used are indirect estimation of gene flow and if it is identified to occur among species may be either due to ancestral shared alleles or ongoing gene flow. The Nm value obtained based on SRAP data, revealed very limited amount of gene flow among the studied species that was also supported by STRUCTURE analysis as *Alcea* species mostly had distinct genetic structure. Reticulation analysis also showed some degree of gene flow for SRAP. We did not observe any intermediate forms in our extensive plant collection, but morphological variability within each species did occur to some extent. To conclude, the present study revealed the use of SRAP molecular markers along with morphological characters in *Alcea* species identification. Some degrees of interspecific genetic admixture occur in *Alcea* species, but the studied species are strongly differentiated during the speciation process and invasion in new habitats. Genetic drift, strong inbreeding and local adaptation are effective evolutionary forces operating in *Alcea* species and population divergence and adaptation.

Plant species identification is of central importance in phylogenetic systematics, evolution, biogeography and biodiversity. It is significant to infer patterns and mechanisms of speciation and hybridization, the evolutionary process by which new biological species arise and gene flow between closely related phylogenetic species can occur (Al-Quran 2008; Bi, *et al.,* 2021; Duan, *et al.,* 2022; Guo, *et al*, 2021; Guo, *et al,* 2022).

Isolation by distance, local adaptation and gene flow are different mechanisms responsible for species differentiation and genetic diversity (Freeland et al. 2011, Frichot et al. 2013).

REFERENCES

Alarcón, M., Vargas, P., Sáez, L., Molero, J., Aldasoro, J.J., 2012. Genetic diversity of mountain plants: Two migration episodes of Mediterranean Erodium (Geraniaceae) Molecular Phylogenetics and Evolution 63, 866–876

Al-Quran S. 2008. Taxonomical and pharmacological survey of therapeutic plants in Jordan. Journal of Natural Products, l (1):10-26.

Azizov U.M., Mirakilova D.B., Umarova N.T., Salikhov S.A., Rakhimov D.A. and Mezhlumyan L.G.(2007). Chemical composition of dry extracts from *Alcea rosea*. *Chemistry of Natural Compounds* 43:508-511.

Alefeld, F.G.C. (1862). Ueber die Malveen. Oesterreichische Botanische Zeitschrift 12: 246–261.

Boissier, P.E. (1867). Flora Orientalis, Vol. 1. Basel, Geneva, Leiden.

Bi, D., C. Dan, M. Khayatnezhad, Z. Sayyah Hashjin, Z. Y. Ma 2021. Molecular Identification And Genetic Diversity In Hypericum L.: A High Value Medicinal Plant Using Rapd Markers Markers. Genetika **53(**1): 393-405.

Chen, Weimiao; Khayatnezhad, Majid; Sarhadi, Nima 2021. Protok gena i struktura populacije kod allochrusa (Caryophylloideae, Caryophyllaceae) pomocu molekularnih markera. Genetika 53(2): 799-812.

Duan, F., Fei Song, Sainan Chen, Majid Khayatnezhad, Noradin Ghadimi, 2022. Model parameters identification of the PEMFCs using an improved design of Crow Search Algorithm. International Journal of Hydrogen Energy, **47**(79): 33839-33849.

Evanno, G., Regnaut, S. & Goudet, J. 2005: Detecting the number of clusters of individuals using the software STRUCTURE: a simulation study. Molecular Ecology 14: 2611–2620.

Escobar G.P., Schönswetter P., Fuertes A.J., Nieto F.G. and Schneeweiss G.M. (2009). Five molecular markers

reveal extensive morphological homoplasy and reticulate evolution in the *Malva alliance* (Malvaceae). *Molecular Phylogenetics and Evolution* **50**:226-239.

Falush, D., Stephens, M. & Pritchard, J.K. 2007: Inference of population structure using multilocus genotype data: dominant markers and null alleles. Molecular Ecology Notes 7: 574–578.

Frichot, E., Schoville, S. D., Bouchard, G. & Francois, O. 2013: Testing for associations between loci and environmental gradients using latent factor mixed models. Molecular Biology and Evolution 30: 1687–1699.

Freeland, J.R., Kirk, H. & Peterson, S.D. 2011: Molecular Ecology (2nded). Wiley-Blackwell, UK, 449 pp.

Fiz O, Vargas P, Alarcon ML, Aldasoro JJ. 2006. Phylogenetic Relationships and Evolution in *Erodium* (*Geraniaceae*) based on trnL-trnF Sequences. *Syst Botany* 31: 739- 763

Guo, H., Wei Gu, Majid Khayatnezhad, Noradin Ghadimi, 2022. Parameter extraction of the SOFC mathematical model based on fractional order version of dragonfly algorithm. International Journal of Hydrogen Energy, **47**(57):24059-24068.

Guo, L.N., She, C., Kong, D.B., Yan, S.L., Xu, Y.P., Khayatnezhad, M. and Gholinia, F. 2021. Prediction of the effects of climate change on hydroelectric generation, electricity demand, and emissions of greenhouse gases under climatic scenarios and optimized ANN model. Energy Reports **7:** 5431-5445.

Huson, D.H. & Bryant, D. 2006: Application of Phylogenetic Networks in Evolutionary Studies. Molecular Biology and Evolution 23: 254–267.

Hammer, O., Harper, D.A. & Ryan, P.D. 2012: PAST: Paleontological Statistics software package for education and data analysis. Palaeonto Electro 4: 9.

Hedrick, P. W. 2005: A standardized genetic differentiation measure. Evolution 59:1633–1638.

Iljin, M.M. 1949. Malvaceae. Flora of the USSR 15: 21–137.

Kazemi M., Aran M. and Zamani S. 2011. Evaluation of genetic diversity of Iranian wild *Alcea rosea* population using RAPD. *World Applied Sciences Journal* **13**:1234-1239.

Jia, Y., M. Khayatnezhad, s. mehri (2020). Population differentiation and gene flow in Rrodium cicutarium: A potential medicinal plant. Genetika 52(3): 1127-1144.

Jost, L. 2008: GST and its relatives do not measure differentiation. Molecular Ecology 17: 4015–4026.

Knowles, L.L., & Carstens, B. 2007: Delimiting species without monophyletic gene trees. Systematic Biology 56: 887-895. doi:10.1080/10635150701701091.

Li, Ang; Mu, Xinyuan; Zhao, Xia; Xu, Jiamin; Khayatnezhad, Majid; Lalehzari, Reza; Developing the non-dimensional framework for water distribution formulation to evaluate sprinkler irrigation; Irrigation and Drainage, **70:** 659-667.

Liu, S., Wang, Y., Song, Y., Khayatnezhad, M., & Minaeifar, A. A. 2021. Genetic variations and interspecific relationships in Salvia (Lamiaceae) using SCoT molecular markers. Caryologia, 74(3), 77-89.

Medrano, M., Lo´ Pez-Perea E. & Herrera, C.M. 2014: Population genetics methods applied to a species delimitation problem: Endemic trumpet daffodils (*Narcissus* section *Pseudonarcissi*) from the Southern Iberian Peninsula. International Journal of Plant Sciences 175: 501-517. doi: 10.1086/675977

Mayr, E. 1982: The Growth of Biological Thought: Diversity, Evolution, and Inheritance. Cambridge, MA: Harvard University Press.1-992

Meirmans, P.G. & Van Tienderen, P.H. 2004: GENOTYPE and GENODIVE: two programs for the analysis of genetic diversity of asexual organisms. Molecular Ecology Notes 4: 792–794.

Meirmans, P.G. 2012: AMOVA-based clustering of population genetic data. Journal of Heredity 103: 744–750.

Öztürk F., Babaoğlu S., Uzunhisarcikli M.E., Açik L., Vural M. and Gürcan I.S. 2009. Genetic differentiation of Turkish *Althaea* L. and *Alcea* L. species. *Advances in Molecular Biology* **1**:47-56.

Pakravan M. 2008. A new species and a new combination in Iranian *Alcea* (Malvaceae). *Annales Botanici Fennici* **45**:133-136.

Peng, X., Khayatnezhad, M. and Ghezeljehmeidan, L. 2021. Rapd profiling in detecting genetic variation in stellaria l. (caryophyllaceae). Genetika-Belgrade **53**: 349-362.

Peakall, R. & Smouse, P.E. 2006: GENALEX 6: genetic analysis in Excel. Population genetic software for teaching and research. Molecular Ecology Notes 6: 288–295.

Podani, J. 2000: Introduction to the Exploration of Multivariate Data English translation. Backhuyes publisher, Leide,407 pp.

Pritchard, J.K., Stephens, M. & Donnelly, P. 2000: Inference of population structure using multilocus genotype Data. Genetics 155: 945–959.

Pérez-Losada, M., Eiroa, J., Mato,S., & Domínguez, J. 2005: Phylogenetic species delimitation of the earth worms *Eiseniafetida* (Savigny,1826) and *Eiseniaandrei* Bouché,1972(Oligochaeta,Lumbricidae) based on mitochondrial and nuclear DNAsequences. Pedobiologia 49: 317–324.doi: 10.1016/j.pedobi.2005.02.004

Riedl I. 1976. Malvaceae. In: Rechinger K.H. Ed. *Flora Iranica 120*, pp 1-86, Akademische Druck und Verlagsanstalt, Graz.

Townsend, C.C., Guest, E. & Al-Rawi, A. 1966– 1985.

Flora of Iraq. Ministry of Agriculture of the Republic of Iraq. Baghdad.

Shi, B., Khayatnezhad, M., Shakoor, A. 2021. The interacting effects of genetic variation in Geranium subg. Geranium (Geraniaceae) using scot molecular markers. Caryologia, 74(3), 141-150.

Sun, Q., Deli Lin, Majid K., Mohammad T., 2021. Investigation of phosphoric acid fuel cell, linear Fresnel solar reflector and Organic Rankine Cycle polygeneration energy system in different climatic conditions. Process Safety and Environmental Protection, **147**:993-1008.

Xu, Y.-P., Ping Ouyang, Si-Ming Xing, Lu-Yu Qi, Majid khayatnezhad, Hasan Jafari,2021. Optimal structure design of a PV/FC HRES using amended Water Strider Algorithm. Energy Reports, **7:** 2057-2067.

Wang, C., Y. Shang, M. Khayatnezhad 2021. Fuzzy Stress-based Modeling for Probabilistic Irrigation Planning Using Copula-NSPSO. Water Resources Management. 35, 4943–4959

Wang, J., Ye, Q., Zhang, T., Shi, X., Khayatnezhad, M., Shakoor, A. 2021. Palynological analysis of genus Geranium (Geraniaceae) and its systematic implications using scanning electron microscopy. Caryologia, 74(3), 31-43.

Wiens, J.J. 2007: Species Delimitation: New approaches for discovering diversity. Systematic. Biology 56: 875-878. doi:10.1080/10635150701748506.

Wiens, J.J. & Penkrot,T.A. 2002: Delimiting species using DNA and morphological variation and discordant species limitsinspinylizards (*Sceloporus*). Systematic. Biology 51: 69–91.

Zohary, M. 1963a. Taxonomical studies in *Alcea* of southwestern Asia. Part I. Bulletin of the Research Council of Israel 11: 210–229.

Zohary, M. 1963b. Taxonomical studies in *Alcea* of southwestern Asia. Part II. Israel Journal of Botany 12: 1–26.

Zhang, J., M. Khayatnezhad, and N. Ghadimi, 2022. Optimal model evaluation of the proton-exchange membrane fuel cells based on deep learning and modified African Vulture Optimization Algorithm. Energy Sources, Part A: Recovery, Utilization, and Environmental Effects, **44**(1):287-305.

Caryologia
International Journal of Cytology, Cytosystematics and Cytogenetics

Firenze University Press
www.fupress.com/caryologia

Citation: Simona Ceraulo, Francesca Dumas (2022). Mapping CAP-A satellite DNAs by FISH in *Sapajus cay paraguay* and *S. macrocephalus* (Platyrrhini, Primates). *Caryologia* 75(4): 87-92. doi: 10.36253/caryologia-1939

Received: September 15, 2022

Accepted: December 24, 2022

Published: April 28, 2023

Data Availability Statement: All relevant data are within the paper and its Supporting Information files.

Competing Interests: The Author(s) declare(s) no conflict of interest.

Mapping CAP-A satellite DNAs by FISH in *Sapajus cay paraguay* and *S. macrocephalus* (Platyrrhini, Primates)

Simona Ceraulo, Francesca Dumas*

Department of Biological, Chemical and Pharmaceutical Sciences and Technologies (STEBICEF), University of Palermo, 90100, Palermo, Italy
*Corresponding author. E-mail: francesca.dumas@unipa.it

Abstract. Satellite DNAs such as Cap-A sequences are potentially informative taxonomic and phylogenetic markers useful for characterizing primate genomes. They have also been used as cytogenetic markers facilitating species identification in many taxa. The aim of this work is to map Cap-A sequences by FISH (fluorescent *in situ* hybridization) on two Platyrrhini (Primates) species genomes, *Sapajus cay paraguay* and *S. macrocephalus*, in order to study their distribution pattern on chromosomes. The Cap-A probes showed bright signals with almost the same interstitial pattern of distribution in correspondence with C and CMA3 rich regions on six pairs of chromosomes in both *Sapajus* species. An additional pair was detected on *S. macrocephalus*. The analysis of the results, compared with previous literature data on other phylogenetically close New World species, shows that Cap-A satellite sequences have a genus-specific pattern, but with slight species-specific patterns that are useful as phylogenetic and taxonomic markers.

Keywords: heterochromatin, karyotype, genome, New World monkeys.

INTRODUCTION

Apart from coding regions (about 2%), the human genome includes highly repetitive sequences (about 98%) which are usually underestimated in genome analyses due to their complexity; these sequences are known as the dark matter of the genome (Ahmad et al. 2020) and consist of satellite DNA (satDNA), defined as tandemly arranged repeats that represent a considerable proportion of the heterochromatic portion of chromosomes in the eukaryotic genome. satDNA, at first seen as serving no useful purpose, is now known to be associated with genome function, chromosome evolution, speciation, and diversity, comprising different kind of elements such as satellite DNAs, SINEs (Short Interspersed Nuclear Elements), LINE retrotransposons (Long Interspersed Nuclear Elements), and rDNA repeats (Ahmad et al. 2020, Ceraulo et al. 2021 a, Dumas et al. 2022).

Thus, satDNAs are potentially informative cytogenetic markers which can be used to study karyotype evolution and address taxonomic issues. They

display high evolutionary rates and consist of tandem repeats organized in the type of large arrays (up to Mb size) typically associated with chromosome landmarks such as centromeres, telomeres, and heterochromatic regions (Ahmed 2020). They evolve by mechanisms of gene conversion, and unequal crossing-over which are involved in what is known as concerted evolution (Sander Lower et al. 2018). satDNAs have high intraspecific sequence homogeneity and interspecific differences, making satDNAs potential taxonomic markers and, in some cases, allowing their use for phylogenetic inference. Furthermore, satDNAs have been used as cytogenetic markers facilitating species identification in many taxa (Prakhongcheep et al. 2013 a,b, Cacheux, et al. 2018).

Among repetitive sequences, Cap-A is a satDNA that has been analyzed in many mammals through molecular comparative sequence analysis (Valeri et al. 2018), and their history has been reconstructed in mammals. This analysis led researchers to show that a Cap-A like sequence is present as a single monomer in most eutherians such as Chiroptera, some Eulipotyphla, and some Rodentia, and also in *Homo sapiens*. Indeed, in *H. sapiens*, it is only a sequence within the intron of the NOS1AP (nitric oxide synthase 1 adaptor protein) gene. No Cap-A like sequence was found among Marsupialia or Monotremata, the sister clades to Eutheria, presumably due to the occurrence of low copy numbers or because the sequence has diverged (Valeri et al. 2018, Valeri et al. 2020). On the other hand, Cap-A duplication and expansion have been shown in New World monkeys (NWMs); this amplification may be explained by a mechanism in which the Cap-A intronic segment was transferred to heterochromatic regions in the ancestral Platyrrhini genome followed by a hyper-expansion through unequal crossing (Valeri et al. 2020).

Comparative cytogenetics using different kinds of repetitive sequence probes mapped by fluorescence *in situ* hybridization (FISH) on chromosomes led us to study sequence pattern distribution among species allowing genomic comparison (Ceraulo et al. 2021 b, c). Cap-A sequence probes have been mapped by FISH in many taxa, including Primates (Valeri et al. 2018, Valeri et al. 2020), in order to study their distribution pattern. This work permits researchers to show that Cap-A is an abundant satDNA in Platyrrhini with a high accumulation in blocks in some genomes. In particular, Cap-A has been found in representatives of the three Platyrrhini families (Cebidae, with the exception of Callitrichines, Atelidae and Pitheciidae, with the exception of the *Callicebus* genus), with genome abundance ranging from less than 1% up to 5%, and chromosome localization which is always associated with non-centromeric constitutive heterochromatin (Valeri et al. 2018, 2020). Furthermore, intragenus research analyzing Cap-A distribution on four *Saimiri* species has also been performed (Valeri et al. 2020) showing slight pattern differences between species.

The fact that Cap-A is present across Platyrrhini led researchers to show its utility as a marker for chromosome and genome evolution studies in NWMs (Valeri et al. 2018). This is especially important because of the extinction to an alarmingly large number of NWM species due to rapid habitat loss.

The Cap-A sequence was first described in the tufted capuchin monkey *Sapajus apella* (previously classified as *Cebus apella*); Cap-A was identified after digestion of genomic DNA with restriction enzymes and with DNA–DNA hybridization (Malfoy et al. 1986, Fanning et al. 1993).

Thus, in order to extend previous studies using Cap-A as a marker in Platyrrhines, two additional *Sapajus* species, *S. cay paraguay* and *S. macrocephalus* (Cebidae), were analyzed, mapping the Cap-A probe by FISH. This study will help clarify *Sapajus* chromosome evolution and add potentially useful data for taxonomic, systematics, and conservation issues.

Indeed, the cytogenetic information about *Sapajus* is poor, whereas more species from the phylogenetically close *Cebus* have been analyzed (Garcia et al. 2002). The number of specimens karyotypically analyzed is low, and most samples have not been studied, especially from the recently recognized *Sapajus* genus. Karyotypes among the two taxa are very similar, and these species have been hypothesized to be distinguishable for the non-centromeric heterochromatin block of some chromosomes, with a differential chromosomal position in each of them (Mudry, 1990, Garcia et al. 2002).

MATERIAL AND METHODS

Peripheral blood from male samples of *S. cay paraguay* and *S. macrocephalus* (Cebidae) was collected from primates at the ISTC-CNR of Rome, in accordance with international and institutional ethics rules. Metaphases were obtained from lymphoblast cell cultures in RPMI culture medium, following standardized protocols. Cell harvesting was performed after 3 h incubation with colcemid 10 µL (10 µg/mL Gibco), followed by hypotonic treatments of 0.075 M KCl for 20 min at 37 °C, following standard protocols (Dumas et al. 2022). Metaphases of the analyzed species were stained pre- and post-FISH using chromomycin A3 (CMA3) and 4',6-diamidino-2-phenylindole (DAPI)

staining, according to a recent protocol (Lemskaya et al. 2018), with some adjustments. CMA3 staining of GC-rich regions and DAPI staining of AT-rich regions were useful for identifying chromosomes and preferential insertion sites of Cap-A sequences.

DAPI images were inverted with a photo editing program (Adobe Photoshop C 2022 V23.3.2); inverted gray bands generally correspond to dark G-bands or light R bands; the DAPI inverted karyotypes for the *S. cay paraguay* and *S. macrocephalus* species were compared with previously published banded karyotypes of the phylogenetically close species *S. apella* and *Cebus capucinus* (Garcia et al. 2002, Milioto et al. 2022).

Human DNA extraction from lymphoblast cell lines was performed using the Pure Link DNA kit (Invitrogen), according to the basic DNA extraction protocol. Cap-A was amplified by Polymerase Chain Reaction (PCR) from human DNA; the following universal set of primers, developed for the PCR of CAP-1 repeats in Primates, were used: (Cap-A F: ACTTCCTCACTGACCTGTCTT; Cap-A R:GGGCTGATGCTTAATGTAGCA).

Genomic DNA was amplified in 50 µL PCR-reactions: five units of Taq GOLD DNA Polymerase (Invitrogen), the template DNA, 500 nM of each primer, 200 µM each of dATP, dCTP, dTTP, and dGTP in 10 mM TRIS-HCl, pH 8.3, 1.5 mM MgCl2, 50 mM KCl. PCR reactions were performed using an Applied Biosystems SimplyAmp (Thermo Fisher Scientific) with the following cycling parameters: 30 cycles each of 94 °C, 60 s; 55 °C, 60 s; 72 °C, 60 s, following a 3 min denaturation at 94 and with a final elongation step of 72 °C, 10 min. A bright band of about 1500 pb was visualized on 1% agarose gel. The PCR products were directly labeled through Nick Translation using 11-dUTP-Fluorescein (green) (Invitrogen).

FISH was performed following previously described protocols (Dumas and Sineo 2014, Dumas et al. 2015) using Cap-A probes obtained by PCR as previous described (Valeri et al. 2018, 2020). The hybridization mix consisted of 2.5 ng/L of probe, 50% formamide, 10% dextran sulfate, and 2xSSC, with an incubation time of 18 h at 37 C. Detection was performed at medium stringency, with washing at low temperatures (45 °C) and at high saline buffer concentration of SSC 0.1 Tween, 15 min, PBS 1min.

C banding was done sequentially post-FISH through a protocol which included denaturation with formamide (Fernàndez et al. 2002).

After FISH, the metaphases were analyzed under a Zeiss Axio2 epifluorescence microscope. Images were captured using a coupled Zeiss digital camera. At least ten metaphase spreads were analyzed for each sample.

RESULTS

Sequential staining, banding, and FISH mapping were performed for the two *Sapajus* species. The inverted DAPI karyotypes of *S. cay paraguay* and *S. macrocephalus* were almost the same as those of the other congeneric species previously published (Garcia et al. 2002, Milioto et al. 2022), with both species having the diploid number 2n = 54; for the karyotype reconstruction, we followed a previous publication (Garcia et al. 2002), with ten pairs of meta/submetacentric chromosomes in *S. cay paraguay* (pairs 1–10), eight pairs in *S. macrocephalus* (1–7, 9), and fourteen and sixteen acrocentric chromosomes, respectively, thus differing over chromosome pairs 8 and 10, which are subtelocentric in the former and acrocentric in the latter. DAPI/CMA3 staining was helpful for identifying chromosomes and preferential sites of Cap- A insertion (Fig. 1, 2).

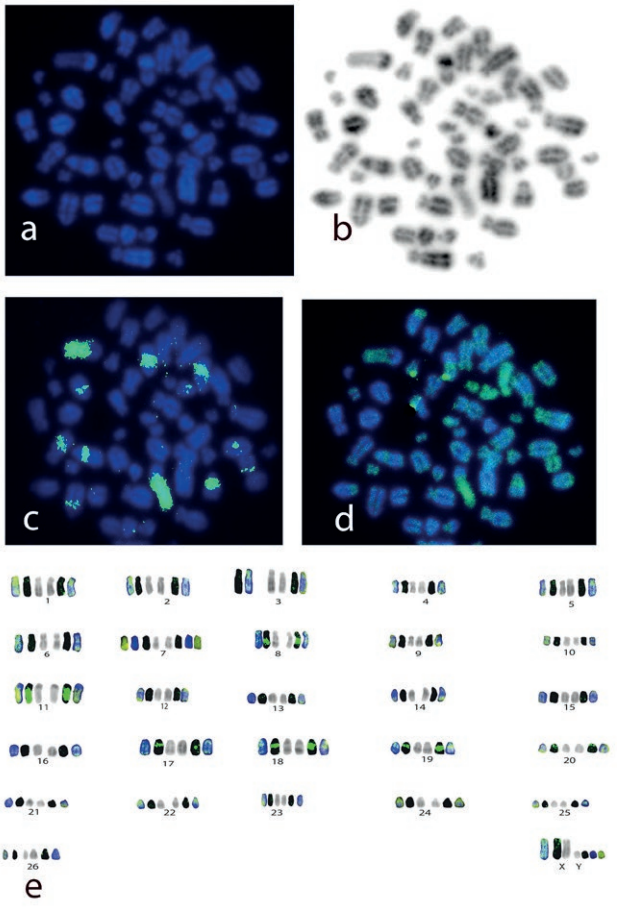

Figure 1. Metaphases of *S. cay paraguay* in DAPI (a), in DAPI inverted (b), Cap-A probe mapping (c), CMA3/DAPI stains (d), the reconstructed karyotype of *S. cay paraguay* from the metaphase in a) after sequential CMA3/ DAPI, DAPI inverted, FISH with Cap-A probes (e).

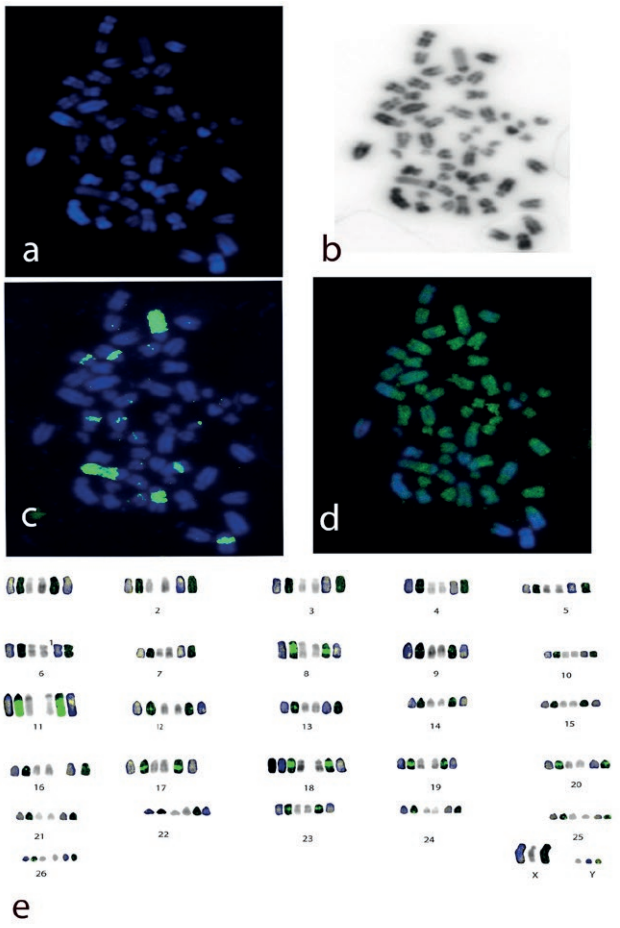

Figure 2. Metaphases of *S. macrocephalus* in DAPI (a), in DAPI inverted (b), Cap-A probe mapping (c), CMA3/DAPI stains (d), the reconstructed karyotype of *S. macrocephalus* from the metaphase in a) after sequential CMA3/ DAPI, DAPI inverted, FISH with Cap-A probes (e).

Cap-A probe mapping revealed bright signals on the metaphases of the two species analyzed, with a similar accumulation pattern and slight differences (Fig. 1, 2): twelve signals were on six chromosome pairs: 5 acrocentric and a subtelocentric chromosome pairs, respectively pairs 11, 17-20 and 8. Additional signals were found on acrocentric chromosome pairs 23 in *S. macrocephalus*, for a total of fourteen (Fig. 2).

The post-FISH C banding pattern obtained was compared with previously published C banding of phylogenetically close species such as *S. apella* (Dumas et al. 2022). Chromosomes pairs with evident C bands were: 8, 11, 18-20; other C bands were at the centromeres of acrocentric chromosomes (Fig. 3), as in the previously analyzed *Sapajus* species.

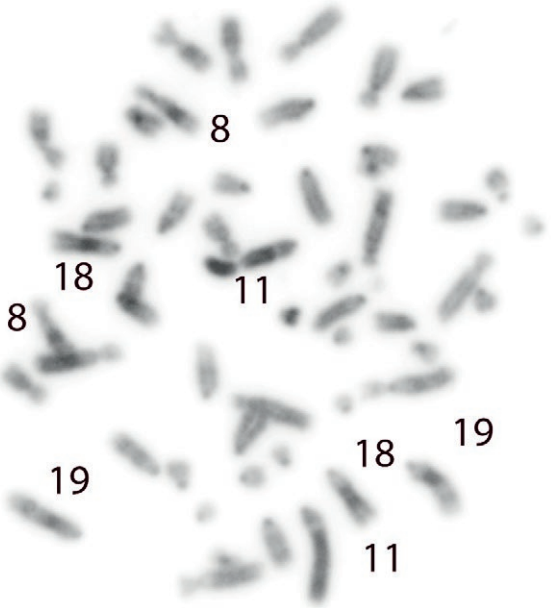

Figure 3. Metaphases of *S. cay paraguay* with C bands. Example of representative chromosome pairs with evident bands are indicated with numbers.

DISCUSSION

Cap-A satDNA have been mapped in many Mammals, including in Primates; previous works have shown that Cap-A is highly amplified in NWMs, localized at non-centromeric positions, with different patterns in the different Platyrrhini species (Valeri et al. 2018, 2020). To extend Cap-A distribution analysis to more primate samples, we used FISH to map Cap-A probes in two species of the genus *Sapajus*. In the two species, chromosome pairs having these signals were identified as 8, 11, 17-20, (Fig. 1, 2); an additional signal was detected on chromosome pair 23 in *S. macrocephalus* (Fig 2); the probe signals fall on CMA3 rich regions in correspondence to the big interstitial C bands (Fig. 3).

Our results for *S. cay paraguay* and *S. macrocephalus* were compared with previous Cap-A mapping data on other platyrrhine species (*Sapajus xanthosternos*, *Saimiri boliviensis, Aotus infulatus, Alouatta guariba, Lagotrix Lagotricha, brachyteles hypoxanthus, Callicebus nigrifrons, Chiropotes satanas, Pithecia irrorata*, *S. boliviensis, S. sciureus, S. vanzolinii* and *S. ustus*) (Valeri et al. 2018, 2020).

The analysis of the results compared with the one from the previous species of the same genus *S. xanthosternos* permitted us to hypothesize that the same chromosome pairs would have these signals. Indeed, in *S. xanthosternos*, six pairs showed signals plus an addtional

on a single chromosome, for a total of thirteen signals. Whereas twelve signals were detected on chromosome pairs in *S. cay paraguay*: on acrocentric chromosome pairs 11, 17-20, and on the subtelocentric chromosome pair 8; moreover, additional signals were found on the acrocentric chromosome pair 23 in *S. macrocephalus*, with a total of fourteen Cap-A signals.

However, one pair seems to have a different Cap-A pattern; indeed, in the previously analyzed *S. xanthosternos* species, the Cap-A probe signal covers both arms, almost all the q and the p arm, while in *S. cay paraguay* and *S. macrocephalus* all the Cap-A probe signals cover just part of the q arm. This difference could presumably be due to an intrachromosomal rearrangement such as an inversion that has amplified and dislocated the sequences differently (presumably on the subtelocentric/acro chromosome pair 8).

Analyzing our results in relation to all the previous available data from different taxa (Valeri et al. 2018, 2020), it is possible to underline that Cap-A localization has high interspecific repeat homogeneity within a genus; indeed, the *Saimiri* species have almost the same chromosomes harboring the Cap-A sequences, with slight differences (Valeri et al. 2020), as it also occurs in the species from the *Sapajus* genus as shown above.

Cap-A probe signals are abundant, around fourteen or fifteen, among *Saimiri* species and are, in the distal regions of the short arms, and in the interstitial heterochromatin of five to seven chromosome pairs. Among *Saimiri* species, signals are on the same chromosome pairs, while others are additional or absent in same specimens. This slightly different location of the Cap-A probe found between the *Samiri* species is particularly evident, especially on chromosomes involved in rearrangements, such as chromosomes 5 and 15. These differences in the Cap-A hybridization pattern in squirrel monkeys has been reported in captivity and in nature; for this reason, it has been hypothesized that Cap-A mapping patterns may be useful in revealing the origin of chromosome sets in hybrids more precisely than chromosome morphology or banding patterns (Valeri et al. 2020).

The link between Cap-A distribution and rearrangements in *Saimiri* is in agreement with the different Cap-A position shown on subtelocentric chromosome between the *Sapajus* species analyzed here and the previously analyzed *S. xanthosternos* (Valeri et al. 2018). Furthermore, *Saimiri* species also show additional chromosomes with Cap-A signals, just as it occurs on *S. microcephalus* in our study. Thus, it can be confirmed the hypothesis that new acquisition of Cap-A occurs; it is presumably due to unequal crossing-over and concerted evolution as previous suggested (Sander Lower et al. 2018).

We observed a slight, variable chromosomal localization of Cap-A signals among the species of the *Sapajus* genus, thus we hypothesized that these differences can be used as taxonomic markers for species identification, in agreement with what was previously shown among *Saimiri* species. This evidence is in agreement with the hypothesis that satDNA sequences, in general, can be used as cytogenetic markers facilitating species identification in many taxa (Prakhongcheep et al. 2013 a,b, Cacheux, et al. 2018).

Furthermore, through the classic cytogenetic approach, detecting heterochromatin with differential chromosomal position has already been hypothesized as distinguishing species (Mudry, 1990, Garcia et al. 2002). The correspondence of the Cap-A signal with heterochromatin block extends the hypothesis regarding the possibility of distinguishing species not only by C bands but also through the Cap-A pattern.

In conclusion, this work demonstrates the presence of Cap-A satellite sequences on chromosomes of *Sapajus* genomes, with a genus specific pattern interstitially in correspondence with C and CMA3 rich regions, but with slight species-specific patterns that can be useful as phylogenetic and taxonomic markers.

ACKNOWLEDGEMENTS

We are grateful to Elsa Addessi, Serena Gastaldi, and Arianna Manciocco for providing the *Sapajus* blood samples from primates of the ISTC-CNR of Rome, Italy.

LITERATURE CITED

Ahmad SF, Singchat W, Jehangir M, Suntronpong A, Panthum T, Malaivijitnond S, Srikulnath K. 2020. Dark Matter of Primate Genomes: Satellite DNA Repeats and Their Evolutionary Dynamics. Cells, 9, 2714. doi.org/10.3390/cells9122714.

Cacheux L, Ponger L, Gerbault-Seureau M, Loll F, Gey D, Richard FA, Escudé C. 2018. The targeted sequencing of alpha satellite DNA in *Cercopithecus pogonias* provides new insight into the diversity and dynamics of centromeric repeats in old world monkeys. Genome Biol. Evol.,10, 1837–1851.

Ceraulo S, Milioto V, Dumas F. 2021. Centromeric enrichment of LINE-1 retrotransposon in two species of South American monkeys *Alouatta belzebul and Ateles nancymaae* (Platyrrhini, Primates). Caryo-

logia, 74, 111–119. https://doi.org/10.36253/caryologia-1296.

Ceraulo S, Perelman LP, Mazzoleni S, Rovatsos M, Dumas F. 2021. Repetitive Sequence Distribution on *Saguinus, Leontocebus and Leontopithecus* Tamarins (Platyrrhine, Primates) by Mapping Telomeric (TTAGGG) Motifs and rDNA Loci. Biology, 10, 844. https://doi.org/10.3390/biology10090844

Ceraulo S, Perelman PL, Dumas F. 2021. Massive LINE-1 retrotransposon enrichment in tamarins of the Cebidae family (Platyrrhini, Primates) and its significance for genome evolution. J. Zool. Syst. Evol. Res., 59, 2553–2561 https://doi.org/10.1111/jzs.12536

Dumas F, Perelman PL, Biltueva L, Roelke ME. 2022. Retrotransposon mapping in spider monkey genomes of the family Atelidae (Platyrrhini, Primates) shows a high level of LINE-1 amplification. J Biol Res doi: 10.4081/jbr.2022.10725

Dumas F, Sineo L, Ishida T. 2015.Taxonomic identification of Aotus (Platyrrhinae) through cytogenetics| Identificazione tassonomica di *Aotus* (Platyrrhinae) mediante la citogenetica. J. Biol. Res 88: 65-66.

Dumas F, Sineo L. 2014. The evolution of human synteny 4 by mapping sub-chromosomal specific probes in Primates. Caryologia. 67, 281–291. https://doi.org/10.1080/0144235X.2014.974357. 30.

Fanning TG, Seuanez HN, Forman L. 1993. Satellite DNA sequences in the new World primate *Cebus apella* (Platyrrhini, Primates). Chromosoma 102,306– 311. (doi:10.1007/BF00661273)

Fernàndez R, Barragàn M, Bullejos M, Marchal J, Diaz de la Guardia R, Sanchez A. 2002. New C-band protocol by heat denaturation in the presence of formamide. Hereditas 137, 145–148. https://doi.org/10.1034/j.1601-5223.2002.01672

Garcia F, Ruiz-Herrera A, Egozcue J, Ponsa M, Garcia M. 2002. Chromosomal homologies between *Cebus* and *Ateles* (Primates) based on ZOO-FISH and G-banding comparisons. Am. J. Primatol. Off. J. Am. Soc. Primatol. 57, 177–188. https://doi.org/10.1002/ajp.10047.

Lemskaya NA, Kulemzina AI, Beklemisheva VR, Biltueva LS, Proskuryakova AA, Hallenbeck JM, Graphodatsky AS. 2018. A combined banding method that allows the reliable identification of chromosomes as well as differentiation of AT-and GC-rich heterochromatin. Chromosome Res., 26, 307–315. https://doi.org/10.1007/s10577-018-9589-9.

Malfoy B, Rousseau N, Vogt N, Viegas-Pequignot E. 1986 Nucleotide sequence of a heterochromatic segment recognized by the antibodies to Z-DNA in fixed metaphase chromosomes. Nucleic Acids Res. 14, 3197–3214. doi:10.1093/nar/14.8.3197

Milioto V, Perelman P L, Paglia LL, Biltueva L, Roelke M, Dumas, F. 2022. Mapping Retrotransposon LINE-1 Sequences into Two Cebidae Species and *Homo sapiens* Genomes and a Short Review on Primates. Genes, *13*(10), 1742.

Prakhongcheep O, Chaiprasertsri N, Terada S, Hirai Y, Srikulnath K, Hirai H, Koga A. 2013. Heterochromatin blocks constituting the entire short arms of acrocentric chromosomes of Azara's owl monkey: Formation processes inferred from chromosomal locations. DNA Res., 20, 461–470.

Prakhongcheep O, Hirai Y, Hara T, Srikulnath K, Hirai H, Koga A. 2013. Two types of alpha satellite DNA in distinct chromosomal locations in Azara's owl monkey. DNA Res., 20, 235–240.

Prakhongcheep O, Thapana W, Suntronpong A, Singchat W, Pattanatanang K, Phatcharakullawarawat R, Muangmai N, Peyachoknagul S, Matsubara K, Ezaz T et al. 2017. Lack of satellite DNA species-specific homogenization and relationship to chromosomal rearrangements in monitor lizards (Varanidae, Squamata). BMC Evol. Biol., 17, 193.

Sander Lower S, McGurk MP, Clark AG, Barbash DA. 2018. Satellite DNA evolution: old ideas, new approaches, Current Opinion in Genetics & Development,Volume 49,, Pages 70-78,ISSN 0959-437X,https://doi.org/10.1016/j.gde.2018.03.003.

Valeri M, Dias GB, Moreira CN, Yonenaga-Yassuda Y, Stanyon R, Svartman M. 2020. characterization of Satellite DNAs in Squirrel Monkeys genus *Saimiri* (cebidae, platyrrhini). Scientific reports, 10 (1), 1-11.

Valeri MP, Dias GB, Pereira VDS, Campos Silva Kuhn G, Svartman, M. 2018. A eutherian intronic sequence gave rise to a major satellite DNA in Platyrrhini. Biology letters, 14(1), 20170686. http://dx.doi.org/10.1098/rsbl.2017.0686

Caryologia
International Journal of Cytology, Cytosystematics and Cytogenetics

Firenze University Press
www.fupress.com/caryologia

OPEN ACCESS

Citation: Peng Zhou, Jiao Li, Jing Huang, Fei Li, Qiang Zhang, Min Zhang (2022). Determination of genome size variation among varieties of *Ilex cornuta* (Aquifoliaceae) by fow cytometry. *Caryologia* 75(4): 93-101. doi: 10.36253/caryologia-1902

Received: November 11, 2022

Accepted: December 15, 2022

Published: April 28, 2023

Data Availability Statement: All relevant data are within the paper and its Supporting Information files.

Competing Interests: The Author(s) declare(s) no conflict of interest.

ORCID
QZ: 0000-0002-2025-9576

Determination of genome size variation among varieties of *Ilex cornuta* (Aquifoliaceae) by fow cytometry

Peng Zhou[1], Jiao Li[2], Jing Huang[1], Fei Li[1], Qiang Zhang[2,*], Min Zhang[1,*]

[1] *Jiangsu Academy of Forestry, Nanjing 211153, Jiangsu, China*
[2] *Co-Innovation Center for Sustainable Forestry in Southern China, Key Laboratory of State Forestry and Grassland Administration on Subtropical Forest Biodiversity Conservation, College of Biology and the Environment, Nanjing Forestry University, Nanjing 210037, Jiangsu, China*
*Corresponding author. E-mail: zhangqiang@njfu.edu.cn; E-mail: nmzhang@163.com

Abstract. *Ilex cornuta* Lindl. & Paxton is a commercially important horticultural species worldwide, and extensive cultivation and hybridization have produced many varieties. Despite the considerable breeding, selection, widespread cultivation and domestication, which may have a significant role in the composition of genomes, there are no other previous reports of intraspecific genome size variation in the different cultivars or hybrids of this species. In the present work, genome size of 12 varieties of *I. cornuta* was assessed and analyzed through high-resolution flow cytometry (FCM). Nuclear DNA was analyzed using nuclei isolated from young leaves, which used propidium iodide (PI) staining, with rice (*Oryza sativa* cv. Nipponbare) as internal reference. As a result, statistically significant differences in genome size were detected among all diploid *I. cornuta* varieties considered. The estimated genome size (2*C* value) of *I. cornuta* varieties ranged from 1.47 to 1.80 pg, with 1.22-fold variation and an average size of 1.65 pg. The domestication and interspecific hybridization induced variation of genome size in *I. cornuta*, and the genome size of hybrids exhibited a wider range of variation compared with that of cultivars. In summary, flow cytometry is a useful tool to analyze the genome size of *I. cornuta*. The first report of the genome sizes of varieties of this species would provide useful data for further research on *I. cornuta*, and enrich the *C* value database of *Ilex* L. What's more, our findings could be the foundation in the future of *I. cornuta* genome sequencing and breeding programs.

Keywords: *Ilex cornuta*, Genome size, DNA content, Flow cytometry, Hybrids, Cultivars.

INTRODUCTION

The *Ilex* L. (holly) is the only living woody dioecious angiosperm genus, accounting for approximately 600 species with a broad distribution from tropics to temperate regions within the monogeneric family of Aquifoliaceae (Loizeau et al. 2016). The *Ilex* species are prized for their glossy evergreen

foliage and abundant showy fruits that can bloom from autumn to early spring, when many other plants in the landscape are dormant (Yao et al. 2021). *Ilex cornuta* Lindl. & Paxton, one of very important native landscape woody materials and distributed only in eastern China and Korea (Hu 1949), has been utilized as a horticultural species because its leaves are distinctive rectangular foliage (one or two spines per side) and its fruits are red berries (Park et al. 2019). *I. cornuta*, the most speciose and commercially significant specie of the diverse genus *Ilex*, has a long and complex horticultural history. Together with *I. aquiforlium* usually distributed in Europe, it is a typical species for Christmas tree inside home. In addition, it has been utilized as medical plant in China so that it contains several useful compounds (Zhang et al. 2012; Kang et al. 2014). Extensive cultivation and hybridization have produced many varieties of *I. cornuta*, including commercially important horticultural species such as cultivated tea and iconic flowering shrubs (Hodges et al. 2001; Park et al. 2019).

Genome size (*C* value/haploid nuclear DNA content) is an important attributes of living organisms, which is correlated with size of nucleus/cell, cellular process including DNA synthesis rate and ecological traits, etc. Genome size has fundamental significance in a wide range of applications including molecular biology, ecology, systematic biology, cytology, evolutionary biology and genomics (Jatt et al. 2019). Genome sizes of more than 7500 plant species have been estimated (Bennett and Leitch 2012), but the genome sizes of higher species are still poorly understood (Bennett and Leitch 2011; Doležel and Bartoš 2005). Flow cytometric analysis in plants has proved to be useful to determine DNA content and ploidy level in different species and accessions (Sliwinska 2018; Pellicer et al. 2014; D'hondt et al. 2011).

The genus *Ilex* is one of the largest plant genera, but of which only 6 species of genome size have been determined (Bennett and Leitch 2012). As the most speciose member of this genus, *I. cornuta* has become widely cultivated throughout Asia, Europe and America. Despite the considerable breeding, selection, widespread cultivation and domestication of *I. cornuta*, which may have a significant role in the composition of genomes, except for *I. cornuta* (Zhang et al. 2013), there are no other previous reports of intraspecific genome size variation in the different cultivars or hybrids of this species. Improved knowledge of genome size of key cultivars and complex hybrids would be a valuable resource for further breeding and improvement of *I. cornuta*. Therefore, in this study, the genome size of cultivars and hybrids of *I. cornuta* were identified and analyzed by FCM. The genome size variation of different *I. cornuta* varieties were explored to provide a basis for the development and utilization of *I. cornuta* germplasm resources.

MATERIALS AND METHODS

Plant materials

The sampling site was located in the National Holly Germplasm Resources Repository of the Jiangsu Academy of Forestry, which is located at Jiangning District, Nanjing City, Jiangsu Province, China. The tested materials were 12 *I. cornuta* varieties in consideration of its commodity value; the age of trees is 5-7a, each was healthy and without pests and diseases. Diploid rice, *Oryza sativa* subsp. japonica cv. Nipponbare (1*C* = 389 Mb, GC = 43.6 %; International Rice Genome Sequence Project 2005), were used as an internal standard, which was provided by Nanjing Agricultural University and germinated in Petri dishes in the laboratory. Leaves were collected from 12 healthy *I. cornuta* varieties and rice.

Flow cytometry analysis

Experimental design

Prior to FCM measurement, flow cytometer parameters were determined, based on external analyses of sample and primary standard. Subsequently, internal FCM procedure was performed.

Preparation of plant nuclei suspensions for flow cytometry

(1) Sampling: 0.05 g of young leaves of *I. cornuta* and 0.05 g of young leaves of rice was collected, washed in distilled and deionized water successively to remove surface dirt, and dried on filter paper.
(2) Dissociation: 1 mL of pre-cooled Tris dissociation solution was added to a pre- cooled culture dish, and the cut leaf tissues were immersed in this solution and then chopped quickly with a razor blade. After chopping, 1 mL Tris dissociation solution was added, well mixed and allowed to stand for 1-3 min at 4 °C.
(3) Filtration: The liquid mixture was drawn from the culture dish, filtered once through a 400 mesh membrane and placed into a centrifuge tube. The mixture was incubated at 4 °C for 5 min.
(4) Centrifugation: The cell nuclear suspension was obtained by centrifugation at 4 °C at 1000 r/min for 5 min.
(5) Dyeing: The supernatant was discarded. The nuclei were stained with propidium iodide (PI), and RNase

was added to a final concentration of 50 μg/mL. The mixture was dyed at 4 °C for 5-10 min in the dark environment before being analyzed.

Settings of flow cytometer and calculations

Samples were run on a BD Influx™ cell sorter (BD, Piscataway, NJ, USA) with an argon laser exciting at 488 nm. Pulse area was detected using 670 mean/30 bandwidth detector, as well as with side (SSC) and forward (FSC) scatters. Prior to analysis, the instrument was checked for linearity and the amplification was adjusted so that the peak corresponding to rice was positioned approximately at channel 10000. The voltage was maintained at a constant high level throughout each experiment. Each plant was measured at least three times by the same operator to eliminate potential artefacts. If the difference among the three measurements exceeded 2%, the most deviating value was discarded and the sample was re-analyzed. Coefficient of variation values (CV) was used to evaluate the results. Nuclear genome size was calculated as a linear relation between the ratio of G_0/G_1 peak of the samples and the standard according to the following formula (Dolezel and Bartos 2005): Sample genome size = [(sample G_0/G_1 peak mean)/(standard G_0/G_1 peak mean)] × standard genome size. Genome size data are presented in absolute terms in pg (1*C* and 2*C* value) and Mbp (1 pg DNA = 978 Mbp; Doležel 2003).

Statistical analyses of genome size

FCM detection results were edited and analyzed by BD FACS sortware1.0.0.650, and a flow histogram was obtained. Variance analysis was carried out using Excel 2003 and SPSS 13.0 with convective detection parameters. A one-way ANOVA (analysis of variance) was used to compare genome sizes among individuals of the same varieties and among 12 sampled varieties respectively. Fisher's least significant difference (LSD) test ($P<0.05$) was used for the multiple comparison. A t test was used to compare genome size values for four cultivars and eight hybrids to determine whether differences were significant between two groups. Genome size data were $\log_{10}$ transformed prior to analyses.

RESULTS

Optimization of flow cytometry for I. cornuta

Based on recommendations from specialized FCM bibliography and small genome size values reported in Aquifoliaceae (Bennett and Leitch 2012), we chose rice as primary standard by internal standardization to lower the bias (Noirot et al. 2003; Lysák et al. 2000). The fluorescence intensity range of standard and sample was determined by observing the position of peak in the flow cytometric histogram, when they were analyzed separately on the machine. As shown in Figure 1 and Figure 2, the debris peak and nuclei peak were effectively separated, and the sample peak had good linearity, indicating that the nuclear dissociation solution was suitable. The G_0/G_1 peak of rice was tuned to fluorescence channel 10000 (Figure 1b), and followed the same protocol, the G_0/G_1 peak of *I. cornuta* sample was positioned at channel number around 18000 (Figure 2b). When rice and *I. cornuta* being chopped simultaneously, the SSC (Figure 3a) showed that the particles of the target species and the internal standard are clearly concentrated with good discrimination, and it was easy to distinguish two dominant G_0/G_1 peaks in histogram (Figure 3b). Nuclear DNA content was calculated as a linear relationship between the ratio of G_0/G_1 peaks of the sample and standard, indicating that the *I. cornuta* nuclei contained more DNA than rice nuclei. Therefore, in the flow cytometry histograms of mixed samples, the peak reflecting the nuclei isolated from rice should be positioned at the left side of the histogram, while the peak reflecting the nuclei isolated from *I. cornuta* sample should be positioned at the right side of the histogram (Figure 3b).

Table 1. Variance analysis of FCM detection parameters of different varieties in *I. cornuta*.

Index	Variation source	Sum of Squares	Degree of freedom	Mean Square	*F* value	Significance level
2*C* value	Between varieties	0.390	11	0.035	17.631	0.000
	Within varieties	0.058	29	0.002		
	Total variation	0.448	40			
1*C* value	Between varieties					
	Within varieties	0.058	29	0.002		
	Total variation	0.448	40			

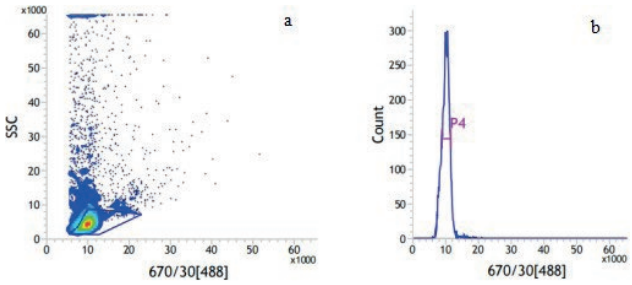

Figure 1. FCM detection analysis result for rice that was separately processed. (a) scatterplot on side scatter (SSC) versus PI fluorescence with manually drawn polygon gate; (b) histogram of relative fluorescence intensity derived from nuclei isolated from rice only. Peak 4 represent G_0/G_1 nuclei of rice.

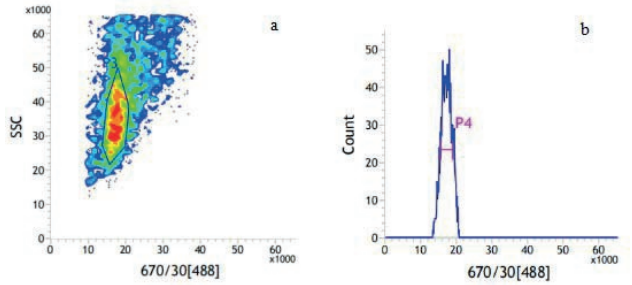

Figure 2. FCM detection analysis result for *I. cornuta* sample that was separately processed. (a) scatterplot on side scatter (SSC) versus PI fluorescence with manually drawn polygon gate; (b) histogram of relative fluorescence intensity derived from nuclei isolated from *I. cornuta* only. Peak 4 represent G_0/G_1 nuclei of *I. cornuta* sample.

FCM histograms of I. cornuta varieties

The peak histograms of different classified *I. cornuta* varieties obtained with FCM were shown in Figure 4. Mean fluorescence values from 12 *I. cornuta* varieties showed G_0/G_1 nuclei peaks in a fluorescence range from 17240 to 23090. Flow cytometry analyses produced high-resolution histograms with CV values for the internal standard and sample peaks varying between 2.77% and 5.10% (mean 4.15%) and between 1.82% and 5.15% (mean 3.95%), respectively, which suggested that the resolutions of the high quality histograms were appropriate for genome size analysis (Table 2).

Assessment of genome size of I. cornuta varieties

The mean 2*C* value was determined for each varieties of *I. cornuta* by comparing the relative G_0/G_1 nuclei PI-fluorescence peak of rice (primary standard) to that of each *I. cornuta* sample. Analysis of variance (ANO-

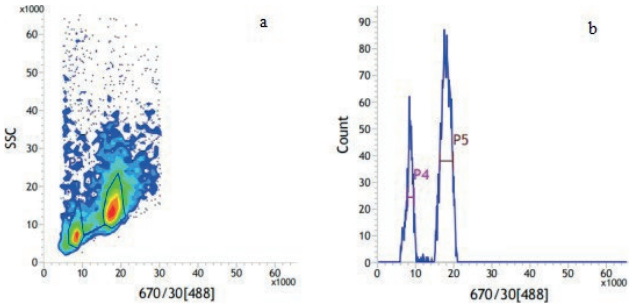

Figure 3. FCM detection analysis result for mixed samples of rice and *I. cornuta* sample that were simultaneously processed (co-chopped). (a) scatterplot on side scatter (SSC) versus PI fluorescence with manually drawn polygon gate, (b) histogram of relative fluorescence intensity derived from nuclei isolated from rice and *I. cornuta* processed simultaneously. Peak 4 represent G_0/G_1 leaf nuclei of rice, peak 5 represent G_0/G_1 nuclei of *I. cornuta* sample.

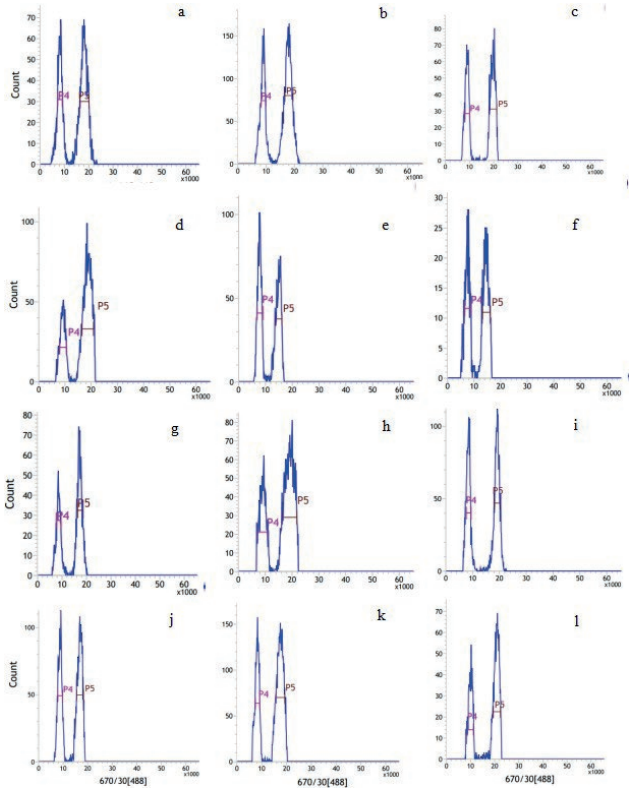

Figure 4. FCM histograms obtained after analyses of propidium iodine-stained nuclei isolated *I. cornuta* varieties 'Burfordii' (a), 'Dwarf Burford' (b), 'Luteocarpa' (c), "O'Spring' (d), 'Emily Bruner' (e), 'James Swan' (f), (g) '*Ilex dabieshanensis* No.1'; 'Mary Nell'(h), 'Nellie R. Stevens' (i) , 'Edward J. Stevens' (j), 'Golden Nellie R Stevens' (k) and 'China Girl'(l) with internal standard rice. Peak 4 represent G_0/G_1 nuclei of rice, peak 5 represent G_0/G_1 nuclei of *I. cornuta* varieties.

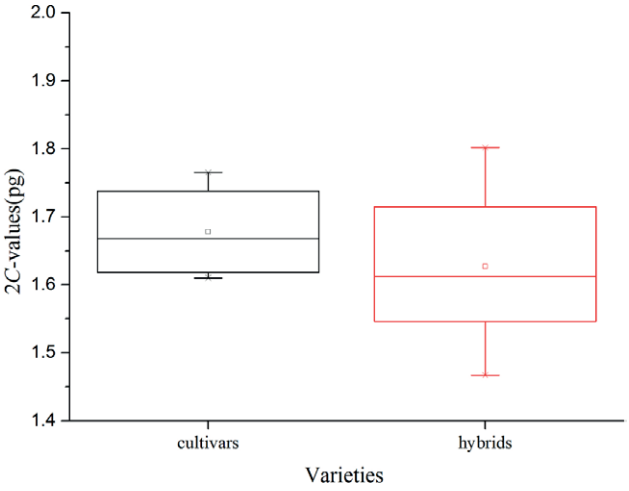

Figure 5. Boxplot of genome sizes in cultivars and hybrids. The horizontal black line within each bar represents the median value of the genome size, while a black dot within the bar denotes the average value of genome size.

VA) of genome sizes variation in different varieties of *I. cornuta* was significant (Table 1). The 2*C* genome sizes (2*C* value) varied 1.22-fold among all *I. cornuta* varieties, ranging from 1.47±0.0217 to 1.80±0.0148 pg, thus with 1*C* genome size estimates for *I. cornuta* ranging from 717 to 881 Mb (0.733–0.901 pg) with an average of 805 Mb (0.823 pg). 'Emily Bruner' had the smallest genome size, whereas 'Nellie R. Stevens' had the largest genome size (Table 2).

Comparison of genome sizes between cultivars and hybrids

The *I. cornuta* varieties measured were distinguished into two groups based on genetic origin, which were significantly different ($P < 0.05$). The first represents four

I. cornuta-related cultivars, whereas the second includes eight interspecific hybrids developed based on *I. cornuta*. The 2*C* value of genome size was estimated between 1.61±0.0048 and 1.77±0.0263 pg for cultivar family and 1.47±0.0217 and 1.80±0.0148 pg for hybrids family (Table 2).

Box and whisker plot showing differences in the 2*C* values assessed with different germplasm sources (Figure 5). The median and average 2*C* value of genome sizes were 1.688 pg and 1.678 pg for cultivars and 1.634 pg and 1.627 pg for hybrids, respectively. The variation in genome size of hybrids (1.22-fold) was somewhat larger than that of cultivars (1.10-fold), possibly due to those hybrid nature.

DISCUSSION

Genome size estimation of I. cornuta

In the present work, the genome sizes of 12 *I. cornuta* varieties were measured, according to their global commodity value in different countries. Results of flow cytometric analysis showed that the mean 2*C* genome size estimated of *I. cornuta* in this study ranged from 1.47 pg to 1.80 pg (1.63 pg on average), corresponding to the 1*C* genome size of 805 Mb or 0.823 pg, which indicated that genome size estimates of *I. cornuta* varieties were very small (1*C*≤1.4 pg; Leitch et al. 1998; Soltis et al. 2003) and considerable variations were found among all varieties. Therefore, caution should be taken when cultivars/genotypes are selected for genome sequencing and other genome-based studies.

Nevertheless, these new data on the genome sizes of both cultivars and complex hybrids are larger than the previous result of *I. cornuta* (2*C*=1.31 pg; Zhang et al. 2013). The possible reasons for this difference might be due to the use of different origins of plant materials, reference plants, methods for lysates, staining protocols and instruments (Wang et al. 2019; Jatt et al. 2019; Kolano et al. 2012). Given the large variation in genome sizes of *I. cornuta* germplasm resources, it is essential to investigate a large number of varieties before a more accurate estimation of their average genome sizes can be achieved.

Optimization of internal reference to estimate genome size accurately

Due to its indirect nature, one of the important steps in FCM analysis was to choose the reference plant species used as an internal standard, which can reveal significant differences in DNA contents among the same cultivar or plant species (Ortega-Ortega et al. 2019; Jatt et al. 2019; Doležel et al. 2003). To be useful as a primary standard, a plant must have similar, but not identical, genome size to the analyzed plant, and the G_0/G_1 peaks of the standard should not overlap to the peaks of the sample and is located relatively at a distance from the samples that can help to decrease the errors in measuring DNA content (Doležel and Greilhuber 2010; Jatt et al. 2019). Ideally, the 2*C* peak of the target species should be located between the 2*C* and 4*C* peaks of the internal reference standard and the genome size of the target and internal standards should not differ more than fourfold (Suda and Leitch 2010). In addition, the standard must be easy to use, genetically stable, nuclei must be obtained in enough amounts for analysis (Ortega-Ortega

Table 2. Genome size of the varieties of *I. cornuta* analyzed in this work.

No	Varieties	Genome size						CV (%) of samples	CV (%) of standard
		2*C* (pg)				1*C* (pg) Mean	1*C* (Mpb) Mean		
		Mean ± SD	Min.	Max.	Significance*				
Ilex cornuta -related cultivars									
1	'Burfordii'	1.77±0.0263	1.72	1.81	ab	0.883	863	4.55	4.40
2	'Dwarf Burford'	1.61±0.0048	1.60	1.62	def	0.805	787	3.50	2.77
3	'Luteocarpa'	1.71±0.0351	1.63	1.81	bc	0.855	836	3.49	4.09
4	'O Spring'	1.63±0.0282	1.57	1.67	de	0.813	794	5.15	4.94
	Average	1.68				0.839	820		
Interspecific hybrids									
Ilex (cornuta x latifolia)									
5	'Emily Bruner'	1.47±0.0217	1.42	1.53	g	0.733	717	4.56	4.81
6	'James Swan'	1.55±0.0294	1.50	1.60	ef	0.774	757	4.85	4.90
Ilex									
7	'*dabieshanensis* No.1'	1.56±0.0355	1.50	1.62	ef	0.781	763	2.81	3.76
Ilex [(cornuta x pernyi) x latifolia]									
8	'Mary Nell'	1.71±0.0048	1.70	1.72	bc	0.856	837	4.57	4.97
Ilex (aquifoilium x cornuta)									
9	'Nellie R. Stevens'	1.80±0.0148	1.78	1.83	a	0.901	881	1.82	3.60
10	'Edward J. Stevens'	1.54±0.0039	1.54	1.55	f	0.772	754	3.98	4.26
11	'Golden Nellie R Stevens'	1.72±0.0146	1.69	1.76	bc	0.859	839	5.08	3.58
Ilex (rugosa x cornuta)									
12	'China Girl'	1.66±0.0093	1.64	1.68	cd	0.831	812	3.09	3.78
Average		1.63				0.813	795		
Overall average		1.65±0.0165	1.42	1.83		0.823	805	3.95	4.15

et al. 2019). Rice has all these characteristics. Initially in this study, rice was selected as internal standard. The G_0/G_1 peak of *I. cornuta* was about twice that of the diploid cultivated rice and they don't overlap each other (Figure 3), which proved the rice was a advisable standard for *I. cornuta* flow cytometric analysis.

Performance of flow cytometry for I. cornuta

The CV has been considered an important FCM parameter, indicating the quality of nuclei suspensions (Favoreto et al. 2012). CV within 9% indicated that test results were relatively reliable (Georgiev et al. 2009); CV below 5% indicated the highest accuracy for FCM assessments in plants (Doležel and Bartoš 2005). In the present work, for 'O Spring' and 'Golden Nellie R Stevens', it was very difficult to obtain CV values at the level of below 5%, which mainly due to the high amount of autofluorescence and phenolics in the gold leaves hampering the dyeing and analysis of the nuclei (Choudhury et al. 2014). Except for these two varieties, the FCM procedure used here provided fluorescence peaks of G_0/G_1 nuclei showing CV are all below 5%, which indicated that the extraction and staining procedure using Tris dissociation solution combined with a centrifugation step can result in the accepted histograms. Thus, the FCM procedure in this work is adequate for determination of genome size for *I. cornuta* and can be applied in other FCM studies of *Ilex*.

Intraspecific variations in genome size

Statistical analysis can help assess the extent of genome size variation among varieties of related species or cultivars. In the case of *I. cornuta* it is important to determine the genetic variability between different cultivars (including genome size) since most of them are not biologically defined species, but rather the result of somatic mutations and artificial hybridization (Hodges et al. 2001). Thus, FCM analysis applied to estimate total nuclear DNA content in *I. cornuta* cultivars can help to identify those cultivars with higher possibilities of hav-

ing sexual compatibility and therefore hybridization via conventional breeding.

Among Angiosperms, there is a great variation in genome sizes, ranging from 0.065 pg/1*C* of DNA in *Genlisea margaretae* Hutch. to 152.23 pg/1*C* in *Paris japonica* Franch (Kolano et al. 2012). Also, numerous studies revealed the existence of considerable variation in genome size at the interspecific level, e.g. *Coffea arabica* (Ortega-Ortega et al. 2019; Noirot et al. 2003), *Phoenix dactylifera* (Jatt et al. 2019), *Chenopodium quinoa* (Kolano et al. 2012), several *Pisum* species (Baranyi et al. 1996), three *Saccharum* species (Zhang et al. 2012), *Agave tequilana* (Palomino et al. 2003) and *Arabidopsis thaliana* (Schmuths et al. 2004). Amongst the cultivars of *I. cornuta* there was a 1.16-fold range of variation, and although some of this might be attributable to methodological variation, it is possible that not all can be explained in this way. Murray (2005) has suggested that intraspecific variation in *C*-value may be indicative of taxonomic heterogeneity and there is no doubt that *I. cornuta* is a highly variable species that exhibits a wide range of morphological variation.

In general, these cultivars, resulting from spontaneous mutations and being thus related, have remarkably similar genome sizes and a different DNA content relative to their progenitors. This is the case of the *I. cornuta* cultivar that gave rise to 'Burfordii', 'Dwarf Burford', 'Luteocarpa' and 'O'Spring'. In contrast, a wider range of variation in the genome size were exhibited among the hybrids, one possible explanation for which was that varieties of hybrid origin have undergone substantial genome size changes as compared with natural mutations (Ortega-Ortega et al. 2019). Other varieties have different genetic origin and yet possess similar DNA content, i.e., 'Luteocarpa' and 'Golden Nellie R Stevens'. It is known that variations in genome size has been primarily attributed to fluctuation within highly repetitive DNA, variation in chromosome number, amplification/deletion of DNA sequences (Wang et al. 2017; Kolano et al. 2012; Sharma et al. 2019). Mechanisms underlying intraspecific and interspecific genome size variation in plants still remain controversial; thus, more research is fairly required in this regard (Ortega-Ortega et al. 2019; Huang et al. 2013).

CONCLUSION

In conclusion, genome size of 12 commercially important *I. cornuta* varieties was analyzed in picograms by flow cytometry technique for the first time. This study can fill a gap in the literature by providing information about the genome size of *I. cornuta* varieties and enrich the *C* value database of *Ilex* L. It also provides a valuable reference for other *Ilex* L. species to determine genome size by flow cytometry. This information can be helpful for *I. cornuta* breeding programs, give the paucity of genome size studies with FCM in different important *I. cornuta* cultivars. Additionally, these results may be relevant for genomic analysis as well as for a better understanding of *I. cornuta* evolutionary relationships, diversification, hybridization, and polyploidy.

ACKNOWLEDGMENTS

Thanks go to Yanwei Zhou and Yiping Zou, who assisted with the material collection and Feng Lin for the technical support with FCM.

AUTHOR CONTRIBUTIONS

Conceptualization, P.Z. and M.Z.; formal analysis, Q.Z.; investigation, J.L. and P.Z.; data curation, J.H.; writing—original draft preparation, P.Z.; writing—review and editing, Q.Z. and M.Z.; visualization, F.L. and J.H.; funding acquisition, M.Z. and P.Z. All authors have read and agreed to the published version of the manuscript.

FUNDING

This research was funded by the Jiangsu Academy of Forestry Youth Foundation [JAF-2022-03], the Jiangsu Province Innovation and extension project of forestry science and technology [LYKJ[2020]02], the Jiangsu Province Innovation and extension project of forestry science and technology [LYKJ[2021]07], the Jiangsu Province Innovation and extension project of agricultural science and technology [2021-SJ-008] and Independent Research Projects of Jiangsu Academy of Forestry [ZZKY202105].

REFERENCES

Baranyi M, Greilhuber J, Święcicki WK. 1996. Genome size in wild *Pisum* species. Theor Appl Genet. 93:717-721.

Bennett MD, Leitch IJ. 2012. Plant DNA C-values database (release 6.0, December 2012). See http://www.kew. org/cvalues.

Bennett MD, Leitch IJ. 2011. Nuclear DNA amounts in angiosperms: targets, trends and tomorrow.
Ann Bot. 107: 467-590.
Choudhury RR, Basak S, Ramesh AM, Rangan L. 2014. Nuclear DNA content of *Pongamia pinnata*
L. and genome size stability of in vitro-regenerated plantlets. Protoplasma. 251: 703-709. Doležel J, Bartoš JAN. 2005. Plant DNA flow cytometry and estimation of nuclear genome size.
Ann Bot. 95: 99-110.
Doležel J, Greilhuber J. 2010. Nuclear genome size: are we getting closer?. Cytom Part A. 77: 635- 642.
D'hondt L, Höfte M, Van Bockstaele E, Leus L. 2011. Applications of flow cytometry in plant pathology for genome size determination, detection and physiological status. Mol Plant Pathol. 12: 815-828.
Doležel J. 2003. Nuclear DNA content and genome size of trout and human. Cytom Part A. 51: 127- 128.
Favoreto FC, Carvalho CR, Lima ABP, Ferreira A, Clarindo WR. 2012. Genome size and base composition of Bromeliaceae species assessed by flow cytometry. Plant Syst Evol. 298:1185- 1193.
Georgiev V, Weber J, Bley T, Pavlov A. 2009. Improved procedure for nucleus extraction for DNA measurements by flow cytometry of red beet (*Beta vulgaris* L.) hairy roots. J Biosci Bioeng. 107: 439-441.
Hodges, G., Ruter, J. M., Kristine Braman, S. 2001. Susceptibility of *Ilex* species, hybrids and cultivars to Florida wax scale (*Ceroplastes floridensis* Comstock). J Environ Hort. 19:32-36.
Hu SY. 1949. The genus *Ilex* in China. J Arnold Arboretum. 30: 233-344.
Huang H, Tong Y, Zhang QJ, Gao LZ. 2013. Genome size variation among and within *Camellia*
species by using flow cytometric analysis. PLoS One. 8: e64981.
International Rice Genome Sequencing Project. 2005. The map-based sequence of the rice genome. Nature. 436:793-800.
Jatt T, Lee MS, Rayburn AL, Jatoi MA, Mirani AA. 2019. Determination of genome size variations among different date palm cultivars (*Phoenix dactylifera* L.) by flow cytometry. 3 Biotech. 9:1- 10.
Kang YF, Wu HM, Chen SJ, Chen WY, Li HT, Chen CY. 2014. Secondary metabolites from the leaves of *Ilex Cornuta*. Chem Nat Comp. 50: 355-356.
Kolano B, Siwinska D, Gomez Pando L, Szymanowska-Pulka J, Maluszynska J. 2012. Genome size variation in *Chenopodium quinoa* (Chenopodiaceae). Plant Syst Evol. 298: 251-255.
Leitch IJ, Chase MW, Bennett MD. 1998. Phylogenetic analysis of DNA C-values provides evidence for a small ancestral genome size in flowering plants. Ann Bot. 82: 85-94.
Loizeau PA, Savolainen V, Andrews S, Barriera G, Spichiger R. 2016. Aquifoliaceae. In *Flowering Plants*; Springer: Cham, Switzerland, 14, p. 31–36.
Lysák MA, Rostková A, Dixon JM, Rossi G, Doležel J. 2000. Limited genome size variation in *Sesleria albicans*. Ann Bot. 86: 399-403.
Murray BG. 2005. When does intraspecific C-value variation become taxonomically significant?. Ann Bot. 95: 119-125.
Noirot M, Poncet V, Barre P, Hamon P, Hamon S, De Kochko A. 2003. Genome size variations in diploid African *Coffea* species. Ann Bot. 92: 709-714.
Ortega-Ortega J, Ramírez-Ortega F A, Ruiz-Medrano R, Xoconostle-Cázares B. 2019. Analysis of genome size of sixteen *Coffea arabica* cultivars using flow cytometry. HortScience. 54: 998- 1004.
Park J, Kim Y, Nam S, Kwon W, Xi H. 2019. The complete chloroplast genome of horned holly, *Ilex cornuta* Lindl. & Paxton (Aquifoliaceae). Mitochondrial DNA B. 4:1275-1276.
Palomino G, Dolezel J, Mendez I, Rubluo A. 2003. Nuclear genome size analysis of *Agave tequilana* Weber. Caryologia. 56: 37-46.
Pellicer J, Leitch IJ. 2014; 1115. The application of flow cytometry for estimating genome size and ploidy level in plants. In Molecular plant taxonomy; Humana Press: Totowa, NJ. pp. 279-307.
Schmuths H, Meister A, Horres R, Bachmann K. 2004. Genome size variation among accessions of *Arabidopsis thaliana*. Ann Bot. 93: 317-321.
Sharma S, Kaushik S, Raina SN. 2019. Estimation of nuclear DNA content and its variation among Indian Tea accessions by flow cytometry. Physiol Mol Biol Plant. 25: 339-346.
Sliwinska E. 2018. Flow cytometry–a modern method for exploring genome size and nuclear DNA synthesis in horticultural and medicinal plant species. Folia Hort. 30: 103-128.
Soltis DE, Soltis PS, Bennett MD, Leitch IJ. 2003. Evolution of genome size in the angiosperms. Am J Bot. 90:1596-1603.
Suda J, Leitch IJ. 2010. The quest for suitable reference standards in genome size research. Cytom Part A. 77: 717-720.
Wang GY, Meng Y, Yang YP. 2017. nome size variation among and within Ophiopogoneae species by flow cytometric analysis. Braz J Bot.40:529-537.
Wang LH, Luo Z, Liu ZG., Zhao J, Deng WP, Wei HR, Liu P, Liu MJ. 2019. Genome Size variation within species of Chinese jujube (*Ziziphus jujuba* Mill.) and

its wild ancestor sour jujube (*Z. acidojujuba* Cheng et Liu). Forests.10:460.

Yao X, Song Y, Yang JB, Tan YH, Corlett RT. 2021. Phylogeny and biogeography of the hollies (*Ilex* L., Aquifoliaceae). J Syst Evol. 59: 73-82.

Zhang JS, Nagai C, Yu QY, Pan YB, Ayala-Silva T, Schnell RJ, Comstock JC, Arumuganathan AK, Ming R. 2012. Genome size variation in three *Saccharum* species. Euphytica. 185: 511-519.

Zhang L, Cao B, Bai C. 2013. New reports of nuclear DNA content for 66 traditional Chinese medicinal plant taxa in China. Caryologia. 66: 375-383.

Zhang SX, Yao ZR, Li J. Tu PF. 2012. Flavonoids from the leaves of *Ilex cornuta*. Chinese J Nat Med. 10: 84-87.

Caryologia
International Journal of Cytology, Cytosystematics and Cytogenetics

Firenze University Press
www.fupress.com/caryologia

OPEN ACCESS

Citation: Weera Thongnetr, Suphat Prasopsin, Surachest Aiumsumang, Sukhonthip Ditcharoen, Alongklod Tanomtong, Prayoon Wongchantra, Wutthisak Bunnaen, Sumalee Phimphan (2022). First report of chromosome and karyological analysis of *Gekko nutaphandi* (Gekkonidae, Squamata) from Thailand: Neo-diploid chromosome number in genus *Gekko*. *Caryologia* 75(4): 103-109. doi: 10.36253/caryologia-1875

Received: September 11, 2022

Accepted: December 13, 2022

Published: April 28, 2023

Data Availability Statement: All relevant data are within the paper and its Supporting Information files.

Competing Interests: The Author(s) declare(s) no conflict of interest.

First report of chromosome and karyological analysis of *Gekko nutaphandi* (Gekkonidae, Squamata) from Thailand: Neo-diploid chromosome number in genus *Gekko*

Weera Thongnetr[1], Suphat Prasopsin[2], Surachest Aiumsumang[3,*], Sukhonthip Ditcharoen[4], Alongklod Tanomtong[5], Prayoon Wongchantra[6], Wutthisak Bunnaen[7], Sumalee Phimphan[3]

[1] *Division of Biology, Department of Science, Faculty of Science and Technology, Rajamangala University of Technology Krungthep, Bangkok 10120, Thailand*
[2] *Research Academic Supports Division, Mahidol University, Kanchanaburi Campus, Saiyok, Kanchanaburi 71150, Thailand*
[3] *Biology program, Faculty of Science and Technology, Phetchabun Rajabhat University, Phetchabun 67000, Thailand*
[4] *Division of Biology, Faculty of Science and Technology, Rajamangala University of Technology Thanyaburi, Khlong Luang, Pathum Thani 12120, Thailand*
[5] *Program of Biology, Faculty of Science, Khon Kaen University, Muang, Khon Kaen 40002, Thailand*
[6] *Center of Environmental Education Research and Training, Faculty of Environment and Resource Studies,Mahasarakham University 44150, Thailand*
[7] *Mahasarakham University Demonstration School (Secondary) Kham Riang Sub-District, Kantharawichai District, Maha Sarakham, 44150, Thailand*
*Corresponding author. E-mail: topthesun1978@gmail.com, surachest.aiu@pcru.ac.th

Abstract. The karyotypes of red-eyed Gecko are not reported yet. Herein, we describe the karyotypes of red-eyed Gecko (*Gekko nutaphandi* Bauer, Sumontha & Pauwels, 2008) from Thailand. Gecko chromosome preparations were directly conducted from bone marrow and testis. Chromosomal characteristics were analyzed by Giemsa staining, Ag-NOR banding as well as fluorescence in situ hybridization (FISH) using microsatellites $d(GC)_{15}$ probe. The results showed that the number of diploid chromosomes is $2n$=34, while the fundamental number (NF) is 46 in both males and females. The types of chromosomes were 4 large metacentric, 6 large submetacentric, 2 medium telocentric, 2 small metacentric and 20 small telocentric chromosomes. The results of conventional Giemsa staining presented the diploid chromosome number differentiation even in the same genus. NORs are located at the secondary constriction to the telomere on the long arm of chromosome pair 5. There are no sex differences in karyotypes between males and females. FISH with $d(GC)_{15}$ sequences were also displayed at the telomeres of most other chromosomes. We found that during metaphase I the homologous chromosomes showed synapsis, which can be defined as 19 ring bivalents and 17 haploid chromosomes (n=17) at metaphase II as a diploid species. The karyotype formula is as follows: $2n$ (34) = $L_4^m+L_6^{sm}+M_2^t+S_2^m+S_{20}^t$.

Keywords: Chromosome, *Gekko nutaphandi*, Karyotype, Red-eyed Gecko.

INTRODUCTION

Geckos of the genus *Gekko* Laurenti, 1768 are members of a relatively large putatively monophyletic group of lizards that also includes *Lepidodactylus* Fitzinger, 1843, *Luperosaurus* Gray, 1845, *Pseudogekko* Taylor, 1922, and *Ptychozoon* Kuhl & van Hasselt, 1822 (Kluge 1968; Russell 1972; Bauer et al. 2008). The genus *Gekko* itself is species rich (84 species) and is generally characterized by regional endemism across its broad range in tropical Asia. Recently, *G. nutaphandi,* is described from Kanchanaburi Province in central western Thailand (Bauer et al. 2008). *G. nutaphandi* is most similar to *G. gecko*, *G. smithii*, *G. siamensis*, *G. verreauxi*, and *G. albofasciolatus* Günther, 1872, which have previously been considered to be closely related based on their shared possession of a suite of features.

Information about karyotypes in *Gekko* is scarce and fragmented, and usually based on conventional staining technique; only a few studies have been published (19 species of 84 species), all of them recent in genus *Gekko,* namely, *G. gecko*: 2n=38 (Singh 1974; Solleder and Schmid 1984; Wu and Zhao 1984; Trifonov et al. 2011; Qin et al. 2012; Patawang et al. 2014), *G. hokouensis*: 2n=38 (Chen et al. 1986; Kawai et al. 2009; Shibaike et al. 2009), *G. japonicus*: 2n=38 (Yoshida and Itoh 1974; Shibaike et al. 2009; Trifonov et al. 2011), *G. shibatai* and *G. vertebralis*: 2n=38 (Shibaike et al. 2009), *G. Vittatus* and *G. ulikovskii*: 2n=38 (Trifonov et al. 2011), *G. tawaensis*: 2n=38 (Ota 1989a; Shibaike et al. 2009), *G. taylori*: 2n=42 (Ota and Nabhitabhata 1991), *G. monarchus*: 2n=44 (Ota et al. 1990), *G. yakuensis*, *G. petricolus* and *G. smithii*: 2n=38-42 (Ota 1989a), *G. kikuchii*: 2n=44 (Ota 1989a), *G. chinensis*: 2n=40 (Lau et al. 1997), *G. subpalmatus*: 2n=38 (Wu and Zhao 1984), *G. swinhonis*: 2n=38 (Chen et al. 1986), *G. petricolus*: 2n=34 (Thongnetr et al. 2022), *Dixonius hangseesom*: 2n=40, *D. Siamensis*: 2n=40, *D. melanostictus*: 2n=42 (Patawang et al. 2022) and *Cyrtodactylus inthanon*: 2n=40 (Prasopsin et al. 2022) and shown in Table 1.

This fact is probably due to the difficulty in obtaining samples for cytogenetic analysis in some species or to problems in obtaining metaphase cells by cell culture induction. Moreover, cytogenetic studies using conventional staining techniques provide valuable information on the excellent karyotype diversity shown by these animals. Analyses of cytogenetic markers, including the number and karyotype formula, sex determination, B chromosomes, number and location of nucleolar organizer regions (NORs), heterochromatin distribution, G-banding, and R-banding, treatments with base-specific fluorochromes and fluorescence *in situ* hybridization techniques allowed the cytogenetic characterization of populations, species, and supra-specific groups (Affonso and Galetti Jr. 2005). The present study is the first report on the chromosomal characteristics of *G. nutaphandi* determined using conventional staining, Ag-NOR banding, and fluorescence *in situ* hybridization techniques.

MATHERIAL AND METHODS

Sample collection, chromosome preparation and chromosome staining

We obtained specimens of *G. nutaphandi* that were collected from Kanchanaburi Province, Western Thailand. Chromosomes were directly prepared *in vivo* (Ota 1989a; Qin et al. 2012) using the following method. With 20% of Giemsa solution, the slides were conventionally stained for 30 minutes (Patawang et al. 2014). After that, the slides were rinsed thoroughly with running tap water to remove excess stain and placed in air-dry at room temperature. Ag-NOR banding was analysed according to the method of Howell and Black (1980). Two drops each of 50% silver nitrate and 2% gelatine solutions were added to the slides, respectively. Then, they were sealed with cover glasses and incubated at 60°C for 5-10 minutes. They were also soaked in distilled water until the cover glasses were separated. Finally, the slides were placed in air-dry at room temperature. They were observed under the microscope. The use of microsatellite investigations which were described by Kubat et al. (2008), was followed here with slight modifications. These sequences were directly labeled with Cy3 at the 5′-terminal during synthesis by Sigma (St. Louis, MO, USA.) Fluorescence *in situ* hybridization (FISH) was performed under highly rigorous conditions on mitotic chromosome spreads (Pinkel et al. 1986).

Chromosomal checks, karyotyping and idiograming

Chromosome counting was carried out on mitotic metaphase cells under the light microscope for 30 cells per specimen to determine the diploid number (2*n*). Twenty clearly observable and well-spread metaphase cells were selected and photographed from each male and female. The short arm length (Ls) and the long arm length (Ll) of each chromosome were measured to calculate the total length of the chromosome for 20 well-spread metaphase cells. The chromosome types were classified from the method of Turpin and Lejeune (1965) as metacentric, submetacentric, acrocentric, and telocentric chromosomes.

Table 1. The karyotype reviews among the genes *Gekko* (Gekkonidae, Squamata).

Species	2*n*	NF	Karyotype formulas	NORs	FISH	Locations	References
Gekko gekko	38	50	6m+4sm+2a+26t	P4	-	Thailand	Patawang et al. (2014)
	38	44	6bi-arms+32uni-arms	-	-	-	Singh (1974)
	38	-	-	-	-	-	Wu and Zhao (1984)
	38	46	8bi-arms+30uni-arms	-	-	-	Solleder and Schmid (1984)
	38	-	-	-	-	-	Trifonov et al. (2011)
	38	50	8 m+2sm+2st(a)+26t			Laos	Qin et al. (2012)
	38	48	8 m+2sm+28t	-	-	China	Qin et al. (2012)
G. hokouensis	38	56	4 m+6sm+20t+8bi-arms*	P19	-	China,	Chen et al. (1986)
	38	58/59	2 m+8sm+10a+16t+Z(t)+W(a)	-	-	Japan	Kawai et al. (2009)
	38	58	4 m+8sm+18t+8bi-arms*	P19	-	Taiwan	Shibaike et al. (2009)
	38	58/59	4 m+8sm+16t+8bi-arms*+Z(t)W(sm)	P19	-	Japan	Shibaike et al. (2009)
	38	42	2m+18sm+16a+ZW	P19	FISH mapping	Thailand	Srikulnath (2015)
G. japonicus	38	-	-	-	-	-	Yoshida and Itoh (1974)
	38	58	4m+8sm+8st+18t	P17	-	Japan	Shibaike et al. (2010)
	38	-	-	-	-	-	Trifonov et al. (2011)
G. shibatai	38	58	4m+8sm+18t+8bi-armed	P19	-	Japan	Shibaike et al. (2009)
G. vertebralis	38	62	4m+14sm+14t+6bi-arme*	P19	-	Japan	Shibaike et al. (2009)
G. vittatus	38	-	-			-	Trifonov et al. (2011)
G. ulikovskii	38	-	-			-	Trifonov et al. (2011)
G. tawaensis	38	58	4m+8sm+18t+8bi-armed	P19	-	Japan	Shibaike et al. (2009)
	38	56	-	P19	-	Japan	Ota (1989a)
G. taylori	42	-	-	-	-	Thailand	Ota and Nabhitabhata (1991)
G. monarchus	44	46	-	-	-	Malaysia	Ota et al. (1990)
G. yakuensis	38	56	-	P19	-	Japan	Ota (1989a)
G. petricolus	38	54	-	-	-	Thailand	Ota (1989a)
G. kikuchii	44	50	-	-	-	Taiwan	Ota (1989a)
G. chinensis	40	46	6bi-armed+34uni-armed	-	-	China	Lau et al. (1997)
G. smithii	38	48	-	-	-	-	Ota (1989a)
G. subpalmatus	38	58	-	-	-	-	Wu and Zhao (1984)
G. swinhonis	38	66	-	-	-		Chen et al. (1986)
G. petricolus	38	54	4m+2sm+10a+22t	P17	$(CA)_{15}$, $(GAA)_{10}$	Thailand	Thongnetr et al. (2022)
G. nutaphandi	34	46	6m+6sm+22t	P5	$(GC)_{15}$	Thailand	Present study
Dixonius hangseesom	40	42	2m+38t	P13	-	Thailand	Patawang et al. (2022)
D. siamensis	40	42	2m+38t	P13	-	Thailand	Patawang et al. (2022)
D. melanostictus	42	44	2a+40t	P8	-	Thailand	Patawang et al. (2022)
Cyrtodactylus inthanon	40	58	12m+4sm+2a+22t	P12	$(CA)_{15}$ $(GC)_{15}$ $(CAG)_{10}$ $(GAA)_{10}$	Thailand	Prasopsin et al. (2022)

Note: 2n = diploid chromosome number, NORs = nucleolar organizer regions, NF = fundamental number (number of chromosome arms), bi-arm = bi-armed chromosome, m = metacentric, sm = submetacentric, a = acrocentric, t = telocentric chromosome, *=small bi-arms chromosome, and - = not available.

RESULTS AND DISCUSSION

Diploid chromosome number, fundamental number and karyotype

The *Gecko* is a large genus (84 species) of Gekkonidae family and until now, no study has investigated the karyotype of *G. nutaphandi*. Furthermore, this is the first report on cytogenetic characterization to use conventional Giemsa staining, NOR-banding, and FISH techniques for this species. For *G. nutaphandi,* the results indicated a diploid chromosome number (2*n*) of 34 in all studied samples (Figure 1). This result dif-

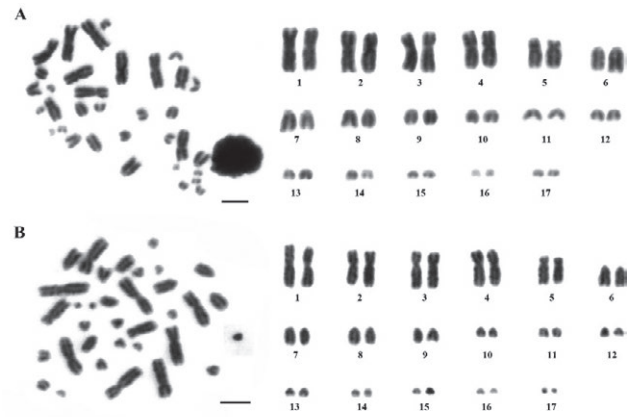

Figure 1. Metaphase chromosome plates and karyotypes of *G. nutaphandi* (A) male (B) female by conventional technique. Scale Bars = 10 μm.

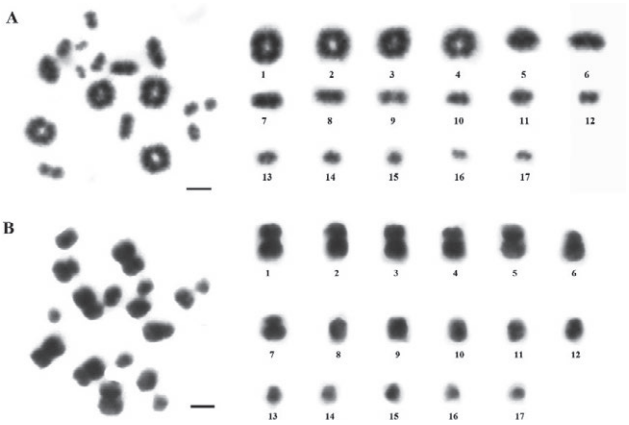

Figure 2. Metaphase chromosome plates and karyotypes of *G. nutaphandi* (A) Metaphase I (B) Metaphase II by conventional technique. Scale Bars = 10 μm.

fers from most species of the genus *Gecko*. The 2*n* of this genus range from 38 to 44. (Singh 1974; Yoshida and Itoh 1974; Solleder and Schmid 1984; Wu and Zhao 1984; Chen et al. 1986; Ota 1989a; Ota et al. 1990; Ota and Nabhitabhata 1991; Lau et al. 1997; Kawai et al. 2009; Shibaike et al. 2009; Trifonov et al. 2011; Qin et al. 2012; Patawang et al. 2014; Patawang et al. 2022 and Prasopsin et al. 2022.

The fundamental number (NF) of *G. nutaphandi* was 46 in both males and females. The karyotype consisted of 4 large metacentric, 6 large submetacentric, 2 medium telocentric, 2 small metacentric, and 20 small telocentric chromosomes (Table 1). These results of NF are agreeable with the previous reports of *G. gecko* (Solleder and Schmid 1984), *G. monarchus* (Ota et al. 1990), and *G. chinensis* (Lau et al. 1997). The NFs of the genus *Gekko* range from 44 to 62, and karyotypes are composed of both mono- and bi-arms chromosomes. Nirchio et al. (2002) proposed that species with high NF is an advanced state or apomorphic character, whereas one with low NF is a primitive state or plesiomorphic character. Thus, the *G. nutaphandi* seems to be a more primitive karyotype than other species. The karyotype formula for this species is $2n$ (34) = $L_4^m+L_6^{sm}+M_2^t+S_2^m+S_{20}^t$. There is no evidence of differentiated sex chromosomes in this species which accord with all species of this genus (Singh 1974; Yoshida and Itoh 1974; Solleder and Schmid 1984; Wu and Zhao 1984; Chen et al. 1986; Ota 1989a; Ota et al. 1990; Ota and Nabhitabhata 1991; Lau et al. 1997; Kawai et al. 2009; Shibaike et al. 2009; Trifonov et al. 2011; Qin et al. 2012; Patawang et al. 2014; Patawang et al. 2022 and Prasopsin et al. 2022.

The present study on the meiotic cell division of *G. nutaphandi* found that during metaphase I (meiosis I), the homologous chromosomes showed synapsis, which can be defined as the 17 bivalent (Figure 2A), and 17 haploid chromosomes at metaphase II (Figure 2B) as diploid species. The largest metacentric chromosome pair 1 is the largest bivalent. No diakinesis and metaphase I cell with partially paired bivalents are speculated to be heteromorphic sex chromosomes, and no metaphase II cells with condensed chromosomes are speculated to be the sex chromosome.

Chromosome markers from Ag-NOR banding

The development of Ag-NOR staining technique (Howell and Black 1980) to detect metaphase chromosome sites of NORs has greatly facilitated comparative studies of NORs variation. Silver staining of NORs is considered as one of the standard banding methods and has assumed considerable importance in characterizing a species' karyotype. The present study was firstly accomplished by using Ag-NOR staining in *G. nutaphandi*. The Ag-NOR positions were shown on the long arm near the centromere of the telocentric chromosome pair 5 (subtelomeric NOR) (Figure 3). The single pair of NOR is the same as in *Gecko* species. Compared with other geckos, the NOR regions showed two NORs appearing near telomeric region of small bi-armed or mono-armed chromosome. An example of the previous reports of the genus *Gekko* had two NORs on one pair of small bi-arms chromosomes. *G. gecko* had two NORs on the near telomere of mono-arms chromosome pair 4 (Patawang et al. 2014), and *G. petricolus* had two NORs on the long arm near telomere of bi-arms chromosome pair 5 (Thongnetr et al. 2022), while there were *G. shibatai*, *G. Yakuensis,*

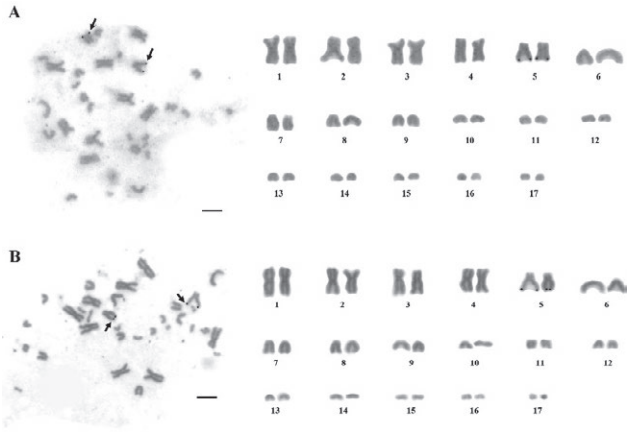

Figure 3. Metaphase chromosome plates and karyotypes of *G. nutaphandi* (A) male (B) female by Ag-NOR banding technique. Scale Bars = 10 μm.

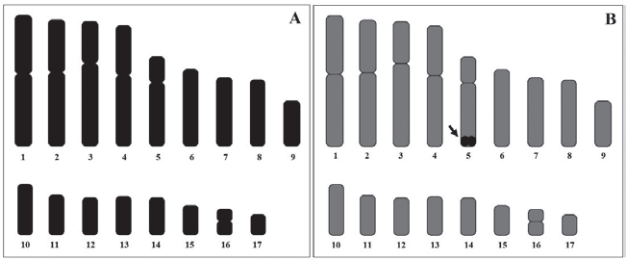

Figure 4. Idiogram represents chromosome type, size, and Ag-NOR banding of *G. nutaphandi*.

G. hokouensis, *G. tawaensis*, *G. vertebralis* and *G. yakuensis* which had two NORs on the long arm near the telomere of small bi-arms chromosome pair 19 (Ota 1989b; Chen et al. 1986; Shibaike et al. 2009). The use of NORs in explaining kinships depends to a considerable extent on the uniformity of this characteristic and the degree of variety within a taxon (Yüksel and Gaffaroğlu 2008).

The idiogram shows a continuous length gradation of chromosomes. The size differences between the largest and smallest chromosomes exhibit approximately two-fold. The data of the chromosome measurement on mitotic metaphase cells (from all specimens) are shown in Table 2. Idiograms by conventional Giemsa staining and Ag-NOR banding are shown in Figure 4.

Microsatellite pattern

Microsatellites or simple sequence repeats (SSRs) are oligonucleotides of 1–6 base pairs in length, forming excessive tandem repeats of usually 4 to 40 units (Tautz and Renz 1984; Ellegren 2004; Chistiakov et al. 2006). They show ample distribution throughout eukaryotic genomes, scattered or clustered in euchromatin and heterochromatin. They are highly polymorphic regarding

Table 2. Mean length of short arm chromosome (Ls), length of long arm chromosome (Ll), length of total chromosomes (LT), relative length (RL), centromeric index (CI), and standard deviation (SD) from 20 metaphases of male and female Red-eyed Gecko (*Gekko nutaphandi*), 2*n* (diploid)=34.

Chro.pairs	Ls	Ll	LT	CI±SD	RL±SD	Chro. size	Chro. type
1	0.932	1.131	2.035	0.548±0.012	0.132±0.007	Large	metacentric
2	0.835	1.160	1.961	0.602±0.015	0.120±0.005	Large	submetacentric
3	0.769	1.303	2.001	0.626±0.023	0.115±0.007	Large	submetacentric
4	0.784	1.113	1.833	0.586±0.020	0.113±0.007	Large	metacentric
5*	0.410	1.003	1.372	0.673±0.019	0.084±0.004	Large	submetacentric
6	0.000	1.216	1.216	1.000±0.000	0.066±0.003	Medium	telocentric
7	0.000	1.016	1.016	1.000±0.000	0.060±0.003	Small	telocentric
8	0.000	1.049	1.049	1.000±0.000	0.055±0.002	Small	telocentric
9	0.000	0.720	0.720	1.000±0.000	0.046±0.003	Small	telocentric
10	0.000	0.800	0.800	1.000±0.000	0.037±0.004	Small	telocentric
11	0.000	0.629	0.629	1.000±0.000	0.032±0.003	Small	telocentric
12	0.000	0.595	0.595	1.000±0.000	0.029±0.003	Small	telocentric
13	0.000	0.615	0.615	1.000±0.000	0.026±0.003	Small	telocentric
14	0.000	0.596	0.596	1.000±0.000	0.023±0.004	Small	telocentric
15	0.000	0.464	0.464	1.000±0.000	0.021±0.003	Small	telocentric
16	0.195	0.220	0.374	0.520±0.038	0.024±0.004	Small	metacentric
17	0.000	0.326	0.326	1.000±0.000	0.016±0.003	Small	telocentric

Note: Chro.=chromosome, * NORs bearing chromosomes (satellite chromosome).

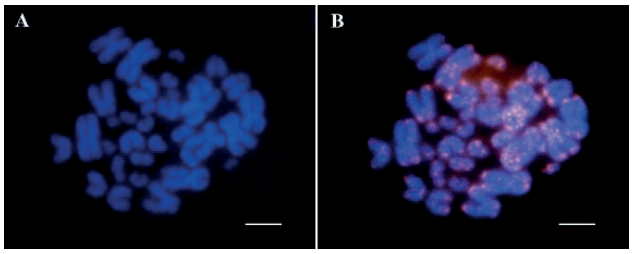

Figure 5. Metaphase chromosome plate of *G. petricolus* (**A**) by FISH technique of DAPI (**B**) microsatellite probe $(GC)_{15}$. Scale Bars = 10 μm.

copy number deviation (Ellegren 2004). Fluorescence hybridization indicates the $(GC)_{15}$ repeat showing abundance at the telomeric ends of most chromosomes (Figure 5), verifying the findings from other gekko groups investigated to date (Srikulnath 2015). The distribution of microsatellites was not only restricted to heterochromatin but also dispersed in euchromatic regions of the chromosomes (Getlekha et al. 2016). Nonetheless, closely related fish species involved in recent speciation events could present a differential pattern in the distribution and quantity of microsatellite sequences on chromosome.

In conclusion, we present the first Karyotype, NOR phenotype, and microsatellite patterns $(GC)_{15}$ on the chromosomes are specific to species in the *G. nutaphandi*. More species and techniques should be further studied for more information about the chromosomal diversity and chromosomal evolution in this genus.

ACKNOWLEDGEMENTS

This research project was financially supported by Thailand science research and innovation (TSRI). Khon Kaen University and Phetchabun Rajabhat University.

REFERENCES

Affonso PRAM, Galetti Jr PM. 2005. Chromosomal diversification of reef fishes from genus *Centropyge* (Perciformes, Pomacanthidae). Genetica 123: 227–233.

Bauer AM, Sumontha M, Pauwels SGO. 2008. A new red-eyed Gekko (Reptilia: Gekkonidae) from Kanchanaburi Province, Thailand. Zootaxa 1750(1750): 32–42.

Chen J, Peng X, Yu D. 1986. Studies on the karyotype of three species of the genus *Gekko*. Acta Herpetologica Sinica 5: 24–29.

Chistiakov DA, Hellemans B, Volckaert FAM. 2006. Microsatellites and their genomic distribution, evolution, function and applications: a review with special reference to fish genetics. Aquaculture 255: 1–29. https://doi.org/10.1016/j.aquaculture.2005.11.031

Ellegren H. 2004. Microsatellites: simple sequences with complex evolution. Nat Rev Genet 5: 435–445. https://doi.org/10.1038/nrg1348

Getlekha N, Molina WF, Cioffi MB, Yano CF, Maneechot N, Bertollo LAC, Supiwong W, Tanomtong A. 2016. Repetitive DNAs highlight the role of chromosomal fusions in the karyotype evolution of *Dascyllus* species (Pomacentridae, Perciformes). Genetica 144(2): 203–211. https://doi.org/10.1007/s10709-016-9890-5

Howell WM, Black DA. 1980. Controlled silver-staining of nucleolus organizer regions with a protective colloidal developer: a 1-step method. Experientia 36: 1014–1015.

Kawai A, Ishijima J, Nishida C, Kosaka A, Ota H, Kohno S, Matsuda Y. 2009. The ZW sex chromosomes of *Gekko hokouensis* (Gekkonidae, Squamata) represent highly conservedhomology with those of avian species. Chromosoma 118: 43–51.

Kluge, A.G. 1968. Phylogenetic relationships of the gekkonid lizard genera *Lepidodactylus* Fitzinger, *Hemiphyllodactylus* Bleeker, and *Pseudogekko* Taylor. *Philippine Journal of Science*, 95: 331–352.

Kubat Z, Hobza R, Vyskot B, Kejnovsky E. 2008. Microsatellite accumulation in the Y chromosome of *Silene latifolia*. Genome 51: 350–356.

Lau MW, Ota H, Bogadek A. 1997. Chromosomes polymorphismand karyotype of *Gekko chinensis* (Tokaynidae: Reptilia) from Hong Kong. J Herpetol 31: 137–139.

Nirchio M, Turner BJ, Perez JE, Gaviria JI, Cequea H. 2002. Karyotypes of three species of toadfish (Batrachoididae: Teleostei) from Venezuela. Sci Mar 66(1): 1–4.

Ota H. 1989a. Karyotypes of five species of *Gekko* (Gekkonidae: Lacertilia) from East and Southeast Asia. Herpetologica 45 (4): 438-443.

Ota H. 1989b. A review of the geckos (Lacertilia: Reptilia) of the Ryukyu Archipelago and Taiwan. In: Matsui M, Hikida T, Goris RC. (eds.). Current Herpetology in East Asia. Herpetological Society of Japan, Kyoto.

Ota H, Hikida T, Matsui M, Mori A. 1990. Karyotype of *Gekko monarchus* (Squamata: Gekkonidae) from Sarawak, Malaysia. Japanese Journal of Herpetology 13: 136–138.

Ota H, Nabhitabhata J. 1991. A new species of *Gekko* (Gekkonidae: Squamata) from Thailand. Copeia 1991: 503–509.

Prasopsin S, Muanglen N, Ditcharoen S, Suwannapoom C, Tanomtong A, Thongnetr W. 2022. First Report on Classical and Molecular Cytogenetics of Doi Inthanon Bent-toed Gecko, *Cyrtodactylus inthanon* Kunya et al., 2015 (Squamata: Gekkonidae) in Thailand. Caryologia, 75(2): 109–117.

Patawang I, Tanomtong A, Jumrusthanasan S, Kakampuy W, Neeratanaphan L, Pinthong K. 2014. Chromosomal characteristics of NORs and karyological analysis of tokay gecko, Gekko gecko)Gekkonidae, Squamata) from mitotic and meiotic cell division. Cytologia 79(3): 315–324.

Patawang I, Prasopsin S, Suwannapoom C, Tanomtong A, Keawmad P, Thongnetr W. (2022). Chromosomal description of three Dixonius (Squamata, Gekkonidae) from Thailand. Caryologia, 75(2): 101–108.

Pinkel D, Straume T, Gray J. 1986. Cytogenetic analysis using quantitative, high sensitivity, fluorescence hybridization. Proceedings of the National Academy of Sciences of the United States of America 83: 2934–2938.

Qin XM, Li HM, Zeng ZH, Zeng DL, Guan QX. 2012. Genetic variation and differentiation of *Gekko gecko* from different populations based on mitochondrial cytochrome *b* gene sequences and karyotypes. Zoological Science 29: 384–389.

Russell AP. 1972. The Foot of Gekkonid Lizards: A Study in Comparative and Functional Anatomy. [Dissertation]. University of London, London.

Singh L. 1974. Study of mitotic and meiotic chromosomes in seven species of lizards. Proceedings of the Zoological Society 27: 57–79.

Solleder E, Schmid M. 1984. XX/XY sex chromosomes in *Gekko gecko* (Sauria, Reptilia). Amphibia-Reptilia 5: 339–345.

Srikulnath K, Uno Y, Nishida C, Ota H, Matsuda Y. 2015. Karyotype reorganization in the Hokou Gecko (*Gekko hokouensis*, Gekkonidae): The Process of Microchromosome Disappearance in Gekkota. PLoS ONE. DOI:10.1371/journal.pone.0134829

Shibaike Y, Takahashi Y, Arikura I, Iiizumi R, Kitakawa S, Sakai M, Imaoka C, Shiro H, Tanaka H, Akakubo N, Nakano M, Watanabe M, Ohne K, Kubota S, Kohno S, Ota H. 2009. Chromosome evolution in the lizard genus *Gekko* (Gekkonidae, Squamata, Reptilia) in the East Asian islands. Cytogenet Genome Res 127: 182–190.

Solleder E, Schmid M. 1984. XX/XY sex chromosomes in *Gekko gecko* (Sauria, Reptilia) amphibia-Reptilia 5: 339–345.

Tautz D, Renz M.1984. Simple sequences are ubiquitous repetitive components of eukaryotic genomes. Nucleic Acids Res 25: 4127–4138. https://doi. org/10.1093/nar/12.10.4127

Thongnetr W, Aiumsumang S, Tanomtong A, Phimphan S. 2022. Classical chromosome features and microsatellites repeat in *Gekko petricolus* (Reptilia, Gekkonidae) from Thailand. *Caryologia* 75(2): 81–88.

Trifonov VA, Giovannotti M, O'Brien PCM, Wallduck M, Lovell F, Rens W, Parise-Maltempi PP, Caputo V, Ferguson-Smith MA. 2011. Chromosomal evolution in Gekkonidae. I. Chromosome painting between *Gekko* and *Hemidactylus* species reveals phylogenetic relationships within the group. Chromosome Res 19: 843–855.

Turpin R, Lejeune J. 1965. Les Chromosomes Humains. Gauther Villars, Paris.

Wu G, Zhao E. 1984. Studies on karyotypes of *Gekko gecko* and *Gekko subpalmatus*. Acta Herpetologica Sinica 3: 61–64.

Yoshida M, Itoh M. 1974. Karyotype of the gecko, *Gekko japonicus*. Chromosome Information Service 17: 29–31.

Yüksel E, Gaffaroğlu M. 2008. The analysis of nucleolar organizer regions in *Chalcalburnus mossulensis* (Pisces: Cyprinidae). Journal of Fisheriessciences.com 2: 587–591.

Caryologia
International Journal of Cytology, Cytosystematics and Cytogenetics

Firenze University Press
www.fupress.com/caryologia

OPEN ACCESS

Citation: Narges Firoozi, Ghasem Karimzadeh, Mohammad Sadegh Sabet, Vahid Sayadi (2022). Intraspecific karyomorphological and genome size variations of *in vitro* embryo derived Iranian endemic Asafoetida (*Ferula assa-foetida* L., Apiaceae). *Caryologia* 75(4): 111-121. doi: 10.36253/caryologia-1721

Received: June 29, 2022

Accepted: December 06, 2022

Published: April 28, 2023

Data Availability Statement: All relevant data are within the paper and its Supporting Information files.

Competing Interests: The Author(s) declare(s) no conflict of interest.

Intraspecific karyomorphological and genome size variations of *in vitro* embryo derived Iranian endemic Asafoetida (*Ferula assa-foetida* L., Apiaceae)

Narges Firoozi, Ghasem Karimzadeh*, Mohammad Sadegh Sabet, Vahid Sayadi

Department of Plant Genetics and Breeding, College of Agriculture, Tarbiat Modares University, Tehran P. O. Box 14115-336, Iran
*Corresponding author. E-mail: karimzadeh_g@modares.ac.ir

Abstract. Asafoetida (*Ferula assa-foetida* L.) is one of the endemic medicinal plants in Iran. Analysis of karyomorphology and 2Cx DNA measurements (monoploid genome size) of 18 Iranian endemic *Ferula assa-foetida* populations were performed. The *in vitro* embryo-derived root tips were examined for karyological studies, via technique of squash and stain with 2% (w/v) aceto-orcein. Seeds of the *Ferula* samples and leaves of *Solanum lycopersicum* as standard reference (2C DNA = 1.96 pg) were stained with propidium iodide (PI), using flow cytometric (FCM) technique. All the studied populations were diploids ($2n = 2x = 22$) with mean chromosome length (CL) of 3.95 µm, varied from 3.05 µm (P7) to 4.94 µm (P18). The mean total chromosome volume (TCV) was 0.98 µm^3, ranged from 0.47 µm^3 (P7) to 1.57 µm^3 (P3). Two-typed chromosomes ("m", "sm") formed three classes of karyotype formula. Karyotypes were mostly symmetrical and fell in 1A and 2A Stebbins category. The monoploid genome size of Iranian endemic *Ferula assa-foetida* populations is being stated for the first time; its mean value was 4.51 pg, ranged from 4.09 (P4) to 4.69 pg (P16). Intraspecific karyomorphological and genome size variations were clearly confirmed in studied *Ferula assa-foetida*.

Keywords: Chromosome, *Ferula assa-foetida*, Flow cytometry, Karyotype, 2Cx DNA.

1. INTRODUCTION

Ferula assa-foetida belongs to Apiaceae family that grows in Iran, Kashmir in Pakistan, and Afghanistan. Asafoetida production from *Ferula assa-foetida* as a source is confined to southern Iran (Farhadi *et al.* 2019; Barzegar *et al.* 2020). Iranian flora consists of 30 species of *Ferula*, most of which are endemic (Khajeh *et al.* 2005; Farhadi *et al.* 2019). It is herbal and permanent and enlarges to 2 cm high (Khajeh *et al.* 2005). Apiaceae family had very low germination owing to seed dormancy (Nadjafi *et al.* 2006). Hence, the germination of *Ferula*'s seeds was complicated. To accelerate the breakage of

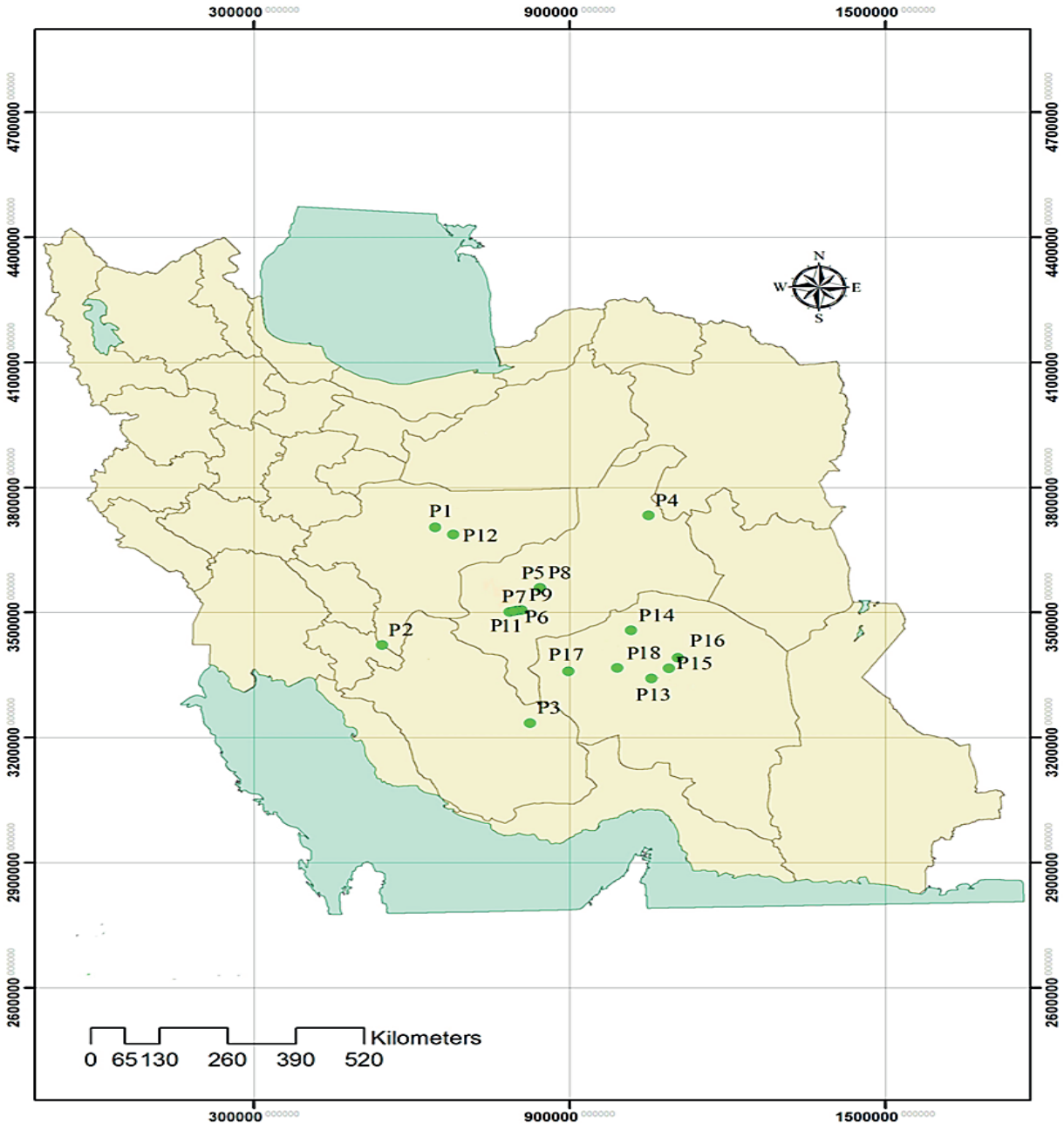

Figure 1. Geographic distribution of sampled *Ferula assa-feotida* L. on the map of Iran, using ArcGIS

its seed dormancy, various methods were applied such as soaking with running water and treating with either chilling temperature or GA_3 (Keshtkar *et al.* 2008; Hassani *et al.* 2009; Zare *et al.* 2011). The oleo-gum-resin has got from taking away of the stems or cut off the roots that have a sulfurous smell and bitter taste. *Ferula* species, due to its chemical compounds, play a useful role in the treatment of various diseases. The oleo-gum-resin is antiseptic, antifungal, antibiotic, laxative, indigestion, antiviral, antidiabetic whooping cough, cramp, infertilitypain, and cancer chemopreventive (Aruna and Sivaramakrishnan 1992; Dehpour *et al.* 2009; Lee *et al.* 2009). The attribute properties of these plants have sesquiterpene coumarins and e few monoterpenes (El-Razek *et al.* 2001). Terpene coumarins have anti-HIV activity (Zhou *et al.* 2000). In plant sciences, for a large number of plants in order to DNA content's screening is used of flow cytometry (FCM) as a powerful and reli-

Table 1. Local information of the collected Iranian endemic *Ferula assa-foetida* L.

Mean rainfall (mm)	Mean Temp (°C)	Altitude (m)	Longitude (E)	Latitude (N)	Local collection locations	Population code
13.66	20.20	1817	52° 33' 00.0"	33° 27' 54.0"	Esfahan, Iran	P1
60.52	15.25	2750	51° 26' 55.3"	30° 55' 49.9"	Kohkiloyeh Boyerahmad, Iran	P2
15.87	20.82	1795	54° 20' 00.0"	29° 12' 00.0"	Fars, Iran	P3
5.54	22.91	669	56° 55' 50.6"	33° 35' 39.1"	Khorasan, Iran	P4
4.32	20.42	2158	54° 38' 23.8"	32° 06' 43.4"	Yazd, Iran	P5
5.08	20.54	1720	54° 09' 53.6"	31° 38' 13.4"	Yazd, Iran	P6
5.08	20.54	831	55° 38' 20.4"	33° 06' 43.2"	Yazd, Iran	P7
4.32	20.42	2158	54° 38' 23.6"	32° 06' 43.4"	Yazd, Iran	P8
5.08	20.54	1950	54° 14' 42.5"	31° 38' 41.7"	Yazd, Iran	P9
5.08	20.54	2160	54° 09' 53.6"	31° 38' 13.5"	Yazd, Iran	P10
5.08	20.54	3279	54° 05' 27.0"	31° 37' 41.2"	Yazd, Iran	P11
9.04	20.00	2164	57° 54' 50.4"	29° 18' 10.8"	Kerman, Iran	P12
12.05	17.07	2000	56° 45' 00.0"	30° 48' 00.0"	Kerman, Iran	P13
9.04	20.00	2200	56° 25' 00.0"	31° 08' 00.0"	Kerman, Iran	P14
12.05	17.07	1900	57° 07' 00.0"	30° 17' 00.0"	Kerman, Iran	P15
4.05	21.05	2600	57° 18' 00.0"	30° 30' 00.0"	Kerman, Iran	P16
11.49	16.67	1850	55° 07' 57.0"	30° 17' 40.0"	Kerman, Iran	P17
7.04	19.23	2335	56° 60' 00.0"	30° 20' 20.4"	Kerman, Iran	P18

able technique (e.g., Loureiro *et al*. 2005; Mahdavi and Karimzadeh 2010; Karimzadeh *et al*. 2010, 2011; Abedi *et al*. 2015; Tarkesh Esfahani *et al*. 2020; Zarabizadeh *et al*., 2022). It mainly focused on cell cycle analysis, measurement of nuclear DNA content, and determination of ploidy level. It can be used to determine monoploid and holoploid genome size (Doležel *et al*. 2003, 2007; Greilhuber *et al*. 2005(. Furthermore, in plant systematics and plant breeding, karyotypes can make available evidence and data for species identification and the study of populations resulting from a cross between individuals (Anjali and Srivastava 2012). In a study on *Ferula assa-foetida*, it was found that this plant is diploid with a chromosome number 22, grouping in 2A class according to Stebbins classification (Zhao *et al*. 2006). Likewise, the same chromosome number of 22 was reported by El-Alaoui-Faris *et al*. (2006) in five different species of *Ferula*; *F. gouliminensis, F. cossoniana, F. tingitana, F. sauvagei,* and *F. atlantica*. Furthermore, in a study conducted in China on two species of *F. liacentiana* and *F. bungeana*, the 22-chromosome number was also reported (Qixin and Menglan, 1993). It is significant to note that some studies and reports on *F. assa-foetida* in outside of its native range have mistakenly identified the species. In other words, some species that produce asafoetida are often misidentified as *F. assa-foetida* (Chamberlain, 1977). Awareness of genetic diversity and the management of genetic resources are considered as the main parts of plant breeding programs. The first step in plant breeding is to understand the genome structure and the germplasm collection (Lee *et al*. 2021). Taken together, these situations indicate the need for basic investigations especially cytogenetic studies. The key aim of the current survey was to study intraspecific genome size and karyo-morphological variations among 18 *F. assa-foetida* populations of Iran.

2. MATERIALS AND METHODS

Seeds of 18 Iranian endemic populations of *Ferula assa-foetida* L. were used for this study. The germplasm collection of the Iranian Biological and Resource Center (IBRC), Tehran, Iran from where the seeds were obtained. Geographical description, climatic information, the population codes used in this study and the gene bank codes are present in Table 1. Since previously reported methods, including chilling temperature and treating $GA_{3,}$ was not satisfactory to achieve good germination, hence, *in vitro* embryo culture was the best, and the most suitable technique (Zare *et al*. 2011; Suran *et al*. 2016).

2.1. In vitro embryo culture

At first, seeds were soaked in running water for 24 h sterilized as follows:

- Wash the seeds with five drops of washing liquid for 2 min.
- Seeds placement under running water for 5 min.
- Seeds placement in ethanol 70% for 2 min.
- Wash seeds with distilled water for 5 min.
- Seeds placement in sodium hypochlorite 5.25 (v/v) for 20 min.
- Wash seeds with dsH_2O three times and each time for 2 min in laminar airflow.

After this step, the embryos were excised by push the bottom of seeds and were transferred to Murashige and Skoog medium (Murashige and Skoog 1962). The embryos in Petri dishes were placed in an incubator at photoperiod with a 16 h light/8 h dark and 25 °C. It was germinated after three to four days.

2.2. Karyomorphological analysis

For the preparations of karyology, actively around one cm-long *in vitro* growing roots were removed and pre-treated in colchicine (0.05% (w/v)) for 4 h in the dark at 4 °C to impel metaphase arrest. After that, the roots were subsequently fixed in freshly Carnoy's fixative (3 absolute ethanol: 1 glacial acetic acid (v/v) ratio) at 4 °C for 24 h (Karimzadeh *et al.* 2010, 2011). Using distilled water, the fixed roots were washed then in a water bath its hydrolyzed in 1M Hydrochloric acid (HCl) for 10 min at 60 °C, after these steps, staining was performed for 3 h with aceto-orcein (2% (w/v)) at 25 °C (Karimzadeh *et al.* 2011). The five well-expand monolayer metaphase plates from various individuals were examined per *Ferula assa-foetida* populations. Photographs were taken in high resolution via a light microscope (BX50 model, Olympus Optical Co., Ltd., Tokyo, Japan) armed with an digital camera (DP12, Olympus Optical Co., Tokyo, Japan).

Eight chromosomal parameters were either investigated as short arm (S) and long arm (L) lengths, or measured as chromosome length (CL = L + S), r-value (S/L), arm ratio (AR; L/S), total chromosome volume (TCV = πr^2 CL, where r = average chromosome radius), form percentage (F% = S/SCL), and centromeric index (CI = S/CL). Chromosome types were determined, via Levan *et al.* (1964) formula and Idiograms were drawn from the mean values. The following parameters were also assessed for analysis karyotype asymmetry: the difference of range relative length ($RL\%_{Max}$ - $RL\%_{Min}$), karyotype total form percentage (TF% = $\Sigma S/\Sigma CL \times 100$), dispersion index (DI = (Mean CI × CV_{CL}) /100), mean centromeric asymmetry (M_{CA}), coefficient of variation of chromosome length (CV_{CL}) (Paszko 2006; Peruzzi *et al.* 2009), Romero-Zarco (1986) intrachromosomal (A1) and interchromosomal (A2) asymmetry indices; and Stebbins asymmetry categories for the investigation of karyotype asymmetry were assessed (Stebbins 1971).

2.3. Flow cytometric analysis

For each Asafetida population, the monoploid 2Cx-value was calculated through Flow cytometric analysis. Hence, to prepare nuclear suspensions, four seeds (Jedrzejczyk and Sliwinska, 2010) of each Asafetida sample along with the healthy fresh young leaves of *Solanum lycopersicum* cv. Stupicke (2C DNA = 1.96 pg; Doležel et al., 2007) as the internal reference standard plant were chopped with a sharp razor blade in ice-cold woody plant buffer (WPB, Loureiro et al., 2007). Flow cytometric analysis was carried out via PI (Propidium Iodide) staining method. The nuclei suspension was examined via the flow cytometer (BD FACSCanto II, BD Biosciences, Bedford, MA, USA), through BD FACSDiva™ Software. The gained data were transferred to Flowing Software (ver. 2.5.0, Cell Imaging Core, Turku Centre for Biotechnology) to be editable in Partec FloMax software (ver. 2.4e, Partec, Münster, Germany). The range of gating zone was calculated on obtained histograms from FCM, via the FloMax. Healthy fresh young leaves of the Asafetida sample's seeds and the standard reference were chopped, using a sharp razor blade. this action performed in ice-cold nuclear extraction buffer WPB (Woody Plant Buffer, Loureiro *et al.* 2007). The chopped seeds and leaves were filtered via a 30 µm green nylon mesh (Partec, Münster, Germany). One ml of staining buffer, 50 µg ml^{-1} of PI (Fluka) solution and 50 µg ml^{-1} of RNase (Sigma-Aldrich Corporation, MO, USA) stock solution were added to each sample. For the stained nuclei, the relative fluorescence intensity was calculated via FCM on a linear scale. For each sample, flow cytometrically minimum 5000 nuclei were evaluated. The values of the means of G1 peak were used to estimate the absolute DNA amount of the sample (Doležel *et al.* 2003, 2007; Greilhuber *et al.* 2005; Doležel and Bartoš 2005; Mahdavi and Karimzadeh 2010; Karimzadeh *et al.* 2011) as follows:

Sample $2C_X$ DNA (pg) = (Sample G1 peak mean/Standard G1 peak mean) × Standard 2C DNA (pg).

Monoploid genome size was estimated based on above converting formula in the form of base pair (Doležel et al. 2003). It should be noted that one pg of DNA equivalent to 978 mega base pairs (Mbp) were considered (Doležel et al. 2003).

2.4. Statistical analysis

In First normality test was carried out for the obtained data from karyotypic and flow cytometric studies and then were investigated for karyological data in five replications and for nuclear DNA content three replications based on a completely randomized design (CRD). Differences between means were measured through the least significant difference (LSD). Minitab 17 software package was used for multivariate statistical analysis. principal components analysis (PCA) was then carried out based on data matrix to evaluate the contribution of each karyotypic parameter to the ordination of populations. A cluster analysis on chromosomal parameters was carried out, through the Ward's method and the Euclidean distance to assess similarities and variations amid the populations.

3. RESULTS

All 18 Iranian endemic populations of *Ferula assa-foetida* were diploid ($2n = 2x = 22$). Obtained karyotypes from somatic complement and the haploid complement's idiograms of studies *F. assa-foetida* populations are demonstrated in figures 2 and 3, respectively. Based on the *ANOVA* results, among populations for either all chromosomal parameters, or monoploid genome size were significant differences ($P < 0.01$; 2Cx DNA; Table 2). The mean chromosome length (CL) was determined as 3.95 µm, varied from 3.05 µm (P7) to 4.94 µm (P18). The mean CI of the complement, varied from 41.15% (P18) to 45.57% (P1). The mean TCV was 0.98 μm^3, ranged from 0.47 μm^3 (P7) to 1.57 μm^3 (P3). According to numerous karyotypic symmetrical indices tested, *F. assa-foetida* populations indicated various symmetrical clusters. The maximum value of TF% was recognized in P1 (45.3%) and the lowest value was identified in P14 (41.3%). The uppermost and the lowermost values of the various range of relative length (DRL) were detected in P8 (4.79%; the most asymmetric) and P1 (2.25%; the most symmetric), respectively. The highest and lowest values of CV_{CL} %were identified in P8 (15.53%; the maximum asymmetric) and P1 (7.17%; the maximum symmetric), respectively. Similar to the results of DRL and

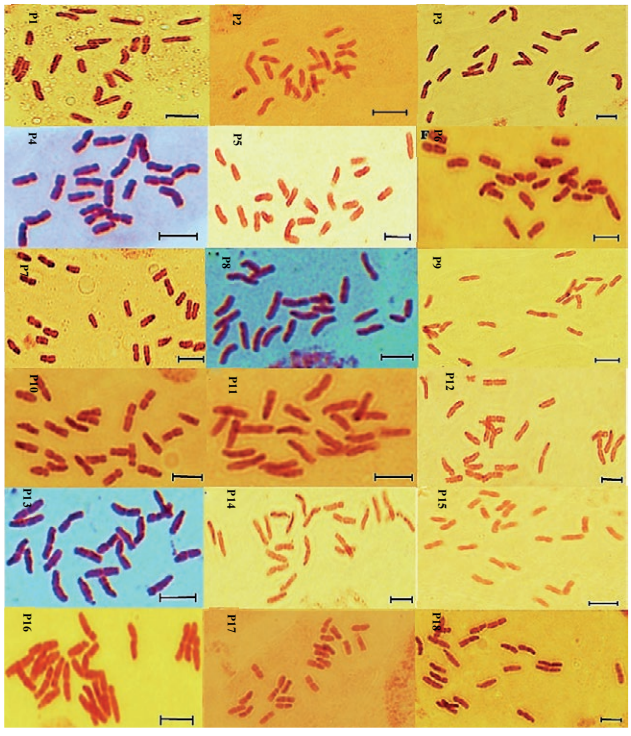

Figure 2. Karyotypes of somatic chromosome complement of 18 Iranian endemic *Ferula assa-foetida* L. ($n = 2x = 22$) populations. Scale bars = 5 µm.

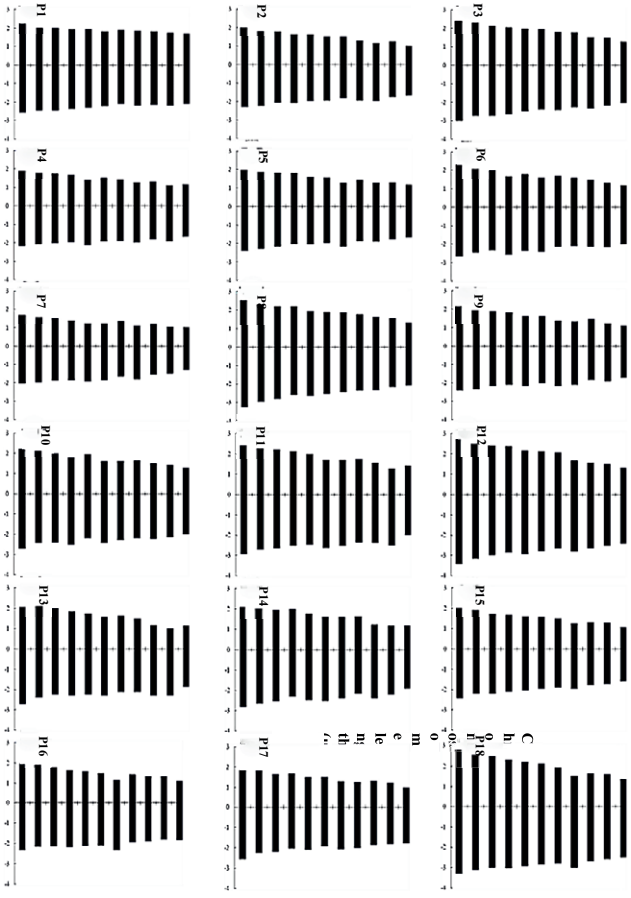

Figure 3. Idiograms of haploid chromosome complement of 18 Iranian endemic *Ferula assa-foetida* L. ($2n = 2x = 22$) populations.

Table 2. *ANOVA* of chromosomal parameters (a) and monoploid genome size (2Cx DNA; b) of *Ferula assa-foetida* L.

S.O.V.	Df	MS							
		S	L	CL	AR	r-value	F%	TCV	CI
a) Chromosomal parameters									
Population	17	12.58**	0.19**	0.18**	2.35**	2.42**	1.85**	20.12**	2.32**
Error	972	0.79	0.005	0.005	0.97	0.97	0.98	0.66	0.97
b) Monoploid genome size (2Cx DNA)									
S.O.V.	Df	2Cx DNA							
Population	17	0.066**							
Error	36	0.004							

** Significant difference ($P < 0.01$).

Table 3. Karyotypic parameters of *Ferula assa-foetida* L. ($2n = 2x = 22$).

Populations	Stebbins' category	Karyotype formula	CV_{CL}%	DI	DRL%	TF%	M_{CA}	Asymmetry Indices (Romero-Zarco, 1986)	
								A_2	A_1
P1	1A	22m	7.17	0.03	2.25	45.30	9.00	0.07	0.16
P2	1A	20m+2sm	13.78	0.06	4.21	43.54	14.11	0.14	0.23
P3	1A	22m	14.45	0.06	4.40	43.34	14.26	0.14	0.24
P4	1A	20m+2sm	10.88	0.05	3.27	43.26	14.24	0.11	0.24
P5	1A	22m	13.16	0.06	3.89	43.21	13.48	0.13	0.23
P6	1A	22m	12.79	0.05	4.03	42.61	15.58	0.13	0.26
P7	1A	22m	14.01	0.06	4.29	42.97	14.92	0.14	0.24
P8	1A	22m	15.53	0.07	4.79	42.95	14.34	0.16	0.24
P9	1A	22m	13.71	0.06	4.22	43.05	14.05	0.14	0.23
P10	1A	22m	11.65	0.05	3.65	42.67	14.89	0.12	0.25
P11	1A	20m+2sm	12.86	0.05	3.99	43.06	15.31	0.13	0.25
P12	1A	20m+2sm	14.94	0.06	4.48	41.78	17.14	0.15	0.27
P13	2A	18m+4sm	13.78	0.06	4.24	41.50	17.59	0.14	0.28
P14	1A	18m+4sm	13.73	0.06	4.07	41.31	18.75	0.14	0.30
P15	1A	22m	14.94	0.06	4.62	42.67	13.03	0.15	0.22
P16	2A	20m+2sm	11.67	0.05	3.43	42.58	16.06	0.12	0.26
P17	1A	20m+2sm	13.37	0.06	4.12	41.39	17.25	0.13	0.28
P18	1A	18m+4sm	13.92	0.06	4.10	41.67	17.69	0.14	0.29

CV_{CL}%, the highest value of dispersion index (DI) was detected in P8 (0.07; the most asymmetric), while P1 displayed the lowest (0.03; the most symmetric). In conclusion, three (DRL, CV_{CL}% and DI) among five karyotypic symmetrical indices examined, confirmed that all 18 *F. assa-foetida* populations examined P8 and P1 performed to have the most asymmetrical and symmetrical karyotypes, respectively. The highest value of M_{CA} was identified in P14 (18.75 %) while P1 demonstrated the lowest value (9.1 %). Two-typed chromosomes were recognized in all populations by using Levan *et al.* (1964) chromosome nomenclature: "m" (centromere at medium region) and "sm" (centromere at sub medium region); formed 3 different karyotypic formulas as follows: 22m (nine populations), 20m+2sm (six populations) and 18m+4sm (three populations; Table 3). Karyotypes of all populations were ordered in the 1A and 2A classes of Stebbins classification (Stebbins 1971). For further detailed studies of asymmetry, A_1 and A_2 indices were also calculated (Romero-Zarco, 1986). The highest $A_1 = 0.30$ was found in P14, showing the highest inter chromosomal difference, resulted in asymmetric karyotype and the lowest $A_1 = 0.16$ is related to the P1 which demonstrations the highest symmetry. The highest $A_2 = 0.16$ was related to

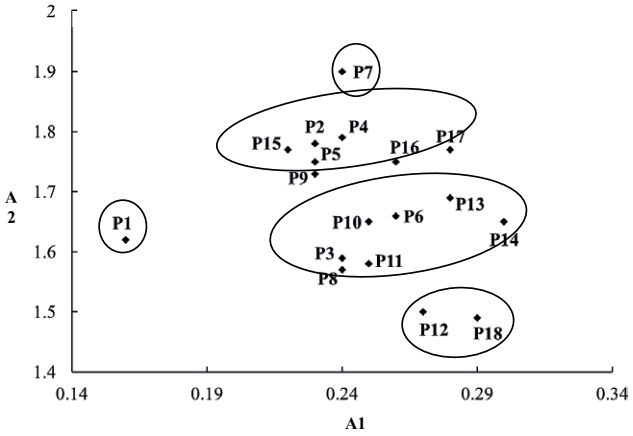

Figure 4. Scatter plot of intrachromosomal (A1) and interchromosomal (A2) asymmetries of 18 Iranian *Ferula assa-foetida* L. populations

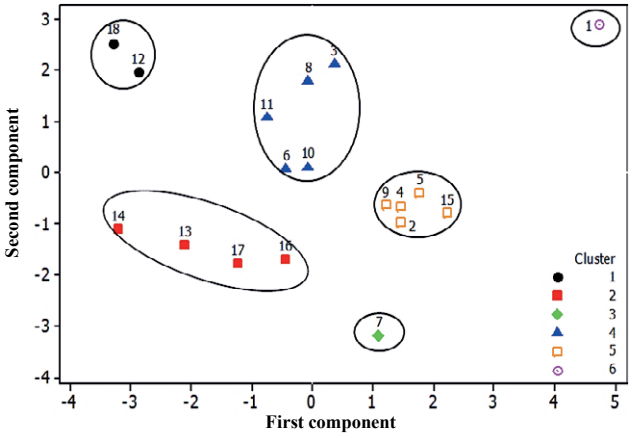

Figure 5. Diagram resulting from principal components analysis (PCA) of *Ferula assa-foetida* L. populations.

P8; they have the highest chromosomal asymmetry and the lowest $A_2 = 0.07$ was related to P1, having the highest intra chromosomal symmetry (Table 3).

The scatter diagram of these indices (Figure 4) shows five groups of populations. The principal component analysis of the karyotypic parameters was carried out to estimate total variation and its parameters quota in populations. The PCA representing that the first three principal components account for 99% of the cumulative variation, and they were plotted in a 2-dimensional graphic (Figure 5). The Ward (Khodadadi *et al.* 2014) phenogram constructed based on karyotype similarities (Figure 6) shows six major clusters. The principal component analysis resulting populations arrangement from this exam entirely fits with that obtained with the Ward grouping analysis. Thus, the obtained results suggested

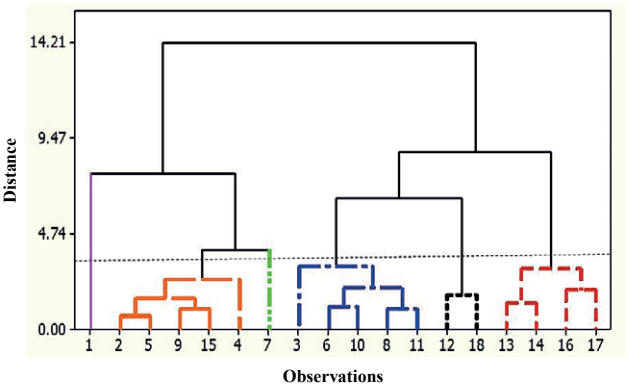

Figure 6. Dendrogram showing the phenetic relationships among the studied populations of *Ferula assa-foetida* L. populations.

Table 4. Mean (± Se) comparisons of monoploid genome size (2Cx DNA) of Iranian endemic *Ferula assa-foetida* L. ($2n = 2x = 22$).

1Cx DNA (Mbp)	1Cx DNA (pg)	Mean 2Cx DNA (pg) ± Se	Population
2166.27	2.215	4.43 ± 0.075^{efg}	P1
2146.71	2.195	4.39 ± 0.047^{fg}	P2
2122.26	2.170	4.34 ± 0.006^{g}	P3
2000.01	2.045	4.09 ± 0.042^{h}	P4
2210.28	2.260	4.52 ± 0.036^{bcde}	P5
2185.83	2.235	4.47 ± 0.010^{def}	P6
2259.18	2.310	4.62 ± 0.035^{ab}	P7
2176.05	2.225	4.45 ± 0.049^{defg}	P8
2244.51	2.295	4.59 ± 0.012^{abc}	P9
2273.85	2.325	4.65 ± 0.015^{a}	P10
2190.72	2.240	4.48 ± 0.060^{cdef}	P11
2176.05	2.225	4.45 ± 0.025^{defg}	P12
2234.73	2.285	4.57 ± 0.019^{abcd}	P13
2229.40	2.280	4.60 ± 0.038^{abc}	P14
2244.51	2.295	4.59 ± 0.026^{abc}	P15
2293.41	2.345	4.69 ± 0.030^{a}	P16
2283.63	2.335	4.67 ± 0.019^{a}	P17
2268.96	2.320	4.64 ± 0.056^{ab}	P18
2000.01-2293.41	2.045-2.345	4.09-4.69	Range

Means with the same symbol letter in a "Mean 2Cx DNA (pg)" column are not significantly different ($P > 0.01$), using LSD test.

that populations within one cluster, having the high homology in chromosomal differences.

The result of FCM data was confirmed for normality and analyzed based on completely randomized design (CRD) with three replicate cells. *ANOVA* showed among- populations high significant difference ($P < 0.01$) for monoploid genome size (2Cx DNA content; Table 2). The mean value was 4.51 pg (Table 4), varied from 4.09 pg in P4 to 4.69 pg in P16. The histograms obtained for

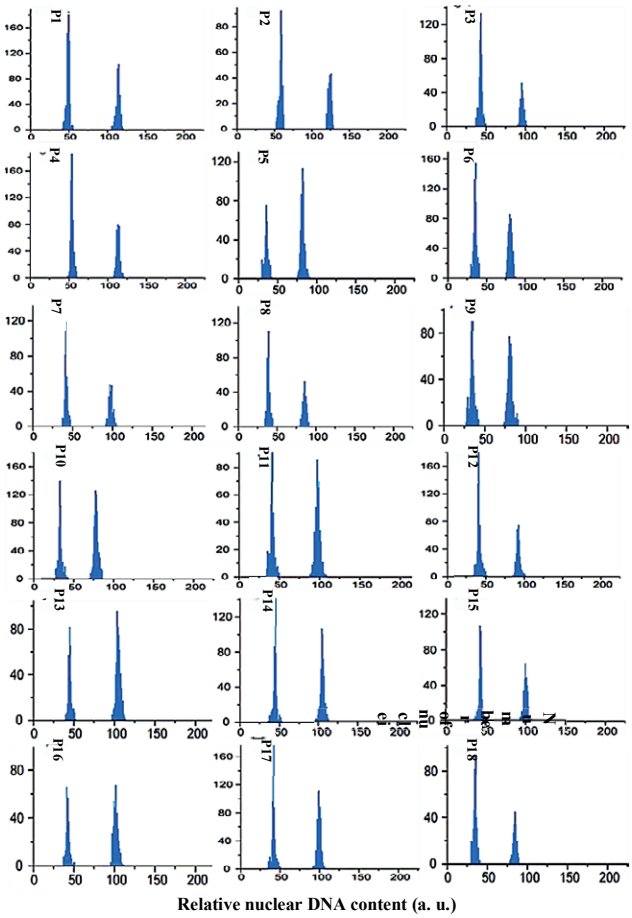

Figure 7. Flow cytometric histograms of monoploid genome size (2Cx DNA (of 18 Iranian endemic *Ferula assa-foetida* L. populations. The left peaks refer to G1 of the *Solanum lycopersicum* cv. Stupicke (2C DNA = 1.96 pg) reference standard and the right peaks refer to G1 of *Ferula assa-foetida* L. samples.

analyzing nuclear DNA amount included two peaks (Figure 7): the left peaks refer to the G1 of *Solanum lycopersicum* cv. Stupicke as reference standard plant (Doležel *et al.* 2007) and the right peaks to the G1 of *F. assa-foetida* samples. In other words, using 1Cx DNA monoploid genome size in Mbp, the mean value of all populations was 2205.39 Mbp (Table 4).

4. DISCUSSION

Ferula assa-foetida belongs to Apiaceae family includes about 170 identified taxa, of which 30 species have been detected in different phytogeographical regions in Iran (Zomorodian *et al.*, 2018). It is an important perennial herb with medicinal benefits which is native to central Asia and Iran *(*Farhadi *et al.* 2019*).* Many pharmaceutical properties and medical benefits had been reported for Ferula (Dehpour *et al.* 2009; Lee *et al.* 2009). For increasing the potential applicability of this genus, this perennial plant still needs more investigation on the genetic variability, expanding the range of research on its genetic characteristics as well as develop breeding methods.

In the current study, we studied the Iranian endemic *Ferula assa-foetida* populations. Eighteen Iranian endemic populations of Asafoetida (*F. assa-foetida* L.) were cytogenetically assessed on the basis of karyomorphology and genome size in the current study; they were all diploids ($2n = 2x = 22$). Mostly, in *Ferula* genera the diploids are more frequent and obtained results in the present study are in agreement with those reported on *Ferula assa-foetida* (Zhao *et al.* 2006) and on other species of *Ferula* (Wanscher 1931; Qixin and Menglan 1993; Ghaffari *et al.* 2005; El-Alaoui-Faris *et al.* 2006; Sağiroğlu and Duman 2006; Bernard *et al.* 2007). The obtained results of *ANOVA* show a significant difference in terms of all chromosomal traits. (Table 2), confirming intraspecific karyomorphological diversity in the studied Iranian endemic Asafoetida populations, which would be beneficial for the success of the breeding programs. The mean chromosome length (CL) was 3.95 µm, varied from 3.05 µm (P7) to 4.94 µm (P18). In other words, a remarkable 1.89 µm variation in chromosome size was detectable among such a number of examined Iranian endemic Asafoetida. In the present investigation two-typed chromosomes ("m", "sm") formed three classes of karyotype formula, comprised: 22m for nine populations (P1, P3, P5- P10, P15), 20m+2sm for six populations (P2, P4, P11, P12, P16, P17(, and 18m+4sm for three populations (P13, P14, P18). Zhao *et al.* (2006), studying on *Ferula fukanensis*, similarly reported the two-typed chromosomes of "m" and "sm". The studied karyotypes were grouped in the 1A and 2A classes based on classification of Stebbins. In a study on *Ferula fukanensis*, karyotypes were classified as 2A (Zhao *et al.* 2006), which was consistent with the results of the current study in the P13 and P16 populations. It has been alleged that symmetric karyotypes have a lower grade of evolution in comparison with asymmetric karyotypes (Stebbins 1971). Understanding taxon evolution, and interrelations are facilitated through the information obtained from karyotype, and chromosome morphology (Furo *et al.* 2020; Sayadi *et al.* 2021). In the current investigation, the scatter diagram shown the populations in five groups that exactly fits with the principal component analysis resulting species arrangement. Furthermore, the results noted that populations inside a cluster have the maximum homology of chromosomes. According to

karyotypes studies, the most fertile offspring can be produced by crossing the populations having the maximum chromosomal homology. The results of principal component analysis, and cluster analysis for the chromosomal traits, it is possible to introduce populations in groups 2 and 3 due to the shortest distance, to intersect and produce maximum fertile offspring. Accordingly, crossing between populations in a cluster is recommended, for instance between P13 with P14, P16, or P17, and also P12 with P18. The karyotypes in the primitive species are usually highly symmetrical, but that is not necessarily the case. In other words, a distinct and more evidence is ever required to evaluate the direction in changes of karyotype (Peruzzi and Eroğlu 2013). It has been noted that the evolutionary relationships via asymmetry indices usage for the establishment may not be straightforward. It can be stated that the genus diversity may have resulted from the structural changes. Some differences in asymmetry indices and karyotype formula between species may have contributed to this diversity (Seijo and Fernandez 2003).

As stated in the Stebbins (1971) classification, the karyotypes were mostly symmetric (Table 3). In the present study, to achieve greater measurement accuracy, additional parameters were also assessed in addition to Stebbins asymmetry categories, including TF%, DI, CV_{CL}, M_{CA}, A_1, and A_2 asymmetry indices for karyotype asymmetry analysis (Table 3). Some have argued and suggested that Stebbins' (1971) classification as a qualitative method is not so strong and lower flexible regarding the types of conclusions it can provide (Paszko, 2006). The average of DI% was 5.6% (from 3% in P1 to 7% in P7). All of the populations were symmetric based on TF% parameter, that the mean value was 42.71%, ranging from 41.3% (P14) to 45.3% (P1). Some chromosomal disorders are probably a factor of gradual changes in the amounts of TF%. The appearance changes in the chromosomes morphology were happens due to the various causes such as translocated or duplicated chromosomes (Das *et al*. 1998). When the populations are similar in Stebbins classification, estimates A1 and A2 parameters of Romero-Zarco (1986) to determine the further asymmetric karyotype are necessary. As A1 index gets lower in P1 represents karyotype symmetry and a higher value in P14 assessed greater asymmetry. The A_2 parameter was 13.22%, ranging from 7% (P1) to 16% (P8). Preventing interspecific cross accomplishment and offspring infertility may have ensued from the difference in resulting karyotype symmetry.

Obvious intraspecific diversity was also detected in terms of monoploid genome size (2Cx DNA) among examined Iranian endemic Asafoetida populations. Hence, on the other hand, the 2Cx DNA amounts of 18 Iranian endemic *F. assa-foetida* L. populations are being reported for the first time, having the mean value of 4.51 pg, varied from 4.09 (P4) to 4.69 pg (P16). In other words, in our knowledge, few reports were found in the literature for the genome size estimation even in other *Ferula* species. For example, 2.90 pg was reported for 2C DNA amount of *F. communis* by Olmedilla *et al*.)1985) and 4.92 pg in *F. heuffelii* by Siljak-Yakovlev *et al*. (2010). Changes in the genome size (increases or decreases) may have participated in the genus diversity and evolution (Seijo and Fernandez 2003). Cytogenetical investigations as a valuable method have been Significantly performed in phylogenetic relationships amongst plants; and its obtained information has been of appreciable value in understanding taxon evolution and interrelations. These results may provide relevant information for *F. assa-foetida* L. breeding studies.

ACKNOWLEDGEMENT

Authors gratefully thank Tarbiat Modares University, Tehran, Iran, for their support to the study.

AUTHOR CONTRIBUTION

N. Firoozi carried out the experiments under the supervision of Prof. G. Karimzadeh and the advisory of Assist. Prof. M. S. Sabet. The manuscript prepared and revised by V. Sayadi. All authors approved the final manuscript.

This research did not receive any specific grant from funding agencies in the public, commercial, or not-for-profit sectors.

REFERENCES

Abedi R, Babaei A, and Karimzadeh G. 2015. Karyological and flow cytometric studies of *Tulipa* (Liliaceae) species from Iran. Plant Syst. Evol. 301(5): 1473-1484.

Aruna K, and Sivaramakrishnan V.M. 1992**.** Anticarcinogenic effects of some Indian plant products. Food Chem. Toxicol. **30(11)**: 953-956.

Anjali M, and Srivastava A.K. 2012**.** Karyological studies in twelve accessions of *Carthamus tinctoriusi*. Caryologia. **65(1)**: 1-6.

Barzegar A, Salim M.A, Badr P, Khosravi A, Hemmati Sh *et al.* 2020. Persian asafoetida vs. sagapenum: chal-

lenges and opportunities. Res. j. pharmacogn. **7 (2)**: 71-80.

Bernard F, Bazarnov H.S, Khatab L.J, Darabi A.S and Sheidai M. 2007. *Ferula gummosa* Boiss. Embryogenic Culture and Karyological Changes. Pak. J. Biol. Sci. **10(12)**: 1977-1983.

Chamberlain David F. 1977. The identity of *Ferula assa-foetida* L. Notes from the Royal Botanic Garden, Edinburgh. **35** (2): 229–233.

Das A.K, Cohen P.T. and Barford D. 1998. The structure of the tetratricopeptide repeats of protein phosphatase 5: implications for TPR-mediated protein-protein interactions. EMBO J. **17(5)**: 1192-1199.

Dehpour A.A, Ebrahimzadeh M.A, Seyed Fazel N, and Seyed Mohammad N. 2009. Antioxidant activity of the methanol extract of *Ferula assafoetida* and its essential oil composition. Grasas y Aceites. **60(4)**: 405-412.

Doležel J, and Bartoš J. 2005. Plant DNA flow cytometry and estimation of nuclear genome size. Ann. Bot. **95**: 99-110.

Doležel J, Bartoš J, Voglmayr H, and Greilhuber J. 2003. Nuclear DNA content and genome size of trout and human. Cytometry. **51**: 127-129.

Doležel J, Greilhuber J, and Suda J. 2007. Flow Cytometry with Plant Cells: Analysis of Genes, Chromosome and Genomes. Weinheim: Wiley-VCH Verlag GmbH & Co., Germany.

El-Alaoui-Faris F.E, Cauwet-Marc A.M, and Cauwet-Marc A.M. 2006. Nombre chromosomique de quelques espèces de férules marocaines (Ferula, Apiaceae). Flora Mediterr. **16**: 341-354.

El-Razek M.H.A, Ohta S, Ahmed A.A, and Hirata T. 2001. Monoterpene coumarins from the roots of *Ferula assa-foetida*. Phytochemistry. **58**: 1289-1295.

Furo I.O, Kretschmer R.O, Brien P.C.M, Pereira J, Ferguson-Smith M.A *et al.* 2020. Phylogenetic analysis and karyotype evolution in two species of core Gruiformes: *Aramides cajaneus* and *Psophia viridis*. Genes. **11(3)**: 307.

Farhadi F, Asili J, Iranshahy M, Iranshahi M. 2019. NMR-based metabolomic study of Asafoetida". Fitoterapia. **139**: 104361.

Ghaffari S.M, Hejazi A, and Pourahmad A. 2005. New chromosome counts in nine endemic species from Iran. Folia Geobot. **40(4)**: 435-440.

Greilhuber J, Doležel J, Lysák M.A, and Bennett M.D. 2005. The origin, evolution and proposed stabilization of the terms 'genome size' and 'C-value' to describe nuclear DNA contents. Ann. Bot. 95: 255-260.

Hassani S.B, Saboora A, Radjabian T, and Fallah Husseini H. 2009. Effects of temperature, GA_3, and cytokinins on breaking seed dormancy of *Ferula assa-foetida*. Iran J Sci Technol Trans A Sci. **33(1)**: 75-85.

Iranshahy M. and Iranshahy M. 2011. Traditional uses, phytochemistry and pharmacology of asafetida (*Ferula asafetida* oleo-gum-resin). J. Ethnopharmacol. **134**: 1-10.

Javadian N, Karimzadeh G, Sharifi M, Moieni A, and Behmanesh M. 2017. *In vitro* polyploidy induction: changes in morphology, podophyllotoxin biosynthesis, and expression of the related genes in *Linum album* (Linaceae). Planta. **245(6)**: 1165-1178.

Jedrzejczyk I. and Sliwinska E. 2010. Leaves and seeds as materials for flow cytometric estimation of the genome size of 11 Rosaceae woody species containing DNA-staining inhibitors. J. Bot. 2010: 1-9.

Karimzadeh G, Danesh-Gilevaei M, and Aghaalikhani M. 2011. Karyotypic and nuclear DNA variations in *Lathyrus sativus* (Fabaceae). Caryologia. **64(1)**: 42-54.

Karimzadeh G, Mousavi S.H, Jafarkhani-Kermani M, and Jalali-Javaran M. 2010. Karyological and nuclear DNA variation in Iranian endemic muskmelon (*Cucumis melo* var. inodorus). Cytologia. **75(4)**: 451-461.

Keshtkar H.R, Azarnivand H, Etemad V, and Moosavi S.S. 2008. Seed dormancy-breaking and germination requirements of *Ferula ovina* and *Ferula gummosa*. Desert. **13(1)**: 45-51.

Khajeh M, Yamini Y, Bahramifar N, Sefidkon F, and Pirmoradei M.R. 2005. Comparison of essential oils compositions of *Ferula assa-foetida* obtained by supercritical carbon dioxide extraction and hydrodistillation methods. Food Chem. **91**: 639-644.

Khodadadi M, Dehghani H, and Fotokian M.H. 2014. Genetic diversity of wheat grain quality and determination the best clustering technique and type for diversity assessment. Genetika. **46(3)**: 763-774.

Lee K.J, Sebastin R, Cho G.T, Yoon M, Lee G.A *et al.* 2021. Genetic diversity and population structure of potato germplasm in RDA-Genebank: utilization for breeding and conservation. Plants. **10(4)**: 752.

Lee C.L, Chiang L.C, Cheng L.H, Liaw C.C, Abd El-Razek M.H *et al.* 2009. Influenza A (H1N1) antiviral and cytotoxic agents from *Ferula assa-foetida*. J. Nat. Prod. **72(9)**: 1568-1572.

Levan A, Fredga K, and Sandberg A. 1964. Nomenculture for centeromeric position on chromosome. Hereditas. **52**: 201-220.

Loureiro J, Pinto G, Lopes T, Doležel J, and Santos C. 2005. Assessment of ploidy stability of the somatic embryogenesis process in *Quercus suber* L. using flow cytometry. Planta. **221(6)**: 815-822.

Loureiro J, Rodriguez E, Doležel J, and Santos C. 2007. Two new nuclear isolation buffers for plant DNA

flow cytometry: a test with 37 species. Ann. of Bot. 100(4): 875-888.

Mahdavi S, and Karimzadeh G. 2010. Karyological and nuclear DNA content variation in some Iranian endemic *Thymus* species (Lamiaceae). J. Agric. Sci. Technol. 12: 447-458.

Murashige T, and Skoog F. 1962. A revised medium for rapid growth and bioassays with tobacco tissue culture. Physiol. Plant. **15**: 473-493.

Nadjafi F, Bannayan M, Tabrizi L, and Rastgoo L. 2006. Seed germination and dormancy breaking techniques for *Ferula gummosa* and *Teucrium polium*. J. Arid Environ. **64**: 542-547.

Qixin L, and Menglan S. 1993. Cytotaxonomy of ***Ferula*** L. in China. Acta Phytotax. Sin. 31(5): 413-421.

Paszko B. 2006. A critical review and a new proposal of karyotype asymmetry indices. Plant Syst. Evol. **258(1)**: 39-48.

Peruzzi L, and Eroğlu H.E. 2013. Karyotype asymmetry: Again, how to measure and what to measure? Comp. Cytogenet. **7(1)**: 1-9.

Romero-Zarco C. 1986. A new method for estimating karyotype asymmetry, Taxon. **35(3)**: 526-530.

Reeves G, Francist D, Davies M.S, Rogers H.J, Hodkinson T.R. 1998. Genome size is negatively correlated with altitude in natural populations of *Dactylis glomerata*. Ann. of Bot. **82**: 99-105.

Sağiroğlu M, and Duman H. 2006. *Ferula parva* Freyn & Bornm. (Apiaceae): A contribution to an enigmatic species from Turkey. Turk. J. of Bot. **30(5)**: 399-404.

Sayadi V, Karimzadeh G, Naghavi M.R, and Rashidi Monfared S. 2021. Karyological studies and chromosome variation among Iranian endemic *Allium* species (Amaryllidaceae). J. of Plant Physiology and Breeding. **11(1)**. 97-108.

Seijo J.G, and Fernandez A. 2003. Karyotype analysis and chromosome evolution in south American species of *Lathyrus* (Leguminosae). Am. J. Bot. 90: 980-987.

Siljak-Yakovlev S, Pustahija F, Šolić E.M, Bogunić F, Muratović E *et al.* 2010. Towards a genome size and chromosome number database of Balkan flora: C-values in 343 taxa with novel values for 242. Adv. Sci. Lett. **3(2)**: 190-213.

Stebbins G.L. 1971. Chromosomal Evaluations in Higher Plants. London: Edward Arnold Publisher, UK, 216 p.

Suran D, Bolor T, Bayarmaa G.A. 2016. *In vitro* seed germination and callus induction of *Ferula ferulaeoides* (Steud.) Korov. (Apiaceae). Mong. J. Biol. Sci. **14(2)**: 53-58.

Tarkesh Esfahani S, Karimzadeh G, and Naghavi M.R. 2020. *In vitro* polyploidy induction in Persian poppy (*Papaver bracteatum* Lindl.). Caryologia, **73(1)**: 133-144.

Wanscher J.H. 1931. Studies on the chromosome numbers of the umbelliferae. Hereditas. **15(2)**: 179-184.

Zarabizadeh H, Karimzadeh G, Rashidi Monfared S, and Tarkesh Esfahani S. 2022. Karyomorphology, ploidy analysis, and flow cytometric genome size estimation of *Medicago monantha* populations. Turk. J. of Bot. **46**: 50-61.

Zare A.R, Solouki M, Omidi M, Irvani N, Oladzad A.A *et al.* 2011. Effect of various treatments on seed germination and dormancy breaking in *Ferula assa foetida* L. (Asafetida), a threatened medicinal herb. Trakia J. Sci. **9(2)**: 57-61.

Zhao X, Ma X.J, Kaisar S, Fu C.L, and Chen R.Y. 2006. Karyotypes analysis of *Ferula fukanensis.* Chin. Med. J. **31(2)**: 114-116.

Zhou P, Takaishi Y, Duan H, Chen B, Honda G *et al.* 2000. Coumarins and bicoumarin from *Ferula sumbul*: anti-HIV activity and inhibition of cytokine release. Phytochemistry. **53(6)**: 689-697.

Zomorodian K, Saharkhiz J, Pakshir K, Immeripour Z and Sadatsharifi A. 2018). The composition, antibiofilm and antimicrobial activities of essential oil of *Ferula assa-foetida* oleo-gum-resin. Biocatal. Agric. Biotechn. **14:** 300-304.

Caryologia
International Journal of Cytology, Cytosystematics and Cytogenetics

Firenze University Press
www.fupress.com/caryologia

OPEN ACCESS

Citation: Seyed Mahmood Ghaffari[1], Seyed Mohsen Hesamzadeh Hejazi[2] (2022). Cytogenetic studies in the *Centaurea aucheri* group (sect. Phaeopappus). *Caryologia* 75(4): 123-131. doi: 10.36253/caryologia-1678

Received: June 06,2022

Accepted: December 06, 2022

Published: April 28, 2023

Data Availability Statement: All relevant data are within the paper and its Supporting Information files.

Competing Interests: The Author(s) declare(s) no conflict of interest.

ORCID
SMG: 0000-0002-6777-6992

Cytogenetic studies in the *Centaurea aucheri* group (sect. Phaeopappus)

Seyed Mahmood Ghaffari[1,*], Seyed Mohsen Hesamzadeh Hejazi[2]

[1] *Institute of Biochemistry and Biophysics, University of Tehran, Tehran, Iran*
[2] *Research Education and Extension Organization (AREEO), Tehran, Iran*
*Corresponding author. E-mail: mghaffary@ut.ac.ir

Abstract. In this study, it was aimed to evaluation of the revision in *Centaurea aucheri* group by the cytogenetical studies and determines the chromosome number for *C. albonitens* species, to determine chromosome morphology and karyotype analysis. Results of meiotic behavior and karyomorphologycal parameters of *Centaurea aucheri* group indicated that raised this group in five distinct species are correct. Somatic and gametic chromosome numbers indicated that *C. albonitens, C. assadii, C. farsestanica, C. indistincta* and *C. phaeopappa* are diploid with n=9 and 2n=18 and *C. aucheri* is tetraploid with n=18 and 2n= 4x= 36+0-2B. Gametic chromosome number and karyomorphology of *C. aucheri* and *C. indistincta* species is reported here for the first time. Also, meiotic behavior and karyomorphology parameters of *C. albonites, C.assadi , C. farsestanica* and *C. phaeopappa* are newly reported here. Analysis of karyotype and behavior of meiosis indicated that *C. aucheri* is a natural allotetraploid species. Karyotype symmetry parameters showed that all the studied species were classified in the class 2A except of *C. aucheri* which was located in class 2B.

Keyword: Allotetraploid, *Centaurea aucheri*, Cytogenetic, Karyomorphology, Meiotic behavior.

INTRODUCTION

Centaurea, as the fourth largest genus among the genera in Asteraceae and also the second largest genus in the tribe Cardueae consist of 200–250 species placed in 40 sections (Wagenitz and Hellwig 1997; López et al. 2011 Hilpold et al. 2014). The present classification of *Centaurea* in 40 sections is highly problematic (Wagenitz 1975) and does not take into account all of the pollen, karyological and carpological evidence (Susanna et al. 1995). In Flora Iranica 88 species belong to 28 sections are reported (Wagenitz 1980). *Centaurea* section *Phaeopappus* (DC.) O. Hoffm.is one of the section comprising of five species in Flora Iranica. Of these, 3 taxa viz: *C. albonitens, C. aucheri* and *C. spectabilis* are distributed in Iran (Wagenitz 1980). Ranjbar and Heydari (2016) elevated this section to 14 species in the world, which 12 are belongs to Iran (10 species are endemic to the country). In flora of Iran 5 subspecies has been cited for *C. aucheri* viz: subsp. *aucheri*, subsp. *elbur-*

sensis, subsp. *farsistanica*, subsp. *indistincta* and subsp. *szowitsii* (Wagenitz 1980; Mozafarian 2018). Ranjbar and Negaresh (2013) raised these five subspecies to the *C. aucheri* (DC.) Wagenitz, *C. assadii* Ranjbar and Negaresh, *C. farsistanica* (Wagenitz) Ranjbar & Negaresh, *C. indisticta* (Wagenitz) and *C. phaeopappa* (DC.) Schultz Bipontinus respectively based on the morphological characteristics. The aims of this present paper is evaluation of the revision in *Centaurea aucheri* group by the cytogenetical studies.

MATERIALS AND METHODS

The origin of the plant material studied here is shown in Table 1. For meiotic studies floral buds of plants found in nature were collected and immediately fixed in Piennr's fluid containing ethanol 96%, chloroform, propionic acid, 6:3:2 (v/v/v)for 24 hours at room temperature. Anthers dissected out from the buds were squashed and stained with 2% acetocarmine. Chromosome counts obtained from a minimum of 50 pollen

Table 1. The species and origin of the material examined.

Taxon	Origin	Altitude(m)	Longitude and Latitude	H. Code
Centaurea albonitens Turrill	Azerbaijan: Tabriz, 20 Km towards Marand	1360	E:46°03'57"; N:38°15'48"	109080
	Azerbaijan: between Khoy and Salmas	1530	E: 44°54'15"; N: 38°24'39"	109081
	Zanjan, 10 Km towards Miyaneh	1500	E: 47°27'35"; N: 37°12'36"	109101
	Zanjan, 30 Km towards Miyaneh	1600	E: 47°30'53"; N: 37°14'41"	109102
Centaurea aucheri	Kordestan:Saqqez to Divandareh	2200	E: 46°54'15"; N: 36°24'39"	109091
	Kordestan: W Saqqez	2160	E: 46°16'13"; N: 36°15'39"	109092
	Qazvin: Avaj, 10 Km. to Hamadan	2400	E: 49°09'38"; N: 35°32'17"	109201
	Qazvin: Neck of Avaj	2320	E: 49°12'05"; N: 35°35'35"	109202
	Qazvin: Abgarm to Avaj	2300	E: 49°14'07"; N: 35°42'58"	109203
	Hamadan: 90 Km. to Qazvin	2070	E: 49°02'19"; N: 35°27'54"	109301
	Lorestan: Doroud, Gahar, Saravand	2110	E: 49°10'03"; N: 33°22'26"	109421
	Markazi: Tafresh, Noghre-kamar	2080	E: 50°08'13"; N: 34°41'53"	109501
Centaurea assadii	Azerbaijan:Miyaneh to Bostanabad	1720	E: 47°18'27"; N: 37°32'05"	109087
	Tehran: Kouhdashteh	1800	E: 51°20'13"; N: 35°44'23"	109701
	Tehran: Kouhdashteh	1950	E: 51°23'50"; N: 35°44'29"	109702
	Tehran: Sorkheh hesar	1500	E: 51°36'03"; N: 35°43'12"	109714
	Tahran: Sorkheh hesar	1700	E: 51°35'46"; N: 35°43'09"	109712
	Tehran: Jajroud	2200	E: 51°29'45"; N: 35°42'39"	109754
	Tehran: Abali	2400	E: 51°57'55"; N: 35°45'54"	109718
Centaurea farsistanica	Shiraz: Bamoo park	1750	E: 52°36'52"; N: 29°42'48"	109614
	Shiraz: Bamoo park	1820	E: 52°37'15"; N: 29°43'11"	109615
	Shiraz: Bamoo park	2000	E: 52°36'33"; N: 29°12'41"	109617
	Fars: Dasht arjan, Khers dareh	2400	E: 51°58'56"; N: 29°39'47"	109687
	Yasouj, Kakan	2300	E: 51°35'57"; N: 30°38'18"	109813
	Yasouj: Kamehr	2400	E: 51°35'38"; N: 30°39'55"	109815
Centaurea indistincta	Tehran: Kouhdashteh	1800	E: 51°20'13"; N: 35°44'23"	109706
	Tehran: Kouhdashteh	2300	E: 51°23'50"; N: 35°44'30"	109709
	Lorestan: Doroud, Gahar	2100	E: 49°10'03"; N: 33°22'25"	109432
	Zanjan	1630	E: 47°33'53"; N: 37°14'41"	109132
Centaurea phaeopappa	Karaj, Eshtehard, Dakin	1550	E: 50°27'36"; N: 35°37'18"	109745
	Qazvin: Abgarm to Avaj	2300	E: 49°14'07"; N: 35°42'58"	109208
	Tahran: Kohdashteh	1800	E: 51°20'13"; N: 35°44'24"	109784
	Karaj, Ziyaran	2000	E: 50°31'43"; N: 36°07'06"	109764
	Azerbaijan: Oroumiyeh to Mahabad	1330	E: 45°19'22"; N: 37°13'52"	109075
	Azarbaijan: Salmas to Oroumiyeh	1375	E: 45°36'08"; N: 37°34'46"	109094
	Azerbaijan: Mishodagh Mt.	2040	E: 45°38'23"; N: 38°17'50"	109049
	Qazvin: Takestan to Hamadan	2350	E: 49°01'44"; N: 35°20'46"	109257

mother cells within each collection. Actively growing root tips were used for mitotic analysis. Roots were pretreated with 0.002M, 8-hydroxyquinoline at 20˚C for 3 hr, and then fixed in 3:1 (ethanol: acetic acid). Staining was carried out with the Feulgen reaction enhanced by squashing in 2% acetocarmine. Nomenclature adopted by Levan et al. (1964) was followed for recognizing chromosome types. Both mitotic and meiotic slides were made permanent by the venetain turpentine (Wilsom 1945). Voucher specimens are preserved in the Herbarium of Research Institute of Forests and Rangelands (RIFR).

RESULTS

Centaurea albonitens *Turrill*

Centaurea albonitens is widely distributed in western Iran, especially Zanjan, west and east Azerbaijan Provinces. Five samples of this taxon showed chromosome numbers of n=9 and 2n=18 in both meiosis and mitotic respectively. Meiosis in this taxon showed 9 bivalents at diakinesis which ring tetravalent in some cells were observed (Figure 1A). Also, two bivalents were associated with the nucleolus at diakinesis, which is confirmed to presence of two satellite chromosomes in this species. First metaphase indicated 9 bivalents, which most of them were in rod shape (Figure 1B). Anaphase I showed (9-9) chromosomes segregation (Figure 1C). Somatic chromosome counts in 50 root tips disclosed a chromosome number of 2n=18 (Figure 1D, E). The representatives of chromosome set at mitotic metaphase are shown in Figure 1F and Table 2. The karyotype of *C. albonitens* consists of one pair of metacentric chromosome and 8 pairs of sub-metacentric chromosomes. The total length of the chromosomes varied from 5.18 µm to 2.96 µm (Table 2). This count (2n=18) agrees with previous reports by Garcia-Jacas et al. (1998) and Ranjbar and Negaresh (2013). Karyotype analysis and meiotic count for this taxon is reported here for the first time.

C. aucheri *(DC.) Wagenitz*

Eight samples of this taxon showed chromosome numbers of n=18 and 2n=36 in both meiosis and mitotic respectively. Meiosis showed some clamping of chromosomes at first metaphase. The bivalents at metaphase I were usually in the shape of rod with one terminal chiasmata (Figure 2A). Many cells were observed in order to ascertain the correct chromosome count. The number

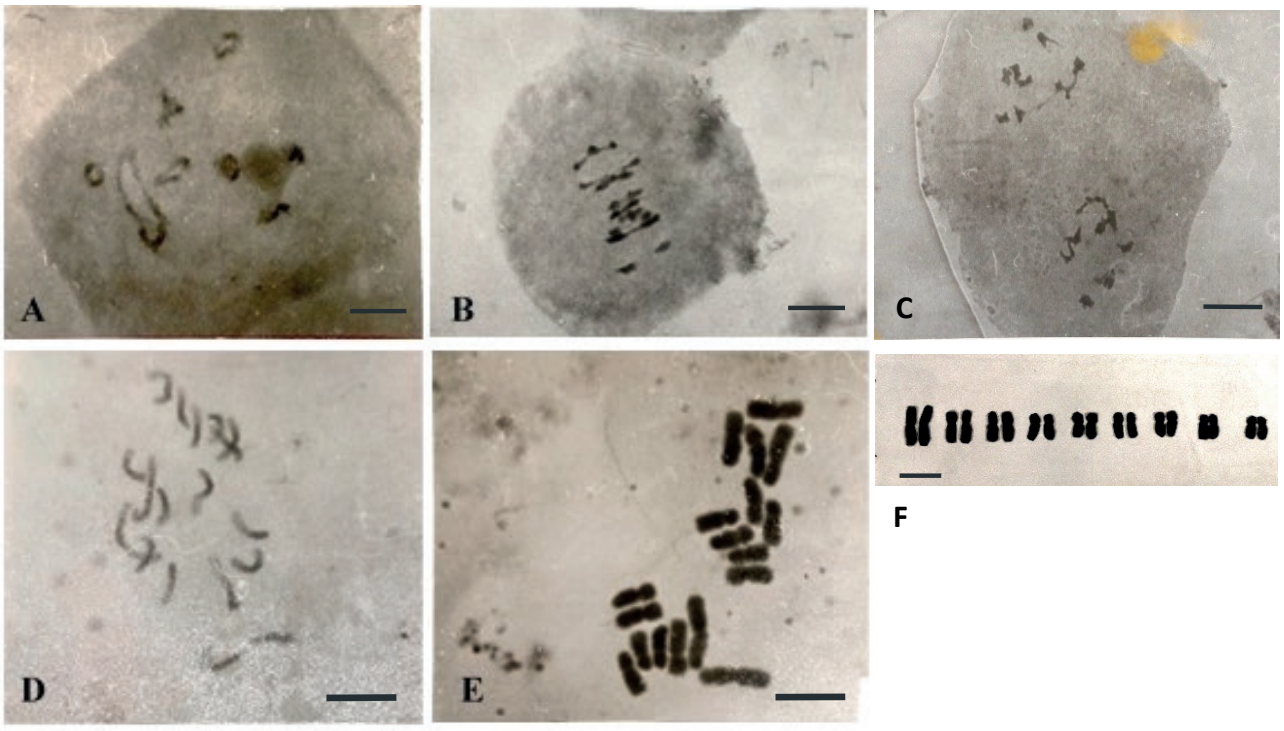

Figure 1. Meiosis and mitotic micrographs of *Centaurea albonitens*. A; Diakinesis, showing ring tetravalent (arrow). B: Metaphase I (n=9). C: Anaphase I (9-9). D: Late prophase (2n=18). E: Metaphase (2n=18). F: Karyotype showing nine pairs of chromosomes. Scale= 5µm.

Table 2. Measurement of somatic chromosomes in a diploid *C. albonitens* (Obtained from 50 cells).

No. of chromosome	Total length (µm)	Long arm (µm)	Short arm (µm)	Arm ratio L/S = r
1	5.18	2.59	2.59	1
2	4.44	2.59	1.85	1.4
3	3.89	2.22	1.67	1.33
4	3.33	2.22	1.11	2
5	3.33	2.04	1.29	1.85
6	3.33	2.04	1.29	1.85
7	3.14	1.85	1.29	1.43
8	2.96	1.85	1.11	1.67
9	2.96	1.85	1.11	1.67

n=18 observed at diakinesis (Figure 2B) and (18-18) segregation at first anaphase (Figure 2C). In the first meiosis stage, we did not observe any tetravalents at metaphase I and diakinesis. Also we did not found any abnormality at first and second anaphase of meiosis, which is prevalent in autopolyploids species. These results indicated that this taxon is natural allotetraploid species. Somatic chromosome counts of 50 root tips disclosed a chromosome number of 2n= 36+0-2B (Figure 2D,E). These B-chromosomes were not found at meiosis stage. The karyotype consisted of 15 metacentric pairs, and 3 submetacentric pairs (Figure 3A). The total length of the chromosomes varied from 6.11 µm to 2.85 µm (Table 3). Different chromosome number of this taxon (2n=36) with others subspecies (2n=18) and allotetraploid behav-

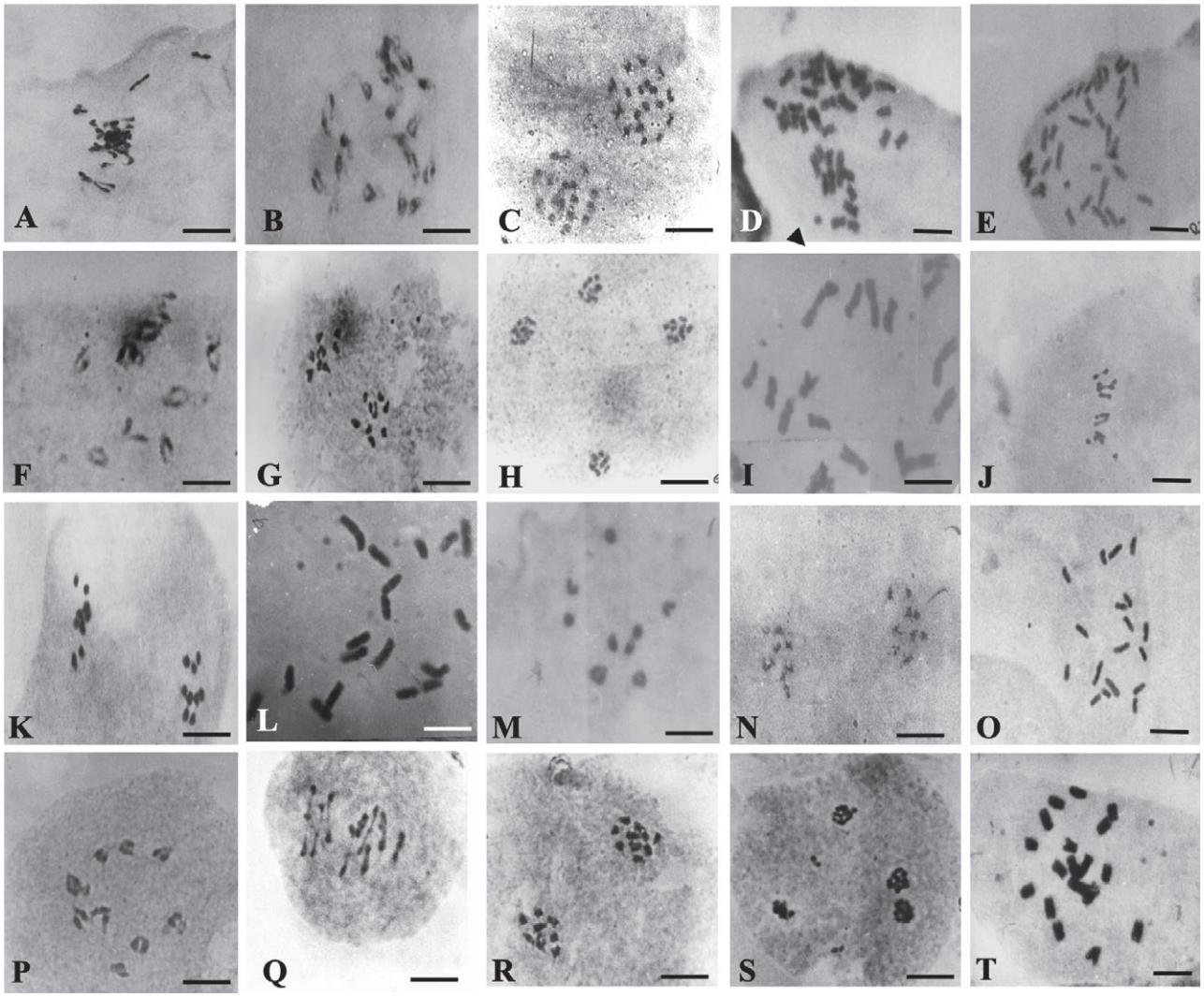

Figure 2. Meiosis and mitotic micrographs of *Centaurea aucheri* group A- E. *C. aucheri*, A: metaphase I. B: diakinesis. C: anaphase I. D: mitotic metaphase, showing B-chromosome (arrow). E: mitotic metaphase, showing 2B-chromosomes (arrows). Scale = 5µm.

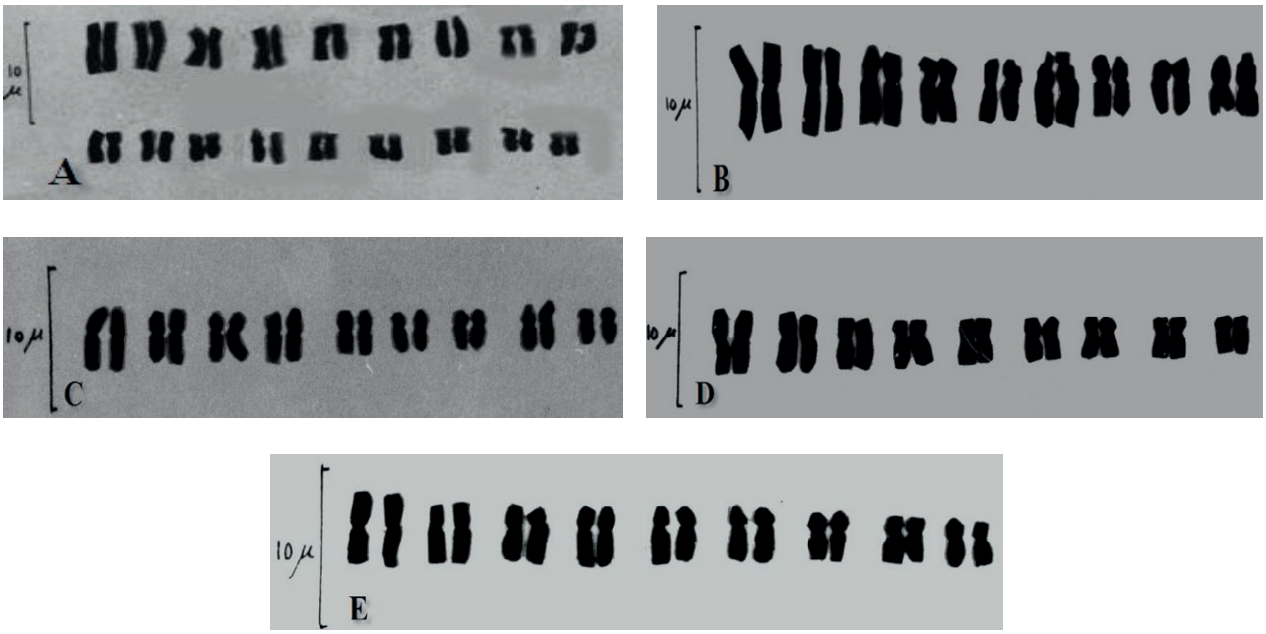

Figure 3. A: Karyotype of *C. aucheri*. B: Karyotype of *C. assadii*. C: Karyotype of *C. farsestanica*. D: Karyotype of *C. indistincta*. E: Karyotype of *C. phaeopappa* Scale bar = 10 µm.

Table 3. Measurement of somatic chromosomes in a tetraploid *C. aucheri* (Obtained from 12 cells).

No. of chromosome	Total length (µm)	Long arm (µm)	Short arm (µm)	Arm ratio L/S = r
1	6.11	3.67	2.44	1.50
2	5.61	3.35	2.26	1.48
3	5.11	3.02	2.08	1.45
4	4.76	2.49	2.26	1.10
5	4.41	2.49	1.91	1.30
6	4.38	2.47	1.91	1.29
7	4.23	2.44	1.79	1.36
8	4.20	2.61	1.58	1.64
9	4.16	2.84	1.32	2.14
10	4.06	2.44	1.61	1.51
11	3.91	1.97	1.94	1.01
12	3.55	2.14	1.41	1.52
13	3.52	2.23	1.29	1.72
14	3.50	2.17	1.32	1.64
15	3.32	2.11	1.20	1.75
16	3.23	1.82	1.41	1.29
17	2.91	1.76	1.14	1.53
18	2.85	1.61	1.23	1.30

ior indicated that upgrade to species rank (*C. aucheri* (DC.) Wagenitz) by Ranjbar and Negaresh (2013) is correct. In addition, we found some specimens of this taxon together with *C. aucheri* subsp. *szowitsii* (*C. phaeopappa*) in one place (Abgarm to Avaj, Table 1), that chromosome examination showed independence in chromosome number for each species (subsp. *aucheri* , n=18, 2n=36: subsp. *szowitsii* n=9, 2n=18) and did not show any hybrid adjective between this two taxon.

C. assadii *Ranjbar & Negaresh*

Wagenitz (1980) is introduced the *C. aucheri* subsp. *elbursensis* (*C. assadii*) as a new endemic subspecies to Iran for the first time. Previous chromosome number report for this taxon is n=9 by Ghaffari (1986). The results obtained in this study showed nine bivalents in pollen mother cells at diakinesis (Figure 2F). Another stages of meiosis showed chromosome segregation (9-9) at anaphase I and 9 chromatid segregation at anaphase II (Figure 2G,H). Chromosome complement at metaphase of mitotic was 2n=18 (Figure 2I). Karyotype consisted of seven pairs of metacentric and two pairs of submetacentric chromosomes (Figure 3B). The total length of the chromosomes varied from 4.74 µm to 2.79 µm (Table 4). This taxon distributed in Azerbaijan, Mazandaran, Qazvin, and Tehran provinces. We found overlapping of this species with *C. indistincta* and *C. phaeopappa* in one place (Tehran, kouhdashteh, see Table 1) and did not see any hybrid between them. Lack of geographical distribution independence, joint with other subspecies, morpho-

logical characteristics and difference in chromosomal characteristics with *C. aucheri*, indicated that this taxon is a distinct species.

C. farsistanica *(Wagenitz) Ranjbar & Negaresh*

Meiosis in this taxon was regular and showed nine bivalents at metaphase I which more of them were in rod shape (Figure 2J). Anaphase I indicated (9-9) chromosomes segregation (Figure 2K). Mitotic study showed 2n=18 chromosomes at metaphase (Figure 2L). This diploid species has a symmetrical karyotype with six pairs of metacentric and three pairs of submetacentric chromosomes (Figure 3C). The total length of the chromosomes varied from 3.98 µm to 2.25 µm (Table 5). This taxon is completely different with others subspecies in morphological characteristic and pattern of distribution (Ranjbar and Negaresh 2013), which are introduced by Wagenitz (1980) and Mozaffarian (2018).

Centaurea indistincta (Wagenitz) Ranjbar & Negaresh

This taxon is reported by Wagenitz (1980) as a new endemic subspecies species (*C. aucheri* subsp. *indistincta*) for flora of Iran, which was introduced by Ranjbar and Negaresh (2013) as a distinct species. Meiosis in this species showed nine bivalents at metaphase I and (9-9) univalents segregation at first anaphase (Figure 2M,N). Chromosome complement in this species was 2n=18 (Figure 2O). Karyotype consisted of five pairs of metacentric and four pairs of submetacentric chromosomes (Figure 3E). The total length of the chromosomes varied from 4.08 µm to 2.52 µm (Table 6).

Centaurea phaeopappa *(DC.) Schulpz & Bipontinus*

Meiotic and mitotic divisions were examined on eight samples of this species (Table 1). Meiosis showed nine bivalents at diakinesis and metaphase I (Figure 2P,Q). Nondisjunction of (8-10) segregation at anaphase I was observed (Figure 2R). Also, in some cells laggard chromosomes at anaphase II were observed (Figure 2S). Mitotic stages in this species indicated chromosome complement of 2n= 18 (Figure 2T) which is agrees with the previous report by Ghaffari (1988). The karyotype consisted of six pairs of metacentric and three pairs of submetacentric chromosomes (Figure 3F). The total length of the chromosomes varied from 4.21 µm to 2.70 µm (Table 7).

Table 4. Measurement of somatic chromosomes in a diploid *C. assadii* (Obtained from 9 cells).

Chromosome No	Total length (µm)	Long arm (µm)	Short arm (µm)	Arm ratio L/S = r
1	4.74	2.43	2.30	1.05
2	4.67	2.51	2.15	1.16
3	4.10	2.45	1.65	1.48
4	3.87	2.43	1.43	1.69
5	3.43	1.94	1.48	1.31
6	3.23	2.28	0.95	2.40
7	3.19	1.84	1.35	1.36
8	3.02	1.80	1.22	1.47
9	2.79	1.54	1.24	1.23

Table 5. Measurement of somatic chromosomes in a diploid *C. farsistanica* (obtained from 14 cells).

Chromosome No	Total length (µm)	Long arm (µm)	Short arm (µm)	Arm ratio L/S = r
1	3.08	2.24	1.73	1.29
2	3.34	1.95	1.39	1.39
3	3.09	1.82	1.27	1.43
4	2.71	1.90	0.80	2.36
5	2.54	1.31	1.23	1.06
6	2.46	1.39	1.06	1.31
7	2.38	1.27	1.11	1.14
8	2.29	1.44	0.85	1.69
9	2.25	1.49	0.76	1.94

Table 6. Measurement of somatic chromosomes in a diploid *C. indistincta* (obtained from 8 cells).

Chromosome No	Total length (µm)	Long arm (µm)	Short arm (µm)	Arm ratio L/S = r
1	4.08	2.21	1.86	1.19
2	3.72	2.30	1.42	1.62
3	3.15	1.95	1.37	1.41
4	2.92	2.08	1.06	1.96
5	2.92	1.59	1.33	1.20
6	2.75	1.55	1.37	1.12
7	2.57	1.73	1.02	1.69
8	2.13	1.64	0.93	1.76
9	2.52	1.59	0.93	1.71

DISCUSSION

The study has detected the somatic and gametic chromosome number and karyomorphology of *C.*

Table 7. Measurement of somatic chromosomes in a diploid *C. phaeopappa* (obtained from 23 cells).

Chromosome No	Total length (µm)	Long arm (µm)	Short arm (µm)	Arm ratio L/S = r
1	4.21	2.13	2.08	1.02
2	3.72	2.21	1.50	1.47
3	3.59	2.04	1.55	1.31
4	3.55	2.21	1.33	1.66
5	3.51	2.21	1.29	1.71
6	3.46	2.17	1.28	1.68
7	2.88	1.68	1.19	1.40
8	2.75	1.86	0.88	2.10
9	2.70	1.68	1.02	1.65

aucheri and *C. indistincta* species for the first time. Also, meiotic behavior and karyomorphology parameters of *C. albonites, C.assadi* and *C. phaeopappa* are newly reported here. *C. albonitens, C. assadii, C. indistincta* , *C. farsestanica* and *C. phaeopappa* are diploid with n= 9, 2n=2x=18 and *C. aucheri* is tetraploid with 2n=4x=36+0-2B. All taxa had the basic chromosome number of x= 9.

By definition, a subspecies designation is applied to a plant that is geographically isolated from other members of its species in habitat and therefore does not interbreed for this reason. Five subspecies (*C. aucheri* subsp. *aucheri, C. aucheri* subsp. *elbursensis, C. aucheri* subsp. *farsestanica, C.aucheri* subsp. *indistincta, C. aucheri* subsp. *szowitsii*) which is introduced by Wagenitz (1980) and Mozafarian (2018) for flora of Iran, were often adjacent to each other [see Table 1 and pattern of distribution of these subspecies in the research article by Ranjbar and Negaresh (2013)]. Therefore, they cannot be considered as subspecies. Eight samples of the *C. aucheri* showed chromosome numbers of n=18 and 2n=36 in both meiosis and mitotic respectively. Meiosis in pollen mother cells in this taxon showed that the most common chromosome configurations were bivalents at diakinesis and first metaphase. Analysis of karyotype and behavior of meiosis indicated that this taxon is a natural allotetraploid species. Therefore, the results of meiotic behavior and karyomorphologycal parameters of five subspecies which are introduced by Wagenitz (1980) and Mozaffarian (2018) are not correct and revision of them by Ranjbar and Negaresh (2013) in five independence species are correct.

In this study, most of the chromosomes of the evaluated species were metacentric (m) or submetacentric(sm). Karyotype symmetry parameters showed that all the studied species were classified in the class 2A of the category of Stebbins (1971), except of *C. aucheri* which was located in class 2B (Table 8). Total form percentage (TF%) for *C. indistincta* and *C. phaeopappa* were 40.41 and 40.02 respectively, that indicated similarity between them. Also, this TF% similarity can be seen between *C. assadii* and *C. farsistanica* with 41.75 and 40.82 respectively. According to the data obtained from the five species (*C. aucheri*, *C. assadii* , *C. farsistanica*, *C. indisticta* and *C. phaeopappa*), the karyotype formulas were different between them (Table 8). Also, the inter and intrachromosomal asymmetry index (A1 and A2) for five taxa were different (Table 8). In this study, C. *farsistanica* had a higher DI value, which is associated with an enhanced order of karyotypic specialization. *C. aucheri* had the highest A_2 values therefore its karyotype was more asymmetric than the other species. To analyze the variability of the karyotypes among species, all karyotype characteristics of *Centaurea* species (Table 8) were compared by one-way design. Using principal components analysis (PCA), the first two independent components accounted for about 81.68% of total variation (Table 9). The first component indicated that TL, LA, SA, CI, TF% and A_2 were important characters for classification of species with about 61% of total variation. AR, LA%, SA%, DRL, A1 and DI were important traits in the second component (21%) (Table 9).

Table 8. Karyotype parameters of *Centaurea* taxa; Total Length of chromosome(TL), Long Arm (LA), Short Arm (SA), Arm Ratio(AR), Centromeric Index(CI), Long Arm percent(LA %), Short Arm percent(SA %); Total Form percent (TF %), Difference of Relative Length (DRL), intrachromosome asymmetry index(A_1), interchromosome asymmetry index(A_2), Dispersion Index(DI), symmetry classes of Stebbins(SC), Haploid Karyotype Formula(H.K.F.) (m: metacentric , sm: submetacentric).

species	TL	LA	SA	AR	CI	%LA	%SA	%TF	DRL	A_1	A_2	DI	SC	H.K.F
C. assadi	3.68	2.14	1.54	1.47	0.41	6.47	4.64	41.75	5.89	0.28	0.19	8.11	2A	7m+2sm
C. aucheri	4.11	2.43	1.68	1.48	0.41	3.29	2.27	40.83	4.41	0.31	0.22	8.41	2B	15m+3sm
C. farsistanica	2.79	1.65	1.14	1.52	0.41	6.58	4.54	40.82	6.87	0.30	0.21	9.12	2A	6m+3sm
C. indistincta	3.11	1.85	1.26	1.52	0.40	6.62	4.49	40.41	5.55	0.32	0.17	7.65	2A	5m+4sm
C. phaeopappa	3.38	2.03	1.35	1.56	0.40	6.66	4.45	40.02	4.96	0.33	0.15	5.47	2A	6m+3sm

Table 9. Eigenvectors from the first two principal components for 12 karyotype parameters to classify *Centaurea* species.

Parameters	First component	Second component
TL	0.328	-0.054
LA	0.336	-0.050
SA	0.316	-0.061
AR	0.294	0.308
CI	-0.320	-0.206
LA%	-0.275	0.381
SA%	-0.304	0.316
TF%	-0.326	-0.169
DRL	-0.204	0.528
A_1	0.133	-0.176
A_2	0.332	0.218
DI	0.215	0.471
Eigen value	7.3257	2.4761
Percentage of Variance	61.0479	20.6346
Cum percentage of variance	61.0479	81.6824

The tree phylogeny (Figure 4) of the five species indicated two major clades. The first major clade consists of two species (*C. indistincta* and *C. phaeopappa*) showed a degree of affinity and were placed close to each other, while, *C. aucheri* joined the other species at a great distance. The second clade contained *C. assadii* and *C. farsestanica*. Thus, these studies could greatly help us in the classification and taxonomic studies. The diagram of species' dispersion, based on two first components, showed that the species separated in three groups, which completely fits with results obtained through the grouping analysis by Ward's method (Figure 5).

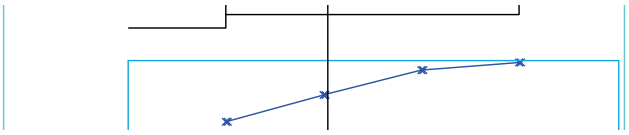

Figure 4. Dendrogram of cluster analysis (Ward) of *Centaurea* species based on karyotype characteristics. Cophenetic correlation r=0.94.

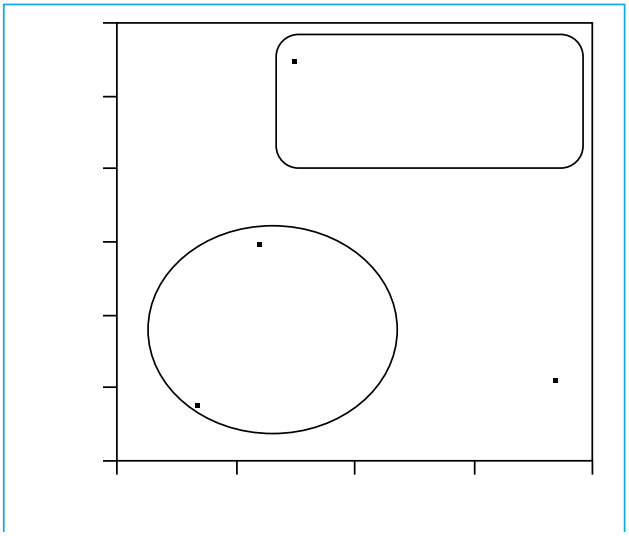

Figure 5. Scatter plot of *Centaurea* species for the first two principal components.

REFERENCES

Garcia-Jacas N, Susanna A, Mozaffarian, V. 1998. New chromosome counts in the subtribe Centaureinae (Asteraceae, Cardueae) from West Asia, III. Botanical Journal of the Linnean Society 128: 413–422.

Ghaffari SM. 1986. Chromosome number reports XCIII. Taxon 35(4):900-901.

Ghaffari SM. 1988. Chromosome number reportsXCIX .Taxon 37(2):397.

Hilpold A, Garcia-Jacas N, Vilatersana R, Susanna A. 2014. Taxonomical and nomenclatural notes on Centaurea: a proposal of classification, a description of new sections and subsections, and a species list of the redefined section Centaurea. Collectanea Botanica 33: e001. Pp. 1-29.doi: 10.3989/ collectbot.2013. v33.001.

Levan A, Fredga K, Sandberg AA. 1964. Nomenclature-forcentromeric position on chromosomes. Hereditas 52:201–220.

López, E, Devesa JA, Arnelas I. 2011. Taxonomic study in the Centaurea longei complex (Asteraceae). Annales Botanici Fennici 48: 1–12.http://dx.doi.org/10.5735/085.048.0101

Mozafarian V. (2018). Tribus Cardueae Cass. In: Mozafarian, V. & al. (eds.), Flora of Iran, Research Institute of Forests and Ranglands.

Ranjbar M, Negaresh K. 2013. A revision of Centaurea sect. Phaeopappus (Asteraceae, Cardueae). Phytotaxa 123 (1): 1–40.

Ranjbar M, Heydari R. 2016. A taxonomic contribution to yellow-flowered members of Centaurea sect. Phaeopappus (Asteraceae) in Iran. Phytotaxa 277: 182–190.

Stebbins G.L. 1971. Chromosomal evolution in higher plsnts. Edward Arnold Ltd. London.

Susanna A, Garcia-Jacas N, Soltis DE, Soltis P.S. 1995. Phylogenetic relationship in tribe Carduae (Asteraceae) based on ITS sequence. American Journal of Botany 82: 1056-1068.

Wagenitz G. 1980. Centaurea. In: Rechinger KH (ed.), Flora Iranica, Lieferung 138b. pp. 313-420. Graz: Akademische Druck-und Verlagsanstalt.

Wagenitz G, Hellwig FH. 1997. Eine neue und eine verschollene Centaurea-Art aus der Türkei und eine neue Volutaria-Art (Compositae-Cardueae). Annalen des Naturhistorischen Museums in Wien 98B: 175–181.

Wilson GB. 1945. The venetian turpentine mounting medium. Stain Technol. 20: 133-135.

Caryologia
International Journal of Cytology, Cytosystematics and Cytogenetics

Firenze University Press
www.fupress.com/caryologia

OPEN ACCESS

Citation: Saeed Mohammadpour, Ghasem Karimzadeh, Seyed Mahmood Ghaffari (2022). Karyomorphology, genome size, and variation of antioxidant in twelve berry species from Iran. *Caryologia* 75(4): 133-148. doi: 10.36253/caryologia-1633

Received: April 18, 2022

Accepted: December 04, 2022

Published: April 28, 2023

Data Availability Statement: All relevant data are within the paper and its Supporting Information files.

Competing Interests: The Author(s) declare(s) no conflict of interest.

Karyomorphology, genome size, and variation of antioxidant in twelve berry species from Iran

Saeed Mohammadpour[1], Ghasem Karimzadeh[1,*], Seyed Mahmood Ghaffari[2]

[1] *Department of Plant Genetics and Breeding, Col lege of Agriculture, Tarbiat Modares University, P.O. Box 14115-336, Tehran, Iran*
[2] *Institute of Biochemistry and Biophysics, University of Tehran, P.O. Box 13145-1384, Tehran, Iran*
*Corresponding author. E-mail: karimzadeh_g@modares.ac.ir

Abstract. Twelve berry species, including *Rubus fruticosus* cv. Qaemshahr, *Rubus occidentalis* cv. Qaemshahr, and *Morus alba* cv. Mashhad, *Morus rubra* cv. Karaj, *Fragaria vesca* subsp. *vesca*, *Ribes nigrum*, *Ribes rubrum*, *Ribes uva-crispa*; *Lycium barbarum*, *Lycium infaustum*, *Lycium ruthenicum*, and *Vaccinium corymbosum* were surveyed for karyomorphology analysis, monoploid genome size, and antioxidant activity. Results indicated that all species were diploid ($2n = 2x = 14$, 16, 24, and 28). Among these species, chromosome counts and karyomorphology parameters of three cultivars including: *R. fruticosus* cv. Qaemshahr ($2n = 2x = 14$), *R. occidentalis* cv. Qaemshahr ($2n = 2x = 14$), and *M. alba* cv. Mashhad ($2n = 2x = 28$) are reported here for the first time. The flow cytometric mean monoploid 2Cx DNA of berry species was 2.35 pg, varied from 0.68 (*Rubus occidentalis* cv. Qaemshahr) to 5.15 pg (*Lycium ruthenicum*). The average antioxidant capacity of berry species was obtained 32.8 μmol g^{-1}. Their average total phenol and flavonoid contents were 4.98 mg g^{-1} (3.08-8.61 mg g^{-1}), and 5.18 (2.47-10.63 mg g^{-1}), respectively.

Keywords: Blueberry, Raspberry, Cytogenetic, Antioxidant, Karyomorphology, Flow cytometry.

INTRODUCTION

Berries are economically important crop in many countries (Umdale *et al*. 2020). Interest in berries has recently increased because they are excellent sources of health-promoting vitamins, anti-oxidants, polyphenols, especially anthocyanins, micronutrients, fiber, and other valuable nutrients (Song and Sing, 2004). Berries are low in calories and are high in moisture and fiber (Basu *et al*. 2010). They contain natural antioxidants such as vitamins C and E, and micronutrients such as folic acid, calcium, selenium, alpha and beta carotene, and lutein (Basu 2019). However, berry production is deficient, even though soil and climate conditions in Iran are excellent for the intensive cultivation of berry fruits (Nestby *et al*. 2019). Some of the berry cultivars that

have recently been introduced to Iran are potentially profitable alternative and non-conventional fruit crops. Among those are cultivars of the blueberry (*Vaccinium corymbosum* L.), the goji berry (*Lycium barbarum*, *L. infaustum*, *L. ruthenicum*), and the raspberry (*Rubus occidentalis*) (Ahmadu and Ahmad 2021). In Iran, the production of blackberry (*Rubus fruticosus*) relies mainly on the collection of the berries from stands of native varieties that grow wild in the mountains. Habitat destruction has led to a reduction in the supply of native blackberries. Although these native wild varieties are not as suitable for intensive culture as the new cultivars, they are still very valuable high dietary value and breeding potential. They can be a versatile raw material for the food processing and pharmaceutical industries. Recently, interest in growing various berry fruits has been increasing among either home gardeners, or small farmers. Berry culture is increasing in the country's mountainous, where soil and climate conditions are more favorable for intensive berry culture than in the lowland areas (Nestby *et al*. 2019).

The consumption of berry fruits and their contribution to improving cardiovascular health is a significant issue (Blumberg *et al*. 2013). The commonly consumed berries in the United States, including blackberry, black raspberry, blueberry, goji berry, cranberry, red raspberry, and strawberries (Yang *et al*. 2019). Display quotations of over 40 words or as needed.

Berry fruits are deciduous shrubbery that grows in different parts of the world (Donno *et al*. 2015). For instance, goji berry grows in China, Tibet, Argentina, Chile, Southern Africa, and other parts of Asia, and its fruits are 1-2 cm long, bright orange-red ellipsoid berries. Goji berry is widely distributed in warm regions of the world, in particular, in the Mediterranean area and Southwest and Central Asia. It is also cultivated in North America and Australia as a hedge plant (Potterat 2010). Mulberry (*Morus alba*) is native to China, but is also found worldwide on not native continents, such as Europe, Africa, North America, and South America. Currant (*Ribes* spp.), is widely cultivated across temperate Europe, Russia, New Zealand, parts of Asia, and to a lesser extent North America (Steffen *et al*. 2015). The main centers of diversity for blueberry are distributed in Europe (Poland, Germany, France, The Netherlands, Spain, and Sweden), New Zealand, Mexico, and North America.

Karyotype analysis and chromosome observation are necessary to elucidate phylogenetic relationships, structure, function, organization, and evolution of plant genes and genomes (Amosova *et al*. 2019). For those reasons, many studies must be performed to observe plant chromosomes. Higher similarity in chromosome shapes suggests a closer phylogenetic relatedness. The base chromosome number in *Rubus* spp. (*R. fruticosus*, and *R. occidentalis*), *Ribes* spp. (*R. nigrum*, *R. rubrum*, and *R. uva-crispa*), Lycieae (*L. barbarum*, *L. infaustum*, and *L. ruthenicum*), Moraceae (*M. alba*, and *M. rubra*) is $x = 7$, 8, 12, and 14, respectively. The base chromosome number in strawberry (*Fragaria vesca*) and blueberry (*Vaccinum corymbosum*) is $x = 7$, and 14, respectively (Zong *et al*. 2021). Most species are diploid with $2n = 24$. Cytological information, including the number of chromosome and karyotypes, is available for many American and Asian *Lycium* and several species in Southern African (Bernardello *et al*. 2008).

Monoploid genome size in the form of base-pair was calculated based on the formula proposed by Doležel et al. (2003), when 1 pg of DNA represents 978 mega base pairs (Mbp). Monoploid genome size was considered as the amount of DNA of one chromosome set, 1C*x*-value, with chromosome base number *x*, and holoploid genome size as the amount of DNA of the whole chromosome complement, 1C-value, with chromosome number n, irrespective of the degree of generative polyploidy (Greilhuber *et al*. 2005; Mahdavi and Karimzadeh 2010; Karimzadeh *et al*. 2011; Abedi *et al*. 2015; Tavan *et al*. 2015). In recent decades, significant progress has been made in the use of flow cytometry in various fields of botany. This growth is due to the advantages of flow cytometry such as high speed, ease of sample preparation, and analysis of inactive mitotic tissues. Despite these advantages, the need for fresh plant materials may often prevent the further development of flow cytometry in field research (Suda and Trávníček 2006). Flow cytometry is known as the most powerful, reliable, and quick method for estimating the genome size (2C DNA) for a wide range of plant communities (e.g. Garcia *et al*. 2004; Doležel and Bartoš 2005; Doležel *et al*. 2007; Loureiro *et al*. 2007; Mahdavi and Karimzadeh 2010; Karimzadeh *et al*. 2010, 2011; Abedi *et al*. 2015; Tavan *et al*. 2015; Tarkesh Esfahani *et al*. 2016, 2020; Javadian *et al*. 2017; Hamidi *et al*. 2018; Zarabizadeh *et al*. 2022). The term "C-value" refers to the constant amount of DNA of an unreplicated haploid chromosome complement (Swift 1950). Monoploid genome size was considered as the amount of DNA of one chromosome set, 1C*x*-value, with chromosome base number *x* (Greilhuber *et al*. 2005). The mean monoploid 2C*x* DNA value was 2.35 pg. On the other hand, the monoploid genome size (1C*x* DNA) varied from 420.54 Mbp (S3; *Rubus occidentalis* cv. Qaemshahr) to 2518.35 Mbp (S9; *Lycium ruthenicum*). Reports of 2C*x* DNA in some berry species have been reported, including S3; *Rubus occidentalis* = 0.60 pg, S5; *Ribes rubrum* = 1.94 pg, and S6; *Ribes*

uva-crispa = 1.88 pg (Meng and Finn 2002; Chiche *et al*. 2003).

Antioxidants are compounds that effectively prevent oxidation in a variety of ways and, by slowing down the oxidation rate, significantly increase the oxidation period (Dorman *et al*. 2003). From one perspective, antioxidants fall into two main categories: synthetic and natural. Phenolic compounds are one of the best sources of natural antioxidants (Dorman *et al*. 2003). Because the use of such plant resources is effective in delaying oxidation and reducing chronic diseases, mutations, and cancer (Briskin 2000). In new research works in the field of natural antioxidants, much attention has been paid to essential oils and extracts of medicinal plants because a wide range of medicinal plants and their aromatic compounds as natural sources with antioxidant properties, (Moure *et al*. 2001; Tepe *et al*. 2006). It is generally recognized that oxygen free radicals (ROS) are associated with many potential risks, including Parkinson's disease, cancer, Alzheimer's, as well as aging (Liochev 2013; Kim *et al*. 2016).Berry species are popular around the world as a 'Super fruit' due to their nutritional value, elevated levels of bioactive phenolic molecules, and excellent sensory evaluation (Kalt *et al*. 2020). In addition to these essential nutrients, berries contain a wide range of antioxidant phenolic molecules such as phenolic acids, flavonoids, flavonols, flavanols, anthocyanins, proanthocyanidins, and ellagitannins (Prior *et al*. 1998; Piljac-Žegarac *et al*. 2009; Nile and Park 2014; Skrovankova *et al*. 2015). Cranberries ranked first in polyphenol content among the commonly consumed fruits in North America which relate to high antioxidant activity (Vinson *et al*. 2001). The Consumption of lingonberries and bilberries has been proved in preventing human cancer which is ascribed to the high levels of phenolic and anthocyanin compounds (Faria *et al*. 2010; Yang and Kortesniemi 2015). The average total antioxidant capacity, total phenol content, total flavonoid content of berries were 32.79, 4.98, and 5.18 μmol g^{-1}, respectively. In the study of Islam *et al*. (2017) on genus *Lycium*, the mean of the antioxidant activity for red goji berry (S7; *Lycium barbarum*) and black goji berry (S9; *Lycium ruthenicum*) were measured as 16.65 and 34.28 μmol g^{-1}, respectively. In the report of Mustafa Ahmed *et al*. (2022) on genus *Vaccinium*, the mean of total phenol content, total flavonoid content, and antioxidant capacity were reported as 3.73 mg g^{-1}, 2.57 mg g^{-1}, and 17.67 μmol g^{-1}, respectively.

In the present study, we provide a detailed karyotype analysis for 12 berries species. Our goals were to confirm the number of chromosomes, karyotype determination, estimate the nuclear genome size, assess the phenolic profile, antioxidant properties, and flavonoid content of these twelve species, and provide scientific insight into the phenolic and antioxidant functions of these species to consumers and nutraceutical industry.

MATERIALS AND METHODS

Plant materials

Seeds were kindly provided by the Cultivation Development Company of Berries (Mazandaran, Iran). The culture medium used was MS (Murashige and Skoog 1962) with macroelements at 1/3 (Rache and Pacheco 2010), 1/8, and 1/16 of its original concentration (NH_4NO_3: 1650 mg l^{-1}, KNO_3: 1900 mg l^{-1}, KH_2PO_4: 170 mg l^{-1}, $CaCl_2H_2O$: 440 mg l^{-1} and $MgSO_4.7H_2O$: 370

Table 1. Specifications of berry species collection sites (Berry spp.) used in this research.

Species codes	English name	Scientific name	Localities	Longitude (E); Latitude (N)	Altitude (m)
S1	Strawberry	*Fragaria vesca* subsp. *vesca*	Iran, Mazandaran, sari	52°59'42.83"; 36°32'25.67"	83
S2	Blackberry	*Rubus fruticosus* cv. Qaemshahr	Iran, Qaemshahr	52°51'28.29"; 36°27'19.11"	282
S3	Black raspberry	*Rubus occidentalis* cv. Qaemshahr	Iran, Qaemshahr	52°51'28.29"; 36°27'19.11"	282
S4	Black currant	*Ribes nigrum*	USA, Arizona, Pinal	111°17'04.21"; 32°48'58.34"	660
S5	Red currant	*Ribes rubrum*	USA, Arizona, Pinal	111°17'04.21"; 32°48'58.34"	660
S6	Goose berry	*Ribes uva-crispa*	USA, Arizona, Pinal	111°17'04.21"; 32°48'58.34"	660
S7	Red goji berry	*Lycium barbarum*	USA, Arizona, Pinal	111°17'04.21"; 32°48'58.34"	660
S8	Goji berry	*Lycium infaustum*	USA, Arizona, Pinal	111°17'04.21"; 32°48'58.34"	660
S9	Black goji berry	*Lycium ruthenicum*	USA, Arizona, Pinal	111°17'04.21"; 32°48'58.34"	660
S10	Blueberry	*Vaccinium corymbosum*	USA, Maine	68°59'05.21"; 45°11'18.34"	426
S11	White mulberry	*Morus alba* cv. Mashhad	Iran, Karaj, Mohammadshahr	51°00'13.27"; 35°44'23.12"	1228
S12	Red mulberry	*Morus rubra* cv. Karaj	Iran, Karaj, Mohammadshahr	51°00'13.27"; 35°44'23.12"	1228

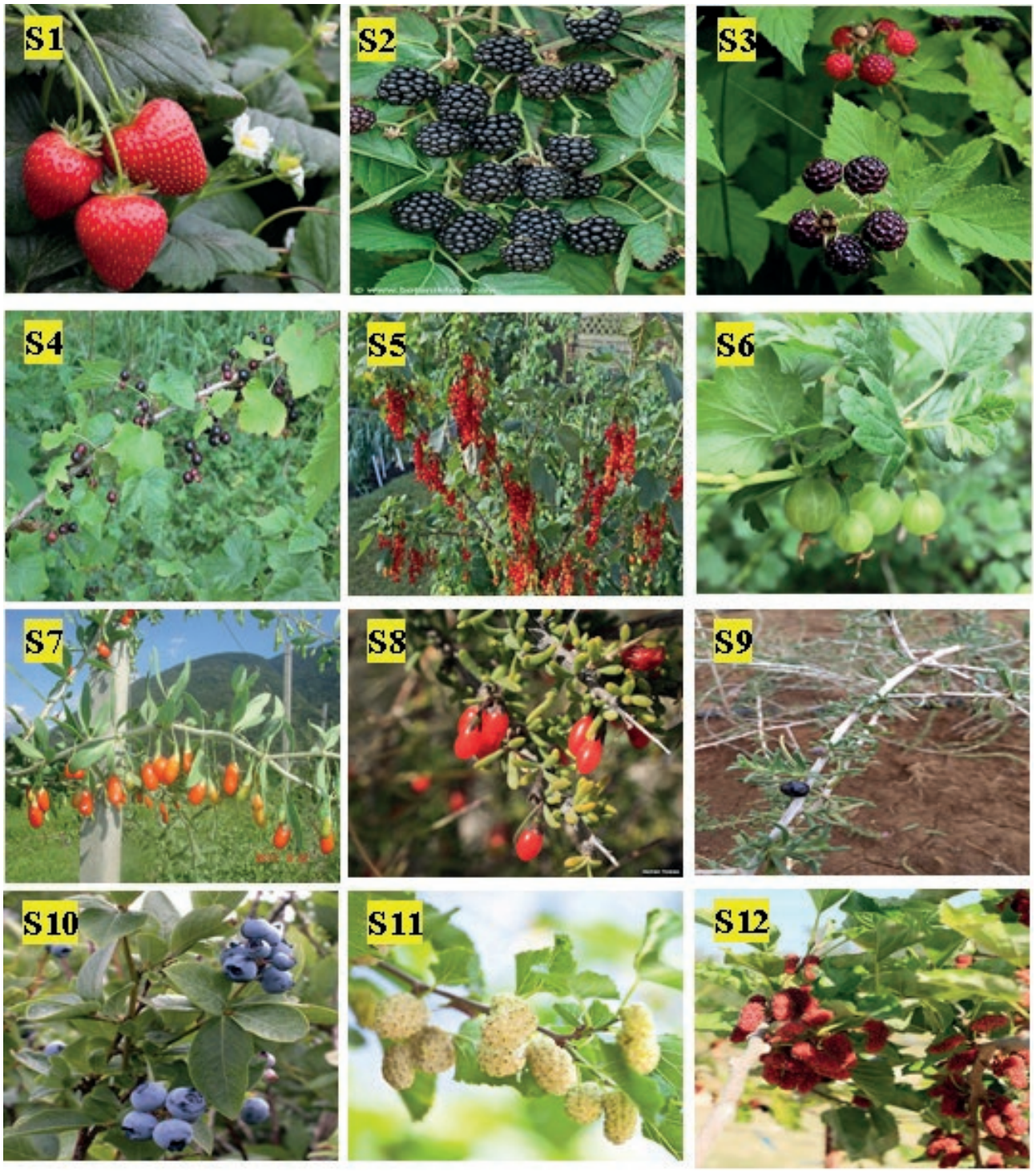

Figure 1. The picture of berry species that studied in this research.

mg l^{-1}). The medium was adjusted to pH = 5.8 and autoclaved for 20 min at 121°C. These plants were grown in a greenhouse at the college of Agriculture, Tarbiat Modares University (TMU). Voucher specimens of the examined species are preserved in the herbarium of the Research Institute of Forests and Rangelands of Iran (TARI) and the Tarbiat Modares University of Iran (TMU). Also, the images of species are shown in Figure

1. All cultures were maintained in a growth chamber at 25 °C, using a 16 h light/8 h dark photoperiod. The light was supplied, using white fluorescent lamps at an intensity of 50 μmol m^{-2} s^{-1}.

Karyomorphology

The best method to study mitosis for preparing a karyotype is root tip meristem tissue, which was used for cytogenetic studies. For the cytological preparations, growing roots about 1 cm long were removed at the appropriate time (when the largest number of cells are in metaphase) and pretreated in 0.002 mol 1–1 8-hydroxyquinoline for 4h at room temperature (RT) in the dark to induce metaphase arrest, followed by washing twice (each for 5 min) in distilled H_2O and fixing in fresh 3:1 (v/v) absolute ethanol: glacial acetic acid for 24 h at 4 °C. The fixed roots were hydrolyzed in 1 M HCl for 7-10 min at 60°C washed two times (each for 5 min) in distilled H_2O and stained in 1% (w/v) aceto-orcein for 3 h or in 4% (w/v) Hematoxylin for 4 h at RT.

Five well-spread monolayer metaphase plates from different individuals were analyzed per species. High-resolution microscopic digital photographs were taken, using an Olympus BX50 microscope (Olympus Optical Co., Tokyo, Japan), equipped with an Olympus DP12 digital camera (Olympus Optical Co.). Eight chromosomal parameters were either measured as long (L) and short (S) arm lengths or calculated as chromosome length (CL), arm ratio (AR; L/S), r-value (S/L), total chromosome volume (TCV = πr^2 CL), where r = average chromosome radius, percentage of total chromosome form (F%), and centromeric index (CI = S/CL). Idiograms were drawn from the mean values, and chromosome types were determined, using the formula of Levan *et al*. (1964). For karyotypic analysis, five parameters, including karyotype total form percentage (TF% = ΣS/ΣCL × 100), coefficient of variation of total chromosome length (CV_{CL}% = (total CL standard deviation/total CL mean) × 100), mean centromeric asymmetry (M_{CA} = A × 100), where the degree of karyotype asymmetry (A = [Σ(L-S/L+S(/n] × 100(, Stebbins (1971) asymmetry categories (ST), and Romero-Zarco (1986) indices: intrachromosomal asymmetry index (A1) and interchromosomal asymmetry index (A2), were measured.

Flow cytometric genome size estimation

Relative DNA content was determined, using PI-stained flow cytometry. Young leaves of the analyzed individuals and a reference standard (either *Solanum lycopersicum*; 2C = 1.96 pg., *Petroselinum crispum*; 2C = 4.45 pg., or *Zea mays*; 2C = 5.43 pg) were co-chopped with a razor blade in a glass petri dish, containing 1 ml of ice-cold WPB buffer (Woody Plant Buffer; 0.02 M Tris-HCl, 4 mM $MgCl_2.6H_2O$, 2 mM EDTA $Na_2.2H_2O$, 86 mM NaCl, 10 mM Sodium metabisulfite, 1% PVP-10, and 1% (v/v) Triton X-100, pH 7.5) (Loureiro *et al*. 2007). The crude nuclei suspension was filtered through a 50-μm nylon mesh. RNase and propidium iodide (each 50 μg ml^{-1}) was then added. After incubation for two min at RT, the relative fluorescence intensity of nuclei was analyzed. At least 5000 nuclei were analyzed in each measurement with CV% (coefficient of variation; %) values below 5.0%. Subjects were randomly selected for the flow cytometric analysis. The DNA amount of a sample was calculated based on the values of the G1 peak means (Doležel *et al*. 2003, 2007; Doležel and Bartoš 2005) as follows:

Sample 2C*x* DNA (pg) = (Sample G1 peak mean/Standard G1 peak mean) × Standard 2C DNA (pg).

The obtained data were initially checked for the normality test and analyzed, using SPSS (Version 22) and Minitab 17. The karyotypic, flow cytometric, and phytochemical content data were first tested for the normality and then analyzed based on a completely randomized design (CRD) with 5, 3, and 3 replications, respectively. The results were statistically evaluated by analysis of variance (*ANOVA*) and expressed as mean. Means comparisons were performed, using the LSD test with SPSS; differences were considered statistically significant at $P \leq 0.01$ and $P \leq 0.05$. Linear regression analysis was carried out to find out the relationship between monoploid 2Cx DNA values and some traits, using Minitab 17.

Chromatographic analysis

The method used to determine total polyphenol content (TPC) was based on Folin-Ciocalteu phenol reagent and spectrophotometric determination at 765 nm. The method used to determine the total flavonoid content (TFC) was based on aluminum chloride and spectrophotometric determination at 420 nm. Antioxidant activity in the berries fruit pulp was evaluated by a 2,2-diphenyl-1-picrylhydrazyl (DPPH) assay (Laczkó-Zöld *et al*. 2018).

Total Antioxidant Capacity (TAC)

The scavenging activity for DPPH radicals was determined using spectrophotometric analysis accord-

ing to a modified method of Lalegani *et al.* (2018). Briefly 100 µl sample solution was added to 900 µl of 0.1 M DPPH solution and mixed thoroughly at RT. Absorbance at 517 nm was determined after 30 min.

Total Phenolic Content (TPC)

The TPC was estimated, using the Folin- Ciocalteu colorimetric method described by Barreca *et al.* (2016). A 20 µl of methanolic extract was added to 2 ml of deionized water, and 100 µl of dilutions Folin- Ciocalteu was then added. After 1-8 min (average 5 min), 300 µl of Sodium carbonate 7% (w/v) was added to it, and the absorbance was measured in the dark at 765 nm after incubation for 2 h at RT. Quantification was done based on the standard curve of gallic acid. Results were expressed as equivalent of the gallic acid (GAE), i.e., mg gallic acid g^{-1} DW.

Total Flavonoid Content (TFC)

The TFC was estimated, using the aluminum chloride method described by Barreca *et al.* (2016). In this method, a 600 µl of methanolic extract was added to 600 µl of 2% (w/v) Aluminum chloride, and after 10 min, the absorbance was measured at 420 nm. Quantification was done based on the standard curve of quercetin. The TFC was calculated and expressed as quercetin equivalents, i.e., mg quercetin g^{-1} DW.

RESULTS

Karyomorphologic analysis

In the current study, one chromosome type "m" formed karyotype formulas of "14m" for *Fragaria vesca* subsp. *vesca* (S1), *Rubus fruticosus* cv. Qaemshahr (S2), and *Rubus occidentalis* cv. Qaemshahr (S3), "16m" for *Ribes nigrum* (S4), *Ribes rubrum* (S5), and *Ribes uva-crispa* (S6), "24m" for *Lycium barbarum* (S7), *Lycium infaustum* (S8), *Lycium ruthenicum* (S9), and *Vaccinium corymbosum* (S10), and "28m" for S11 and S12 (*Morus alba* cv. Mashhad (S11), *Morus rubra* cv. Karaj (S12). The base chromosome number in *Fragaria vesca* subsp. *vesca*, *Rubus fruticosus* cv. Qaemshahr, *Rubus occidentalis* cv. Qaemshahr; is $x = 7$; *Ribes nigrum*, *Ribes rubrum*, *Ribes uva-crispa* $x = 8$; *Lycium barbarum*, *Lycium infaustum*, *Lycium ruthenicum*, *Vaccinium corymbosum* $x = 12$; *Morus alba* cv. Mashhad, *Morus rubra* cv. Karaj $x = 14$, and all of these species are diploid with $2n = 14$, 16, 24, and 28.

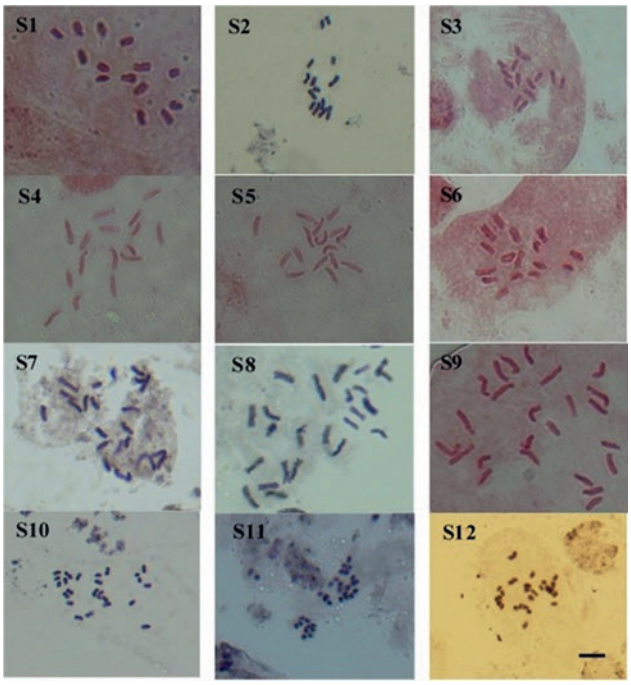

Figure 2. Somatic chromosomes of 12 berry species. Scale bar = 5 µm.

ANOVA shows significant ($P < 0.01$) differences between the berries species for the most studied chromosomal parameters (Table 2). Karyotypes of somatic complement and the idiograms of the haploid comple-

Table 2. ANOVA for chromosomal parameters of berry species.

S.O.V.	DF	MS							
		S	L	CL	AR	r-value	F%	TCV	CI
Species	11	7.413**	8.825**	20.685**	0.128**	0.128**	23.661**	49.778**	0.199**
Error	593	0.039	0.046	0.11	0.017	0.017	0.121	0.422	0.057
Total	604								

**Significant difference at $P < 0.01$

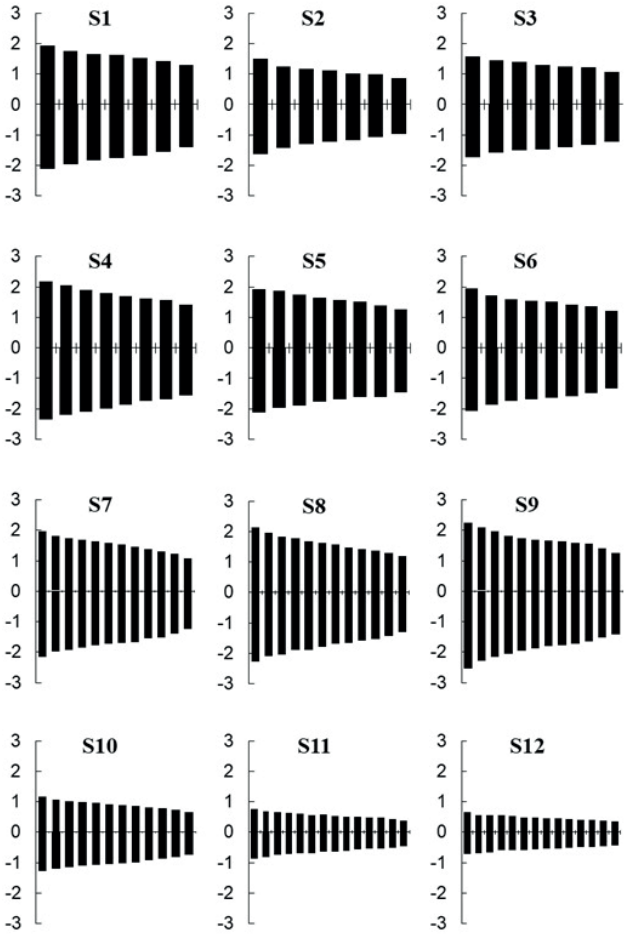

Figure 3. Idiograms of haploid chromosomes of 12 berry species.

ment of studied berries are demonstrated in Figures 2 and 3, respectively. The mean value of chromosome length (CL) was 2.83 µm, varying from 1.06 µm (*Morus rubra* cv. Karaj; S12) to 3.75 µm (*Ribes nigrum*; S4). The mean TCV was 1.6 µm, ranging from 0.10 µm (S10) to 6.19 µm (S1). The mean CI of the complement varied from 46% (S12) to 51% (S5). The studied berry species showed different symmetrical groups according to various karyotypic symmetrical indices. For instance, the highest value of total form percentage of karyotype (TF%) was detected in S5 (50.51%; Table 3; the most symmetric), and the lowest value was identified in S12 (46.28%; the most asymmetric). The highest and the lowest values of coefficient of variation (CV_{CL}%) were identified on S11 (18.03%; the most asymmetric) and S3 (11.98%; the most symmetric), respectively. On the other hand, karyotypes of all these species were classified in 1A class of Stebbins classification (Stebbins 1971; Table 3). The basic chromosome number for these ber-

Table 3. Karyotypic symmetry formula and flow cytometric genome size of 12 berry species. Total form percentage of karyotype (TF%), mean centromeric asymmetry (M_{CA}%), coefficient of variation of chromosome length (CV_{CL}%), karyotype formula (KF), Stebbins asymmetry categories (ST), intrachromosome asymmetry index (A1), interchromosome asymmetry index (A2), m: metacentric, M: metacentric. Means with the same symbol letter in the "2C*x* DNA (pg)" column are not significantly different (P > 0.01), using LSD test.

Species	Asymmetry indices (Romero-Zarco, 1986)		ST	KF	CV_{CL}%	M_{CA}%	TF%	2C*x* DNA (pg)
	A1	A2						
S1	0.46	0.13	1A	14m	13.38	4.37	47.79	2.10^{d}
S2	0.47	0.18	1A	14m	17.71	4.91	47.59	1.55^{g}
S3	0.47	0.12	1A	14m	11.98	4.73	47.66	0.86^{i}
S4	0.39	0.14	1A	16m	14.21	4.31	47.86	1.86^{e}
S5	0.33	0.16	1A	16m	16.17	4.54	50.51	1.94^{e}
S6	0.39	0.15	1A	16m	14.61	4.30	47.98	1.94^{e}
S7	0.10	0.16	1A	24m	15.82	5.35	47.38	3.93^{b}
S8	0.09	0.17	1A	24m	16.65	4.73	47.68	3.82^{b}
S9	0.09	0.16	1A	24m	16.51	4.75	47.60	5.15^{a}
S10	0.11	0.16	1A	24m	15.63	5.91	47.07	2.53^{c}
S11	0.00	0.18	1A	28m	18.03	7.31	46.37	1.65^{f}
S12	0.00	0.16	1A	28m	16.05	7.58	46.28	1.18^{h}

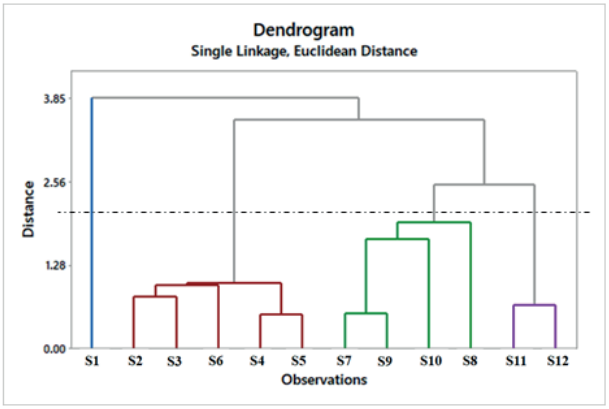

Figure 4. Dendrogram shows relationships of similarity among studied 12 berry species related to all chromosomal characteristics, constructed using Euclidean distance and Single method; cophenetic correlation r = 0.75.

three groups. To determine total variation in berries and parameters quota in total variation, the principal component analysis (PCA) of the karyotypic parameters was performed. The single dendrogram constructed based on karyotype similarities (Figure 3) shows four major clus-

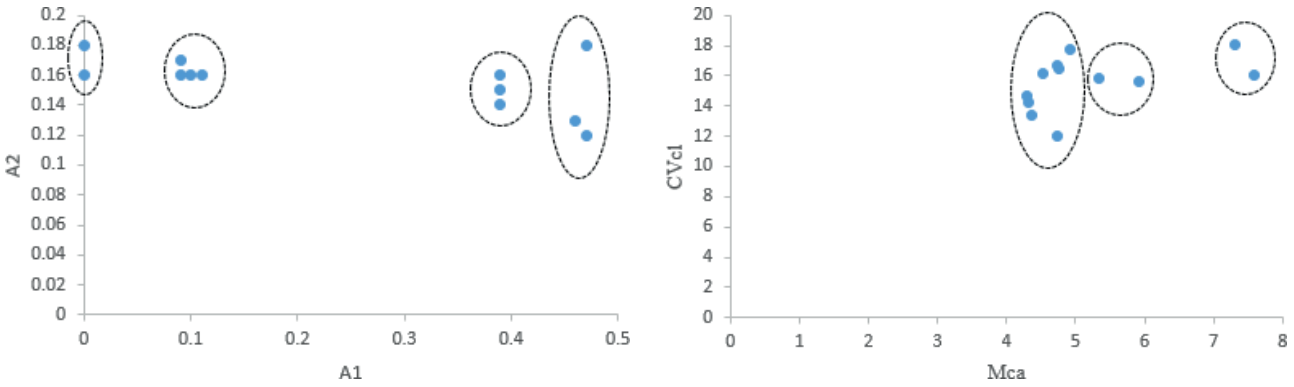

Figure 5. Scatter diagram of 12 berry species: Romero-Zarco asymmetry indices (a), CVCL and MCA (b).

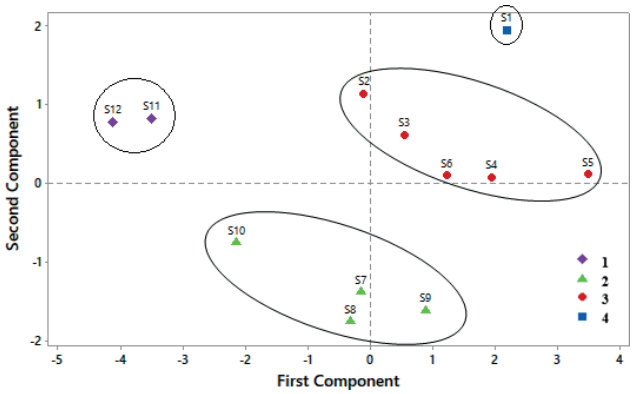

Figure 6. Diagram resulted from principal components analysis 1 (highly related to the position of centromere) and 2 (strongly related to the length of the complements) of studied berry species.

ters. The first cluster consists of S11 and S12, the second cluster consists of S7-S10, and the third cluster consists of S2-S6, while S1 is separated within the fourth cluster.

Nuclear genome size estimation

The resultant flow cytometric data were first tested for normality test and then analyzed according to a completely randomized design (CRD) with 3 replicate cells. The monoploid genome size (2C*x* DNA) of these twelve species (*Fragaria vesca* subsp. *vesca*, *Rubes fruticosus* cv. Qaemshahr, *Rubus occidentalis* cv. Qaemshahr, *Ribes nigrum*, *Ribes rubrum*, *Ribes uva-crispa*, *Lycium barbarum*, *Lycium infaustum*, *Lycium ruthenicum*, *Vaccinium corymbosum*, *Morus alba* cv. Mashhad, *Morus rubra* cv. Karaj) were 2.1, 1.55, 0.68, 1.86, 1.94, 1.94, 3.93, 3.82, 5.15, 2.53, 1.65, and 1.18 pg, respectively (Table 3). The differences in nuclear DNA contents among these analyzed species were statistically significant ($P < 0.01$). The highest value was detected in *Lycium ruthenicum* (S9, 5.15 pg), while *Rubus occidentalis* cv. Qaemshahr (S3) was the lowest (0.68 pg), and the mean total value was 2.36 pg (Table 3).

The histograms obtained for analyzing nuclear DNA contained two peaks (Figure 6). The left peaks in S7 to S10 refer to the known samples reference standard, and the right peaks to the unknown samples. In other species, the peaks on the left refer to unknown specimens, and the peaks on the right refer to the reference standard of known specimens. Young leaves of berries spe-

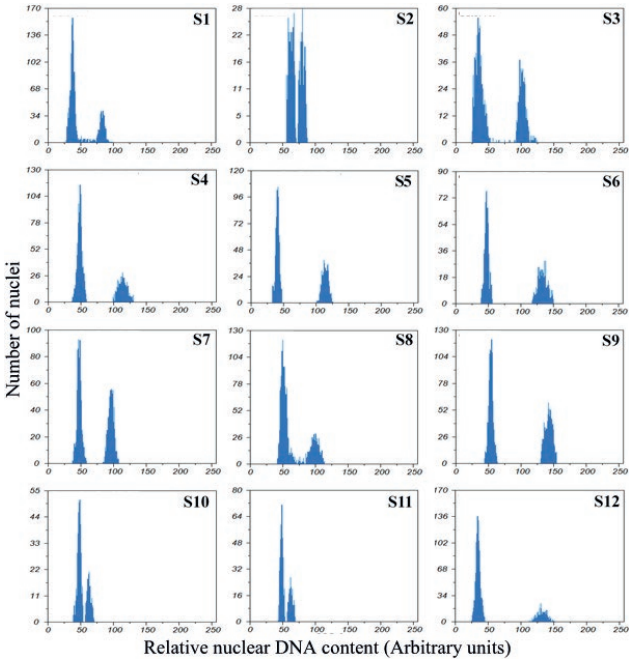

Figure 7. Histograms of relative fluorescence intensity were obtained, using WPB isolation buffer after simultaneous analysis of nuclei isolated from standard plant and berry species plants. The mean channel number and coefficient of variation (CV%) value of each peak are also given.

cies contain many cytosolic compounds such as phenolic acids and flavonoids, which can interfere with the fluorescent staining of nuclear DNA. To compensate this problem, a new isolation buffer, WPB, was developed to analyze problematic or woody species because the Sodium metabisulfite and PVP-10 in WPB act as reducing and binding agents to prevent the action of interfering phenols and secondary metabolites. This buffer was found to be suitable for the analysis of *Lycium* species, as evidenced by the CV of DNA peak and flow cytometric histograms of relative fluorescence intensity. Phylogenetic analysis revealed that *Lycium* species are included in a monophyletic group, indicating a very close evolutionary relationship. This study discovered significant differences in the genome size among these three species (*L. barbarum, L. ruthenicum,* and *L. infaustum*). It was also shown in *Ribes*, *Rubus*, and *Morus* species. There is excellent genome size variation between species. It has been proposed that having a large genome has direct physiological consequences for plants, such as earlier flowering time, larger stomata size, and longer life cycles than small genomes. The flowering time may be partly affected by differences in DNA content.

Phytochemical studies

ANOVA shows significant ($P < 0.01$) differences between the berries species for the three studied phytochemical traits, including total antioxidant capacity (TAC), total phenol content (TPC), and total flavonoid content (TFC). The mean comparisons are shown in Table 4, using LSD test at 0.01 probabilty level. The average total antioxidant capacity (TAC; Table 4) of berries was 32.79 μmol g^{-1}, ranging from 6.92 μmol g^{-1} (S1; *Fragaria vesca* subsp. *vesca*) to 63.84 μmol g^{-1} (S3; *Rubus occidentalis* cv. Qaemshahr). The average total phenol content (TPC; Table 4) of berries was 4.98 μmol g^{-1}, ranging from 3.08 μmol g^{-1} (S12; *Morus rubra* cv. Karaj) to 8.61 μmol g^{-1} (S9; *Lycium ruthenicum*). The average total flavonoid content (TFC; Table 4) of berries was 5.18 μmol g^{-1}, ranging from 2.43 μmol g^{-1} (S12; *Morus rubra* cv. Karaj) to 10.63 μmol g^{-1} (S9; *Lycium ruthenicum*). Black raspberry (S3; *Rubus occidentalis* cv. Qaemshahr) in terms of all three phytochemical traits, had the highest score among all berry species.

Interestingly, the level of antioxidant activity of black raspberry (S3; *Rubus occidentalis* cv. Qaemshahr) had statistically significant difference among all studied berry species in the present study at a probability level of 1%. For example, it had 6.6-fold increase over strawberry (S1; *Fragaria vesca* subsp. *vesca*) and a 24% increase over Black currant (S4; *Ribes nigrum*). In the next positions, Goose berry (S6; *Ribes uva-crispa*) and Black currant (S4; *Ribes nigrum*) had the highest values, respectively. Moreover, strawberry (S1; *Fragaria vesca* subsp. *vesca*) and Goji berry (S8: *Lycium infaustum*) had the lowest one.

Table 4. Information obtained from phytochemical evaluation of studied 12 berry species. Total Antioxidant Capacity (TAC), Total Flavonoid Content (TFC), Total Phenol Content (TPC). In each column, means with the same symbol letter are not significantly different ($P > 0.01$), using LSD test.

Species	TAC (μmol g^{-1})	TFC (mg g^{-1})	TPC (mg g^{-1})
S1	9.62^{h}	2.47^{f}	3.08^{f}
S2	38.40^{c}	5.40^{c}	5.75^{b}
S3	63.84^{a}	9.60^{a}	7.92^{a}
S4	51.57^{b}	6.50^{b}	5.82^{b}
S5	24.56^{e}	3.43^{d}	3.73^{d}
S6	52.19^{b}	9.23^{a}	7.68^{a}
S7	25.06^{e}	3.45^{d}	4.07^{c}
S8	16.38^{g}	2.57^{ef}	3.17^{ef}
S9	34.95^{c}	10.63^{a}	8.61^{a}
S10	27.50^{de}	2.77^{e}	3.28^{e}
S11	29.11^{d}	3.70^{d}	3.59^{d}
S12	20.32^{f}	2.43^{f}	3.08^{f}
Average (range)	32.79 (9.62-63.84)	5.18 (2.43-10.63)	4.98 (3.08-8.61)

DISCUSSION

Our results provided the basic genetic, genomic and phytochemical information for these species, which are helpful for the construction of genetic and physical maps and whole-genome sequencing in the future and provide scientific insight into the phenolic and antioxidant functions to consumers and the nutraceutical industry.

For the first time, some of these species' chromosome number and karyotype were determined in Iran. Chromosome numbers $2n = 2x = 14$, 16, 24, and 28 in these berry species are consistent with other reports. Differences in the karyotype formula of these species, which are geographically, climatically, and habitually different from each other, indicating the existence of chromosomal structural changes in the process of karyotype evolution and species formation in these species. It varies according to geographical and climatic conditions. Structural changes in the speciation process of these species can be changed such as displacements, inversions, and other structural changes. According to Stebbins

(1971), cytogenetic studies can be used to understand better the relationships between species and different populations of a species and to orient the evolutionary tendencies of plants. Each of these plants shows a unique adaptation to the environment in which they grow. As this compromise increases, new varieties or species may appear in plant communities. This study developed an important tool to assess berries' chemical composition and bioactivity, using different chromatographic methods for its fruits' comprehensive authentication and quality control. In the present study, all chromosomal parameters were significantly different. Differences between species for all karyological parameters confirm the intraspecific chromosomal variations. These results are in agreement with those reported by Chen *et al*. (2013). In the current study, one chromosome type ("m") formed karyotype formulas of "14m" for S1-S3 (*Fragaria vesca* subsp. *vesca*, *Rubus fruticosus* cv. Qaemshahr, *Rubus occidentalis* cv. Qaemshahr), "16m" for S4-S6 (*Ribes nigrum*, *Ribes rubrum*, *Ribes uva-crispa*), "24m" for S7-S10 (*Lycium barbarum*, *Lycium infaustum*, *Lycium ruthenicum*, *Vaccinium corymbosum*), and "28m" for S11 and S12 (*Morus alba* cv. Mashhad, *Morus rubra* cv. Karaj). Similar to our findings, Chen *et al*. (2013) reported the same one chromosome type in *Lycium* species. In the present study, the average total length of chromosomes (CL) in the studied species is 2.83 μm. Karyotype symmetry was more indicative of evolutionary traits in the studied berries species, regardless of ploidy levels. To determine the karyotypic symmetry, several properties were examined in 12 species. Based on TF%, S6 with the highest value (47.98%) has the most symmetric, and S12 with the lowest value (46.28%) has the most asymmetric karyotype. Gradual changes and changes in TF% values may be due to chromosomal abnormalities. Structural changes in chromosome morphology probably due to chromosome duplication or translocation (exchange and displacement) between chromosomes (Das and Teng 1998). According to the CV_{CL}% index, S3 (11.98%) has the most symmetrical karyotype and S11 (18.03%) has the most asymmetric karyotype among other species. Overall, the coefficient of variation in the sample was low due to the metacentric nature of most chromosomes, indicating the symmetry and the uniformity of these karyotypes. In general, it can be concluded, species that are more evolutionarily advanced have variations in chromosome type and size and are therefore asymmetrically karyotypically. This asymmetry is exacerbated by the displacement of chromosomal fragments. Karyotypic dissimilarity in terms of karyotype symmetry measurement parameters can lead to failure in reproduction and inadequate seed production in the offspring while preventing successful intraspecific crosses. In other words, the results of such crosses may be somewhat sterile. In the study of Chen *et al*. (2013) on the genus *Lycium*, the chromosomal base number for red goji berry (S7; *L. barbarum*) and black goji berry (S9; *L. ruthenicum*) was reported to be 12, which is in complete agreement with the findings of the present study (Table 3). Costich *et al*. (1993) worked on the blueberry plant (S10; *Vaccinium corymbosum*) showed that the chromosomal base number was 12, which is consistent with the findings of the current study. For the genus *Ribes*, the base chromosome number 8 was reported by Chiche *et al*. (2003), which is matched for the three different species of this genus (S4; *R. nigrum*, S5; *Ribes rubrum*, S6; *R. uva-crispa*) in the present study.

On the other hand, karyotypes of all species were classified in 1A (Table 3) . For more detailed studies of asymmetry, Romero-Zarco (1986) indices of A1 and A2 were also calculated. The scatter diagram of these indices (Figure 4) presents four species groups. According to the analyzed asymmetry indices, S3 was demonstrated as the most symmetric species, while S2 and S11 were among the most asymmetric species. It has been suggested that karyotypes with more asymmetry have a derived status in comparison to those with more symmetrical morphology (Lakshmi *et al*. 1984). For example, differences in chromosome length (CL) may indicate the occurrence of cyclic changes in genome size during the diversification of the genus. Thus, the study of asymmetry indices and variation in genome size is a valuable means for the establishment of the evolutionary relationship between the species and the origin of diversification of the populations (Karimzadeh *et al*. 2011).

To determine the total diversity in the population and the quota of the parameters in the total diversity, principal component analysis (PCA) of the karyotypic parameters was performed. It shows that the first two main components make up 82% of the cumulative changes and they are predicted in a two-dimensional graph (Figure 5). The single dendrogram constructed on the basis of karyotype similarities (Figure 3) shows four major clusters. The first cluster consists of S11 and S12, the second cluster consists of S7-S10, and the third cluster consists of S2-S6, while S1 is separated within the fourth cluster. The arrangement of PCA species from this experiment is fully consistent with the analysis obtained by single grouping analysis. Therefore, the results of this study proposed that species within a cluster have the most homology in chromosomal variations. For this purpose, a cross between S7 and S8 or S9 is suggested because they have the most similarity in their chromosomal characteristics.

The mean monoploid 2C*x* DNA value was 2.35 pg in the studied species, verifying intraspecific genome size variation. On the other hand, the monoploid genome size (1C*x* DNA) varied from 420.54 Mbp (S3; *Rubus occidentalis* cv. Qaemshahr) to 2518.35 Mbp (S9; *Lycium ruthenicum*). According to the results (Chen *et al*. 2013), red goji berry (S7; *Lycium barbarum*) and black goji berry (S9; *Lycium ruthenicum*) had 2C*x* DNA values of 4.35 pg and 5.45 pg, respectively. In the present study, the genome size for the those was 3.93 pg and 5.15 pg, correspondingly, which is almost in agreement with the findings of the previous report. The existence of some deviation from this species may be due to the inter-species and intersex diversity. Knowing genome size may be useful in genome research and studies of relationships between DNA content, physiology, and plant ecology (Thiem and Sliwinska 2003). Reports of 2C*x* DNA in some berry species have been published, including S3; *Rubus occidentalis* = 0.60 pg, S5; *Ribes rubrum* = 1.94 pg, and S6; *Ribes uva-crispa* = 1.88 pg (Meng and Finn 2002; Chiche *et al*. 2003). In the present study (Table 3), the monoploid genome size (2C*x* DNA) for the latter three species is 0.68 pg, 1.86 pg, and 1.94 pg, respectively, which is in complete agreement with the findings of the two previous reports. In the present study, the existence of a statistically significant difference in the monoploid genome size indicates the interspecific and intersex diversity among berry species. On the other hand, the correlation between 2C*x* DNA with environmental conditions (longitude, latitude, and altitude), chromosome length, and the chromosome number showed that 2C*x* DNA in the studied berry species had a significant correlation with the chromosome length and chromosome number, and there were no significant correlations between 2C*x* DNA with environmental conditions. Hence, it is concluded that the genome size of berries species is independent of changes in environmental conditions.

Antioxidant properties estimated by antioxidant assays (DPPH) showed significant differences among different concentrations. Evaluation of total polyphenol content in samples is a widely used method to determine the number of antioxidants in the samples. A rapid, simple, and inexpensive method to measure the antioxidant capacity of food involves the use of the free radical 2,2-Diphenyl-1-picrylhydrazyl (DPPH). DPPH radicals are frequently utilized in antioxidant studies. DPPH is widely used to test the ability of compounds to act as free radical scavengers or hydrogen donors and evaluate the antioxidant activity of foods. Antioxidants in a sample can scavenge the DPPH radicals. A gradual reduction in absorbance is observed, indicating that DPPH radicals are being scavenged. Through adding samples, which are rich in antioxidants, to a DPPH solution. Therefore, the percentages we have presented pertain to DPPH radical scavenging capacity, which is directly proportional to antioxidant capacity. The total phenolic content of dry fruits showed a wide range, with values ranging from 3.08 mg GAE/g (S1; *Fragaria vesca* subsp. *vesca*) to 8.61 mg GAE/g (S9; *Lycium ruthenicum*) shown in Table 4. By comparing these data, it can be concluded that the S3 (*Rubus occidentalis* cv. Qaemshahr) has a high amount of antioxidants. The total flavonoid content (TFC) of dried fruits showed a wide range, with values ranging from 2.43 g QE/g (S12; *Morus rubra* cv. Karaj) to 10.63 g QE/g (S9; *Lycium ruthenicum*) as shown in Table 4.

Based on the above studies and considering the diversity of these 12 species in terms of cytology and phytochemistry, it is concluded that some of these species are prone to enter the daily food basket. Black raspberry (S3; *Rubus occidentalis* cv. Qaemshahr) had the highest value in terms of all three phytochemical traits, followed by goose berry (S6; *Ribes uva-crispa*) and black currant (S4; *Ribes nigrum*), respectively. Strawberry (S1; *Fragaria vesca* subsp. *vesca*) and red mulberry (S12; *Morus rubra* cv. Karaj) had the lowest value. We report that black raspberry (S3; *Rubus occidentalis* cv. Qaemshahr) is a remarkable source of antioxidant compounds compared to other fruits. Hence, research supports deep-colored fruits as potent antioxidant sources. Berries and dried fruit compose a relatively small part of the average diet, but they are important antioxidant sources. Highly pigmented berries have the highest antioxidant activity. Such fruits are rich in antioxidant compounds that are known for their enhanced stability and bioaccessibility. Based on our findings and the cited literatures, it can be suggested that black raspberries are among the fruits that provide antioxidants. In the study of Islam *et al*. (2017) on genus *Lycium*, the mean of total phenol content, total flavonoids content, and antioxidant activity for red goji berries (S7; *Lycium barbarum*) were measured as 3.16 mg g^{-1}, 2.83 mg g^{-1}, and 16.65 μmol g^{-1} respectively. These values were 8.33 mg g^{-1}, 11.03 mg g^{-1}, and 34.28 μmol g^{-1} respectively for black goji berry (S9; *Lycium ruthenicum*). In the present study (Table 4), these values were 4.07 mg g^{-1}, 3.45 mg g^{-1}, and 25.06 μmol g^{-1} respectively, for S7 with a significant increase of 29%, 22%, and 50% in all three cases, respectively, compared to the previous report of red goji berry (S7; *Lycium barbarum*). Also for S9, these values are reported 8.61 mg g^{-1}, 10.63 mg g^{-1}, and 34.95 μmol g^{-1}, respectively, which is almost equal to the previous report for (S9; *Lycium ruthenicum*). In the study of Mustafa Ahmed *et al*. (2022) on genus *Vaccinium*, the mean of total phenol

Table 5. Correlation coefficients between phytochemical traits of 12 berry species with chromosome number, chromosome length, the monoploid genome size (2C*x* DNA), and environmental conditions

Phytochemical traits	Latitude (N)	Longitude (E)	Altitude (m)	Chromosome (No.)	CL (µm)	2C*x* DNA (pg)
Total phenol content (mg g^{-1})	-0.28^{ns}	0.29^{ns}	-0.30^{ns}	-0.38*	0.40*	0.10^{ns}
Total flavonoid content (mg g^{-1})	-0.29^{ns}	0.29^{ns}	-0.25^{ns}	-0.34*	0.39*	0.09^{ns}
Antioxidant capacity (DPPH) (µmol g^{-1})	-0.09^{ns}	0.10^{ns}	-0.19^{ns}	-0.44*	0.08^{ns}	-0.34*

^{ns}, *, **: Non significant (P > 0.05), significant differences (P < 0.05) and (P < 0.01), respectively.

content, total flavonoid content, and antioxidant capacity were reported as 3.73 mg g^{-1}, 2.57 mg g^{-1}, and 17.67 µmol g^{-1}, respectively. In the present study (Table 4), these values were 3.28 mg g^{-1}, 2.77 mg g^{-1}, and 27.50 µmol g^{-1}, respectively which are almost in agreement with those in the previous report.

In the current study, the correlation was carried out between phytochemical traits with chromosome number, chromosome length, the monoploid genome size (2Cx DNA), and environmental conditions (latitude and altitude). The results showed no significant correlation between phytochemical traits of species with environmental conditions, but there was a significant correlation between phytochemical traits with chromosome number, antioxidant activity with genome size, total phenol with chromosome length, and total flavonoid with chromosome length (Table 5). From these results, it is inferred that phytochemical traits in the studied species are independent of changes in environmental conditions.

For traits that had a significant correlation between them in the table above, linear regression analysis was performed (Figure 7).

Figure 7 shows that the monoploid genome size (2C*x* DNA) has a direct linear relationship with chromosome length and chromosome number of berry plants (Figures a, and b). Antioxidant has an inverse linear relationship with the genome size and chromosome number (Figures c, and d). It means that berries with fewer chromosomes and smaller genome sizes produce more antioxidants. Phenol and flavonoid have an inverse linear relationship with the chromosome number (Figures e, and f), but a direct relationship with the chromosome length (Figures g, and h).

For further study, the correlation between genome size and chromosome length for four species (S7, S8, S9, S10) with the same chromosome number ($2n = 2x = 24$) was also calculated and was significant at the 1% probability level ($r = 0.89^{**}$). Therefore, Figure 8 shows the relationship of the direct linear regression between the monoploid genome size and chromosome length for the four species mentioned above.

In another study, the effect of different ploidy levels on the quantity and quality of essential oils of different species of berry was investigated and their genetic modification was provided. It is suggested that these berry species should be compared with other species in Iran in terms of cytogenetics and phytochemistry. It is suggested that due to significant differences in genome size and morphology, further research should pin-point rDNA (5S and 45S) sites and additional repetitive DNA elements, using fluorescence *in situ* hybridization (FISH) to better uncover the processes involved in the chromosome evolution of these twelve berry species.

ACKNOWLEDGMENTS

Thanks to Tarbiat Modares University for financial support, and to the Cultivation Development Company of Berries for sharing berry species from the USA.

REFERENCES

Abedi R, Babaei A, Karimzadeh G. 2015. Karyological and flow cytometric studies of Tulipa (Liliaceae) species from Iran. Plant Systematics and Evolution. 301: 1473-1484.

Ahmadu T, Ahmad K. 2021. An introduction to Bioactive natural products and general applications. In Bioactive Natural Products for Pharmaceutical Applications. Springer, Cham.140: 41-91.

Amosova AV, Zoshchuk SA, Rodionov AV, Ghukasyan L, Samatadze TE, Punina EO, Loskutov IG, Yurkevich OY, Muravenko OV. 2019. Molecular cytogenetics of valuable Arctic and sub-Arctic pasture grass species from the Aveneae/Poeae tribe complex (Poaceae). BMC genetics. 20(1): 1-16.

Barreca D, Laganà G, Leuzzi U, Smeriglio A, Trombetta D, Bellocco E. 2016. Evaluation of the nutraceutical, antioxidant and cytoprotective properties of ripe pistachio (Pistacia vera L., variety Bronte) hulls. Food Chemistry. 196: 493-502.

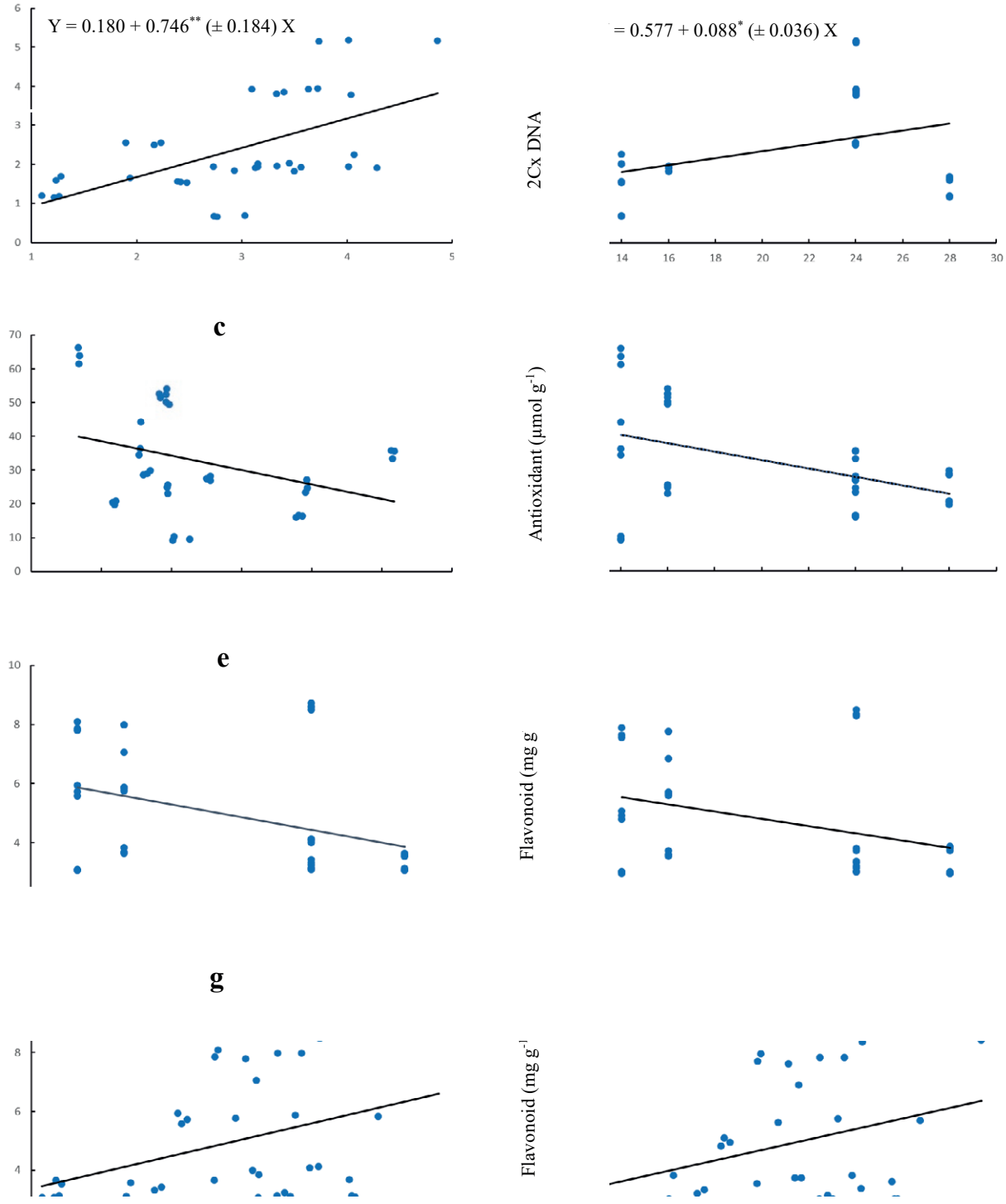

Figure 8. Diagrams of linear regression relationships between different traits of studied berry plants

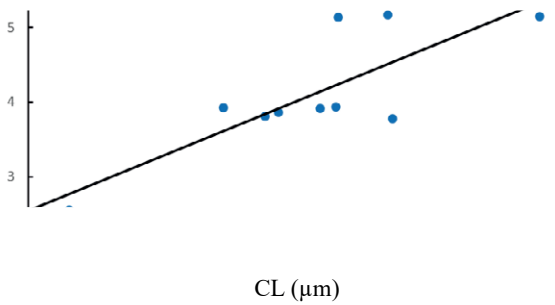

Figure 9. Diagram of the linear regression relationship between genome size and chromosome length for four species (S7-S10) with the same chromosome number ($2n = 2x = 24$).

Basu A, Rhone M, Lyons TJ. 2010. Berries: emerging impact on cardiovascular health. Nutrition reviews 68(3): 168-177.

Basu A. 2019. Role of berry bioactive compounds on lipids and lipoproteins in diabetes and metabolic syndrome. Nutrients. 11(9): 1983.

Bernardello G, Stiefkens L, Las Penas ML. 2008. Karyotype studies in Grabowskia and Phrodus (Solanaceae). Plant Systematic and Evolution. 275: 265-269.

Blumberg JB, Camesano TA, Cassidy A, Kris-Etherton P, Howell A, Manach C, Ostertag LM, Sies H, Skulas-Ray A, Vita JA. 2013. Cranberries and their bioactive constituents in human health. Advances in Nutrition. 4(6): 618-632.

Briskin DP. 2000. Medicinal plants and phytomedicines. Linking plant biochemistry and physiology to human health. Plant Physiology. 124(2): 507-514.

Chen J, Liu X, Zhu L, Wang Y. 2013. Nuclear genome size estimation and karyotype analysis of *Lycium* species (Solanaceae). Scientia Horticulturae. 151: 46-50.

Chiche J, Brown SC, Leclerc JC, Siljak-Yakovlev S. 2003. Genome size, heterochromatin organisation, and ribosomal gene mapping in four species of Ribes. Canadian Journal of Botany. 81(11): 1049-1057.

Costich DE, Ortiz R, Meagher TR, Bruederle LP, Vorsa N. 1993. Determination of ploidy level and nuclear DNA content in blueberry by flow cytometry. Theoretical and Applied Genetics. 86(8): 1001-1006.

Das, TK, Teng BS. 1998. Between trust and control: Developing confidence in partner cooperation in alliances. Academy of Management Review. 23(3):491-512.

Doležel J, Bartoš J 2005. Plant DNA flow cytometry and estimation of nuclear genome size. Annals of Botany. 95: 99-110.

Doležel J, Bartoš J, Voglmayr H, Greilhuber J 2003. Nuclear DNA content and genome size of trout and human. Cytometry. 51: 127-129.

Doležel J, Greilhuber J, Suda J. 2007. Flow Cytometry with Plant Cells: Analysis of Genes, Chromosomes and Genomes. Wiley-VCH Verlag GmbH and Co., Weinheim, Germany.

Donno D, Beccaro GL, Mellano MG, Cerutti AK, Bounous G. 2015. Goji berry fruit (*Lycium* spp.): antioxidant compound fingerprint and bioactivity evaluation. Journal of Functional Foods. 18: 1070-1085.

Dorman HD, Koşar M, Kahlos K, Holm Y, Hiltunen R. 2003. Antioxidant properties and composition of aqueous extracts from Mentha species, hybrids, varieties, and cultivars. Journal of Agricultural and Food Chemistry. 51(16): 4563-4569.

Faria A, Pestana D, Teixeira D, de Freitas V, Mateus N, Calhau C. 2010. Blueberry anthocyanins and pyruvic acid adducts: anticancer properties in breast cancer cell lines. Phytotherapy Research. 24(12): 1862-1869.

Greilhuber J, Doležel J, Lysák MA, Bennett MD. 2005. The origin, evolution and proposed stabilization of the terms 'genome size' and 'C-value' to describe nuclear DNA contents. Annals of Botany. 95: 255-260.

Greilhuber J. 2007. Cytochemistry and C-values: the less-well-known world of nuclear DNA amounts. Annals of Botany. 101(6): 791-804.

Hamidi F, Karimzadeh G, Rashidi Monfared S, Salehi, M. 2018. Assessment of Iranian endemic Artemisia khorassanica: karyological, genome size, and genes expression involved in artemisinin production. Turkish Journal of Biology. 42: 322-333.

Javadian N, Karimzadeh G, Sharifi M, Moieni A, Behmanesh M. 2017. In vitro polyploidy induction: changes in morphology, podophyllotoxin biosynthesis, and expression of the related genes in *Linum album* (Linaceae). Planta. 245(6): 1165-1178.

Kalt W, Cassidy A, Howard LR, Krikorian R, Stull AJ, Tremblay F, Zamora-Ros R. 2020. Recent research on the health benefits of blueberries and their anthocyanins. Advances in Nutrition. 11(2): 224-236.

Karimzadeh G, Danesh-Gilevaei M, Aghaalikhani M. 2011. Karyotypic and nuclear DNA variations in *Lathyrus sativus* (Fabaceae). Caryologia. 64(1): 42-54.

Karimzadeh G, Mousavi SH, Jafarkhani-Kermani M, Jalali-Javaran M. 2010. Karyological and nuclear DNA variation in Iranian endemic muskmelon (*Cucumis melo* var. Inodorus). Cytologia. 75(4): 451-461.

Kim H, Lee GR, Kim J, Baek JY, Jo YJ, Hong SE, Kim HM. 2016. Sulfiredoxin inhibitor induces preferential death of cancer cells through reactive oxygen species-

mediated mitochondrial damage. Free Radical Biology and Medicine. 91: 264-274.

Laczkó-Zöld E, Komlósi A, Ülkei T, Fogarasi E, Croitoru M, Fülöp I, Domokos E, Ştefănescu R, Varga E. 2018. Extractability of polyphenols from black currant, red currant and gooseberry and their antioxidant activity. Acta Biologica Hungarica. 69(2): 156-169.

Lakshmi N, Venkateswara Rao T. 1984. Karyological and morphological investigations on some inbred strain of *Trigonella*. Genetica-Ibrica. 43: 187-200.

Lalegani S, Gavlighi HA, Azizi MH, Sarteshnizi RA. 2018. Inhibitory activity of phenolic-rich pistachio green hull extract-enriched pasta on key type 2 diabetes relevant enzymes and glycemic index. Food Research International. 105: 94-101.

Liochev SI. 2013. Reactive oxygen species and the free radical theory of aging. Free Radical Biology and Medicine. 60: 1-4.

Loureiro J, Rodriguez E, Doležel J, Santos C. 2007. Two new nuclear isolation buffers for plant DNA flow cytometry: a test with 37 species. Annals of Botany. 100: 875-888.

Lu Y, Guo S, Zhang F, Yan H, Qian DW, Wang HQ, Jin L, Duan JA. 2019. Comparison of functional components and antioxidant activity of *Lycium barbarum* L. fruits from different regions in China. Molecules. 24(12): 2228.

Mahdavi S, Karimzadeh G. 2010. Karyological and nuclear DNA content variation in some Iranian endemic *Thymus* species (Lamiaceae). Journal of Agricultural Science and Technology (JAST). 12(4): 447-458.

Meng R, Finn C. 2002. Determining ploidy level and nuclear DNA content in *Rubus* by flow cytometry. Journal of the American Society for Horticultural Science. 127(5): 767-775.

Moure A, Cruz JM, Franco D, Domınguez JM, Sineiro J, Domınguez H, Núñez MJ, Parajó JC. 2001. Natural antioxidants from residual sources. Food Chemistry. 72(2): 145-171.

Murashige T, Skoog F. 1962. A revised medium for rapid growth and bio-assays with tobacco tissue cultures. Physiologia Plantarum. 15(3): 437-497.

Mustafa AM, Angeloni S, Abouelenein D, Acquaticci L, Xiao J, Sagratini G, Maggi F, Vittori S, Caprioli G. 2022. A new HPLC-MS/MS method for the simultaneous determination of 36 polyphenols in blueberry, strawberry and their commercial products and determination of antioxidant activity. Food Chemistry. 367: 130743.

Nestby R, Hykkerud AL, Martinussen I. 2019. Review of botanical characterization, growth preferences, climatic adaptation and human health effects of Ericaceae and Empetraceae wild dwarf shrub berries in boreal, alpine and arctic areas. Journal of Berry Research. 9(3): 515-547.

Nile SH, Park SW. 2014. Edible berries: Bioactive components and their effect on human health. Nutrition. 30(2): 134-144.

Nin S, Petrucci WA, Del Bubba M, Ancillotti C, Giordani E. 2017. Effects of environmental factors on seed germination and seedling establishment in bilberry (*Vaccinium myrtillus* L.). Scientia Horticulturae. 226: 241-249.

Piljac-Žegarac J, Belščak A, Piljac A. 2009. Antioxidant capacity and polyphenolic content of blueberry (*Vaccinium corymbosum* L.) leaf infusions. Journal of Medicinal Food. 12(3): 608-614.

Potterat O. 2010. Goji (*Lycium barbarum* and *L. Chinense*): phytochemistry, pharma-cology and safety in the perspective of traditional uses and recent popularity. Planta Medica. 76: 7-19.

Prior R.L, Cao G, Martin A, Sofic E, McEwen J, O'Brien C, Lischner N, Ehlenfeldt M, Kalt W, Krewer G, Mainland CM. 1998. Antioxidant capacity as influenced by total phenolic and anthocyanin content, maturity, and variety of *Vaccinium* species. Journal of Agricultural and Food Chemistry. 46(7): 2686-2693.

Rache L, Pacheco JC. 2010. Propagación *in vitro* de plantas adultas de *Vaccinium meridionale* (Ericaceae). Acta Botanica Brasilica. 24(4): 1086-1095.

Skrovankova S, Sumczynski D, Mlcek J, Jurikova T, Sochor J. 2015. Bioactive compounds and antioxidant activity in different types of berries. International Journal of Molecular Sciences. 16(10): 24673-24706.

Sliwinska E, Zielinska E, Jedrzejczyk I. 2005. Are seeds suitable for flow cytometric estimation of plant genome size. Cytometry Part A. 64(2): 72-79.

Song Q, Sing KC. 2004. *Agrobacterium tumefaciens*-mediated transformation of blueberry (*Vaccinium corymbosum* L.). Plant Cell Reports. 23(7): 475-484.

Stebbins GL. 1971. Chromosome Evolution in Higher Plants. London: Edward Arnold, UK.

Steffen K, Grousset F, Schrader G, Petter F, Suffert M. 2015. Identification of pests and pathogens recorded in Europe with relation to fruit imports. EPPO Bulletin. 45(2): 223-239.

Suda J, Trávníček P. 2006. Reliable DNA ploidy determination in dehydrated tissues of vascular plants by DAPI flow cytometry-new prospects for plant research. Cytometry Part A. 69(4): 273-280.

Swift H. 1950. The constancy of desoxyribose nucleic acid in plant nuclei. Proceedings of the National Academy of Sciences of the USA. 36(11): 643-654.

Tarkesh Esfahani S, Karimzadeh G, Naghavi MR. 2016. 2C DNA value of Persian poppy (*Papaver bracteatum* Lindl.) medicinal plant as revealed by flow cytometry analysis; a quick effective criteria for distinguishing unidentified *Papaver* species. International Journal of Advanced Biotechnology and Research. 7(2): 573-578.

Tarkesh Esfahani S, Karimzadeh G, Naghavi MR. 2020. *In vitro* polyploidy induction in Persian poppy (*Papaver bracteatum* Lindl.). Caryologia. 73(1): 133-144.

Tavan M, Mirjalili MH, Karimzadeh G. 2015. *In vitro* polyploidy induction: changes in morphological, anatomical and phytochemical characteristics of *Thymus persicus* (Lamiaceae). Plant Cell, Tissue and Organ Culture. 122(3): 573-583.

Tepe B, Sokmen M, Akpulat HA, Sokmen A. 2006. Screening of the antioxidant potentials of six *Salvia* species from Turkey. Food Chemistry. 95(2): 200-204.

Thiem B, Sliwinska E. 2003. Flow cytometric analysis of nuclear DNA content in cloudberry (*Rubus chamaemorus* L.) *in vitro* cultures. Plant Science. 164: 126-134.

Umdale S, Ahire M, Aiwale V, Jadhav A, Mundada P. 2020. Phytochemical investigation and antioxidant efficacy of wild, underutilized berries of economically important Indian Sandalwood (*Santalum album* L.). Biocatalysis and Agricultural Biotechnology. 27: 101705.

Vinson JA, Su X, Zubik L, Bose P. 2001. Phenol antioxidant quantity and quality in foods: fruits. Journal of Agricultural and Food Chemistry. 49(11): 5315-5321.

Yang B, Kortesniemi M.. 2015. Clinical evidence on potential health benefits of berries. Current Opinion in Food Science. 2: 36-42.

Yang H, Tian T, Wu D, Guo D, Lu J. 2019. Prevention and treatment effects of edible berries for three deadly diseases: Cardiovascular disease, cancer and diabetes. Critical Reviews in Food Science and Nutrition. 59(12): 1903-1912.

Zarabizadeh H, Karimzadeh G, Rashidi Monfared S, Tarkesh Esfahani S. 2022. Karyomorphology, ploidy analysis, and flow cytometric genome size estimation of *Medicago monantha* populations. Turkish Journal of Botany. 46: 50-61.

Zarco CR. 1986. A new method for estimating karyotype asymmetry. Taxon. 35(3): 526-530.

Zong Y, Gu L, Shen Z, Kang H, Li Y, Liao F, Xu L, Guo W. 2021. Genome-wide identification and bioinformatics analysis of auxin response factor genes in highbush blueberry. Horticulturae. 7(10): 403.

Finito di stampare da
Logo s.r.l. – Borgoricco (PD) – Italia

OPEN ACCESS POLICY

Caryologia provides immediate open access to its content. Our publisher, Firenze University Press at the University of Florence, complies with the Budapest Open Access Initiative definition of Open Access: By "open access" , we mean the free availability on the public internet, the permission for all users to read, download, copy, distribute, print, search, or link to the full text of the articles, crawl them for indexing, pass them as data to software, or use them for any other lawful purpose, without financial, legal, or technical barriers other than those inseparable from gaining access to the internet itself. The only constraint on reproduction and distribution, and the only role for copyright in this domain is to guarantee the original authors with control over the integrity of their work and the right to be properly acknowledged and cited. We support a greater global exchange of knowledge by making the research published in our journal open to the public and reusable under the terms of a Creative Commons Attribution 4.0 International Public License (CC-BY-4.0). Furthermore, we encourage authors to post their pre-publication manuscript in institutional repositories or on their websites prior to and during the submission process and to post the Publisher's final formatted PDF version after publication without embargo. These practices benefit authors with productive exchanges as well as earlier and greater citation of published work.

PUBLICATION FREQUENCY

Papers will be published online as soon as they are accepted, and tagged with a DOI code. The final full bibliographic record for each article (initial-final page) will be released with the hard copies of *Caryologia*. Manuscripts are accepted at any time through the online submission system.

COPYRIGHT NOTICE

Authors who publish with *Caryologia* agree to the following terms:

- Authors retain the copyright and grant the journal right of first publication with the work simultaneously licensed under a Creative Commons Attribution 4.0 International Public License (CC-BY-4.0) that allows others to share the work with an acknowledgment of the work's authorship and initial publication in Caryologia.
- Authors are able to enter into separate, additional contractual arrangements for the non-exclusive distribution of the journal's published version of the work (e.g., post it to an institutional repository or publish it in a book), with an acknowledgment of its initial publication in this journal.
- Authors are permitted and encouraged to post their work online (e.g., in institutional repositories or on their website) prior to and during the submission process, as it can lead to productive exchanges, as well as earlier and greater citation of published work (See The Effect of Open Access).

PUBLICATION FEES

Open access publishing is not without costs. *Caryologia* therefore levies an article-processing charge of € 150.00 for each article accepted for publication, plus VAT or local taxes where applicable.

We routinely waive charges for authors from low-income countries. For other countries, article-processing charge waivers or discounts are granted on a case-by-case basis to authors with insufficient funds. Authors can request a waiver or discount during the submission process.

PUBLICATION ETHICS

Responsibilities of *Caryologia*'s editors, reviewers, and authors concerning publication ethics and publication malpractice are described in *Caryologia*'s Guidelines on Publication Ethics.

CORRECTIONS AND RETRACTIONS

In accordance with the generally accepted standards of scholarly publishing, *Caryologia* does not alter articles after publication: "Articles that have been published should remain extant, exact and unaltered to the maximum extent possible".

In cases of serious errors or (suspected) misconduct *Caryologia* publishes corrections and retractions (expressions of concern).

Corrections

In cases of serious errors that affect or significantly impair the reader's understanding or evaluation of the article, *Caryologia* publishes a correction note that is linked to the published article. The published article will be left unchanged.

Retractions

In accordance with the "Retraction Guidelines" by the Committee on Publication Ethics (COPE) *Caryologia* will retract a published article if:

- there is clear evidence that the findings are unreliable, either as a result of misconduct (e.g. data fabrication) or honest error (e.g. miscalculation)
- the findings have previously been published elsewhere without proper crossreferencing, permission or justification (i.e. cases of redundant publication)
- it turns out to be an act of plagiarism
- it reports unethical research.

An article is retracted by publishing a retraction notice that is linked to or replaces the retracted article. *Caryologia* will make any effort to clearly identify a retracted article as such.

If an investigation is underway that might result in the retraction of an article *Caryologia* may choose to alert readers by publishing an expression of concern.

COMPLYNG WITH ETHICS OF EXPERIMENTATION

Please ensure that all research reported in submitted papers has been conducted in an ethical and responsible manner, and is in full compliance with all relevant codes of experimentation and legislation. All papers which report in vivo experiments or clinical trials on humans or animals must include a written statement in the Methods section. This should explain that all work was conducted with the formal approval of the local human subject or animal care committees (institutional and national), and that clinical trials have been registered as legislation requires. Authors who do not have formal ethics review committees should include a statement that their study follows the principles of the Declaration of Helsinki

ARCHIVING

Caryologia and Firenze University Press are experimenting a National legal deposition and long-term digital preservation service.

ARTICLE PROCESSING CHARGES

All articles published in *Caryologia* are open access and freely available online, immediately upon publication. This is made possible by an article-processing charge (APC) that covers the range of publishing services we provide. This includes provision of online tools for editors and authors, article production and hosting, liaison with abstracting and indexing services, and customer services. The APC, payable when your manuscript is editorially accepted and before publication, is charged to either you, or your funder, institution or employer.

Open access publishing is not without costs. *Caryologia* therefore levies an article-processing charge of € 150.00 for each article accepted for publication, plus VAT or local taxes where applicable.

FREQUENTLY-ASKED QUESTIONS (FAQ)

Who is responsible for making or arranging the payment?

As the corresponding author of the manuscript you are responsible for making or arranging the payment (for instance, via your institution) upon editorial acceptance of the manuscript.

At which stage is the amount I will need to pay fixed?

The APC payable for an article is agreed as part of the manuscript submission process. The agreed charge will not change, regardless of any change to the journal's APC.

When and how do I pay?

Upon editorial acceptance of an article, the corresponding author (you) will be notified that payment is due.

We advise prompt payment as we are unable to publish accepted articles until payment has been received. Payment can be made by Invoice. Payment is due within 30 days of the manuscript receiving editorial acceptance. Receipts are available on request.

No taxes are included in this charge. If you are resident in any European Union country you have to add Value-Added Tax (VAT) at the rate applicable in the respective country. Institutions that are not based in the EU and are paying your fee on your behalf can have the VAT charge recorded under the EU reverse charge method, this means VAT does not need to be added to the invoice. Such institutions are required to supply us with their VAT registration number. If you are resident in Japan you have to add Japanese Consumption Tax (JCT) at the rate set by the Japanese government.

Can charges be waived if I lack funds?

We consider individual waiver requests for articles in Caryologia on a case-by-case basis and they may be granted in cases of lack of funds. To apply for a waiver please request one during the submission process. A decision on the waiver will normally be made within two working days. Requests made during the review process or after acceptance will not be considered.

I am from a low-income country, do I have to pay an APC?

We will provide a waiver or discount if you are based in a country which is classified by the World Bank as a low-income or a lower-middle-income economy with a gross domestic product (GDP) of less than $200bn. Please request this waiver of discount during submission.

What funding sources are available?

Many funding agencies allow the use of grants to cover APCs. An increasing number of funders and agencies strongly encourage open access publication. For more detailed information and to learn about our support service for authors.

APC waivers for substantial critiques of articles published in OA journals

Where authors are submitting a manuscript that represents a substantial critique of an article previously published in the same fully open access journal, they may apply for a waiver of the article processing charge (APC).

In order to apply for an APC waiver on these grounds, please contact the journal editorial team at the point of submission. Requests will not be considered until a manuscript has been submitted, and will be awarded at the discretion of the editor. Contact details for the journal editorial offices may be found on the journal website.

What is your APC refund policy?

Firenze University Press will refund an article processing charge (APC) if an error on our part has resulted in a failure to publish an article under the open access terms selected by the authors. This may include the failure to make an article openly available on the journal platform, or publication of an article under a different Creative Commons licence from that selected by the author(s). A refund will only be offered if these errors have not been corrected within 30 days of publication.

2022
Vol. 75 – n. 4

Caryologia

International Journal of Cytology, Cytosystematics and Cytogenetics

Table of contents